University of Southampton

Faculty of Environmental and Life Sciences

Biological Sciences

Regulation of Endocytosis in Embryos: A Mechanism to Overcome Poor Maternal Nutrition but with Long-Term Health Implications

by

Laura Carvalho Nunes Coelho Caetano, MSc.

Thesis for the degree of Doctor of Philosophy

February 2020

University of Southampton

Abstract

Faculty of Environmental and Life Sciences

Biological Sciences

Thesis for the degree of Doctor of Philosophy

REGULATION OF ENDOCYTOSIS IN EMBRYOS: A MECHANISM TO OVERCOME POOR MATERNAL NUTRITION BUT WITH LONG-TERM HEALTH IMPLICATIONS

by

Laura Carvalho Nunes Coelho Caetano

Our group have previously shown that the period around mammalian conception is sensitive to environmental factors that can affect the early embryo before implantation with enduring consequences over the lifetime. Our past work in mice has shown maternal low protein diet exclusively during preimplantation development with normal nutrition thereafter (Emb-LPD diet) leads to increased endocytosis in trophectoderm (TE) of blastocysts followed by growth, cardiovascular and metabolic dysfunctions. The maternal nutrient depletion associates with a reduction in mammalian target of rapamycin complex 1 (mTORC1) signalling (pathway regulating cellular growth) in the early embryos, which is responsive to insulin and BCAAs, both reduced in the Emb-LPD maternal serum and uterine luminal fluid, respectively. We reasoned that the reduced uterine metabolite composition is sensed by embryos through mTOR, activating endocytosis as an early biomarker of adversely programmed embryos, to increase nutrient uptake to counter the poor quality of maternal diet, yet associating with later health complications.

The current mouse study determined the role of individual BCAA and insulin depletion conditions on endocytosis in TE after establishing an improved *in vitro* embryo culture and endocytosis model. Thus, 2-cell embryos were cultured to the blastocyst stage in KSOM medium supplemented with BCAA and insulin at normal (N, NBCAA/N-INS; 100% of concentrations found in control-fed mothers) or with a combination or individual BCAA and/or insulin (INS) depleted by 50% (L-): low valine (L-VAL), low isoleucine (L-ISO), low leucine (L-LEU). After culture, blastocyst fluorescent markers for lysosomes (LysoTracker)

and endocytosed and processed bovine serum albumin (BSA-BODIPY) were used with confocal microscopy and VOLOCITY imaging software for quantitative analysis. From many combinations of media with individually varying BCAAs and insulin, my 48 h cultures showed: (i) Culture with L-ISO was sufficient with control concentrations of other BCAAs and insulin to induce enhanced endocytosis in blastocysts; (ii) L-LEU alone had a weaker effect on endocytosis than L-ISO but L-VAL had no effect; (iii) L-INS with control BCAAs had no effect on endocytosis; (iv) Combinations of L-ISO and L-LEU enhanced endocytosis, also when combined with L-INS; (v) Control and experimental culture conditions had no effect on embryo development rate or blastocyst cell number. Additional studies on the enhanced endocytosis phenotype revealed that induction with L-ISO/N-INS also stimulated expression of the structural endocytosis vesicle protein, clathrin, and the main multi-ligand endocytic receptor, megalin, in blastocysts. Induction also increased active lysosomes containing the hydrolase cathepsin B. The timing of the change in endocytosis phenotype, assessed by screening earlier stage morulae, showed that the response only occurred from the early blastocyst stage onwards when the endocytosis system had fully matured.

I also explored whether deficiency in mTORC1 signalling in blastocysts could activate the enhanced endocytosis phenotype and, in particular, if the mTORC1-associated transcription factor for lysosome expression, TFEB, was involved. Experimental analysis showed that embryos cultured in control medium with NBCAA/N-INS with increasing concentrations of the mTORC1 inhibitor, rapamycin, led to a dramatic relocation of TFEB from mainly cytoplasmic (inactive) to nuclear (active) localisation, where it acts to promote transcription for lysosomal biosynthesis. Furthermore, treatment with the L-ISO/N-INS protocol in the absence of rapamycin also stimulated nuclear localisation of TFEB and subsequently, increased lysosomes.

Collectively, these mouse model experiments indicate L-ISO, and to lesser extents L-LEU and L-INS, act as environmental cues to stimulate compensatory blastocyst endocytosis in low nutrient conditions, mediated through altered TFEB activation shown to be responsive to reduced mTORC1 signalling.

In separate experiments, the same endocytosis assay markers were used (BSA-BODIPY and LysoTracker Red) on human embryos donated for research, and compared outcomes based upon maternal BMI and conventional IVF versus intracytoplasmic injection (ICSI). In the first experiment, patients were separated based on normal (18-23) or high (28-33) BMI as a

measure of normal or dysfunctional physiological/nutritional states. Whilst no difference was found between blastocysts in terms of embryo survival and cell number, those from the high BMI group exhibited the enhanced endocytosis phenotype using LysoTracker Red. Moreover, the range of scores varied across the high BMI group showing individual embryo variation. Lastly, examination of human embryos for TFEB localisation revealed increased nuclear versus cytoplasmic location for the high BMI group, but not quite at significance level. ICSI procedure showed no effect on endocytosis phenotype, although ICSI embryo scores showed high variation in the high BMI group. Collectively, this preliminary data supports the concept that maternal nutrition/metabolism affects embryo endocytosis phenotype in the human as shown in the mouse model, with the potential to be a biomarker for embryo long-term health.

Table of Contents

Table of Tables

Table of Figures

Research Thesis: Declaration of Authorship

Print name:

Title of thesis:

I declare that this thesis and the work presented in it are my own and has been generated by me as the result of my own original research.

I confirm that:

1. This work was done wholly or mainly while in candidature for a research degree at this University;
2. Where any part of this thesis has previously been submitted for a degree or any other qualification at this University or any other institution, this has been clearly stated;
3. Where I have consulted the published work of others, this is always clearly attributed;
4. Where I have quoted from the work of others, the source is always given. With the exception of such quotations, this thesis is entirely my own work;
5. I have acknowledged all main sources of help;
6. Where the thesis is based on work done by myself jointly with others, I have made clear exactly what was done by others and what I have contributed myself;
7. None of this work has been published before submission.

Signature: ..... Date: .....

Acknowledgements

Firstly, I would like to thank my supervisor, Professor Tom Fleming, for his support, patience, motivation and valuable advice for my PhD and related research. I could not have imagined having a better advisor and mentor.

I would like to extend my gratitude to my second supervisor, Dr Judith Eckert, for always making an effort to help me and for being so interested.

I am also very thankful to the Biomedical Imaging Unit staff, specially Dr David Chatelet for helping me with the *Volocity* software and Dr David Johnson for confocal microscopy training and for having all the patience in the world to answer my questions and to help me with my project.

I would also like to thank Dr David Tumbarello for sharing his knowledge in endocytosis and cell signalling with me and for his output in some crucial details.

A big thank you to the BRF staff, in particular Lorraine House, for helping me with mouse handling during my experiments.

I would like to thank the Wessex Fertility Clinic staff, in particular the embryology manager Tony Price and previous staff member Dr Matthew Cotterill for bringing the donated embryos to the University laboratory and for showing me how to handle them.

I am very appreciative of all former fellow lab members of the Developmental Biology group: Diego Ojeda, Dr Reyna Peñailillo, Dr Pooja Khurana, Dr Anan Aljahdali, Dr Joanna Gould, Georgie Dawes, Dr Bhav Sheth and Dr Patrick Vilela. Thank you for all the support, help and good moments we spent together. It would have not been the same without them.

A big thank you to all the people I shared the common office space with, in special my friends Dr María Martín, Monica Guerrero, Liam Barry Carroll and Joe Chouhan, for the stimulating discussions, chitchat and all the fun we had even throughout difficult times.

I'm immensely grateful to my parents and family for standing by me, through their long-distance support, motivation and love during not only this unique and demanding journey but also at each and every step through life.

And finally to my husband Miguel, for being my rock and for believing in me even when I doubted myself and thought I did not have the strength to continue.

Abbreviations

AA	Amino Acids
Akt	Protein Kinase B
AMPK	5' AMP-activated protein kinase
ATP	Adenosine triphosphate
ART	Artificial reproductive techniques
BCAA	Branched chain amino acid
Blast	Blastocyst
BMI	Body mass index
bp	Base pair
BSA	Bovine Serum Albumin
cDNA	Complementary DNA
Cdx2	Caudal-type homeobox-2
COP	Coat Protein Complex
Ct	Cycle threshold
Ctsb	Cathepsin B
DNA	Deoxyribonucleic acid
DAPI	4’,6’-Diamino-2-Phenylindole
DMSO	Dimethyl sulfoxide
Dnmt	DNA methyltransferase transcript
dNTP	Deoxynucleotide triphosphates
DEPTOR	Domain-containing mTOR-interacting protein
DOHaD	Developmental Origins of health and Disease
E	Embryonic day
EB	Embryoid body
E-Cad	E-cadherin
Emb-LPD	Embryonic low protein diet
EDTA	Ethylenediaminetetraacetic acid
Eomes	T-box gene eomesodermin

ESC	Embryonic stem cell
FITC	Fluorescein isothiocyanate
GLUT	Glucose transporter
GR	Glucocorticoid receptor
H2afz	H2A Histone Family Member Z
hESC	Human ES cells
IGF	Insulin-like growth
INS	Insulin
ISO	Isoleucine
IVF	*In vitro* fertilisation
KSOM	Potassium simplex optimized medium
LAMP1	Lysosomal-associated membrane protein 1
LBCAA	Low Branched chain amino acid
L-	Low
LEU	Leucine
Log	Logarithm
LPD	Low protein diet
LRP2	Low density lipoprotein-related protein 2
mESC	Mouse embryonic stem cell
MetS	Metabolic Syndrome
$MgCl_2$	Magnesium chloride
M-MLV	Moloney murine leukemia Virus
mRNA	Messenger RNA
mTOR	Mammalian target of Rapamycin
N-	Normal
NBCAA	Normal Branched chain amino acid
NPD	Normal protein diet
Oct4	Octamer binding transcription factor 4
ParE	Parietal endoderm
PBS	Phosphate-Buffered Saline

PBS-T	Tween-20 in PBS
PCOS	Polycystic ovarian syndrome
PCR	Polymerase chain reaction
PE	Primitive endoderm
PGK1	Phosphoglycerate Kinase 1
PPIB	Peptidylprolyl Isomerase B
pH	Potential of hydrogen
PI3K	Phosphatidylinositol 3-kinase
PIKK	Phosphatidylinositol kinase-related kinase
PKC	Protein Kinase C
(Ppara)-α	Peroxisomal proliferator activated receptor
PVP	Polyvinylpyrrolidone
qPCR	Quantitative PCR
qRT-PCR	Quantitative real time PCR
RhoA	Ras homolog gene family, member A
RNA	Ribonucleic acid
rRNA	Ribosomal RNA
RT	Reverse transcriptase
RT-	Negative control of reverse transcriptase
S6K	P70 ribosomal S6 kinase
SDHA	Succinate dehydrogenase complex flavoprotein subunit A
SEM	Standard error of mean
SOX2	SRY-related HMG box-containing transcription factor
TBE	Tris/Borate/EDTA
TBP	TATA-Box-Binding protein
TE	Trophectoderm
TFEB	Transcriptor factor EB
TSC	Tuberous sclerosis complex
TUBA	Tubulin Alpha

VAL	Valine
VE	Visceral endoderm
VPS18	Vacuolar protein sorting 18 homolog
VYS	Visceral yolk sac
ZP	Zona pellucida
0BCAA	Branched chain amino acid absence
3Rs	Replacement, Reduction and Refinement

Project Overview

Non-communicable diseases, also known as chronic diseases, are on the rise throughout the world, particularly conditions affecting the comorbidity of cardiovascular, metabolic and neurological disease, such as the Metabolic Syndrome (MetS). In fact, 25% of the World's adult population suffers from MetS, which is defined as a cluster of severe heart attack risk factors, including diabetes and prediabetes, abdominal obesity, high cholesterol and high blood pressure (World Health Organization and International Diabetes Federation information). This rise accounts for an increase in health care costs as well as loss of working capacity. Although genetic mutations and lifestyle contribute for MetS and related conditions, it is the *in utero* environment (which is affected by maternal nutrition) that is the most significant driver of disease risk - the framework of the Developmental Origins of Health and Disease (DOHaD) hypothesis (Barker and Thornburg, 2013).

The period right after conception and during early embryonic development (periconceptional period) has been identified as a vulnerable time for the embryo, when environmental factors may cause permanent changes in the pattern and characteristics of development leading to higher risk of adult MetS-related diseases. Several *in vivo* and *in vitro* studies have been conducted in human and animal models showing the association between periconceptional conditions such as poor maternal diet, assisted reproductive techniques (ART) and maternal inflammatory sickness and an increased risk of adult MetS-related diseases (Fleming et al, 2018).

Our research group developed a mouse periconceptional model of developmental origin of disease where a low protein diet (LPD) - detailed diet composition is described in *Appendix 8.1* - specifically during this period (from conception until blastocyst formation) and replaced by a normal diet thereafter (Emb-LPD), proved to be sufficient to cause adult cardiometabolic and neurological disease (Watkins et al., 2010; Watkins et al., 2008a; Gould et al., 2018). These offspring showed high blood pressure associated with impaired arterial vasodilatation in male offspring, female excess weight and adiposity, abnormal brain development, anxiety related behaviour and memory loss throughout adult life. This model shows that programming of later-life disease can be induced by conditions experienced during the preimplantation period. In the human, nutrient programming of early embryos might occur due to short famine periods, as occurred in the Dutch Hunger

Winter in 1944-1945, which have revealed an enhanced risk of cardiometabolic and neurological disease in adults conceived in that period (Roseboom et al., 2015; Roseboom et al., 2001). Moreover, studies in IVF children showed a higher risk of developing cardiometabolic disease (Hart and Norman, 2013a; Ceelen et al., 2009; Sunde et al, 2016).

Since embryos sense the quality of extracellular nutrients available in the maternal reproductive tract, our group have investigated the uterine fluid and serum of LPD mothers, showing a significant depletion in branched chain amino acids (BCAAs) such as leucine, valine and isoleucine by approximately 30% compared to normal protein diet (NPD) mothers, and decreased serum insulin (Eckert et al., 2012). The maternal nutrient depletion associates with a reduction in mammalian target of rapamycin (mTOR) signalling (pathway regulating cellular growth) in the early embryos, which is responsive to insulin and BCAAs. When the availability of nutrients is reduced, embryos sense it through mTOR, causing a series of compensatory mechanisms to promote adaptation and survival to the adverse environment. One of these compensatory mechanisms is to stimulate endocytosis in the extra-embryonic lineages, trophectoderm (TE) and primitive endoderm (PE), the progenitors of the placenta and yolk sac, respectively (Sun et al., 2014), which can be seen as a way of improving the nutrient supply so that the extra-embryonic lineages accomplish their role in embryonic nutrient delivery. However, this adaptation comes with the establishment of an increased nutrient-storage metabolism in offspring, which becomes a maladaptation in cases where the postnatal environment is substantially different, leading to adult chronic diseases.

Endocytosis regulates the internalisation of extracellular nutrients and signalling molecules by receptor-mediated, micropinocytosis or phagocytosis, and its intrinsic regulation is well characterised. However, the endocytosis extrinsic regulation, how this system senses the external environment, is not well understood. In fact, this research subject becomes of extreme interest, as lysosomes have been proposed not only to be responsible for protein degradation but also for signalling and homeostasis of cellular metabolism with implications for health and disease (Settembre et al, 2013).

Our group previously showed, using the Emb-LPD model and embryo culture in deprived environments (depleted BCAAs), an increased ligand uptake and internalised vesicles, increased number and volume of lysosomes per cell and increased expression of megalin (a major endocytic receptor in the extra-embryonic lineages) in blastocyst TE and in PE

formed in embryoid bodies cultured from mouse embryonic stem cells (mESCs) (Sun et al., 2014). However, the precise induction conditions of endocytosis, how the embryo mediates such a response, and whether such a compensatory mechanism occurs and acts in the same way in the human, are unknown. These issues will be the main topics of my research.

Chapter 1 Literature Review

1.1 Mouse Embryo Development

Since the time of conception, the mouse embryo spends approximately 5 days preparing for implantation. During this period, the preimplantation mouse embryo undergoes several morphogenetic changes, including around six cleavage divisions, the activation of the embryonic genome, the process of compaction through the development of intercellular adhesion and junctions (Saiz and Plusa, 2013), the accumulation of intercellular fluid – blastocoel cavity formation (Smith and McLaren, 1977) and the formation of distinct cell lineages. During this development, the embryo remains enclosed by the zona pellucida (ZP), a protective glycoprotein coat, from which it hatches prior to implantation into the receptive maternal uterine endometrium (Enders and Schlafke, 1967).

Compaction, first reported by Lewis and Wright, (1935), starts at the 8-cell stage in mouse and consists of the flattening and approximation of blastomeres (*Figure 1.1*) so that individual cells are no longer visible (Saiz and Plusa, 2013). This process is calcium-dependent and marks the beginning of tight-junction formation between the basolateral membranes of the blastomeres (Ducibella and Anderson, 1975). Compaction also coincides with polarisation of each blastomere, forming a proto-epithelial phenotype with outward-facing apical and contact localised basolateral membranes (Fleming et al., 1994). 8-cell blastomeres can either divide symmetrically producing two polar daughter cells or asymmetrically into one polar and one apolar cell. By this time, the morula stage is formed *(Figure 1.1*). Cells located on the inside of the morula (descendent from asymmetric division) will become, after subsequent cell divisions, the pluripotent inner cell mass (ICM) – embryonic cell lineage - of the blastocyst, whereas cells positioned on the surface will develop into the trophectoderm (TE) – extra-embryonic epithelial cell lineage (Tarkowski and Wróblewska, 1967).

The blastocyst is formed through cavitation at around the 32-cell stage (Suwiska et al., 2008; Smith and McLaren, 1977) at embryonic day 3.5 (E3.5), and it is characterised by the presence of a fluid-filled cavity (the blastocoel) and the ICM, both surrounded by the

TE *(Figure 1.1*). The blastocoel fluid is released from TE cytoplasmic vesicles to expand the intercellular area (Calarco and Brown, 1969) and by vectorial transport of fluid across the TE driven by basolateral Na^+/K^+-ATPase (Watson, 2001) such that the ICM becomes placed in one pole (embryonic pole), surrounded by polar TE, while mural TE surrounds the blastocoel (abembryonic pole). The region of TE that is in contact with ICM gives rise to the extraembryonic ectoderm in response to paracrine signals (e.g. Fgf4 produced by ICM) (Gardner, 1982; Nichols et al., 1998). At this time the embryo is at the "egg cylinder" stage and it is connected to the uterine tissue via the ectoplacental cone (also derived from TE) (Rossant and Tam, 2009). Furthermore, a population of ICM cells gives rise to the primitive endoderm (PE) in the late blastocyst (which will differentiate into extra-embryonic parietal and visceral endoderm around the time of implantation) on the surface that is facing the blastocoel whilst the remaining ICM forms the epiblast, the tissue that produces all of the foetal lineages (Marikawa and Alarcon, 2009; Rossant and Tam, 2009). While the exposure of the ICM surface to the blastocoel can trigger the differentiation of ICM to the PE, recent studies also suggest that the precursor cells for PE are present within the ICM in a mosaic pattern at the blastocyst stage, which later migrate towards this surface (Plusa et al., 2008) – further discussed.

The parietal endoderm (ParE) cells derived from the PE will then form a discontinuous layer responsible for nutrient transport and secrete Reicherts's membrane (a thick extracellular basement membrane which may function as a filter between the foetus and the mother) (Familari, 2006). After gastrulation, these cells contribute to parietal yolk sac formation while the visceral endoderm (VE), also derived from PE, will contribute to the visceral yolk sac (VYC) (Gardner, 1982), which includes functions such as early histiotrophic nutrition for the embryo from uterine secretions. It covers the extraembryonic ectoderm and the epiblast which develops into the three primary germ layers (embryonic ectoderm, endoderm and mesoderm) that contain the progenitors of all the tissues of the foetus (Gardner, 1982).

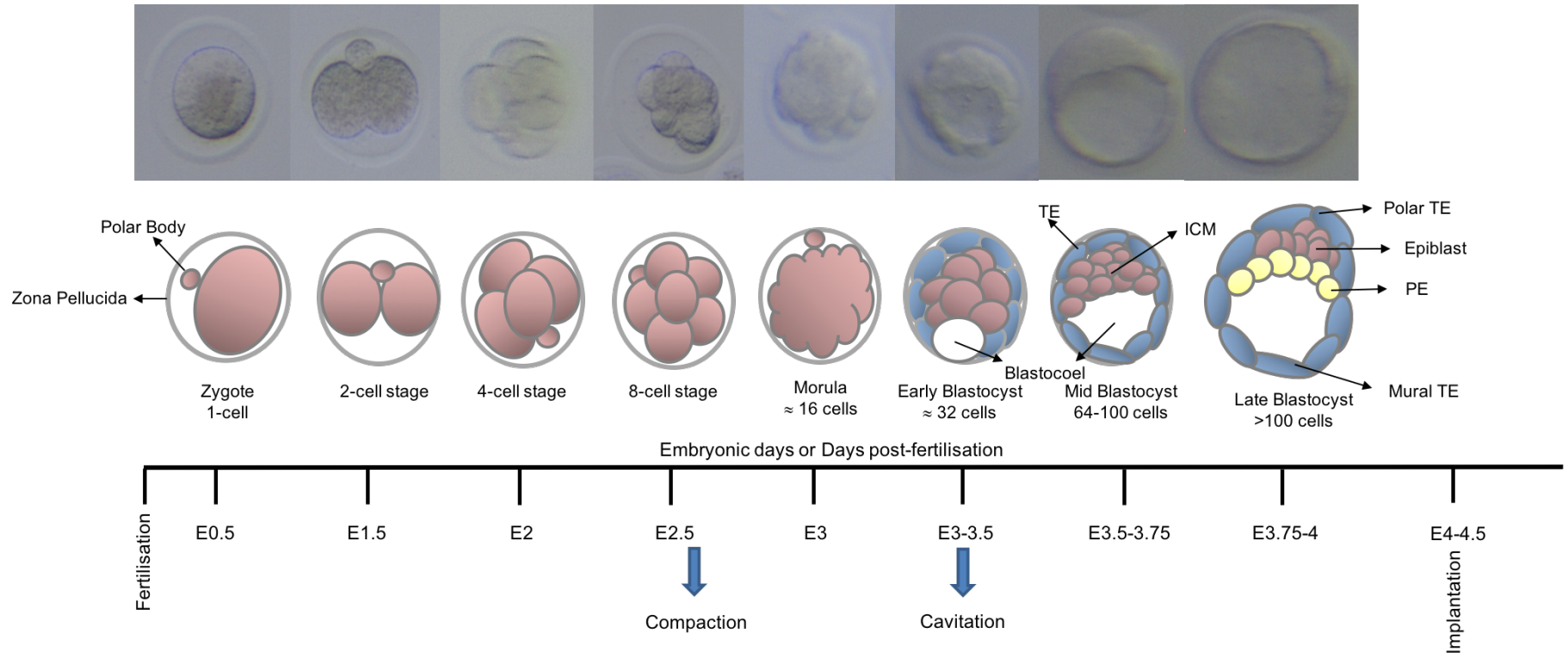

Figure 1.1 - Schematic representation of the stages of mouse preimplantation development. The polar body is a product of the second meiotic division of the oocyte and degenerates during preimplantation development. The timeline (not to scale) indicates the time elapsed since fertilisation in embryonic days (E). ICM, inner cell mass; TE, trophectoderm; PE, primitive endoderm. Adapted from Saiz and Plusa, (2013).

1.1.1 Differences in mouse and human early embryonic development

Pre-implantation development is morphologically similar in humans and mice, although there are notable differences in developmental timing, gene expression, signalling requirement for pluripotency and lineage segregation (Niakan and Eggan, 2013). For instance, the timing of embryonic genome activation (EGA), the process by which an embryo begins to transcribe its newly formed genome, initiates between the 1- and 2-cell stage for mice (Flach et al., 2004), while in humans it occurs between the 4- and 8-cell stage (Braude et al., 1988; Tesařék et al., 1988). A fertilized egg is initially transcriptionally inactive as it is in a transcriptionally oppressive environment. Thus, the first cell cycles are driven by maternal mRNA and proteins deposited in the oocyte during oogenesis. EGA is essential to synthesise new proteins and for further cleavage to take place (Latham, 1999). Changes in chromatin structure and protein content (particularly histone proteins) appear to regulate the availability of the genome for transcription. The major activation of the embryonic genome is followed by a progressive decline in the expression of maternal mRNA between 26 and 47 h post-insemination. Moreover, blastocyst formation happens at E3–3.5 in mice in contrast to E4–5 in humans (reviewed in Tang et al., 2016).

After implantation, human and mouse embryos become structurally distinct. Mouse blastocyst implantation occurs at E4–4.5, the pluripotent epiblast cells become polarized and transform into a cup-shaped epithelium (Bedzhov and Zernicka-Goetz, 2014; Beddington and Robertson, 1999) with an inverted cup on top formed by the TE-derived extra-embryonic ectoderm (ExE) (*Figure 1.2)* while human embryos undergo an additional cell division and implant between E6-8 (Norwitz et al., 2001). Following implantation at E7–E8, the amniotic cavity is formed and the epiblast and the underlying PE flatten into a round bilaminar embryonic disc (*Figure 1.2)* between the fluid-filled amniotic cavity and the yolk sac (formerly the blastocoel) (reviewed in Tang et al., 2016). With the differentiation of vessels in the mesoderm, a vascular yolk sac is formed. The ExE in mouse (*Figure 1.2)* corresponds to the structural equivalent of the amnion epithelium or the peripheral epiblast in humans (*Figure 1.2),* while the extra-embryonic VE corresponds to the human yolk sac epithelium (reviewed in Tang et al., 2016). The

primitive streak - a transient structure whose formation marks the start of gastrulation at around E16 in humans and E6-6.5 in mice - is formed at the posterior end of the embryonic disc and it extends towards the anterior region of the epiblast (reviewed in Tang et al., 2016). The proliferating epiblast cells and the streak undergo epithelial–mesenchymal transition and migrate to the space between the epiblast and PE, giving rise to the mesoderm layer (*Figure 1.2)* and they also replace the PE cells to become the definitive endoderm, resulting in the transformation of the bilaminar embryonic disc into a trilaminar disc, which contains the three germ layers - ectoderm, mesoderm and endoderm (reviewed in Tang et al., 2016).

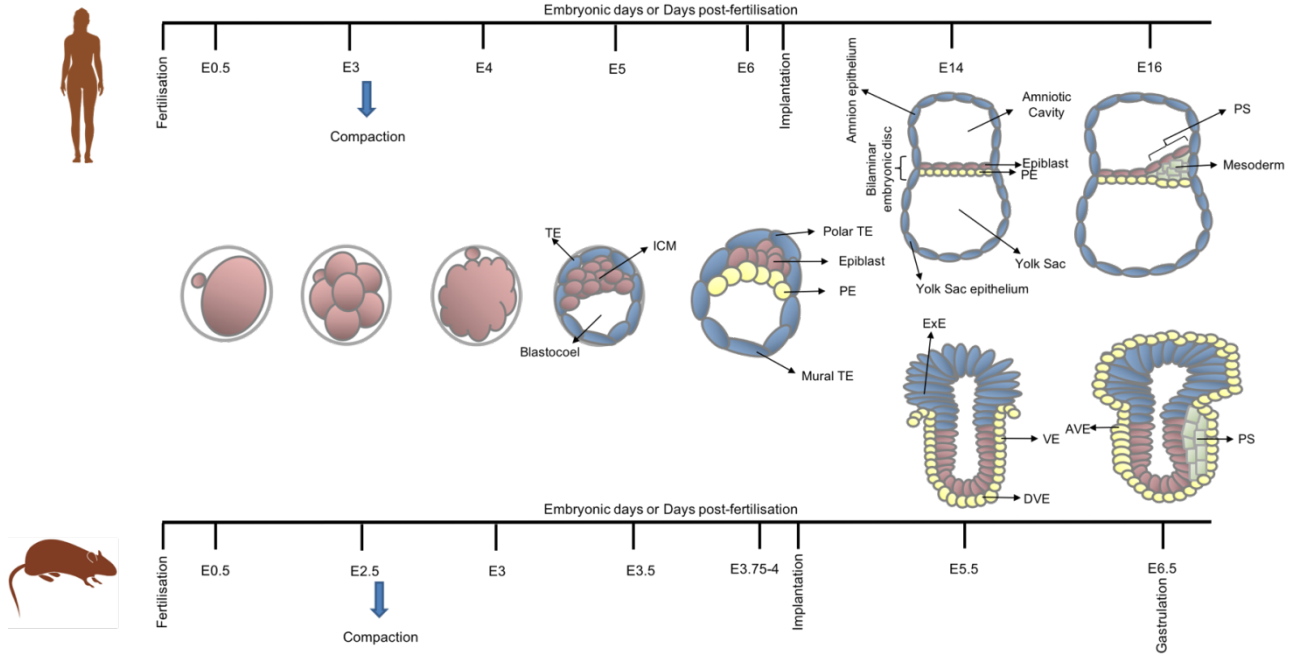

Figure 1.2 - Schematic representation of the differences in mouse and human early embryonic development. Human and mouse embryos become structurally distinct after implantation. In the mouse, implantation occurs at approximately E4.5, with the pluripotent epiblast cells becoming polarized and transformed into a cup-shaped epithelium, whereas the TE-derived extra-embryonic ectoderm (ExE) forms an inverted cup on top. The primitive endoderm (PE) develops as the visceral endoderm (VE) and envelops the epiblast and ExE. At E5.5, the distal VE (DVE) thickens and migrates to become the anterior VE (AVE). Gastrulation occurs at the posterior epiblast at E6.5, where the primitive streak (PS) emerges and gives rise to mesoderm and definitive endoderm. Human embryos exhibit a planar structure during the peri-gastrulation period. Following implantation at E7–E8, the epiblast moves away from the trophoblast, creating the amniotic cavity. The epiblast and the underlying PE flatten into a bilaminar embryonic disc, which is located between the amniotic cavity and the yolk sac. At E16, gastrulation begins and the PS is formed at the posterior end of the embryonic disc extending halfway across the epiblast towards the anterior region. The proliferating epiblast cells along the PS undergo epithelial to mesenchymal transition and migrate to the space between the epiblast and PE, becoming the mesoderm layer. The epiblast cells replace the PE cells to become the definitive endoderm, thus resulting in the formation of a trilaminar disc. Adapted from Tang et al., (2016).

1.1.2 Extra-embryonic Cell Lineages

Extra-embryonic membranes surround and protect the embryo and mediate the uptake of nutrients and gases as well as the disposal of waste products. In eutherian mammals, the TE and the PE are the main origin of these tissues. The TE contributes to the embryonic part of the placenta while the PE develops into the VE and ParE after implantation, which form the majority of the yolk sac (Gardner, 1982). In the mouse embryo, the most extensively studied model, the formation of these lineages takes place over 3 days in two successive and critical differentiation events, the division of TE and ICM followed by the division of the epiblast and PE (as reviewed in Saiz et al., 2013), detailed in the next section.

1.1.2.1 TE, ICM, PE and Epiblast formation and specification

In the embryo through to the early morula stage, all the blastomeres are totipotent as well as the ICM of early cavitating blastocysts, as these cells are able to give rise to all embryonic and extraembryonic lineages (Garner and McLaren, 1974; Grabarek et al., 2012; Handyside, 1978; Hogan and Tilly, 1978; Kelly, 1977; Spindle, 1978; Suwinska et al., 2008; Tarkowski et al., 2010). On the other hand, the epiblast is pluripotent, as it can produce all tissues except those derived from the TE and PE (Gardner and Rossant, 1979). This pluripotency will be lost as cells start to differentiate into specialised tissues.

Blastomeres at the 8-cell stage (E2.5) acquire a polarised apical surface upon compaction, which becomes isolated from the basolateral surfaces with the gradual development of intercellular junctions (Ducibella and Anderson, 1975). This ‘polarity model’ (*Figure 1.3a*) assumes that it is the differential inheritance of this polarised surface, after division from 8- to 16- and from 16- to 32-cells, which determines a TE or ICM fate (Johnson and Ziomek, 1981). Thus, blastomeres can either divide symmetrically producing two daughter cells that inherit the polarised domain and therefore will differentiate into TE or asymmetrically into one polar and one apolar daughter, which will differentiate into TE and ICM lineages, respectively. However, some studies have indicated that as early as the first cleavage, cells may already have a tendency to differentiate in specific lineages (Fujimori et al., 2003; Gardner, 2001; Piotrowska et al.,

2001) – further described. The ratio of outside to inside cell number varies widely during the 16-cell stage, although they are inversely proportional and compensated at the next division, resulting in a relatively consistent number of ICM cells in the 32-cell blastocyst and suggesting that mechanisms are in place to ensure an ICM of adequate size is produced (Fleming, 1987).

At the end of ICM and TE differentiation, the outer TE destined cells express caudal-type homeobox-2 (Cdx2), which is one of the first markers for TE cells, and T-box gene eomesodermin (Eomes) (Russ et al., 2000; Strumpf et al., 2005). Cdx2 expression in embryonic stem (ES) cells is sufficient to induce TE differentiation (Niwa et al., 2005; Strumpf et al., 2005). On the other hand, the inner cells remain pluripotent being regulated by Octamer-binding transcription factor 4 (Oct4), SRY-related HMG box-containing transcription factor (Sox2) and Nanog (Avilion et al., 2003; Nichols et al., 1998; Niwa et al., 2000; Puy et al., 2011; Singh et al., 2007).

As mentioned before, there is a controversial theory, suggesting that cells may already have a tendency to differentiate in specific lineages during the first cleavages. Piotrowska et al., (2001) showed by labelling individual cells, that the first cell to divide to the four-cell stage contributes preferentially to the embryonic part (*Figure 1.3b*). Therefore, at the 2-cell stage it is already possible to predict which cell will supply a greater proportion of its progeny to the embryonic part of the blastocyst and to the abembryonic part. However, this view is controversial and other studies have not identified evidence of 'pre-patterning' (Kurotaki et al., 2007). In accordance with this concept, Bischoff et al., (2008) showed through a 3D time-lapse lineage analysis that there is a spatial and temporal relationship between symmetric and asymmetric divisions and that descendants of individual blastomeres give rise to distinct regions of the blastocyst *(Figure 1.3c*). Plachta et al., (2011) showed that each cell in an early embryo shows one of two distinct Oct4 kinetic patterns, before there are any morphologically distinguishable differences or signs of lineage segregation. Cells with high Oct4 kinetics (high rate of Oct4 import and export to and from the nucleus) have increased accessibility to DNA making the cells prone to become TE, while slower Oct4 kinetics are more likely to give rise to the pluripotent cell lineage that contributes to the ICM. However, these early differences found between blastomeres are not

determinative, and these cells can be reprogrammed if the development is perturbed as they show plasticity (Zernicka-Goetz, 2006)

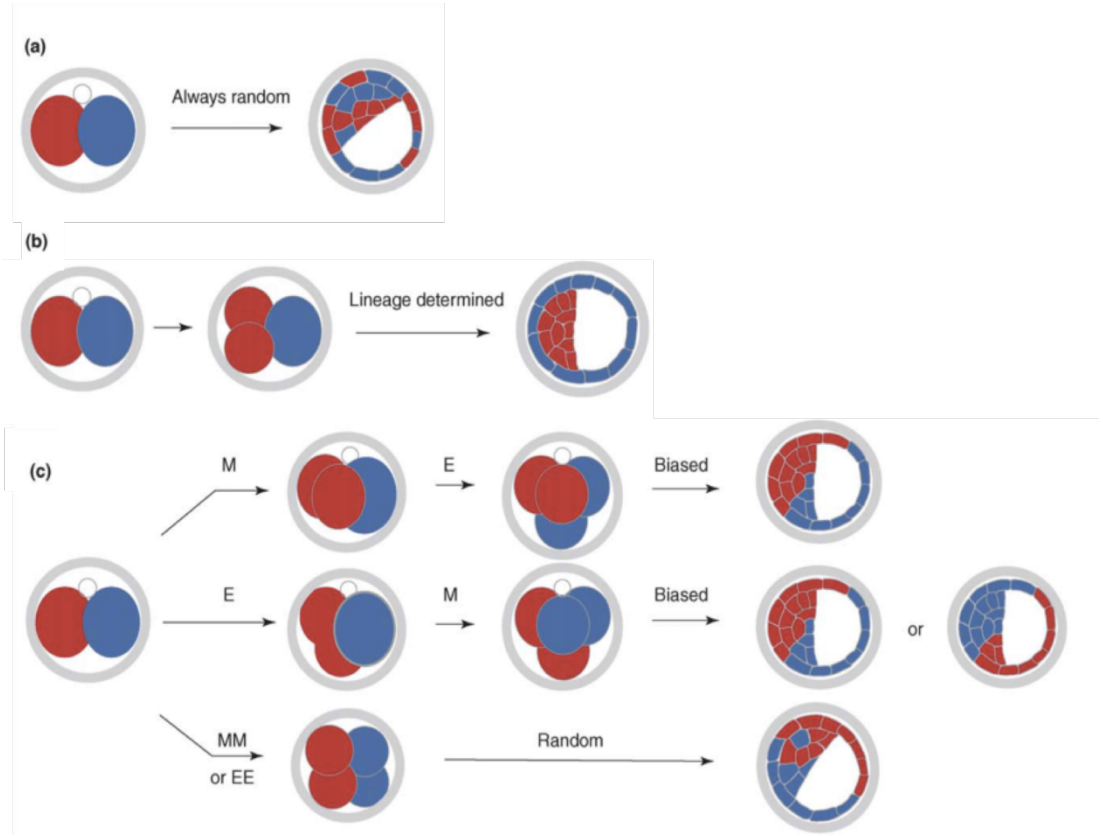

Figure 1.3 - Three viewpoints for allocation of the progeny of 2-cell stage blastomeres at the blastocyst stage. (a) 'Random' development: The different blastocyst parts and lineage formation is entirely independent of the 2-cell stage blastomere progeny. (b) 'Determined' development in which one 2-cell stage blastomere divides earlier and contributes to the ICM whereas the other divides later and contributes to the TE. (c) 'Biased' development: Both 2-cell stage blastomeres contribute to both ICM and trophectoderm lineages, but one contributes more cells to the embryonic part of the blastocyst and the other to the abembryonic part. Allocation of blastomere progeny depends on the order and orientation of cleavage from the 2- to the 4-cell stage. When the first blastomere to divide to the 4-cell stage undertakes meriodional division (M) with respect to the polar body and the second an equatorial–oblique division (E), the first blastomere to divide contributes more cells to the embryonic and the second to the abembryonic part of the blastocyst. When the order of division is the other way around, the earlier to divide blastomere contributes either to the embryonic or to the abembryonic part. When both blastomeres divide equatorially or meriodionally, the allocation of blastomere progeny is random. Adapted from Zernicka-Goetz, (2006).

The TE is the first epithelium to arise during mammalian development. Thus, its cells are bound through an extensive network of intercellular junctions developed during TE formation, which ensure selective permeability and epithelial cohesion (Ducibella and Anderson, 1975; Calarco and Epstein, 1973). The compaction of the 8-cell embryo is Ca^{2+}-dependent and it is mediated by changes in the cytoskeleton and by the formation of adherens junctions (Hyafil et al., 1980; Ducibella and Anderson, 1975). E-cadherin is present in adherens junctions and it is essential for the formation of an organised TE epithelium (Larue et al., 1994; Vestweber and Kemler, 1984; Hyafil et al., 1980). Adherens junction formation is followed by the development of tight junctions and desmosomes, which provide cohesion to the cells allowing the formation and expansion of the blastocoel (Eckert and Fleming, 2008; Thomas et al., 2004; Fleming et al., 1989, 1991; Ducibella and Anderson, 1975).

As mentioned above, the second differentiation event during preimplantation development results in the formation of the PE and the epiblast. The precise moment when these two lineages first emerge is still unclear, although it is now known that the PE and epiblast precursors are found intermingled in the ICM of the blastocyst (E3.5), in a 'salt and pepper' pattern – expressing Nanog (epiblast) and Gata6 (PE) lineage-promoting transcription factors (Grabarek et al., 2012; Guo et al., 2010; Morris et al., 2010; Plusa et al., 2008; Chazaud et al., 2006; Rossant et al., 2003). Cells mainly expressing Nanog retain pluripotency and become epiblast cells (Chambers et al., 2003; Mitsui et al., 2003). On the contrary, cells predominately expressing Gata6 (earliest PE gene to be expressed) migrate to form the outer layer of the ICM – PE. PE is marked by a number of other endodermal proteins, such as platelet-derived growth factor receptor alpha (PDGFRA), SOX17, SOX7, hepatic nuclear factor 4 (HNF4), HNF1b, or hematopoietically expressed homeobox (HEX), which appear sequentially during PE development (Artus et al., 2011; Niakan et al., 2010; Plusa et al., 2008; Rossant et al., 2003; Barbacci et al., 1999; Koutsourakis et al., 1999; Thomas et al., 1998; Chen et al., 1994; Duncan et al., 1994; Arceci et al., 1993). Nanog is necessary for maintaining the epiblast (Mitsui et al., 2003), and it is considered, alongside Oct4, the core of the pluripotency network. On the other hand, Gata6 and Gata4 in the PE repress Nanog expression, thus restricting their pluripotency. Expression of either Gata6 or Gata4 in ES

cells is sufficient to induce differentiation towards extra-embryonic endoderm (Fujikura and Yamato, 2002).

1.1.2.2 Extra-embryonic Cell Lineage Functions

The primary function of the extra-embryonic derivatives is nutrient transport. Before the establishment of blood flow through the placenta (hemotrophic nutrition), nutrients available to the embryo are absorbed by histotrophic mechanisms involving endocytosis by phagocytosis, pinocytosis, and receptor-mediated endocytosis from the maternal environment (Bielinska et al., 1999; Jauniaux et al., 2003). From the 32-cell stage, nutrient uptake is regulated by the TE and transported to the blastocoel (Fleming and Goodall, 1986; Pemble and Kaye, 1976). Later, between E3.5-4.5, the TE starts to attach to the endometrial epithelium and to implant into the uterine wall. At this time the TE becomes the trophoblast, which together with the maternal tissue will form the chorio-allantoric placenta. The placenta allows foetal nutrient uptake, waste elimination and gas exchange via the mother's blood supply, fights against internal infection and produces hormones to support pregnancy and provide thermo-regulation to the foetus.

Besides synthesizing a number of specialized proteins that facilitate endocytosis, digestion, and secretion of nutrients (due to its large number of phagocytic and pinocytic vesicles and microvilli), the visceral endoderm (VE) influences the differentiation and development of blood islands and vessels in the adjacent extraembryonic mesoderm (Boucher and Pedersen, 1996), ensuring efficient exchange of nutrients and gases between the mother and embryo (Bielinska et al., 1999). VE is also responsible for the synthesis and secretion of proteins involved in nutrient transport, such as transferrin and apolipoproteins (Bielinska et al., 1999). Moreover, it has also been suggested to influence myocardial differentiation, primitive streak formation (where cell migrations associated with gastrulation occur) and the development of the forebrain (Brown et al., 2010).

The ParE synthesizes large amounts of type IV collagen and laminins (Smith and Strickland, 1981). These extracellular matrix proteins are assembled into Reichert's membrane, which passively filters nutrients from the maternal environment (Gardner, 1982).

By E10, the visceral yolk sac (VYS) has been fully developed from the VE. The principal specialized functions of the yolk sac itself, beyond storage, are to transport to the embryo (through endocytosis) and metabolize maternally-derived macromolecules and to synthesize serum proteins (Jollie, 1990; Palis, 2006). The importance of the VYS in nutrient delivery has been demonstrated in several experiments. For instance, the disruption of yolk sac endoderm function by injection of certain chemicals (e.g. trypan blue), or the use of antibodies against yolk sac endoderm, are teratogenic for rodents (Brent et al., 1990; Jollie, 1990).

Cubilin, megalin, and amnionless are endocytic receptors which mediate uptake of several nutrients including proteins, cholesterol, lipids, iron, calcium, folic acid, retinoic acid, and vitamins B12 and D (Kozyraki and Gofflot, 2007). They are localized at the apical side of polarized epithelium and in the endocytic apparatus of the cell including coated pits, endosomes, and recycled vesicles (Christensen and Birn, 2002).

1.1.3 Energy supply for embryo development

The environmental requirements of the embryo change as development progresses and these are met by changes in the maternal environment. Pyruvate is required to support early embryo development until the 8-cell stage acting as a major source of energy (Biggers et al., 1967). Glucose is unable to support development prior to compaction (Brinster and Thomson, 1966; Brinster, 1965) although it becomes the main energy substrate during compaction and blastocyst formation (Leese and Barton, 1984). However, the reliance of the morula on glucose-derived energy is not absolute, as 2-cell stage embryos cultured in the absence of glucose are still able to form blastocysts by increasing their rate of consumption of pyruvate to meet the energy demands of cavitation (Martin and Leese, 1995). In contrast, freshly fertilised zygotes deprived of glucose can form morula *in vitro*, but fail to develop to further stages and subsequently degenerate (Martin and Leese, 1995; Brown and Whittingham, 1991; Chatot et al., 1989). These embryos do not develop the capacity of compensation by increasing pyruvate consumption (Martin and Leese, 1995; Brown and Whittingham, 1991; Chatot et al., 1989). Furthermore, and despite the fact that glucose is not required as an energy substrate prior to the 8-cell stage (Leese and Barton, 1984), there is an absolute requirement of glucose exposure in order to form a blastocyst (Martin and Leese, 1995; Chatot et al., 1994). This exposure enables the expression of the facilitative glucose transporter (GLUT) (Pantaleon et al., 2001), essential for blastocyst formation (Pantaleon et al., 1997), and allows the adaptive response in the absence of glucose. Glucose can be transported across membranes by two different mechanisms: mainly through the sodium-independent GLUT system (Wheeler and Hinkle, 1985), which is further described in *1.1.3.1* ,or by a sodium-dependent system (Esposito, 1984).

Proteins and amino acids are also required as an energy substrate for embryo development (Biggers et al., 2000; Lane and Gardner, 1997; Takahashi and First, 1992; Pullar et al., 1990; Epstein and Edwards, 1975; Schlafke and Enders, 1972). Amino acids are transported across membranes by membrane transport proteins which can change according to the embryonic developmental stage (Gonzalez et al., 2012). Martin and Sutherland, (2001) showed in an *in vitro* study using embryos cultured in medium lacking amino acids, that these cannot form trophoblast cell outgrowths on fibronectin (*in vitro*

model of implantation) but remain viable for up to 3 days in culture and will form outgrowths after being transferred into complete medium with amino acids. They showed that the amino acid requirement at this point is a developmental checkpoint event that occurs during a 4 to 8 hours period at the early blastocyst stage (Martin and Sutherland, 2001), and depends on mTOR signalling pathway. In accordance, other studies also support an important role for amino acids in regulating trophoblast differentiation, where embryos in diapause (delaying implantation), show very low rates of amino acid uptake (Van Winkle, 1981; Weitlauf, 1973). Since amino acid uptake and rates of protein synthesis are relatively low before the morula stage (Epstein and Edwards, 1975), it is likely that cells from these early developmental stages obtain most of their amino acid substrates from degradation of existing proteins and/or by synthesis *de novo*. By the blastocyst stage, embryos have acquired more extensive and sophisticated amino acid transport systems (DiZio and Tasca, 1977; Epstein and Edwards, 1975) which is correlated with an increasing dependence upon an exogenous source of amino acids as the rate of protein synthesis approaches, and eventually exceeds the degradation rate (Sellens and Sherman, 1981). Amino acid transport systems in preimplantation embryos is further described in *1.1.3.2*.

The proteins and glycoproteins found in the maternal reproductive tract are products of both transudation from the blood and specific synthetic and secretory activity of cells (Feigelson and Kay, 1972; Daniel and Krishnan, 1969). Embryos developing *in vivo* take up protein through endocytosis mechanisms (Fleming and Pickering, 1985; Pullar et al., 1990; Schlafke and Enders, 1972), which is indispensable for growth particularly in the earlier developmental stages, as the amino acid transport system is not yet fully developed and amino acid substrates are mainly a product of protein degradation or synthesis de novo.

1.1.3.1 GLUTs in preimplantation embryos

Several facilitative glucose transport proteins (GLUT family) – expressed by the SLC2 family of genes - have been described to date. Glucose transport across cell membranes via GLUT proteins is an energy independent process in which glucose is transported down its concentration gradient.

Currently, there are thirteen members of the GLUT family identified. GLUT1, GLUT2 and GLUT3 were first identified as glucose transporters in preimplantation embryos (Hogan et al., 1991;Pantaleon et al., 1997), although more recently additional GLUTS were detected in preimplantation embryos but with functions still unknown. GLUT1 and GLUT 3 are responsible for mediating maternal-placental transfer of glucose (Shin et al., 1997). In mice, GLUT1 is expressed throughout preimplantation development on the basolateral surface of TE cells and on the plasma membrane of the ICM (Pantaleon et al. 1997). Given its cell surface expression in the ICM it is hypothesized that the function of GLUT1 in developing embryos is to transport glucose into these cells from TE and or blastocoel (Pantaleon et al. 1997). GLUT3 is also critical for development of the preimplantation mouse embryo (Pantaleon et al., 1997; Pantaleon et al., 2008) as well as later in embryonic development (Ganguly et al., 2007). GLUT3 protein is detected from 4-cell to 8-cell stages in cytoplasmic vesicles (Pantaleon et al. 1997); in the plasma membrane of uncompacted morulae and on the apical surface of the polarized TE cells at blastocyst stage (Riley and Moley, 2006). GLUT3 in TE functions as the main glucose transporter responsible for maternal glucose uptake into the blastocyst. Its apical localization in the TE together with the basolateral GLUT1 provides the ICM with glucose (Pantaleon and Kaye, 1998). GLUT2 expression in preimplantation embryos is controversial, as some studies demonstrated its expression in 8-cell/compacted morula and mouse blastocysts (Aghayan et al., 1992; Hogan et al., 1991), while others failed to show its expression (Morita et al., 1992; Tonack et al., 2004). However, it has been speculated that GLUT2 may be responsible for glucose transport into the blastocoel cavity (Pantaleon et al. 1997).

The activation of growth factor receptors, including insulin and IGF-I, during the preimplantation period in mammals is vital for embryo survival and development. The signal transduction mechanisms by which these factors mediate their effects in preimplantation embryos are beginning to be elucidated. Phosphatidylinositol 3-kinase (PI3-K) is a known regulator of several physiologic responses including cellular proliferation, growth and survival as well as glucose metabolism in the preimplantation embryo (Riley and Moley, 2006). In other cell systems, insulin has been shown to activate the PI3-K pathway, thus stimulating glucose uptake by causing the translocation of insulin responsive GLUTs to the plasma membrane (reviewed in Welsh et al., 2005).

It is still not fully established whether insulin-stimulation results in the activation of this pathway in preimplantation embryos. However, Riley et al., (2005) showed that blastocysts treated with insulin results in increased protein kinase B (Akt) phosphorylation, suggesting that insulin triggers the activation of the PI3-K/Akt pathway and thereby might regulate glucose homeostasis in mammalian blastocysts.

1.1.3.2 Amino acid transport system in preimplantation embryos

The ability to maintain intracellular amino acids at equal or higher concentrations than that found in the extracellular environment is facilitated by the presence of amino acid transporters present in the plasma membrane, normally coupled with ion gradient or amino acid gradient. Some transporters function to actively concentrate amino acids inside cells, whereas others may facilitate cellular efflux by counter exchange mechanisms (Bertran et al., 1994; Hundal and Taylor, 2009). These transporters also function as nutrient sensing and signal delivery into cells. Several amino acids transporters have been described to date in different tissues, including mammalian placenta and in less extent in the preimplantation embryo, which will be focused in this chapter.

Amino acid transporters can be highly regulated during early embryonic development. During preimplantation development, embryonic amino acid use is bi-phasic, amino acid uptake and rates of protein synthesis are relatively low before the morula stage (Epstein and Edwards, 1975) with the embryo relying more on those amino acids present at higher levels in the oviduct; however, later stage blastocysts increase amino acid uptake and use all amino acids (Lane and Gardner, 1997; Steeves and Gardner, 1999). Oviduct fluid is characterised by high concentrations of L-alanine, L-aspartate, glycine, L-serine, L-glutamine, L-threonine and taurine (Harris et al., 2005). Most mammalian cells require mechanisms for volume regulation (Friedrich et al., 2006). Preimplantation mouse embryos appear to develop in a hypertonic environment in oviductal fluid. *In vitro*, glycine, alanine, glutamine, and taurine protect preimplantation embryos from detrimental effects of hypertonic media (Dawson and Baltz, 1997). These amino acids have a Na^+-dependent system for their transport in cleavage-stage conceptuses, thus they are able to improve development *in vitro* in hypertonic medium. For instance, Na^+-dependent systems Gly (for glycine) and β (taurine) protect embryos from hyperosmotic

media, while lysine and leucine, which transport systems are not fully developed in early cleavage embryos, do not. Volume-sensitive organic osmolyte/anion channels (VSOAC) transport taurine, glycine, aspartate, and chloride through Na^+ -independent channel proteins in 1- and 2-cell embryos and in blastocysts (Kolajova and Baltz, 1999). System Gly, whose preferred substrate is glycine, is expressed throughout cleavage but not at blastocyst stage and it is essential for regulating oocyte size (Van Winkle and Campione, 1996). Similarly, system X_{AG}^- and mRNA encoding excitatory (anionic) amino acid transporter (EAAT) are expressed in blastocysts but not at earlier stages of development (Van Winkle and Campione, 1996). Its preferred substrates are aspartate and glutamate. Moreover, a transport system for glutamine, system N, appears to be developmentally regulated in early embryos and appears transiently at 4- to 8- cell stage (Van Winkle and Dickinson, 1995). In contrast, taurine transport by system β and mRNA encoding the taurine transporter (TAUT) are expressed throughout all preimplantation development (Van Winkle et al., 1994). All these transporters are dependent on sodium (*Table 1.1*).

Essential amino acids increase the cleavage rate in embryos after the 8-cell stage. Incubation of blastocysts with the essential amino acid methionine increases the amount of the internalised amino acid, with a 10-fold greater accumulation of this amino acid than its total chemical potential gradient (Kaye et al., 1982). This was attributed to the Na^+-dependent system $B0,^+$ activity present at blastocyst stage (Van Winkle et al., 1990). System $B0,^+$ and system $b0,^+$ (Na^+-independent) transport a wide variety of zwitterionic and cationic amino acids in blastocysts. Their preferred substrates are leucine and arginine, respectively (reviewed in Van Winkle, 2001), which are among the most effective essential amino acid signalling molecules. Leucine uptake through $B0,^+$ activates the mTOR pathway and induces the formation of motile trophoblast cells, regulating the onset of embryo penetration into the uterine wall (Van Winkle et al., 2006). System x_c^- (Na^+-independent) for cystine and glutamate transport has relatively high activity in unfertilized and fertilized mouse eggs, but its activity is greatly reduced in 2-cell conceptuses and appears to be lost by the time that blastocysts form (Van Winkle et al., 1992). Cystine is exchanged for intracellular glutamate that had been derived from glutamine previously taken up from the medium. The cystine that is taken up is reduced and utilized for the synthesis of glutathione, which appears to help cells resist oxidative stress *in vitro* (Van Winkle et al., 1992) associated with fertilization.

Systems L and T (Na^+-independent) in embryos are present at all stages of preimplantation development. System L operates as a 1:1 heteroexchanger facilitating uptake of branched chain amino acids (BCAAs) in exchange for certain cytoplasmic amino acids accumulated via secondary active transporters such as system A: Sodium-coupled neutral amino acid transporter (SNAT) (Hundal and Taylor, 2009). System L preferred amino acid subtracts are BCAAs and benzenoid amino acids while system T has benzenoid amino acids as preferred substrate.

Amino acid transport systems in early mouse embryos are likely regulated at the genetic level to appear during development when the transport they facilitate is physiologically beneficial. For instance, upregulation of System A transport activity in response to global amino acid withdrawal in mammalian cells is known as “adaptive regulation” (reviewed in Hundal and Taylor, 2009). The increase in System A activity associated with cellular amino acid withdrawal is linked with increased expression of SNAT2 (Ling et al., 2001). 2- and 4-cell stage embryos express SNAT1 and SNAT2 in the cytoplasm and nuclei of blastomeres while in morulae these are excluded from the nucleus. In blastocysts SNAT1 is localised to the cytoplasm/cell surface of the TE and it is not expressed in the ICM, whereas SNAT2 is detected in the nucleus and cytoplasm of TE and in ICM of fully expanded blastocysts but not in early formed blastocysts (Tan et al., 2016). These changes in transporter expression likely reflect different amino acid requirements during development.

Amino acid transport in preimplantation embryos is regulated by female reproductive tract constituents in order to optimize the functions of the systems. However, the precise mechanisms of regulation and how components of the uterine environment regulate transport system activities in early embryos are yet to be fully described. *Table 1* shows a summary of amino acid transport systems and their preferred substrates and functions in preimplantation mouse embryos.

System in embryos	*Stages most highly expressed*	*Preferred aa substrate(s)*	*Proposed physiological function*
Na^+ and Cl^- -dependent transporter superfamily			
Gly	1- to 8- cell	Glycine	Cellular volume (or protein concentration) regulation and concomitant effects on metabolism especially during early cleavage
β	All	Taurine	1. Cellular volume (or protein concentration) regulation and concomitant effects on metabolism throughout preimplantation development 2. Resistance to oxidant stress
$B^{0,+}$	Blastocyst	Most zwitterionic and cationic amino acids (e.g., leucine and tryptophan)	1. Net amino acid uptake for protein synthesis and accumulation in blastocysts 2. Regulation of protein kinases involved in protein synthesis regulation in blastocysts
Na^+ -dependent EAAT family			
X_{AG}^-	Blastocyst	Glutamate and aspartate	Uptake of anionic amino acid signaling molecules and their depletion from uterine secretions if activated *in vivo*
X_A^-	Blastocyst	Aspartate	
B	Blastocyst	Zwitterionic	
Na+ -dependent A/N family			
N	4- to 8- cell	Glutamine	Transient glutamine accumulation, cell volume (or protein concentration) regulation) and consequent metabolic effects at 4 to 8-cell stage
A	Blastocyst	BCAA Alanine Proline	"Adaptive regulation" to amino acid withdrawal
Na+ -independent channel proteins			
$VSOAC_1$	1- to 2- cell	Taurine Glycine Aspartame	Cellular volume (or protein concentration) regulation and concomitant effects on metabolism especially during early cleavage
$VSOAC_2$	Blastocyst	Taurine Glycine Aspartame	

Na+ -independent aa transporter superfamily			
b^{+}_{1a} b^{+}_{1b}	1- to 2-cell	Arginine	1. Regulation of polyamine and NO production possibly through direct delivery of arginine to sites of synthesis 2. Net amino acid uptake for protein synthesis and accumulation in blastocysts in conjunction with system $B^{0,+}$ 3. Regulation of protein kinases involved in protein synthesis regulation
b^{+}_{i}	1- to 8-cell	Arginine	
b^{+2}	Blastocyst	Arginine	
$b^{0,+}$	Blastocyst	Most bulky cationic and zwitterionic (e.g., arginine)	
L	All	BCAA and benzenoid	
T	All	Benzenoid	
X_c	1-cell	Glutamate Cystine	

Table 1.1 -Mammalian amino acid transport protein superfamilies and corresponding systems in preimplantation mouse embryos (Adapted from Van Winkle, 2001).

1.2 Developmental Origin of Health and Disease (DOHaD)

An association between the reproductive environment and later disease risk in adulthood was first hypothesized by Professor David Barker in Southampton, UK, and it is now recognised as *DOHaD* or *Developmental Origin of Health and Disease* (Barker et al., 2002). The Dutch Hunger Winter in 1944-1945 was critical in the establishment of the DOHaD hypothesis. The effects of a 5-month famine experienced during early gestation have revealed an enhanced risk of cardiometabolic and neurological disease in the offspring's later life, such as coronary heart disease, glucose intolerance, obesity and accelerated ageing (Roseboom et al., 2015; Roseboom et al., 2001; Franke et al., 2017), identifying the periconceptional period as a vulnerable window for adverse programming (reviewed in Velazquez et al., 2019). Furthermore, the Hertfordshire and Helsinki cohort studies (1930s-1940s) demonstrated that risk factors for adult cardiovascular and metabolic disease, such as hypertension, coronary heart disease and Type II diabetes, are positively correlated with poor foetal growth and birth weight and associated with a 'catch-up' growth in infancy (reviewed in Barker and Thornburg, 2013). Such associations have been replicated in different cohorts across the world (Barker, 2004).

The DOHaD concept is based on the "developmental plasticity" phenomenon by which one genotype can give rise to a range of different persistent physiological or morphological changes as a strategy to adapt to different environmental conditions during development (Barker, 2004). However, such permanent responses may become maladaptive in cases where the post-natal environment is substantially different (*Figure 1.4*).

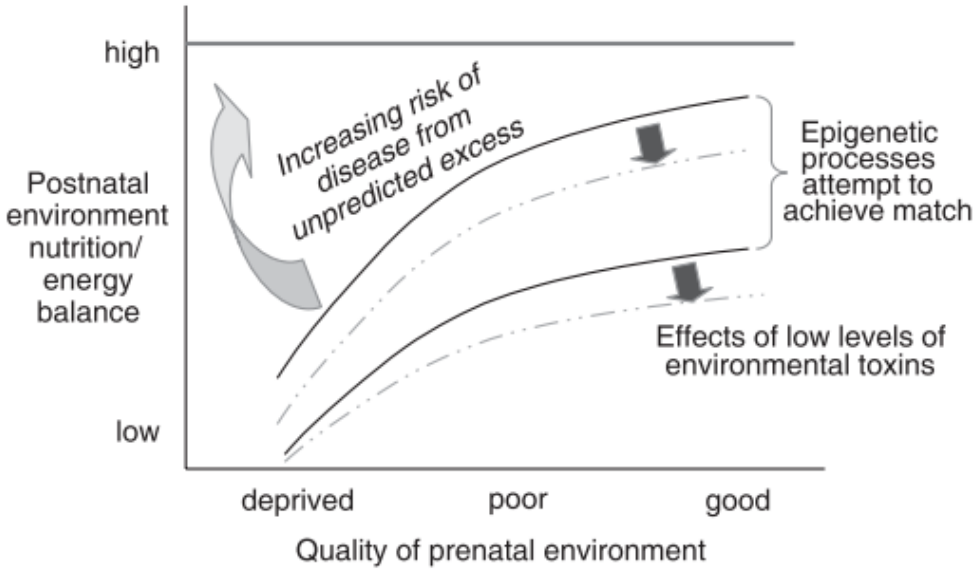

Figure 1.4 - Diagram showing how mismatch between prenatal and postnatal environment increases risk of chronic disease later in life. The space represented between the continuous lines show the range of postnatal environments for which the phenotypes induced by the prenatal environment are matched, and therefore able to remain healthy. Epigenetic processes have an enormous importance in attempting to produce an optimal match during development. As the quality of the prenatal environment decreases, this range becomes narrower, increasing the disease probability from unpredicted excess in the postnatal environment. Even low levels of environmental toxins that alone would not be pathogenic can induce substantial effects on risk of later chronic disease by altering the epigenetic matching, as shown by the discontinuous lines (Hanson and Gluckman, 2008).

1.2.1 Embryonic and periconceptional environment and developmental programming

Several *in vivo* and *in vitro* studies, including the effect of poor parental nutrition, artificial reproductive techniques (ART) and health status have been carried out, suggesting the susceptibility of the preimplantation embryo to the environmental conditions which can lead to long-term phenotype alterations and increased disease risk (Eckert et al., 2012, 2016; Velazquez, 2015; Watkins et al., 2015; Sinclair and Watkins, 2014; Watkins and Sinclair, 2014; Fleming et al., 2012; Watkins et al., 2008a; Gould et al., 2018). These crucial influences on lifetime health occurring so early in development

might reflect perturbations or adaptations in epigenetic, cellular, metabolic, and physiological mechanisms (Fleming et al., 2018).

The metabolic syndrome (MetS) is a major and escalating public-health and clinical challenge worldwide which is defined by the co-occurrence of several factors such as obesity, insulin resistance, hypertension and dyslipidemia. MetS confers a 5-fold increase in the risk of type 2 diabetes mellitus and 2-fold risk of developing cardiovascular disease over the next 5 to 10 years (Kaur, 2014). Studies in experimental animals showed a developmental origin of adult MetS correlated with maternal nutrient-restriction during gestation, followed by a compensatory growth associated with post-natal food consumption (Parlee and MacDougald, 2015). Not only poor maternal nutrition, but also maternal smoking, stress, inflammation, obesity and hypertension are related with offspring MetS (Kaur, 2014). The way maternal nutrition correlates with offspring MetS is believed to be related with different pathways including foetal oxidative stress (malnutrition can directly lead to a pro-oxidative state by creating protein/micronutrient deficiencies), an altered hypothalamic-pituitary-adrenal (HPA) axis (nutrient restriction results in the birth of offspring with elevated basal or stress-induced glucocorticoid secretion), neuropeptides (maternal nutrition induces changes in the hypothalamic circuitry and in the expression, localization, and action of specific neuropeptides altering the level of energy intake in the offspring) (Brenseke et al., 2013) and epigenetic modification of transcription factors.

Studies regarding maternal inflammatory sickness mediated by endotoxin exposure at the time of conception showed that the pro-inflammatory cytokine activation within the mother leads to changes in the blastocyst morphogenesis (Williams et al., 2011). However, unlike nutritional programming, inflammation has minimal or no effect on the offspring growth or adult cardiometabolic phenotype but rather alters the innate immune system in a way that responsiveness to endotoxin is suppressed (Williams et al., 2011).

The use of assisted reproductive technologies (ART) to overcome infertility has been increasing, with over eight million children born from *in vitro* fertilisation (IVF) worldwide (De Geyter, 2018). The first IVF baby, Louise Brown, was born 41 years ago, and since that time, extensive epidemiological investigations have been done

(Hyrapetian et al., 2014; Hart and Norman, 2013a, 2013b; Bay et al., 2019; Zhao et al., 2018). Increased incidence compared to natural conception has been reported for perinatal complications (Hyrapetian et al., 2014), low birth weight (Bay et al., 2019), abnormal placental growth (Bloise et al., 2014; Haavaldsen et al., 2012), foetal congenital malformations (Zhao et al., 2018) and imprinting disorders (Lazaraviciute et al., 2014). Moreover, an increased risk of cardiometabolic disease in ART children has been reported, with increased incidence of high blood pressure, adiposity and glucose intolerance (Hart and Norman, 2013a; Ceelen et al., 2009), although more epidemiological studies are required. It has also been proposed that ART offspring may have a small increase in neurodevelopmental delay and risk of clinical depression (Hart and Norman, 2013b). However, the causes of any adversity in ART children, whether related to clinical and/or embryological treatment (superovulation, IVF, embryo culture, cryopreservation, embryo transfer, etc.) or the parental reproductive capacity, still needs to be elucidated.

1.2.1.1 Low protein diet

Considering the legal and moral issues of human embryonic research, several animal models, especially rodent models, have been used to study the DOHaD concept. Strong evidence suggests that a maternal low protein diet restricted to the preimplantation window – Emb-LPD - (until E3.5 in mice and E4.5 in rat) results in compromised embryo development (Watkins et al., 2015; Fleming et al., 2012; Langley-Evans, 2000; Kwong et al., 2000). Emb-LPD induces changes in the maternal serum metabolites at the time of mouse blastocyst formation, including reduction in insulin and increase in glucose, together with reduced levels of free amino acids including branched chain amino acids (BCAA) leucine, isoleucine and valine (Eckert et al., 2012). These uterine fluid modifications, sensed by the embryos, stimulate changes in their phenotype in order to promote embryo adaptation and survival. However, as mentioned before, these might become future maladaptations if conditions of nutrient restriction change.

Langley-Evans, (1997) showed that rats born from mothers fed with a LPD throughout the entire pregnancy had a decreased birth weight and higher blood pressure compared to controls. Kwong et al., (2000) showed that also Emb-LPD induced programming of altered birth weight and hypertension, highlighting for the first time the

periconceptional diet programming in rats. Later, Watkins et al., (2010, 2008a) using the mouse Emb-LPD model, showed high blood pressure associated with impaired arterial vasodilatation in male offspring, elevated serum and lung angiotensin-converting enzyme (ACE) activity in female and male offspring, respectively, highlighting the importance of the periconceptional period for embryo reprogramming. Anxiety related behaviour and female excess weight and adiposity throughout adult life were also described in this model (Watkins et al., 2008a). Moreover, Gould et al., (2018) showed that these animals present reduced neural stem cells in the foetal brain and a compensatory mechanism to upregulate neuronal differentiation and increase cortex thickness and neuron ratio, leading to adult memory deficits.

1.3 Nutrients availability and embryo sensing

Studies using the Emb-LPD model showed several alterations in the maternal serum at the time of blastocyst formation such as reduced insulin level, increased glucose and a reduced concentration of amino acids including the 3 branched chain amino acids (BCAAs) - leucine, isoleucine and valine (Eckert et al., 2012). Moreover, a reduction in the BCAAs within the maternal uterine fluid at the blastocyst stage coincident with an altered content of blastocyst amino acids and reduced mammalian target of rapamycin complex 1 (mTORC1) signalling was also reported (Eckert et al., 2012). mTOR is crucial for cellular growth regulation and amino acids and insulin are known to be potent activators of the pathway (Kim, 2009). Therefore, the nutrient depletion found in the maternal uterine fluid which is sensed by the embryo by the mTOR pathway leads to compensatory mechanisms in order to promote embryo adaptation and survival to adverse environment. These compensatory mechanisms include an increased blastocyst TE endocytosis (Sun et al., 2014); increased TE proliferation and invasive behaviour by the time of implantation (Eckert et al., 2012) and an increased growth phenotype in late gestation and postnatally (Watkins et al., 2008a).

1.3.1 mTOR pathway

Mammalian target of rapamycin complex 1 (mTOR) is a serine/threonine protein kinase and a member of phosphatidylinositol kinase-related kinase (PIKK) family which

phosphorylates specific downstream effectors and in turn promotes overall cellular growth via the translation of specific populations of mRNAs (Gonzalez et al., 2012; Schmelzle and Hall, 2000). mTOR can form two different multiprotein complexes, mTORC1 and mTORC2, responsible for protein synthesis regulation necessary for cell growth and proliferation, but with different downstream targets and cellular effects (Hara et al., 2002; Kim et al., 2002; Sarbassov et al., 2004). mTORC1 consists of mTOR, Raptor, GβL and domain-containing mTOR-interacting protein (DEPTOR), and it is partially inhibited by rapamycin (Kim et al., 2002). It combines multiple signals to promote cellular growth during stress by indicating the availability of growth factors, nutrients and energy. Growth factors and hormones, such as insulin, recruit the phosphatidylinositol 3-kinase (PI3K) by binding the insulin receptor, thus activating Akt to signal mTORC1 which inactivates tuberous sclerosis complex 2 (TSC2) to prevent inhibition of mTORC1 (Sato et al., 2008). Active mTORC1 exerts several biological effects, including the activation of mRNA translation by phosphorylating crucial regulators of protein synthesis including 4E-BP1 and ribosomal protein S6 kinase (S6K), the suppression of autophagy through Atg13 and ULK1, ribosome biogenesis, and activation of transcription that leads to increased mitochondrial activity or adipogensis (reviewed in Zarogoulidis et al., 2014). Thus, mTORC1 suppression leads to the activation of 4E-BP1 and S6K repression which will supress mRNA translation (*Figure 1.5*). Amino acid sensing does not depend on the TSC complex, but it is carried out by Rag protein which regulates mTORC1 directly, which can in turn negatively affect the Akt activation (Manning, 2004).

mTORC2, which consists of mTOR, Rictor, GβL, Sin1, PRR5/Protor-1 and DEPTOR, promotes cell survival through the activation of Akt, regulating cytoskeletal dynamics by activating protein kinase C (PKC) (Jacinto et al., 2004). mTORC2 activity is not inhibited by rapamycin at least in a short time period (Sarbassov et al., 2004) and it is activated by growth factors such as insulin but not by nutrients.

AMPK is a highly conserved sensor of cellular energy status which is activated under conditions of low intracellular ATP, as occurs during nutrient deprivation or hypoxia (Gwinn et al., 2008). AMPK responds to energy stress by suppressing cell growth and biosynthetic processes, in part through its inhibition of the mTOR (mTORC1) pathway. AMPK phosphorylation of the TSC2 contributes to suppression of mTORC1 (Gwinn et al.,

2008) which could in turn down-regulate the phosphorylation of S6K and 4E-BP1, suppressing mRNA translation (*Figure 1.5*). Alternatively, energy stress could stimulate endocytosis thus internalising receptors from the plasma membrane including amino acids transporters (Feng and Levine, 2010). These would stop cell growth and division and prevent damage caused by the energy stress (Feng and Levine, 2010).

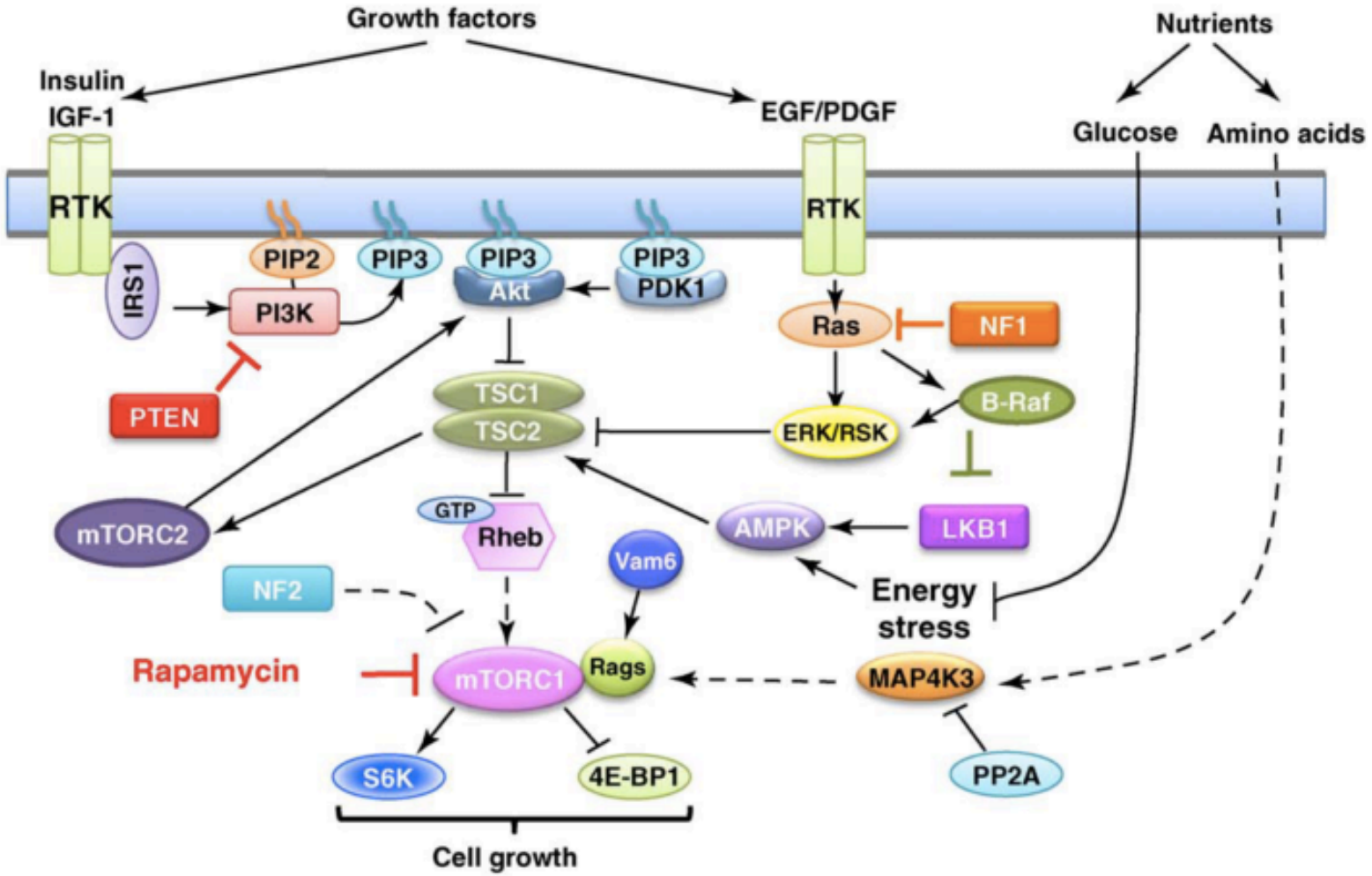

Figure 1.5 – Diagram showing a simplified mTOR pathway. (Mieulet and Lamb, 2010)

1.4 Endocytosis and Exocytosis

Endocytosis is a complex process by which cells take up components including fluid, nutrients, ligands and pathogens from the extracellular space while exocytosis describes the reverse process of releasing internal contents to the cell exterior. Endocytic and exocytic pathways are critical for cellular homeostasis, tissue function, and overall cell survival. These processes have been suggested to play a critical role in regulating the internalisation of extracellular nutrients, signalling molecules, pathogens and neuronal communications (Ivanov, 2008).

The endocytic pathways can be categorized as clathrin-dependent or clathrin-independent. Clathrin is composed by a 190 kDa heavy chain and two light chains with 25 kDa each, assembled into a triskelion (Royle, 2006). Clathrin-dependent endocytosis *(Figure 1.6)* involves the formation of vesicles coated with clathrin and it is primarily but not exclusively actin-independent. Similarly, the vesicles of the early exocytic pathway can be formed with participation of coat protein complex I and II (COPI and COPII, respectively). Specific coat proteins function to recruit different cargo as well as determine different intracellular destinations of the endocytic and exocytic vesicles.

Clathrin-independent endocytosis includes several internalization pathways that use an alternative protein coat or do not require a protein coat for the formation of endocytic vesicles (Ivanov, 2008). Clathrin-independent macro- and micropinocytosis, including apical epithelial surface internalisation of fluid, ligands and macromolecules, is clearly more actin-dependent than clathrin-dependent endocytosis and can be regulated through small GTPases including Ras homolog gene family, member A (RhoA) (Garred et al., 2001).

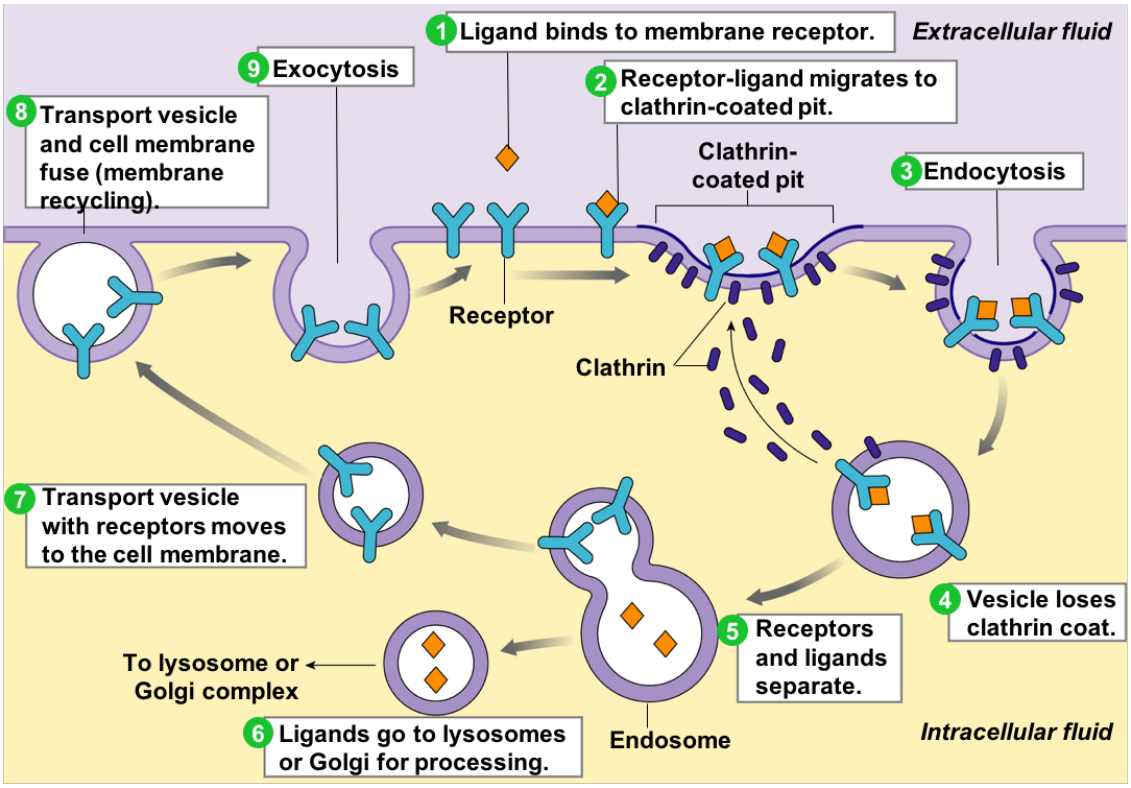

Figure 1.6 – Schematic representation of clathrin-dependent endocytosis. Copyright © 2007 Pearson Education, Inc., publishing as Benjamin Cummings.

1.4.1 Endocytosis in early developing embryos

Embryos developing *in vivo* take up protein, an indispensable element for growth and metabolism particularly in the earlier developmental stages, through endocytosis mechanisms. This has been supported by *in vitro* studies in several species which revealed endocytosis and lysosomal hydrolysis of extracellular tracers, including horseradish peroxidase, ferritin, bovine serum albumin (BSA), uteroferrin, and myoglobin (Pullar et al., 1990; Fleming and Pickering, 1985; Hastings and Enders, 1974; Schlafke and Enders, 1972).

Oocytes, zygotes and blastomeres in early developmental embryos contain clusters of pre-lysosomal endocytic vesicles (endosomes) distributed randomly in the cortical cytoplasm. From the 8-cell stage and continuing until early 16-cell stage, endosome distribution becomes progressively localized to the apical cytoplasm (Fleming and Pickering, 1985). At the late 16-cell stage, secondary lysosomes are formed and polarized to the basal cytoplasm (Fleming and Pickering, 1985) and the endocytic system becomes progressively more stable. At the blastocyst stage, the endocytic system is

mature and the TE, which is exposed to the uterine fluid, constitutes an exchange barrier between the ICM and the external medium (Assemat, 2005). *In vitro* studies have shown the influence of exogenous protein in the endocytosis uptake rate and further embryonic growth (Sun et al., 2014; Kaye and Gardner, 1999; Dunglison and Kaye, 1995), suggesting the protein and amino acid availability as an environmental signal sensed by early embryos with the capability of reprograming their development.

1.4.1.1 Endocytosis in the extra-embryonic lineages

The polarised endocytic and lysosomal system within the outer TE lineage of preimplantation embryos comprises megalin (or low density lipoprotein-related protein 2 - LRP2) and cubilin LDL-family receptors (Assemat, 2005; Gueth-Hallonet et al., 1996). Before VE formation, TE constitutes the single nutrient exchange barrier between embryo and environment. After implantation, the PE differentiates to form VYS, which is the sole functional interface between mother and foetus until the formation of the allantoic placenta (Jollie, 1990). Several experiments with radiolabelled macromolecules and proteins demonstrated that proteins are endocytosed by the VYS and hydrolysed into amino acids in the lysosome before being delivered to the embryo (Lloyd et al., 1998). This process is ATP and calcium dependent.

1.4.2 Endocytosis receptors

Megalin, a 600 kDa transmembrane protein, is a member of the LDLR (Low Density Lipoprotein Receptor) gene family that forms a complex and drives endocytosis of cubilin, a multi-ligand receptor, and its ligands (Assemat, 2005). Megalin and cubilin first appear at the 8-cell stage and are expressed by the TE and VE, localized at the apical pole of the cells exposed to the maternal environment (Assemat, 2005). The megalin/cubilin complex appears to be crucial for embryonic survival and normal growth, playing a critical role in protein, lipid and folate absorption (Assemat, 2005). Megalin receptor-mediated endocytosis is clathrin-dependent. With the formation of clathrin-coated pits, megalin internalises its ligands into endocytic compartments being subsequently recycled to the cell surface. Administration of anti-cubilin antibodies to the pregnant rat induces foetal malformations (Sahali et al., 1988) and disorganize the apical endocytic apparatus of the VE which affects the uptake of essential maternal nutrients (Le Panse et al., 1994).

1.4.3 Endocytosis and mTOR pathway

One of the targets through which mTOR regulates the cellular growth is endocytosis. In fact, in mammalian cells, mTOR localization to late endosomal and lysosomal compartments is involved in amino acid-induced mTORC1 signalling (Wang and Torbett, 2015) suggesting a mechanistic co-regulation between cell growth and cell catabolism (Settembre et al., 2013). Different mechanisms have been reported to stimulate endocytosis in response to mTOR signalling. Transferrin, for instance, is a nutrient receptor known to be upregulated by mTOR, thus facilitating nutrient uptake (Galvez et al., 2007).

The lysosome maintains cellular homeostasis and mediates several physiological processes, including cellular clearance, energy metabolism, lipid homeostasis, plasma membrane repair, bone remodelling, and pathogen defence (Settembre et al., 2012). All these processes require a dynamic and adaptive response of the lysosome to the environment, but how this response process occurs is not yet well understood. The cellular clearance process requires a coordinated action of hydrolases, acidification apparatus and membrane proteins (Settembre et al., 2013) to allow optimal lysosomal function in different environmental conditions, such as growth, starvation, infection, and intracellular accumulation of storage products (Settembre et al., 2013). It has become evident that the lysosome plays an important role in nutrient sensing and in signalling pathways that are involved in cell metabolism and growth. Autophagy is one of the cellular processes that cells use to preserve amino acids when these are depleted in the environment. In autophagy, double-membrane vesicles are formed around cytoplasmic proteins, protein complexes and organelles forming the autophagosomes, which are transported bi-directionally along microtubules (mediated by the motor protein dynein) and ultimately fuse with lysosomes, where their contents are degraded (Jahreiss et al., 2008).

In circumstances of extra- or intracellular stress and signals such as starvation and growth factor deprivation, mTORC1 is inactivated, releasing nutrient reserves through autophagy activation (He and Klionsky, 2009). Other studies showed that the level of amino acids accumulated in the lysosome lumen is responsible for mTORC1 docking on the lysosomal surface, which is a specific requirement for its activity (Zoncu, 2012).

When amino acids are depleted in the environment, lysosomal mTORC1 are translocated close to nuclei, driven by changes in intracellular pH (Korolchuk et al., 2011). In case of amino acid replenishment, lysosomes will be translocated to peripheral areas (close to the upstream signalling modules) facilitating mTORC1 stimulation (Korolchuk et al., 2011). This observation supports the idea that mTORC1 activity is dependent on the lysosome and clarifies why mTORC1 is reactivated upon lysosomal degradation of autophagic substrates (Yu et al., 2010). The discovery of a "lysosomal gene network" - the coordinated lysosomal expression and regulation (CLEAR) network (Sardiello et al., 2009) and its master gene transcriptor factor EB (TFEB) – member of the microphthalmia/transcription factor E (MiT-TFE) family - has revealed that lysosomal function can be coordinated to respond and adapt to different environments. TFEB interacts with mTOR on the lysosomal membrane sensing the lysosomal content. When nutrients are present, TFEB is phosphorylated by mTORC1, inhibiting its activity. However, mTORC1 inhibition upregulates TFEB by promoting its nuclear translocation (Settembre et al., 2012). Such dynamic changes in subcellular localization occur in response to various forms of cell stress, including nutrient fluctuations, and are mediated by changes in the phosphorylation of multiple conserved amino acids (Puertollano et al., 2018). Hence, TFEB acts both as a sensor of lysosomal content, when on the lysosomal surface, and as a promoter of lysosomal biosynthesis when in the nucleus (Settembre et al., 2012). This lysosome-to-nucleus signalling mechanism permits a lysosome auto-regulation of its function, through TFEB and mTOR interactions. Recently, TFEB was also shown to regulate the induction of protein synthesis via mTORC1 upon amino acid feeding after starvation or physical exercise. This effect is mediated by the transcriptional regulation of RagD GTPase and is important for an efficient mTORC1 recruitment to the lysosomal surface (Di Malta et al., 2017).

Interestingly, TFE3, another member of the MiT-TFE family, was also found to control lysosomal biogenesis and autophagy by regulating a gene network that largely overlaps with the one regulated by TFEB (Martina et al., 2015) suggesting that these two transcription factors play a cooperative role by regulating very similar sets of genes (Puertollano et al., 2018).

Furthermore, tumour protein p53 is another candidate associating cell growth with endocytosis regulation. p53 is responsible for cell-cycle arrest and apoptosis which

works together with mTOR to suppress cell growth in environmental stress such as nutrient deficiency. p53 senses the cellular stress which activates TSC2, thus inhibiting mTOR (Feng and Levine, 2010). Since p53 was reported to bind to specific gene promoters and to change histone acetylation status, it could be a promising candidate for epigenetic reprogramming embryo responses to the maternal uterine environment (Feng and Levine, 2010; Barlev et al., 2001). Epigenetic reprogramming is discussed in detail in 1.5.

1.4.4 Low protein diet and compensatory endocytosis

As discussed previously, the periconceptional period is considered a vulnerable period for the embryo, since environmental factors may cause permanent changes in the pattern and characteristics of development leading to risk of adult onset disease (Fleming et al., 2015, 2018). The embryonic endocytosis system, which functions as a primary contact between embryo and maternal fluid, was suggested to play an important role in embryo sensing and adaptation to the external environment. Sun et al. (2014) compared endocytosis in blastocyst (E3.5) extraembryonic lineages coming from two maternal diet treatments – Emb-LPD and NPD. The results showed alterations in both clathrin-dependent and -independent endocytosis at this early preimplantation stage regarding number and volume of endocytic vesicles. In the TE (intact blastocysts) and PE-like lineages [from embryoid bodies (EB) cultured from Emb-LPD / NPD mouse embryonic stem cell lines (mESCs)], there was an enhanced endocytosis in response to maternal Emb-LPD with increased uptake of endocytosed fluid and ligand and increased numbers of lysosomes. In fact, stimulated endocytosis was previously found to be up-regulated in mouse VYS of LPD (Watkins et al., 2008a), which derives from the PE. Interestingly, the increased passage number of mESCs for EB derivation did not alter this endocytic phenotype, suggesting this compensatory mechanism to be a heritable characteristic.

The mechanisms leading to stimulated endocytosis in blastocyst TE in this model probably derive from the nutrient levels within the immediate maternal tract environment or through indirect changes in factors regulating cellular behaviour mediated through the diet (Sun et al., 2014). Embryos cultured *in vitro* from early developmental stages (2-cell) to blastocyst or cultured for short periods at blastocyst in

a decreased concentrations of protein (BSA) show an increased endocytosis (Sun et al., 2014; Dunglison and Kaye, 1995). Interestingly, this endocytosis activation is sustained even after changing the culture by increasing the protein level. Again these characteristics are compatible with a compensatory model designed for long-term protection in response to nutrient restriction.

As reported by Eckert et al., (2012), BCAAs (leucine, valine and isoleucine) are depleted by ~30% in the maternal Emb-LPD uterine fluid and E3.5 blastocysts from the Emb-LPD model showed suppressed mTORC1 activity. 2-cell stage embryos cultured until the blastocyst stage in altered BCAA concentrations mimicking the Emb-LPD uterine fluid also showed stimulated endocytosis (Sun et al., 2014).

Megalin receptor has been reported to be up-regulated in the VYS of E17 embryos as well as in the TE from E3.5 blastocysts and PE from EBs from the Emb-LPD or LPD models at the protein level (Sun et al., 2014; Watkins et al., 2008). Furthermore, cubilin was found to be less expressed than megalin in the Emb-LPD model suggesting that it might be a limiting factor for the megalin-cubilin complex, thus contributing to a megalin compensatory effect (Sun et al., 2014).

1.4.4.1 Reprogramming of endocytosis pathway

As mentioned before, the uterine luminal fluid environment at the time of blastocyst formation in Emb-LPD mothers is depleted in BCAAs (Eckert et al., 2012) which are involved in the mTORC1 signal transduction pathway regulating cellular growth (Wang and Proud, 2009). Blastocysts from this LPD model show a reduction in mTORC1 signalling (Eckert et al., 2012). Reduced mTORC1 is known to be generally associated with increased autophagy in order to supplement nutrient supply for growth (Martina et al., 2012). However, there is no evidence of increased autophagy within Emb-LPD TE cells (Sun et al., 2014). Instead, the reduced availability of BCAAs led to reduced mTORC1 activation and increased activation of endocytosis in TE cells (Sun et al., 2014). However, other systems showed a positive correlation between reduced mTORC1 activity and suppression of different steps in early endocytic processing and nutrient uptake (Galvez et al., 2007; Tenay et al., 2013), which makes the association between reduced mTORC1 and increased endocytosis in the Emb-LPD model distinct. Therefore, mTORC2 emerges as a possible “bridge” between mTORC1 signalling of reduced nutrient levels via BCAA

availability in the LPD model and increased endocytosis (Sun et al., 2014). Unlike mTORC1, mTORC2 is not sensitive to rapamycin and functions primarily in cytoskeletal reorganisation (via PKC) and cell survival mechanisms in response to external stimuli and it also modulates the activation state of RhoA GTPase (Jacinto et al., 2004; Populo et al., 2012). Furthermore, the increased actin and surface RhoA in Emb-LPD blastocysts implicates nutrient sensing to stimulate endocytosis by this pathway (Sun et al., 2014). However, Sun el al (2014) showed that treatment with the exoenzyme C3 transferase - an inhibitor of RhoA (Aktories et al., 2005) - inhibited FITC-dextran endocytosis in Emb-LPD TE cells and also in NPD TE cells (but to a lesser extent), resulting in an equivalent level of internalisation across groups. This indicates that RhoA-mediated endocytosis is specifically increased in response to Emb-LPD but that other regulators of endocytosis also exist. Lastly, the increased motility and invasiveness phenotype showed by Eckert et al (2012) to occur in Emb-LPD trophoblast outgrowths was rapamycin-insensitive, suggesting mediation through mTORC2 cytoskeletal reorganisation to support implantation potential. Collectively, this suggests clathrin-independent endocytosis as the primary mechanism involved in the altered TE phenotype and leading to early compensatory mechanisms to protect nutrient provision and enhance survival.

The mTOR pathway is required to sustain glucose metabolism and glycolysis and is important in the transcriptional programme of glucose transporters and glycolytic enzymes. The GLUT family is regulated by insulin stimulation and it is considered as an effector of external nutrient environment crucial for development. Several studies reported a GLUT4 upregulation in offspring from restricted maternal nutrient environment. In fact, Muhlhausler et al., (2009) showed that lamb foetuses from LPD mothers, had GLUT4 downregulated in skeletal muscles but an increased expression after birth, compliant with the growth retardation *in uterus* and the later postnatal catch-up. Moreover, endocytosis in blastocysts is also known to be insulin sensitive (Dunglison and Kaye, 1995), however, since Emb-LPD reduces the maternal insulin level (Eckert et al., 2012), it is unlikely to be a contributory factor of enhanced endocytosis in this model. Since glucose transport is altered in response to the maternal environment, other mTOR targets might also be affected. Collinet et al., (2010) showed that enhanced expression of metabolic genes leads to increased endocytosis of nutrients, which reflects a compensatory response to a metabolic deficit. Thus, these maternal

environment alterations may affect the endocytosis system through epigenetic modifications caused by mTOR suppression during this developmental window.

1.5 Epigenetics in the developing embryo

The periconceptional period is considered an especially vulnerable period for programming since maturing gametes and early embryos may demonstrate persistent responses to environmental conditions due to the unique metabolic, epigenetic and developmental events associated with this reproductive stage, which may affect the later life phenotype, possibly promoting a clinical disease (reviewed in Fleming et al., 2018).

The term epigenetics refers to transmissible changes in gene expression without DNA sequence alterations, mediated by altered methylation of the DNA and remodelling of chromatin (Wolffe and Matzke, 1999). DNA modifications occur as cytosine methylation within CpG dinucleotides (cytosine followed by guanine) which is usually associated with transcriptional repression through blocking the binding of transcription factors (reviewed in Watkins et al., 2008b). In addition, the core histones forming the nucleosome can be subject to several post-translational modifications, which affect the access to the DNA for transcription factors (Kouzarides, 2007). DNA methylation and histone modification marks are thought to interact and confer heritability though still allowing plasticity and reversibility if necessary. The regulation of mammalian imprinted genes is an important epigenetic mechanism for growth regulation during gestation. These genes are marked by a cluster of methylated DNA and are only expressed from either maternal (expressed exclusively in growth-inhibiting genes) or paternal alleles (growth-promoting genes only) (Hanley et al., 2010). Imprinted gene expression is increased in extraembryonic tissues and there is a progressive upregulation during embryonic development (Zaitoun et al., 2010). In fact, preimplantation development (together with gametogenesis) is one of the most dynamic epigenetic reprogramming periods during mammalian life cycle. This period starts with fertilization with the paternal genome being demethylated while the maternal genome is progressively demethylated by lack of methylation maintenance (Borgel et al., 2010). During the early cleavage divisions, there is a loss of genome methylation although the imprinted alleles will retain their status. From the morula stage onward, the ICM undergoes extensive

remethylation which is mediated by the *de novo* DNA methyltransferase Dnmt3b (Watanabe et al., 2002).

The first lineage allocations in mouse occur early in development before implantation, under genetic control and it is thought that the first blastomeres will undergo lineage decisions based on asymmetries between transcription factor genes (reviewed in Ralston and Rossant, 2005). Torres-Padilla et al., (2007) showed that as early as the 4-cell stage, differential histone modifications exist between blastomeres, which act as a predictive factor of their respective lineage contributions. Overexpression of H3 methylation at specific arginine residues in individual blastomeres results in expression of specific transcription factors which predispose blastomeres to contribute to the pluripotent cells of the ICM, resulting also in a dramatic upregulation of Nanog and Sox2. In the morula ICM cells, Oct4 is highly expressed while outer cells are characterized by Cdx2, thus differentiating into TE. The second lineage separation takes place in the blastocyst ICM between epiblast cells expressing Nanog and the cells facing the blastocoel expressing Gata6, thus becoming PE (reviewed in Watkins et al., 2008b). Together, this suggests that epigenetic mechanisms occurring in this early developmental period could lead to changes in lineage allocation and further divergent development of the embryo, reinforcing the significance of this window of development as particularly vulnerable to environmental cues.

1.5.1 Epigenetic reprograming induced by low protein diet

The insulin-like growth factor (IGF) family has a major role in promoting growth during gestation and it is highly susceptible to environmental factors. In fact, there is accumulating evidence that different embryo culture conditions as well as altered maternal uterine environment induce changes in epigenetic status, such as reduced IGF-2 and H19 imprinting (Khosla et al., 2001).

A well-known example of epigenetic environmental regulation is the wild-type expression of the agouti protein which results in a phenotypic brown coat colour in the mouse. In this mouse model, Cooney et al., (2002) showed that maternal diet supplemented with methyl donors, can alter the phenotype of the agouti mouse, increasing the proportion of offspring with the wild-type agouti coat colour as compared to the offspring from mothers fed a standard diet. These findings suggest that the

maternal methyl donor diet leads to increased methylation and silencing of the offspring's retrotransposon, thus allowing the wild-type agouti promoter to be expressed. These results corroborate that maternal nutritional environmental exposure can change the stable expression of genes in the offspring through an epigenetic modification *in utero* (Simmons, 2011).

The environmental regulation of epigenetics in the offspring has been established by experiments in different animal species, and the maternal LPD model has been intensively studied. Maternal Emb-LPD in rats resulted in mild transient maternal hyperglycemia, reduced blastocyst cell numbers, gender-specific programming of imprinted gene expression, and altered postnatal growth and hypertension (Kwong et al., 2000; Kwong et al., 2006). A different study showed that when pregnant rats were fed LPD throughout pregnancy, offspring showed a reduced DNA methylation of the glucocorticoid receptor (GR) and peroxisomal proliferator activated receptor (Ppara)-α genes and increased their expression. However, folic acid supplementation could stop these effects (Lillycrop et al., 2005). Furthermore, GR hepatic promoter showed histone modification which facilitate transcription were increased in addition to DNA hypomethylation (Lillycrop et al., 2007). Intriguingly, DNA methyltransferase 1 (Dnmt1) was implicated in these epigenetic changes and hence metabolic phenotype because Dnmt1 expression was significantly reduced and its variation could explain variation in GR promoter methylation (Lillycrop et al., 2007).

In another example, Emb-LPD mouse embryoid bodies (EBs) were shown to grow to a larger size and to express reduced Gata6 transcription factor - regulator of PE differentiation - at mRNA and protein levels compared to control NPD (Sun et al., 2015). The same study showed a significant reduction in histone H3 and H4 acetylation and RNA polymerase II binding, all markers of reduced gene expression. Moreover, Denisenko et al., (2016) showed that maternal Emb-LPD and LPD treatments altered offspring embryonic somatic lineages (eg, liver, kidney) via epigenetic mechanisms. Here, diet restriction reduced ribosomal RNA production through increased methylation of the rDNA gene promoter, thereby limiting ribosome biogenesis and global protein translation during poor nutrient availability. Interestingly, upon lifting of the dietary challenge (eg, foetal or postnatal stages after Emb-LPD; postnatal stages after LPD), rDNA promoter methylation reduced, allowing rRNA production to increase beyond that

of control (NPD) levels, an over-compensation leading to catch-up growth and disease risk (Denisenko et al., 2016). This regulation of rDNA expression offers a molecular explanation of the phenotype concept of restricted growth during nutrient challenge and excess growth after release from challenge (Denisenko et al., 2016). Moreover, rDNA has also been found to be a genomic target for growth regulation in models of maternal high-fat or obesogenic diets (Holland et al., 2016). Additionally, in the rat Emb-LPD/LPD model, altered expression of imprinted H19 and/or IGF2 genes occurs in male blastocysts and foetal liver, further indicating an epigenetic basis for embryonic programming (Kwong et al., 2006).

1.6 Study models

1.6.1 LPD/NPD model

Our group have been using a maternal Emb-LPD (9% casein) substituted by a NPD (18% casein) for the remainder of pregnancy and postnatally as a model of early embryonic reprogramming. This diet was formulated by Professor Alan Jackson's laboratory in Southampton (Langley and Jackson, 1994) and has been used worldwide in rodent models of DOHaD. It is important to mention that the protein concentration in the LPD is a mild restriction and would be a suitable nutrient base for a non-pregnant rodent. Hence, the effects of the diet illustrate the potential variation across the normal range rather than an attempt to model starvation (Fleming et al., 2015).

Mouse blastocysts collected from Emb-LPD mothers and transferred into NPD fed recipients before and following the transfer exhibit enhanced foetal growth and caused excess weight and increased adiposity through to late adult life in female offspring (Watkins et al., 2008a), highlighting the importance of the periconceptional period for embryo reprogramming through the induction of compensatory mechanisms. Endocytosis in the extra-embryonic lineages (TE and PE) was also shown to be increased in the Emb-LPD model by evaluating the expression of markers and proteins involved in endocytosis using quantitative imaging (Sun et al., 2014). This overexpression is seen as a compensatory mechanism to promote adaptation and survival to the adverse nutritional environment. Therefore, this model becomes an excellent system to further

investigate how the endocytosis response to maternal diet is precisely induced and regulated at a cell biological level, which is one of the main goals of this project.

1.6.2 Human embryos model

It is recognized that lifestyle such as smoking, psychological factors, age and body mass index (BMI) are correlated with subfertility and IVF outcome (Klonoff-Cohen, 2005; Lintsen et al., 2005; Smeenk et al., 2001). Although several studies report a decreased clinical pregnancy rate associated with increased BMI (Van Der Steeg et al., 2008) and age (Leridon, 2004), there is no direct effect of age and BMI on the amino acid concentration of uterine fluid (Kermack et al., 2015). However, as in the mouse, the amino acid composition of the uterine fluid is significantly influenced by the diet (Kermack et al., 2015).

In clinical practice, embryo culture medium was first developed based on data from mouse embryo development (Gardner and Lane, 1998) whereby the nutritional content may not reflect the nutritive requirement of the developing human embryo (Kermack et al., 2015). Moreover, human embryo metabolism changes throughout development, thus the medium should reproduce the requirements of the growing embryo (Zollner et al., 2004). Before the 8-cell stage the metabolism of the early embryo is low and pyruvate is the major source of energy while glucose plays only a small role (Hardy et al., 1989). After the activation of the embryonic genome, the embryo needs more glucose while protein synthesis also increases (Hardy et al., 1989). The late preimplantation embryo additionally needs amino acids, vitamins and fatty acids (Quinn, 2014). Thus, it is possible that the inclusion of physiological concentrations of nutrients could further enhance the success of clinical IVF (Kermack et al., 2015). Different culture systems used in IVF laboratories have different compositions which may condition early embryonic development. Since the commercial companies do not divulge the exact composition of their media, it becomes difficult to study what might be responsible for different embryonic development outcomes (Zollner et al., 2004).

Animal studies have shown that culture media constituents are responsible for changes in foetal and birth weight of offspring (Velazquez et al., 2018; Ecker et al., 2004; Fernandez-Gonzalez et al., 2004; Khosla et al., 2001). In the human, a recent meta-analysis showed that children conceived by IVF and ICSI (intracytoplasmic sperm

injection) have a lower weight during the first 4 years of age, with a rapid growth afterwards (Bay et al. 2019). However, even though most culture media share the same basic components, the addition of extra supplementation, alterations in amino acid or carbohydrate compositions and/or concentrations and the lack of information on the exact amount of each component makes it difficult to compare different studies (Zandstra et al., 2015). Besides that, there are some additional difficulties in human studies compared with animal studies. For example, it is difficult to exclude the influence of other factors that might have evolved and changed over time - such as alterations in the culture conditions, including oxygen and temperature; technical procedures, such as the introduction of undisturbed extended embryo culture; hormonal stimulation protocols and altered population characteristics - and to define the relative influence of the different ART procedures. Moreover, it is also difficult to differentiate between effects mediated through parental infertility and the actual ART treatments (reviewed in Fleming et al., 2018). Nevertheless, there has been a progressive birth weight increase in IVF singletons over the past 25 years, which may reflect such changes in ART practice or procedures made overtime (Castillo et al., 2019).

The Dutch Famine studies emphasised that the exposure to suboptimal conditions during early development rather than later in gestation leads to large and long-term negative consequences for both mental and physical health (Roseboom et al., 2011), making compelling the research of these potential effects in IVF (Bloise et al., 2014). Despite the major technological advances in ART in the last decades, intense studies must be carried out to follow potential long-term complications that may only manifest over time, as the oldest child conceived with IVF was born only forty-one years ago (Wang and Sauer, 2006). Thus, identifying the major inductive factors that may initiate adverse embryo programming (such as BCAAs and protein levels in Emb-LPD mouse) and potential compensatory responses (such as enhanced endocytosis) occurring at this time will permit a preventative strategy to protect future health.

1.6.3 Aims

i. To optimise an *in vitro* culture protocol to analyse the effects of extrinsic metabolite factors on endocytosis in mouse preimplantation embryos at sub-cellular resolution and with quantitative imaging, thereby to model Emb-LPD programming.

ii. To identify specific environmental metabolites that activate endocytosis in mouse embryos.

iii. To identify how stimulated endocytosis in mouse embryos is regulated at cellular and molecular levels.

iv. To investigate if stimulated endocytosis occurs in human blastocysts and whether the endocytosis phenotype associates with particular maternal demographics.

1.6.4 Hypothesis

A combination of amino acids and/or insulin depletion *in vitro* is responsible for activation of compensatory endocytosis in preimplantation mouse embryos. The developing embryo senses nutrient depletion by the mTOR pathway, activating compensatory mechanisms in order to promote embryo adaptation.

1.6.5 Long-term vision

This project aims to determine the mechanistic basis and precise induction conditions that activate a stimulated endocytosis phenotype in mouse preimplantation embryos and whether such a phenomenon occurs in the human. Since activation of stimulated blastocyst endocytosis has been shown to be an early marker of adverse developmental programming induced by poor maternal diet, a long-term vision will be to supplement maternal diet and/or IVF culture media to suppress this condition and to protect the health of offspring.

Chapter 2 General Methods

2.1 Animals

MF1 mice used in this study were kept under a UK Home Office project license (PPL 30/3001 held by Professor Tom Fleming and Personal Licence IC326AA53) and standard animal housing conditions in accordance with the Animals (Scientific Procedures) Act of 1986 and associated Codes of Practise. Mice were bred in-house (University of Southampton Biomedical Research Facility) on a 07.00 to 19.00 h light cycle, fed with standard chow. Cages contained wood chip bedding, shredded paper for nesting and, for environmental enrichment, a crimson Perspex nesting house and compressed cotton wool pellets. The room temperature was 20.5 ± 2°C and humidity 50-55%. Non-superovulated, chow-fed MF1 virgin females aged 7 to 9 weeks were naturally mated overnight with MF1 males (aged 2.5 to 8 months – optimal mating age) and plug checked (presence of copulation plug) to detect a successful mating the following morning. The mating period takes variable time (usually between 1 to 4 days), depending on the female oestrus cycle stage (unknown). Matings were spaced a minimum of 5 days apart between experiments and plug-positive females were considered to be on E0.5 at 14.00 h on the day the vaginal plug was detected. Plug positive females were transferred to individual cages and culled the next day for embryo collection (E1.5) or later depending on the experimental design.

2.1.1 Mouse embryo collection

Mice were culled by cervical dislocation and embryos were collected at different time points of preimplantation development following reproductive tract dissection. Oviducts and uterine horns were placed in warm (37 °C) saline solution (BR0053G, OXOID, UK) and then transferred to an empty petri dish where they were gently flushed under a stereomicroscope (Wild Heerbrugg, Germany) with 1 ml of pre-warmed H6 medium supplemented with 4 mg/ml bovine serum albumin (BSA), (A3311, Sigma-Aldrich, UK) (H6BSA – *appendix 8.2.1.*) or 6 mg/ml Polyvinylpyrrolidone (H6PVP) (Sigma-Aldrich, UK) using a 30G needle. 2-cell stage embryos (at E1.5) and blastocysts (at E3.5) were flushed from the oviduct and uterine horns, respectively.

2.1.2 Mouse embryo culture

Embryos collected at E1.5 were cultured in 30 μl drops of potassium simplex optimized medium (KSOM) (*Appendix 8.2.2.*) in a 6 cm petri dish (Sterilin) submerged in embryo tested mineral oil (M8410, Sigma, UK) to develop to later stages at 37°C and 5% CO_2. For *in vitro* culture experiments the medium contained different concentrations and combination of BCAAs (leucine, valine and isoleucine) and insulin in KSOM (*Appendix 8.2.3.*) with omitted BSA. To remove H6BSA medium, embryos were washed three times in their respective culture medium before *in vitro* culture.

2.2 Patients

Wessex Fertility is an IVF clinic in Southampton with over 15 years experience and over 5,000 assisted conception cycles per annum. The clinic provided us with frozen (slow and vitrified) embryos. Collection and analysis of human embryos was carried out with written informed consent from all patients under HFEA licence number R0142 given to the Centre for Human Development, Stem Cells and Regeneration, University of Southampton. All frozen embryos have an expiry date and all experiments on live embryos must be completed before that date which was adhered to throughout the project.

2.2.1 Human embryo thawing and culture – Slow frozen embryos

0.5M Sucrose Thawing Medium with 12 mg/mL Human Serum Albumin (STM) and 0.2 M Sucrose Thawing Medium with 12 mg/mL Human Serum Albumin (Origio, Quinn's Advantage Thaw Kit ART 8016) covered with mineral oil (Sigma) were calibrated at 37°C in a 4-well dish (60 mm NUNC culture dish). Slow frozen embryos kept in straws in liquid nitrogen were collected and pulled down from the straw to the centre of the 4-well dish. Using 300 μm (Cook, K-FPIP-1300-10BS-5) or 170 μm (Research Instruments, 7-72-2170/5) flexipet pipettes, embryos were first transferred to the 0.5 M STM and incubated for 10 minutes and then to the 0.2 M STM for 10 minutes at 37°C. Drops (40 μl) of Sage 1-step™, with HSA and phenol red culture medium (Origio, 67010010) in a 6 cm dish and covered with mineral oil (Origio, Oil for Tissue Culture ART-4008) were previously calibrated overnight (37°C) and the embryos were then transferred to the

drops and incubated at 37°C with 5% CO_2 and 5% O_2 in order to develop to blastocyst stage.

2.2.2 Human embryo thawing and culture – Vitrified embryos

0.5ml of thawing solution (Irvine Scientific, Vit Kit®-Thaw 90137-SO) was calibrated at 37°C in a 4-well dish (60mm NUNC culture dish) inside the class II hood heated stage for a minimum of 5 minutes after the vitrification thaw kit warmed at room temperature for 5 minutes. A 40µl drop of dilution solution (Irvine Scientific, Vit Kit®-Thaw 90137-SO) and two 40µl drops of wash solution (Irvine Scientific, Vit Kit®-Thaw 90137-SO) were placed in a properly labelled 60mm culture dish placed on the non-heated area of the stage. Vitrified embryos kept in HSV straws in liquid nitrogen were pulled down from the Dewar to the warming dish (thawing solution) within 2 seconds and left for 1 minute. With 300µm (Cook, K-FPIP-1300-10BS-5) or 170µm (Research Instruments, 7-72-2170/5) flexipet pipettes, embryos were then transferred to the dilution medium at room temperature for 4 minutes followed by 4 minutes in washing solution drop 1 and 4 minutes in drop 2. Drops (40µl) of culture medium Sage 1-step™, with HSA and phenol red culture medium (Origio, 67010010) in a 6cm dish and covered with mineral oil (Origio, Oil for Tissue Culture ART-4008) were previously calibrated overnight (37°C) and the embryos were then transferred to the drops and incubated at 37°C with 5% CO_2 and 5% O_2 in order to develop to blastocyst stage.

2.3 Embryo whole-mount immunocytochemistry

Appendix 8.3 contains all the protocols for the preparation of solutions used and the full protocols for immunocytochemistry. After collection, culture or endocytosis assay (described in the next chapter), mouse embryos were treated with pre-warmed Tyrode's Solution pH 2.5±0.3 - (T1788, Sigma-Aldrich, UK) (37°C) in a cavity block (under the dissecting microscope) until the zona pellucida was removed (around 30 seconds). Embryos were then rapidly washed and kept in H6BSA medium at 37°C for 2 hours and fixed in 1% formaldehyde (Sigma) in PBS for 20 minutes. In some experiments (when mentioned), the zona was left on, thus the previous steps were skipped. During the fixation period, immunocytochemistry chambers were prepared. These comprised steel washers (M6 x 40 mm penny washers – Farnell UK, 2506031) attached with commercial

superglue to a pre- acid washed (1 M HCl, Sigma-Aldrich, UK) 22 mm coverslip (Thermo Scientific). Washers with coverslip attached were washed 3 times in PBS followed by 20 minutes in 2.5 mg/ml Poly-L-Lysine hydrobromide (P8954, Sigma-Aldrich, UK) in PBS on a hot plate (37°C) to make inner coverslip surface adhesive to embryos, the solution was then removed and replaced by PBS and further washed again in PBS. After fixation, embryos were transferred to the chambers (with PBS) by pipetting under the microscope. Embryos attached to the bottom coverslip and were then treated with 0.25% Triton-X-100 (Sigma-Aldrich) in PBS for 15 minutes in order to permeabilize the cells, to allow penetration of the antibodies, followed by washing in Tween-20 (Sigma-Aldrich) 1:1000 in PBS (PBS-T). Then embryos were treated with 2.6 mg/ml NH_4Cl (Sigma-Aldrich) in PBS for 10 minutes to block free aldehydes, thus preventing/reducing fixative-induced autofluorescence. Embryos were then washed 3 times (5 minutes each) in PBS-T before being incubated with the primary antibody (diluted in PBS-T) overnight at 4°C. The following day, embryos were washed with PBS-T (3 times for 10 minutes each) and then incubated with the secondary antibody for 1 h at room temperature which was then removed by washing in PBS-T (3 times for 10 minutes). DAPI (Invitrogen) was diluted in PBS-T (0.2 μg/ml) and was used as a nuclear counterstain. After 20 minutes' incubation with DAPI, embryos were washed 3 times in PBS-T. Finally, 20 μl Citifluor (an anti-fading agent) dissolved in PBS (Agar AF3 PBS solution) was added to the chamber well and a coverslip (Thermo Scientific - 18 mm, 0.13-0.16 mm) was applied on the top and sealed with nail varnish.

Antibodies used for immunolabelling were: rabbit polyclonal anti E-Cadherin (generated in house to mouse E-cadherin GST fusion protein; 1:250), rabbit polyclonal anti transcription factor EB (TFEB) gene 7942 (A303-673A-T Bethyl Laboratories; 1:50), mouse monoclonal to megalin (Protein G purified, 1:400) (Meads and Wild, 1993) and rabbit polyclonal anti clathrin (Cell Signaling P1663, 1:400); Secondary antibodies were: Alexa Fluor 568 Goat anti-mouse (ab175473, Abcam), Alexa Fluor 488 Donkey anti-rabbit (ab150073, Abcam) and Alexa Fluor 647 Donkey anti-rabbit (ab150075, Abcam) (1:300). Negative controls were included by omitting the primary antibody.

2.4 Confocal microscopy image capture and analysis

A Leica SP5 was used for image capture and the VOLOCITY 6.3 (PerkinElmer) 3D software to analyse the data. VOLOCITY is an innovative, high performance 3D imaging software product designed specifically for Life Science research. It allows the visualization and analysis of multi-channel 3D volumes, based on their intensity.

Control and immunolabelled embryos were either scanned (i) using several xy optical sections at 1 μm intervals to generate a z-series corresponding to half embryo (the half closest to the coverslip) or (ii) only on the surface closest to the coverslip (50-60 xy sections at 0.15 μm intervals to generate a z-series range of the TE layer attached to coverslip – known as high resolution assay). In this last approach, measurements were made in individual cells - 1 to 3 TE cells per embryo. These embryos were also stained with CellMask^{TM} Deep Red (Thermo Fisher Scientific, Molecular Probes - C10046) for 1 h at room temperature after fixation (1:200), which is a plasma membrane stain, in order to label the cell boundaries and to crop them (using the VOLOCITY software) to make measurements on individual TE cells. Cell numbers were determined by nuclear staining (DAPI). The second half of the embryo farthest from the coverslip was not included due to the reduced confocal signal and to maintain reliability of results. A VOLOCITY protocol (described in *2.4.1* and A*ppendix 8.4)* was created for each individual labelling protocol based on vesicles/structures sizes and the same protocol applied to all embryos in different treatment groups.

2.4.1 VOLOCITY protocol

VOLOCITY 6.3 (PerkinElmer) is a software that converts fluorescent signals into measurable 3D structures. There are several configurations in the programme that can (and should) be altered in order to create the most appropriate protocol to what is being studied and to minimise programme pitfalls. One useful tool is to exclude objects by size, thus decreasing the chance of counting nonspecific signal. Furthermore, the intensity threshold (which defines the percentage of signal regarded as being specific or not by setting a background threshold) must be set the same for all embryos in order to obtain comparable results across treatments. “Normalisation” was set in the Image Acquisition control of the confocal microscope so that all embryos were imaged based on having a

minimal saturation point. The first step in the data analysis is to select the number of channels each image has and alter the image size in x, y and z orientations. This information can be obtained in the *lif* file saved during image acquisition using the Leica LAS AF software.

After designing and optimising the VOLOCITY protocol, it was saved and performed without any further alterations for all embryos, thus avoiding any bias. Changing these settings between embryos or treatments would mean individual and incomparable feedback per embryo. The optimised protocol consisted of:

1. Crop cell (for TE high resolution approach only)

2. Find object (based on channel) – red channel for LysoTracker Red or MagicRed™; green channel for BSA-BODIPY, LysoTracker Green or FITC-Dextran

3. Remove noise from objects (fine filter)

4. Separate touching objects (by 2 µm)

5. Exclude objects by size: chosen based on the literature, according to Tsichlaki and Fitzharris, (2016) the blastocyst nuclei size is 690±20 μm^3 while a lysosome size range between 0.1 – 1.2 µm diameter (Kuehnel, 2003)

   5.1. vesicles <0.01 μm^3 and > 20 μm^3

   5.2. nuclei < 150 μm^3

6. Nuclei – fill holes in objects

7. Objects of interest were selected by automatic threshold using an offset of 50%.

8. Measure distance from vesicle centre to nucleus edge (TE).

9. Object data were exported to Excel for analysis.

Using these settings, VOLOCITY was used to calculate number and volume of labelled vesicles (combined total volume and mean individual vesicles volume) and nuclei, and to measure the distance from the vesicles centre to the nucleus edge (in individual TE

cells). A*ppendix 8.4* contains screen shots images “step-by-step” to perform the optimised protocol in VOLOCITY 6.3.

2.5 Single embryo RNA extraction and reverse transcription reaction

2.5.1 RNA extraction

After culture, blastocysts were washed through three 50 µL PBS drops supplemented with 1 % of Polyvinyl-pyrrolidone (PVP). For qPCR assay, embryos were transferred individually into nuclease-free thin walled non-stick tubes in a minimal volume (< 1 µL) and immediately snap frozen on dry ice prior to storage at -80°C.
Poly A+ RNA was extracted from single blastocysts using the Dynabeads mRNA direct kit (Invitrogen). Poly-A tail, a long chain of adenine nucleotides, is added to the mRNA to increase its stability during RNA processing.

Individual embryos (previously stored at -80°C) were lysed in 150 µL lysis buffer for 10 minutes at room temperature. Meanwhile, Dynabeads were washed twice in lysis buffer using the magnet (1:1 Dynabeads to buffer). 10 µL Dynabeads were added to each embryo, gently mixed and roller-incubated for 10 minutes at room temperature. After incubation, bead-mRNA complex was concentrated by a magnet, its supernatant was removed and placed on dry ice immediately and stored at -80 °C (to be used later for DNA extraction – *2.7*). Beads were washed twice with Buffer A and three times with Buffer B before being resuspended in 10 µL nuclease-free water (Fisher, UK). For the elution step, tubes were incubated in a heating block at 65 °C for 2 minutes, and placed immediately on ice in the magnet. The supernatant was removed and used for reverse transcription reaction.

Due to the small amount and volume of RNA of the final elution, RNA was not quantified or assessed by electrophoresis gel. However, previous quantification using Nanodrop with single blastocyst showed less than 1 ng of RNA per µl.

2.5.2 Reverse transcription (cDNA synthesis)

For cDNA conversion, immediately after RNA extraction, 8 µL RNA elution (with 3 µL nuclease free water) were used for sample, while the remaining 2 µL (with 9 µL nuclease free water) were used for a negative control of reverse transcription (RT-). Reverse

transcription was performed by adding the previous RNA (or negative control) to a previously made mastermix composed by: 1 µL 10 mM Deoxynucleotide Triphosphates (dNTPs) mix (U1240, Sigma-Aldrich, UK), 1 µL Random Nonamers (50 µM) (R7647-100UL, Sigma-Aldrich, UK), 4 µL Buffer Reverse Transcriptase (5x reaction buffer, M531A, Promega, UK) and 5 µL nuclease-free water in thin-walled, nuclease-free tubes. This mastermix was mixed and incubated at 70°C for 10 minutes in a controlled heat block and immediately chilled on ice before adding 1 µL M-MLV Reverse transcriptase enzyme (200 units) (M1705, Promega, UK) to the sample or nuclease free water to the negative control. This negative control allows the detection of genomic DNA during quantitative PCR (qPCR). The samples were then incubated at 21°C for 10 minutes (annealing), followed by 50 minutes at 37°C (extension) and 90°C for 10 minutes (reverse transcriptase inactivation) using the Thermal Cycler (MJ Research Tetrad 2 with 4 blocks, Marshall Scientific, US). Prepared blastocyst cDNA products were diluted until 65 µL with nuclease free water to be used in qPCR and were stored at -20°C. *Table 2.1* summarises the components used for reverse transcription.

Components	Supplier	Volume (per embryo)
Deoxynucleotide Triphosphates (dNTP's) 10 mM- U1240	Sigma-Aldrich, UK	1 µL
Random Nonamers 50 µM - R7647-100UL	Sigma-Aldrich, UK	1 µL
Buffer Reverse Transcriptase (5x reaction buffer) - M531A	Promega, UK)	4 µL
Nuclease-free water	Fisher, UK	5 µL
M-MLV Reverse transcriptase enzyme (200 units) - M1705	Promega, UK	1 µL

Table 2.1 – Components used for reverse transcription.

2.6 Polymerase chain reaction (PCR)

2.6.1 Single embryo quantitative real-time PCR (qRT-PCR)

For qRT-PCR, product amplification took place in the CFX96TM Real-Time System/C1000TM Thermal Cycler (BioRad, UK) and was analysed with Opticon Monitor v3.1 software. Each lyophilised primer mix vial (forward and reverve primer mix; PrimerDesign, UK) was diluted in nuclease-free water according to the manufacture's handbook.

All reactions were run in duplicate, using low profile, non-skirted, clear 96-well plates (Starlab), and for each reaction standard curve points and no template controls (NTC) – water samples - were included. As controls, RT- samples were also tested to confirm absence of genomic DNA.

All the assays were performed using SYBR Green in a volume of 10 µL, using 5 µL 2x Quantifast SYBR Green (204054, Quiagen, UK), 1 µL primer mix (forward and reverse) and 4 µL blastocyst cDNA. SYBR green is a dye-based fluorescent labelling method that enables the quantification and collection of data as it intercalates with every new copy of dsDNA molecule. The fluorescence is measured in each cycle and increases as the PCR progresses. Therefore, the fluorescence intensity is proportionate to the number of dsDNA copies formed.

The amplification programme used included enzyme activation at 95°C for 5 minutes, followed by 40 cycles of denaturation at 95°C for 10 seconds, annealing at 60°C for 40 seconds, and a final extension step at 72°C for 10 minutes. Melting curves were generated for each sample to confirm target-specific amplification (verification of a single product for each run) by fluorescence detection between 60°C and 90°C at 0.1°C, holding for 2 seconds before the programme ended and was maintained at 4°C until the plates were retrieved from the machine. Specific product amplification was determined by the generation of a single peaked melting curve (*Figure 2.1*). RT- and NTC controls should not show any amplification. If there is amplification but the melting curves do not coincide with positive targets' curves, they may be ignored. If the melting curves and melting temperatures coincide, then the Ct values of these negative controls should be at least 10 Ct values less than the samples.

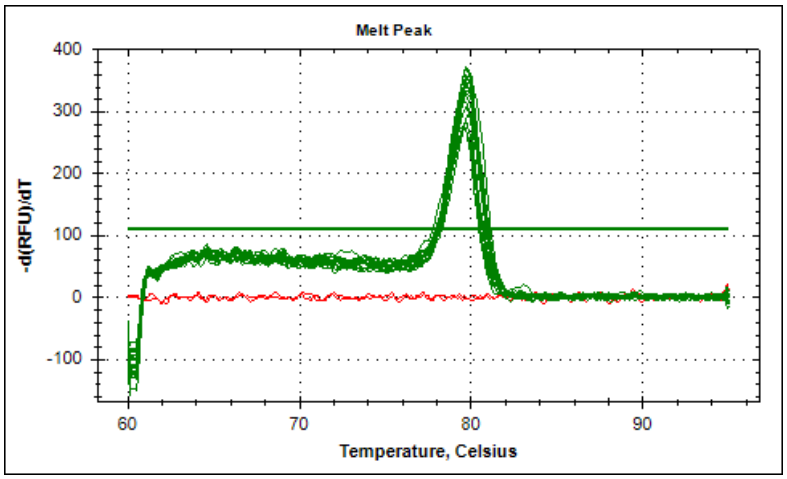

Figure 2.1 – Melting curve example. Specific amplification of the target (megalin) by SYBR Green. The presence of a single peak (green) is interpreted as the amplification of one single product. The plain expression of the NTC samples (red) confirms no presence of contamination of the reaction. Green – cDNA samples; red – NTC controls.

Data was saved from the Opticon Monitor and plates were kept in the fridge at 4°C protected from light. Agarose gel electrophoresis was done after qPCR in order to check the presence of the correctly sized amplicon (*see 2.6.3*).

For each gene of interest, the standard curve analysis method (described in *2.6.4*.) was used to measure relative changes in gene expression.

Table 2.2 shows the list and sequences of primers used for single blastocyst gene expression.

Gene		Sequence (5'-3')	PCR product size
H2afz*+	For Rev	'ACAGCGCAGCCATCCTGGAGTA' 'TTCCCGATCAGCGATTTGTGG'	202 bp
Ppib*	For Rev	'TTCTTCATAACCACAGTCAAGACC' 'ACCTTCCGTACCACATCCAT'	92 bp
Sdha*+	For Rev	'TGTTCAGTTCCACCCCACA' 'TCTCCACGACACCCTTCTGT'	66 bp
Tbp*	For Rev	'GGGAGAATCATGGACCAGAA' 'GATGGGAATTCCAGGAGTCA'	90 bp
Tuba*	For Rev	'CTGGAACCCACGGTCATC' 'GTGGCCACGAGCATAGTTATT'	114 bp
Megalin$^{\Delta}$	For Rev	'CAATGGAGGATGCAGCCATATCT' 'GTGTGGACACTGGCACTCAG'	64 bp

Gene	Supplier
Ctsb$^{\Delta}$	PrimerDesign
Lamp1$^{\Delta}$	PrimerDesign
Vps18$^{\Delta}$	PrimerDesign

Table 2.2 – List of primers for qRT-PCR used for blastocyst samples. As no DNAse treatment was performed in these samples (due to the small concentration of RNA per sample) and to ensure no DNA amplification, all primers were designed as span-exon/intron boundary. * Potential reference genes well expressed in mouse blastocysts used for GeNorm. + Selected reference genes according to Genorm. $^{\Delta}$Target genes. Ctsb, Lamp1 and Vps18 were designed by PrimerDesign.

2.6.2 Selection of reference genes (geNorm)

Reference or house-keeping genes are invariant endogenous controls that remains consistent in expression across experimental conditions. They are expressed in all cells of the organism under normal (control) or patho-physiological (experimental) conditions. Therefore, these unaltered genes are used to correct for sample to sample variations in mRNA levels from different samples within a given experiment.

To identify the best reference genes, a set of five potential reference genes were run in a qPCR with five samples per group (control and treatment). These genes were: H2A

Histone Family Member Z (H2afz), Peptidylproyl Isomerase B (Ppib), Succinate dehydrogenase complex, subunit A (Sdha), TATA-Box-Binding protein (Tbp) and Tubulin Alpha (Tuba).

Reference gene stability was determined using Biogazelle qbase+ 3.0 (Biogazelle, Belgium), a relative quantification software. geNorm analysis is based on geNorm M and V values. The M value indicates the average expression stability value of remaining reference genes at each step during stepwise exclusion of the least stable reference gene. The optimal number of reference genes is calculated according to the geNorm V (variation) value (geNorm V < 0.15). This value represents the pairwise variation between two sequential normalization factors containing an increasing number of genes (Vandesompele et al., 2002). Out of five candidate genes, four genes showed a high average expression stability of low M value (M < 0.5). Figure 2.2A shows the M values for the five tested genes, ranking from the least to the most stable gene (left to right). The optimum number of reference genes for the current experiment was two, calculated by V2/3 (normalising factor < 0.15) (Figure 2.2B). Therefore, Sdha and H2afz (lowest M values) were identified as the most stable reference genes.

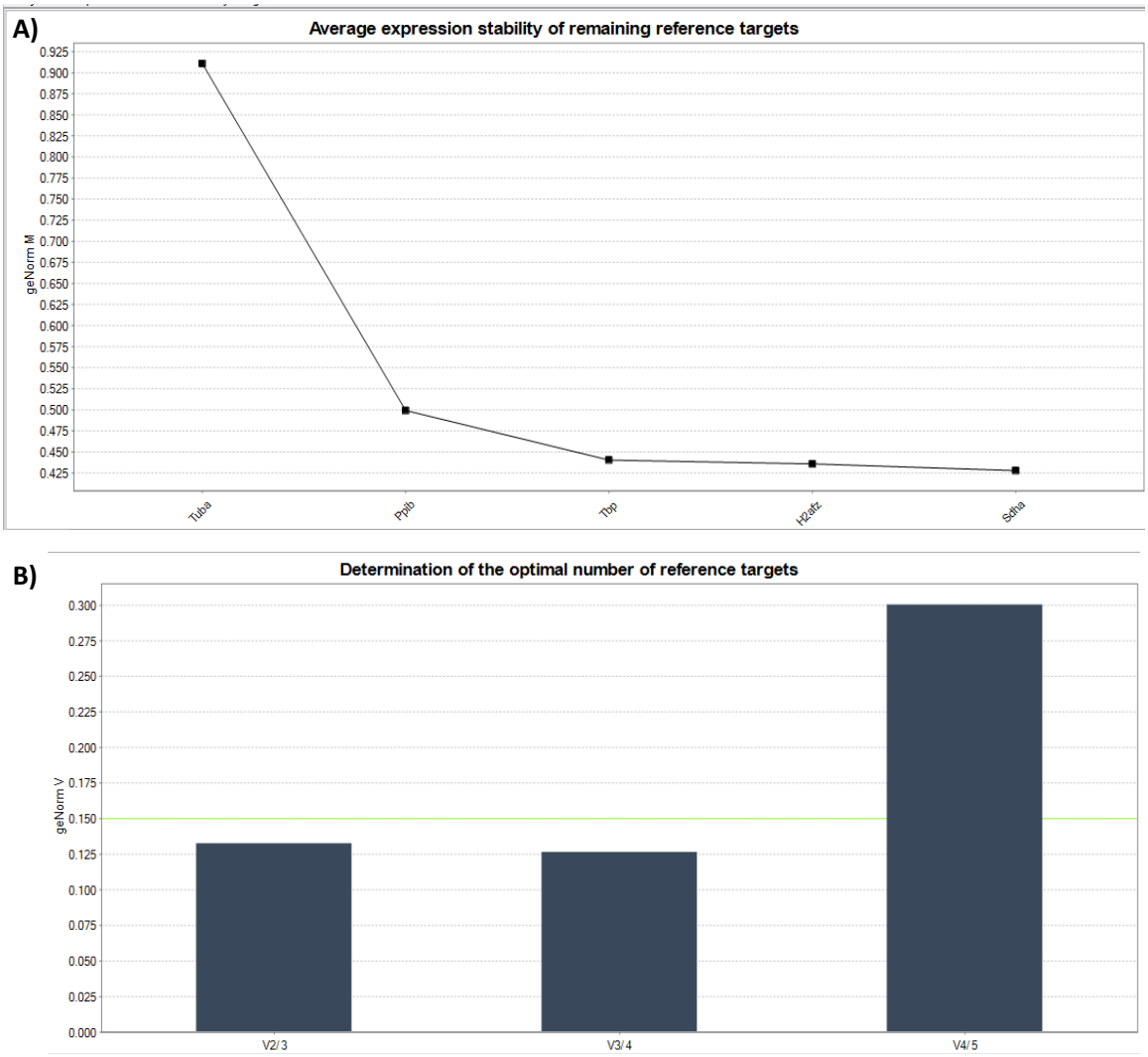

Figure 2.2 – GeNorm output for reference gene targets analysed for male blastocysts (cultured in L-ISO/N-INS medium from 2-cell until blastocyst stage). A) geNorm analysis showing average gene expression stability M. M was calculated by comparing average pairwise variation of expression between 5 target reference genes (x-axis). Genes with highest reference target stability (average geNorm, M ≤ 0.5) are shown on the right most side on the x-axis and were selected for normalisation. B) Shows optimal number of reference genes selected for normalisation. geNorm V is less than 0.15 when comparing a normalisation factor based on the 2 or 3 most stable targets and suggests that no more than 2 genes are required for accurate normalisation, therefore the optimal number of reference targets is 2 (H2afz and Sdha).

2.6.3 Qualitative analysis of PCR products

Amplified DNA products were separated by gel electrophoresis with 2% agarose gel in 1X TBE (100 mM Tris base, 100 mM Boric acid, 2 mM EDTA (disodium salt), pH 8.0) buffer. 3 g agarose was diluted in 150 ml 1x TBE buffer. The gel-buffer solution was microwaved for 3 minutes (with occasional stirring) until a clear solution was obtained. 15 μl ethidium bromide (500 μg/ml) was added to the solution followed by 15 seconds in the microwave. The solution was poured into the electrophoresis chamber and left to solidify for 30 minutes. The chamber was filled with 1X TBE buffer (running buffer). Stored samples (duplicates were mixed into one well – 20 μl total) were mixed with 5 μl gel loading solution (Sigma, G2526-5ML) and loaded onto subsequent wells (25 μl/well). 6 μl of 100 base pair (bp) ladder (Promega, G210A) was added in some lanes. The gel was then run for 1.5h at 130 V and immediately visualised under ultraviolet (UV) light using a UV camera. *Figure 2.3* shows a representative agarose gel electrophoresis image of PCR products of selected target genes.

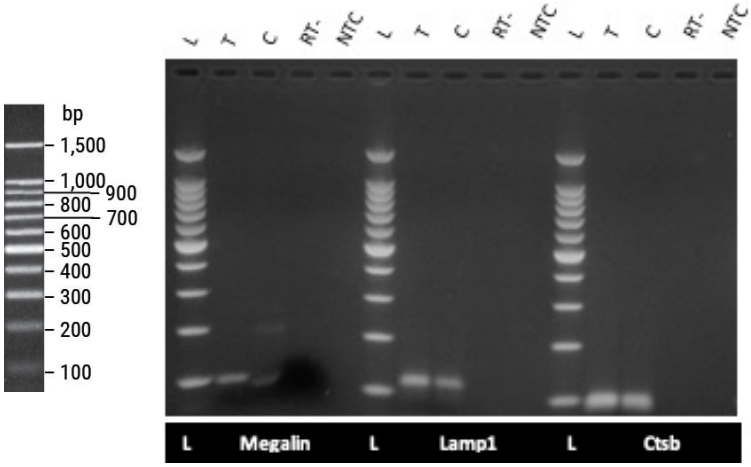

Figure 2.3 - Representative images of PCR products in 2% agarose gel electrophoresis. PCR products for selected target genes (Megalin – 64 bp, Lamp1 and Ctsb). For each gene, 100bp ladder (L), treatment (T) and control (C), RT- and NTC samples were loaded. Size bands of the ladder are shown on the left.

2.6.4 Quantification of gene expression by standard curve method

Standard curve method was used to quantify gene expression in blastocysts. RNA was extracted from non-treated/E3.5 blastocysts and converted to cDNA, pooled and diluted 2-fold 5 times generating six serial dilutions. These were run in duplicates for every assay performed (in the same 96-well plate). Due to the small amount and volume of RNA, it

was not quantified; thus, we assumed a theoretic concentration of 1 for the initial most concentrate dilution. *Figure 2.4* shows an example of standard curve for target gene Lamp1. With the average Ct values and the known concentration of each point, a graph with a trend line and R-squared (R^2) - coefficient of variance between replicates at a single concentration - is generated (*Figure 2.4*). The interpretation of the equation allows to define the efficiency of the primers. The line slope suggests the efficiency of the assay – slopes between -3.1 and -3.6 are considered acceptable (90 and 110% efficient, respectively). This represents an efficiency (E) of 92.54% for the example represented in *Figure 2.4* (slope of -3.5146) calculated by the equation $E = -1+10(^{-1/slope})$.

Furthermore, using the equation from the plot, new values per sample can be calculated considering the efficiency of the equation. Quantity = $10^{(ct-b)/m}$, where b is the interception (28.678 in *Figure 2.4*) and m is the slope (-3.5146 in *Figure 2.4*) of the linear regression.

EMB STD	[]theoretic	Log []	Ct1	Ct2	Average Ct	Standard Deviation (SD)
A	1	0	28,73	29,6	29,17	0,62
B	0,5	-0,301029996	29,49	29,74	29,62	0,18
C	0,25	-0,602059991	30,36	30,9	30,63	0,38
D	0,125	-0,903089987	31,46	31,13	31,30	0,23
E	0,0625	-1,204119983	32,55	32,59	32,57	0,03
F	0,03125	-1,505149978	34,64	34,69	34,67	0,04

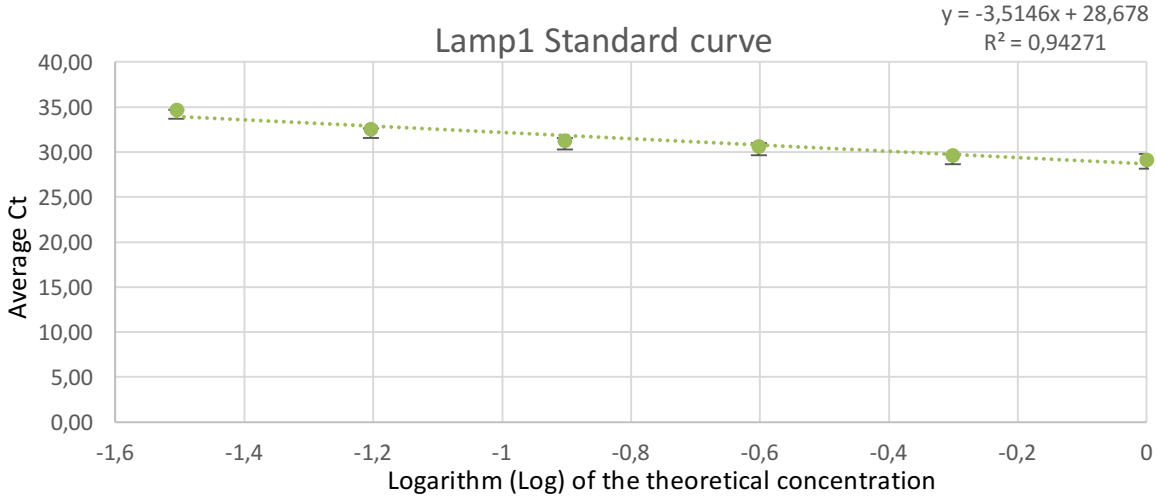

Figure 2.4 - Example of standard curve graph of Lamp1 using the logarithm (x-axis) of the theoretical concentration of six points of serial dilutions of cDNA (from blastocysts pooled together) against the Ct values of each point (y-axis). Equation and R^2 are displayed on the top right of the graph, showing a slope of -3.5146 (92.54% efficiency). Error bars showing SD.

2.7 DNA extraction from single embryos

After blastocysts were lysed in Dynabeads lysis buffer and RNAs were bound to Dynabeads (described in 2.5.1), lysis buffer containing genomic DNA was collected into an Eppendorf tube and stored at -80 °C. DNA was then extracted from one blastocyst by adding 1 µL Glycogen (Fisher, UK) (20 µg/µL) and 0.1 volume of the DNA supernatant of 3M sodium acetate (Sigma-Aldrich, UK) to the previously measured DNA supernatant. Subsequently, 2.5 volume of 100% ethanol (Fisher, UK) was added to the solution. After vortexing DNA was chilled for 30 minutes in -80°C followed by spinning in chilled centrifuge at 4°C for 15 minutes at 10,000 rpm. Supernatant was removed and the DNA pellet washed with 70% ethanol followed by a second spin in the same conditions. After that, the pellet was dried at room temperature for 5 minutes and resuspended in 5 µl nuclease free water to be used for Multiplex PCR.

2.7.1 Multiplex PCR and sex determination/genotyping of blastocysts

DNA was used for sex determination through Nested PCR (method adapted from Kunieda et al. 1992). 5 µl DNA were added to a tube containing master mix with 10X Buffer containing 15 mM $MgCl_2$, 2.5 mM dNTP mix, 2.5 µM each outer primer (Sry2, Sry4, Zfy3, Zfy4, Nds3, Nds4) (*Table 2.3*), 25 mM $MgCl_2$, 5U/µl HotStarTaq polymerase and nuclease free water until a complete volume of 50 µl. Primers amplifying Sry and Zfy genes are located in the sex-determining regions of the Y- chromosome while DXNds3 (or Nds) is located in the sex-determining region of the X chromosome. The PCR conditions were: 95°C for 15 min for activation, followed by 30 cycles of denaturation at 94°C for 1 min, annealing at 55°C for 30 s, and extension at 72°C for 1 min to finish at 72°C for 10 min. 5 µl template from the previous PCR were used for the second PCR with the same reagents except $MgCl_2$ and using inner primers (Sry1, Sry3, Zfy11, Zfy12, Nds1, Nds2) (*Table 2.4*) at the same PCR conditions.

Male and female controls were also included. These were generated by extracting DNA from mouse tails using KAPA Biosystem extract kit. In summary, 2 mm of a mouse tail was mixed with 10x Kapa express Extract buffer, Kapa express extract enzyme and nuclease free water, according to the manufacture's protocol. For lysis, samples were heated for 10 minutes at 75°C, followed by 5 minutes at 95°C (enzyme inactivation). Samples were then centrifuged to pellet cellular debris prior to diluting the DNA

extracted 1:10 with nuclease free water and storage at -20°C.

Gene		Primer name	Outer primers (5'-3')
Polymorphic X Chromosome Microsatellite locus (DXNds3)	For Rev	Nds3 Nds4	'GAGTGCCTCATCTATACTTACA' 'TCTAGTTCATTGTTGATTAGTT'
HMG box sex-determining region Y (SRY)	For Rev	Sry2 Sry4	'TCTTAAACTCTGAAGAAGAGAC' 'GTCTTGCCTGTATGTGATGG'
Zinc finger Y-chromosome (ZFY)	For Rev	Zfy3 Zfy4	'AAGATAAGCTTACATAATCACATGGA' 'CCTATGAAATCCTTTGCTGCACATGT'

Table 2.3 - Outer primers for genotyping (Kunieda et al., 1992)

Gene			Inner primers (5'-3')
Polymorphic X Chromosome Microsatellite locus (DXNds3)	For Rev	Nds1 Nds2	'ATGCTTGGCCAGTGTACATAG' 'TCCGGAAAGCAGCCATTGGAGA'
HMG box sex-determining region Y (SRY)	For Rev	Sry1 Sry3	'GTGAGAGGCACAAGTTGGC' 'CTCTGTGTAGGATCTTCAATC'
Zinc finger Y-chromosome (ZFY)	For Rev	Zfy11 Zfy12	'GTAGGAAGAATCTTTCTCATGCTGG' 'TTTTTGAGTGCTGATGGGTGACGG'

Table 2.4 - Inner primers for genotyping (Kunieda et al., 1992)

The amplified PCR products were run on 1.5% agarose gel at 120 V for 1 h to identify the bands associated with female or male sex. Four bands representing Zfy (217 and 199 bp), Sry (147 bp) and DXNds3 (111 bp) were defined as male and a single band representing Dxnds3 (111 bp) was defined as a female embryo. *Figure 2.5A* shows a representative gender-specific reaction for male and female embryos and controls. Some samples could not be identified due to unclear visualisation on the gel (*Figure 2.5B*). Primers for Zfy amplified two fragments of slightly different sizes (217 and 199 bp). According to Kunieda et al., (1992) this may have been due to the presence of the two highly homologous sequence, Zfy1 and Zfy2 genes, on the mouse Y chromosome, because the sequences of regions chosen for the Zfy primers are identical between the Zfr1 and Zfy2 genes, and an 18-bp deletion is present in the segment of the Zfy2 gene defined between the primers.

Table 2.5 shows the results of multiplex PCR sex analysis for all embryos analysed. The total number of male blastocysts collected and analysed was much higher than the number of females for both treatments (67.4% total male vs. 32.6% female blastocysts). Due to the low number of female blastocysts, only male blastocysts were used for qPCR (10 embryos per group from 10 mothers).

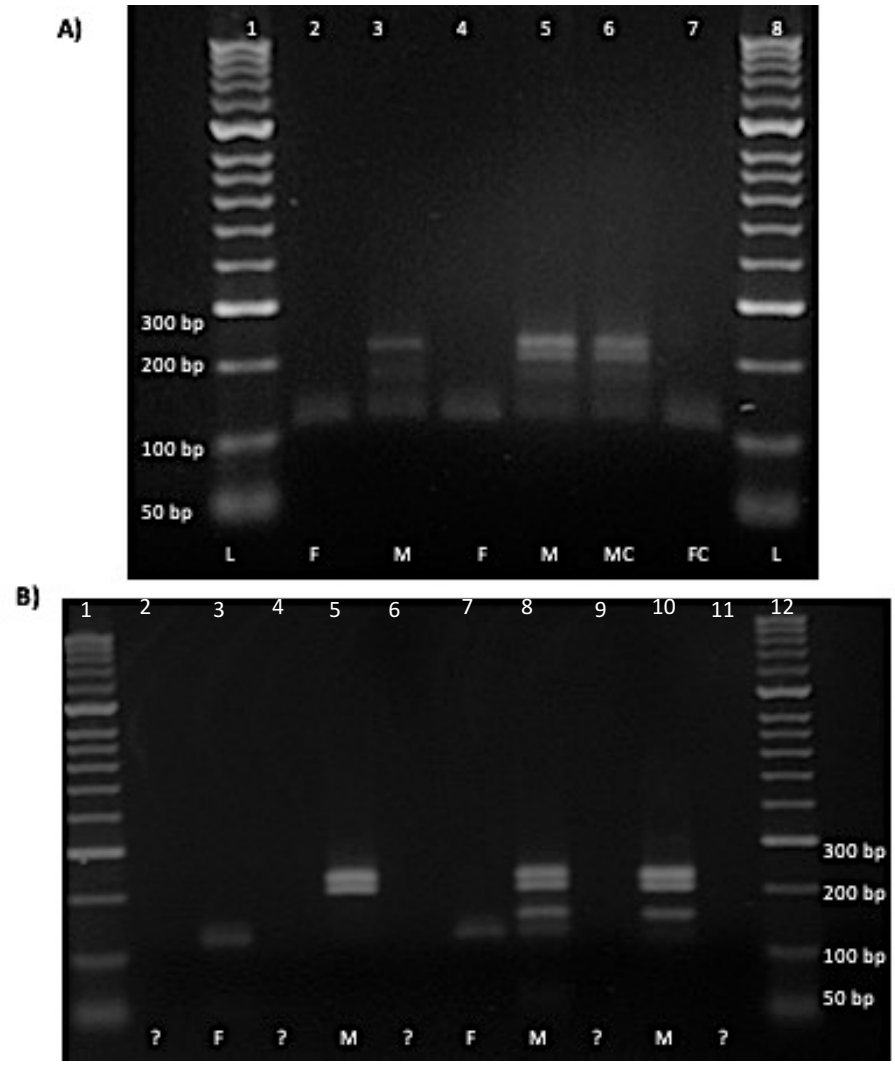

Figure 2.5 - Examples of electrophoresis agarose gels for gender analysis of DNA isolated from single blastocysts by multiplex PCR. A) Lanes 2 and 4 correspond to female (F) blastocysts (DXNds3 – 111 bp) and lanes 3 and 5 to male (M) blastocysts (DXNds3 – 111 bp, Sry – 147 bp and Zfy – 217 and 199 bp). L – ladder (lanes 1 and 8); MC- male control (lane 6); FC – female control (lane 7). B) Lanes 3 and 7 correspond to female (F) blastocysts (DXNds3 – 111 bp); lanes 5, 8 and 10 to male (M) blastocysts (DXNds3 – 111 bp, Sry – 147 bp and Zfy – 217 and 199 bp) and samples in lanes 2, 4, 6, 9 and 11 could not be identified (correspondent RNA was not used for qPCR). L – ladder (lanes 1 and 12).

	Male (%)	Female (%)
Control	14 (73.7)	5 (26.3)
Treatment	15 (62.5)	9 (37.5)
Total	29 (67.4)	14 (32.6)

Table 2.5 – Results of PCR sex analysis of blastocysts – proportion of male and female blastocysts. We obtained valid multiplex results for a total of 43 embryos (from 14 mothers). The total number of male blastocysts collected and analysed was higher than the number of females for control and experimental treatments (defined in *Chapter 4*; 67.4% total male vs. 32.6% female blastocysts). Due to the low number of female blastocysts, only male blastocysts were used for qPCR (10 embryos per group from 10 mothers).

2.8 Statistical analysis

In all statistical analyses, significance was considered as P value <0.05. A trend was assumed if P value was between 0.1 and 0.051. Data regarding mouse embryos was first assessed for normality using the Shapiro–Wilk normality test. Data analysis was performed using One-Way Anova and Tukey's *post hoc* test for multi comparisons for normally distributed data or Student's t-test (when two groups were compared); Kruskal-Wallis test with Dunn's multiple comparisons *post hoc* test or Mann-Whitney (if two groups were compared) for non-normally distributed data. Data are presented as mean ± SEM.

Human embryo endocytosis and immunocytochemistry data were assessed using the multilevel random effects regression model (SPSS version 25) which takes into account potential hierarchical nature of the data with between-patient and within-patient variation and different parameters measured from individual embryos (Kwong et al., 2004). Thus, differences identified between groups (maternal BMI or ICSI procedure) throughout the study are independent of factors like cell volume, cell number and if there was a resultant pregnancy from the same cycle as the one the embryos studied were retrieved. The random effects model was developed by Prof Clive Osmond, Senior Medical Statistician at Medical Research Council Epidemiology unit at Southampton General Hospital.

Chapter 3 Endocytosis System in Extra-Embryonic Lineages – Protocol Optimization

3.1 Introduction

3.1.1 Endocytosis system in mouse embryo development

Endocytosis is the process of internalization of extracellular material. This membrane invagination process gives rise to an independent cytoplasmic vesicle, which acquires a more specific name (e.g. phagosome, pinosome, coated vesicle) depending on the cell type being studied and the type of endocytosis involved (*Figure 3.1*) (Besterman and Low, 1983). The endocytosis system is the main mechanism for nutrient uptake used by preimplantation embryos. Endocytic organelles such as clusters of pre-lysosomal endocytic vesicles (endosomes) are randomly distributed in the cortical cytoplasm from the oocyte stage onwards up to the early 8-cell stage. From the 8-cell stage until the early 16-cell stage, endosomes become progressively localized in the apical cytoplasm and the system progressively becomes more stable (Fleming and Pickering, 1985). Simultaneously, pinocytotic activity (clathrin-independent) at the cell surface becomes segregated preferentially to the apical rather than the basolateral membrane, whereas the final maturation phase occurs at the late 16-cell stage when secondary lysosomes form and polarize in the basal cytoplasm (Fleming and Pickering, 1985). Pinocytosis can be regulated by energy such as ATP, which regulates the quantity of extracellular fluid internalised, and plays an important role in nutrient uptake by embryos at early embryonic stages and in the VYS. Phagocytosis, the internalisation of large particles (1-3 μm of diameter) starts with the formation of the morula stage and by E3.5 the mouse embryo already possesses a phagocytic potential (Rassoulzadegan et al., 2000), mainly in the mural TE opposite to the ICM. In receptor-mediated endocytosis, ligands bind to specific membrane receptors, and the cell membrane invaginates into the cytoplasm, with the formation of clathrin-coated pits. Clathrin is then recycled and the uncoated vesicles fuse with the acidic (pH<5) endosomes which will fuse with lysosomes to degrade the ligands. Lysosomes were shown to have proton-pumping vacuolar ATPases,

which maintain the luminal environment at a pH of 4.6–5.0 (Mellman et al., 1986). This is the most common form of endocytosis used by embryos in the maternal reproductive tract, where the degraded products are either included into the TE or transported and accumulate in the basolateral compartment and then transported into the blastocoel, from where they are taken up by the ICM (Miller and Schultz, 1985) by different transport pathways. Receptor-mediated endocytosis occurs as early as the oocyte stage (Lowther et al., 2011).

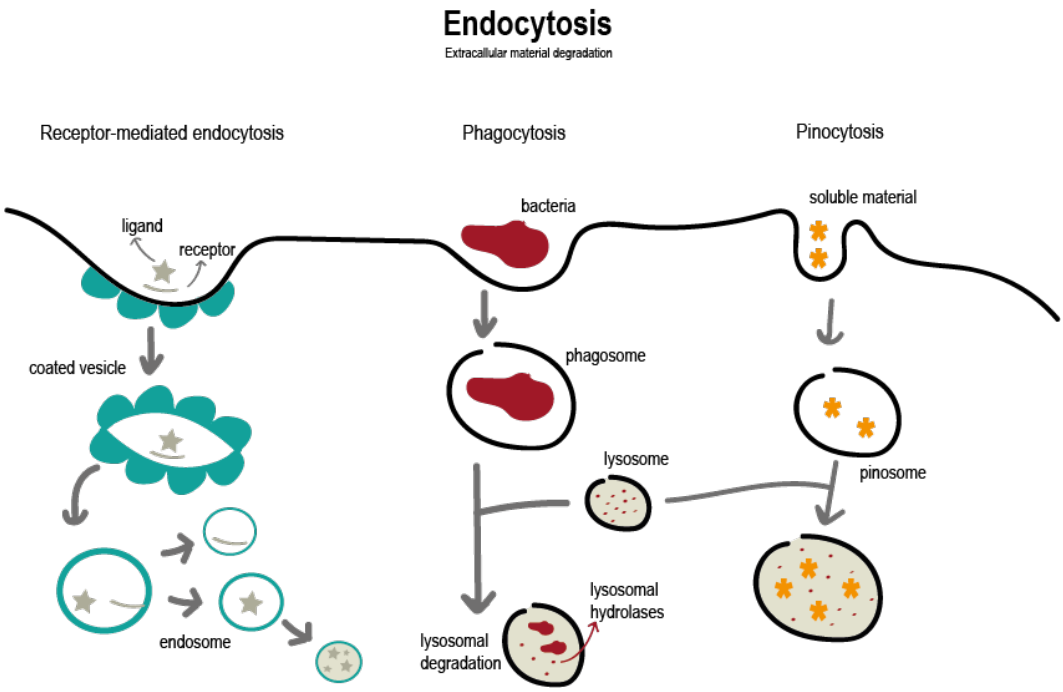

Figure 3.1 – Diagram showing three types of endocytosis – Receptor-mediated endocytosis, phagocytosis and pinocytosis.

Appropriate nutrients support embryonic cell growth and proliferation, while a deficient nutrition can alter cellular activities and induce epigenetic modifications responsible for several adult diseases. Previous studies have shown that blastocysts collected from Emb-LPD mothers displayed an enhanced TE endocytosis with respect to the number and collective lysosome volume per cell with endocytosed ligand and fluid compared with embryos from control NPD mothers (Sun et al., 2014). Endocytosis is also stimulated in the outer PE-like lineage of embryoid bodies formed from embryonic stem cell lines generated from Emb-LPD blastocysts (Sun et al., 2014). In this chapter, I describe the detailed optimisation of the endocytosis assay protocol used in the next chapters.

3.2 Materials and Methods

3.2.1 Animals

Described in section *2.1Animals*.

3.2.2 Embryos collection

Described in *section 2.1.1.*

3.2.3 Endocytosis Assays

Mouse embryos were collected at early blastocyst stage (E3.5) from the uterine horns with H6BSA and different protocols (described in this section) were tested in order to develop and optimise the embryonic endocytic assay. *Appendix 8.5.* contains the optimised steps for the endocytosis assay.

3.2.3.1 Self-Quenched BODIPY FL Conjugate of BSA (BSA-BODIPY)

Self-Quenched BODIPY FL Conjugate of BSA [BioVision, 7932-2] (BSA-BODIPY) was used for degraded protein detection after endocytosis. Bovine serum albumin (BSA) is a common endocytic cargo, which is usually degraded by proteases in the lysosome. BSA-BODIPY derives from BSA heavily labelled with a fluorescence dye BODIPY FL. The high concentration of the fluorophore on BSA causes prominent self-quenching of the dye conjugate. However, when BSA degradation occurs, the peptide fragments that carry the fluorophores are released, thereby relieving the dye from self-quenching *(Figure 3.2).*

From 10 mg/ml BSA-BODIPY stock solution, a final working solution of 0.5 mg/ml was prepared using KSOM. After washing the embryos in KSOM followed by 3 washes in KSOM with BSA-BODIPY (0.5 mg/ml) and LysoTracker (100 nM), embryos were cultured in combined BSA-BODIPY and LysoTracker drops submerged in mineral oil for 1 hour in the incubator at 37°C and 5% CO_2. After the incubation, embryos were washed 3 times in H6BSA.

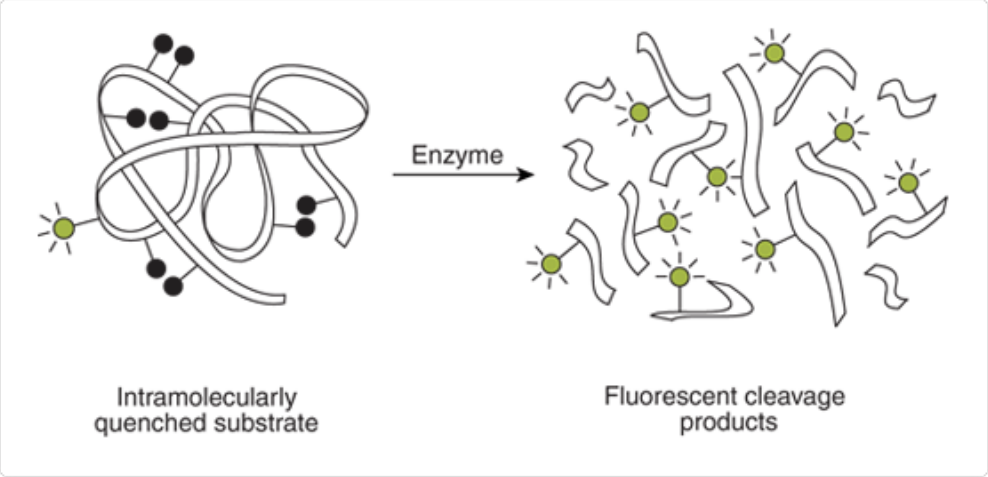

Figure 3.2 - Principle of enzyme detection via the disruption of intramolecular self-quenching (Thermo Fisher, Molecular Probes handbook, available at https://www.thermofisher.com/uk/en/home/references/molecular-probes-the-handbook/enzyme-substrates/detecting-peptidases-and-proteases.html accessed on 03/02/2020).

3.2.3.2 Lysosomes staining with LysoTracker® Red DND-99

LysoTracker® Red DND-99 (Molecular Probes, ThermoFisher Scientific, L7528) is a red-fluorescent acidotropic probe for labelling and tracking acidic spherical organelles in live cells. It consists of a fluorophore linked to a weak base that is only partially protonated at neutral pH and that is permeant to cell membranes. The mechanism of retention within the organelles has not been firmly established but is likely to involve protonation and retention in the membranes of the organelles. The co-localisation of LysoTracker with BSA-BODIPY allows the detection of lysosomes (LysoTracker) and the proteins after degradation (BSA-BODIPY) within this organelle.

From 1 mM stock solution a final working solution of 100 nM was prepared by dilution in KSOM. After washing the embryos in KSOM followed by 3 washes in LysoTracker and BSA-BODIPY (0.5 mg/ml) in KSOM, embryos were cultured in drops of LysoTracker and BSA-BODIPY combined in KSOM submerged in mineral oil for 1 hour in the incubator at 37°C and 5% CO_2. After the incubation embryos were washed 3 times in H6BSA.

3.2.3.3 Activated lysosomes activity – Magic Red™ Cathepsin B

The Magic Red™ Cathepsin B kit measures cathepsin B protease activity by detecting active cathepsins in whole, living cells. The Magic Red (MR) reagent is a cell-permeable and non-cytotoxic substrate that fluoresces red upon cleavage by active cathepsin enzymes. It contains a cathepsin B target sequence peptide (arginine-arginine - RR) linked to a photostable red (Cresyl Violet) fluorescent probe. Following enzymatic cleavage at one or both arginine amide linkage sites, the mono and non-substituted cresyl violet fluorophores generate red fluorescence when excited at 550-590 nm. The red fluorescent product will stay inside the cell and will aggregate inside enzymically active lysosomes (cathepsins are lysosomal). Cathepsins B are the most abundant lysosomal proteases and are highly expressed in early mouse embryos (Tsukamoto et al., 2013). Cathepsins are transported from the Golgi to lysosomes through late endosomes, and during the carriage, inactive proenzymes (immature) are converted to active (mature) enzymes through a sequence of proteolytic process (reviewed by Reiser et al., 2010). Thus, MR was used as a marker of active lysosomes. MR substrate is supplied as a highly concentrated lyophilized powder which was reconstituted in DMSO, forming a 260X stock concentrate, and was then diluted 1:10 in distilled H_2O to form the final staining solution at 26X. Embryos collected were washed with KSOM followed by three washes in 1:20 MR final solution and BSA-BODIPY (0.5 mg/ml) in KSOM or 1:20 MR final solution and LysoTracker (100 nM) in KSOM before been cultured for 1 h in the same solution submerged in mineral oil for 1 hour in the incubator at 37°C and 5% CO_2. After the incubation, embryos were washed 3 times in H6BSA.

3.2.4 Zona pellucida removal vs non-removal

Three different protocols were tested regarding the removal of the zona pellucida (ZP). The endocytosis assay was either performed 1) before removing the ZP, 2) after removing ZP or 3) without removing the ZP. In scenarios 1 and 2, blastocysts were treated with acid Tyrode's medium (Sigma) in a cavity block for 15 to 40 seconds under the microscope until the ZP was completely removed, either after or before the endocytosis assay, respectively, followed by 2 h incubation at 37°C in H6BSA in order to completely recover from the acid treatment.

3.2.5 Cell membrane boundaries staining

As described before in *2.4* - the TE plasma membrane of embryos was labelled in order to visualise and crop individual cells (using the VOLOCITY program) to further evaluate the endocytosis uptake in individual TE cells. The following section describes the optimisation of the protocol used to stain the cell plasma membrane. Negative controls were included by omitting the primary antibody.

3.2.5.1 Immunocytochemistry: E-Cadherin

E-Cadherin, which is present in blastocysts at the adherens junctions and along cell membranes where cells are in contact, was first used to attempt to label the boundary between TE cells. Embryos were first washed and incubated 1h (37°C and 5% CO_2) with LysoTracker (100 nM) and BSA-BODIPY (0.5 mg/ml) or FITC-Dextran (5 mg/ml) submerged in mineral oil followed by fixation. The immunocytochemistry protocol is detailed in *Appendix 8.3*. Controls consisted of secondary antibodies only with omitted primary antibodies.

3.2.5.2 CellMask™ Deep Red

The CellMask™ (Thermo Fisher Scientific, Molecular Probes - C10046) plasma membrane stains are amphipathic molecules providing a lipophilic moiety for membrane loading and a negatively charged hydrophilic dye for “anchoring” of the probe in the plasma membrane. The protocol used for staining with CellMask™ was optimised in order to obtain the best results. Different concentrations of CellMask™ diluted in KSOM were tried in this method (1:200; 1:800 and 1:1000) after 1 h incubation in LysoTracker with BSA-BODIPY or FITC-Dextran for different time points (30 min, 1 h and 1.5 h). In this first optimisation approach embryos were first washed and incubated 1 h (37°C and 5% CO_2) with LysoTracker (100 nM) and BSA-BODIPY (0.5 mg/ml) or FITC-Dextran (5 mg/ml) submerged in mineral oil followed by different incubation time points in CellMask™ (in 3 different concentrations) in the same conditions. In this approach SYTO® Blue Fluorescent Nucleic Acid Stain Sampler Kit (SYTO® dyes 40, 41, 42, 45) was also tested for nuclear staining for live cells. These dyes are cell-permeant nucleic acid stains that differ from each other in one or more characteristics, including cell permeability,

fluorescence enhancement upon binding nucleic acids, excitation and emission spectra, DNA/RNA selectivity and binding affinity. After this last incubation, embryos were washed and mounted in chambers (as detailed in 2.3 – Immunocytochemistry).

CellMask™ staining pattern is also maintained after fixation with formaldehyde, thus, another method tested in order to improve the final methodology to be used, was to incubate the embryos for 1 h (37°C and 5% CO_2) with LysoTracker (100 nM) and BSA-BODIPY (0.5 mg/ml) or FITC-Dextran (5 mg/ml) followed by fixation with 1% formaldehyde (20 min) and 1 h in CellMask™ (1:200) at room temperature. After the incubation with CellMask™, embryo nuclei were stained with DAPI (as described in *Appendix 8.3*).

3.2.6 Live vs fixed embryos

Since CellMask™ can be used in live cell imaging as well as in fixed cells, we decided to also image live embryos to remove possible artefacts caused by fixation. The SP8 confocal microscope in the University Imaging Unit has a closed chamber with controlled temperature and CO_2, which was used to maintain the live embryos in the appropriate conditions. However, since the CellMask™ is only stable for 30–90 minutes in live cells (as opposed to up to 24 h in fixed cells) depending on the cell type and experimental conditions, it makes the method inviable as it takes approximately 20 minutes to image each embryo (using the two different approaches mentioned in 2.4 – Confocal microscopy image capture and analysis).

3.2.7 Image acquisition and data analysis

Control and immunolabelled samples were imaged using confocal microscopy (Leica SP5 or SP8). The excitation wavelength of BSA-BODIPY is 505 nm with an emission wavelength of 515 nm (green fluorescence). FITC-Dextran excitation maximum is 490 nm and the emission is 520 nm (green fluorescence). LysoTracker® Red DND-99 excitation wavelength is 577 nm and the emission wavelength is 590 nm (red fluorescence). CellMask™ Deep Red excitation wavelength is 649 nm while the emission is 666 nm.

As mentioned before, embryos were scanned using the confocal system with two different approaches - half-embryo (with xy = 1 µm intervals) and high resolution (xy = 0.15 µm intervals) only for 2-3 TE cells. In both methods, only the embryo surface closest to the coverslip was imaged (brightest signal obtained) while the other half (distal to the coverslip) was not included due to the reduced signal strength. Image acquisition in the confocal microscope was "normalised" by adjusting the gain of each channel to the lowest saturation point. Using the Leica Application Suite Advanced Fluorescence (LAS AF), the image acquisition configuration was set as: 1024x1024 format, 600 Hz speed, line average of 4 (number of scans performed per embryo in order to decrease the image graininess – noise) and rotation of 90°. Embryos were imaged with a 1.41 zoom and -1.0% smart offset in each channel.

All images acquired in the confocal were analysed with VOLOCITY 6.3 software (PerkinElmer). Two different protocols were created and optimised in VOLOCITY – one for the half embryo approach and one for the high resolution top TE cell approach. The software converts fluorescent signals into measurable 3D structures. However, there are several configurations in the programme that can be altered in order to create the most appropriate protocol and to minimise the programme pitfalls (described in *2.4*). The final protocol was set as:

1) Find object and remove noise from objects using fine filter (individually for each channel – red for LysoTracker and green channel for BSA-BODIPY and FITC-Dextran);
2) Select the size guide (exclude vesicles >20 μm^3 for BSA-BODIPY and LysoTracker and <200 μm^3 for nuclei);
3) Separate touching objects (in order to minimise the effect of combining touching vesicles).

In the half embryo approach, the total number and volume of vesicles was divided by the number of nuclei counted, giving an approximate number and volume of vesicles per cell. However, in this approach both TE and ICM cells are included. After the protocols were designed and optimised, they were saved and performed without any further alterations for all embryos, thus avoiding any bias.

3.3 Results

3.3.1 BSA-BODIPY/LysoTracker endocytosis assay development

BSA-BODIPY was used for the first time in early embryo development studies by Sun et al., (2014). The BSA-BODIPY and LysoTracker concentrations and incubation time usually used together, at 0.5 mg/ml and 100 nM in KSOM medium for 1 h respectively, were based on the optimisations previously made by our research group (Sun et al., 2014).

3.3.1.1 Controls

In order to confirm the specificity of the signal obtained, E3.5 embryos were cultured for 1 h in 0.5 mg/ml BSA-BODIPY at 4°C, since endocytosis is inhibited at this temperature. No strong fluorescent signal was detected even when the gain (in the confocal image acquisition) was increased (*Figure 3.3a*). Furthermore, 8-cell stage embryos were also used as control since BSA is known to be taken up by the Megalin-Cubilin receptor complex, which only starts to appear in the outer cells around the morula stage (Assemat, 2005), meaning that BSA cannot be endocytosed. These embryos were cultured for 1 h at 37°C with 0.5 mg/ml BSA-BODIPY and no signal was obtained *(Figure 3.3b).*

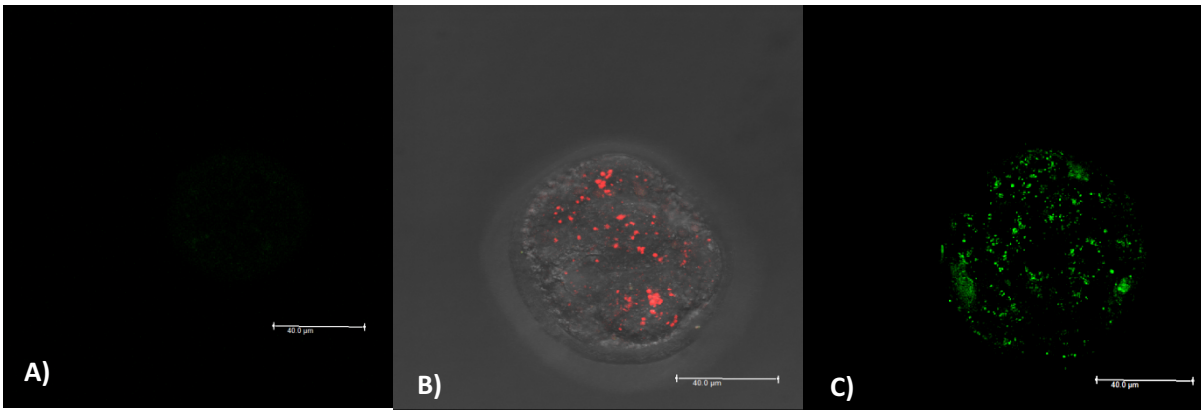

Figure 3.3 – Negative controls for BSA-BODIPY uptake. A) Blastocysts cultured at 4°C for 1 h in BSA-BODIPY (0.5 mg/ml) B) 8-cell embryo stained with LysoTacker (red) and BSA-BODIPY (green) [phase contrast] which is not taken up at this developmental stage. C) Blastocysts cultured at 37°C for 1 h in BSA-BODIPY (0.5 mg/ml). Scale bar = 40 µm.

The incubation with both BSA-BODIPY and LysoTracker allowed the further confirmation of the assay reliability, since BSA is degradated inside lysosomes, thus these two should co-localize. E3.5 blastocysts were co-cultured with 100nM LysoTracker and 0.5mg/ml BSA-BODIPY at 37°Cfor 1h, and these were further imaged in the SP5 confocal microscope. *Figure 3.4* shows the same embryo imaged in the red (lysosomes stained by LysoTracker) and green channel (BSA being degraded) separately. It is possible to verify that both vesicles are co-localised around the cell nuclei, suggesting that the BSA is being degraded inside the lysosomes.

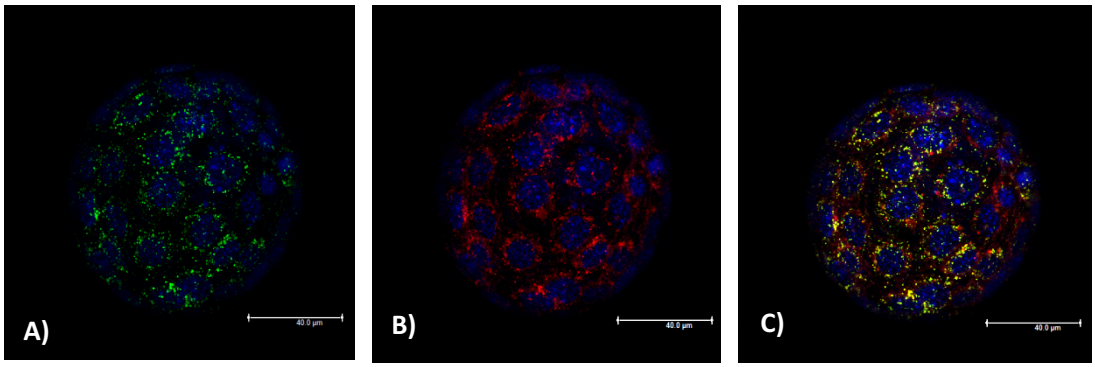

Figure 3.4 – Blastocyst stained with BSA-BODIPY (green), LysoTracker (red) and DAPI (blue) A) BSA-BODIPY localised around the nuclei; B) Lysosomes localised around the nuclei. C) BSA-BODIPY and LysoTracker colocalization. Scale bar = 40 µm.

Figure 3.5 is a cross-section (one xy section from z-stack) image of an embryo stained with both LysoTracker and BSA-BODIPY. It is possible to see lysosomes (red) in both the ICM and TE, while BSA is only present (and co-localised with the LysoTracker) in the TE. No staining was present in the blastocoel. This result suggests that the BSA is not endocytosed directly by the ICM. These findings are in accordance with the findings of Sun et al., (2014) and Dunglison and Kaye, (1995), who also showed the presence of endocytosed albumin in the TE but not in the ICM. The TE tight junctions are responsible to prevent this access to the embryo interior.

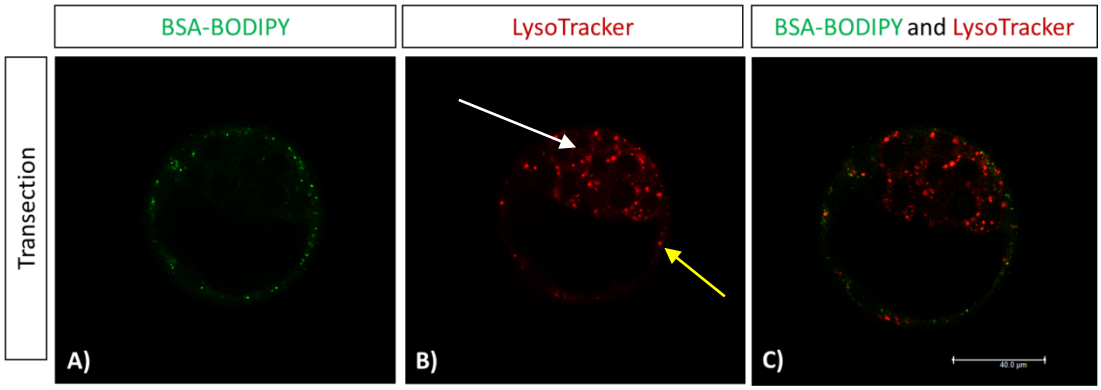

Figure 3.5 - Cross-section image of an embryo stained with both BSA-BODIPY (A) and LysoTracker (B). It is possible to see lysosomes (red) in both the ICM (white arrow) and TE (yellow arrow), while BSA is only present (and co-localised with the LysoTracker) in the TE (C). No staining is present in the blastocoel. Scale bar = 40µm.

A final confirmation of the reliability of this assay, was achieved by staining E3.5 blastocysts individualy with LysoTracker, BSA-BODIPY and CellMask and imaging all the channels in order to account for possible bleaching from one channel to another. From *Figure 3.6* it is possible to verify the reliability of the staining since there is no bleaching to other channels, thus meaning that the vesicles counted and measured in each channel (by the VOLOCITY software) are specific and not a bleaching artifact.

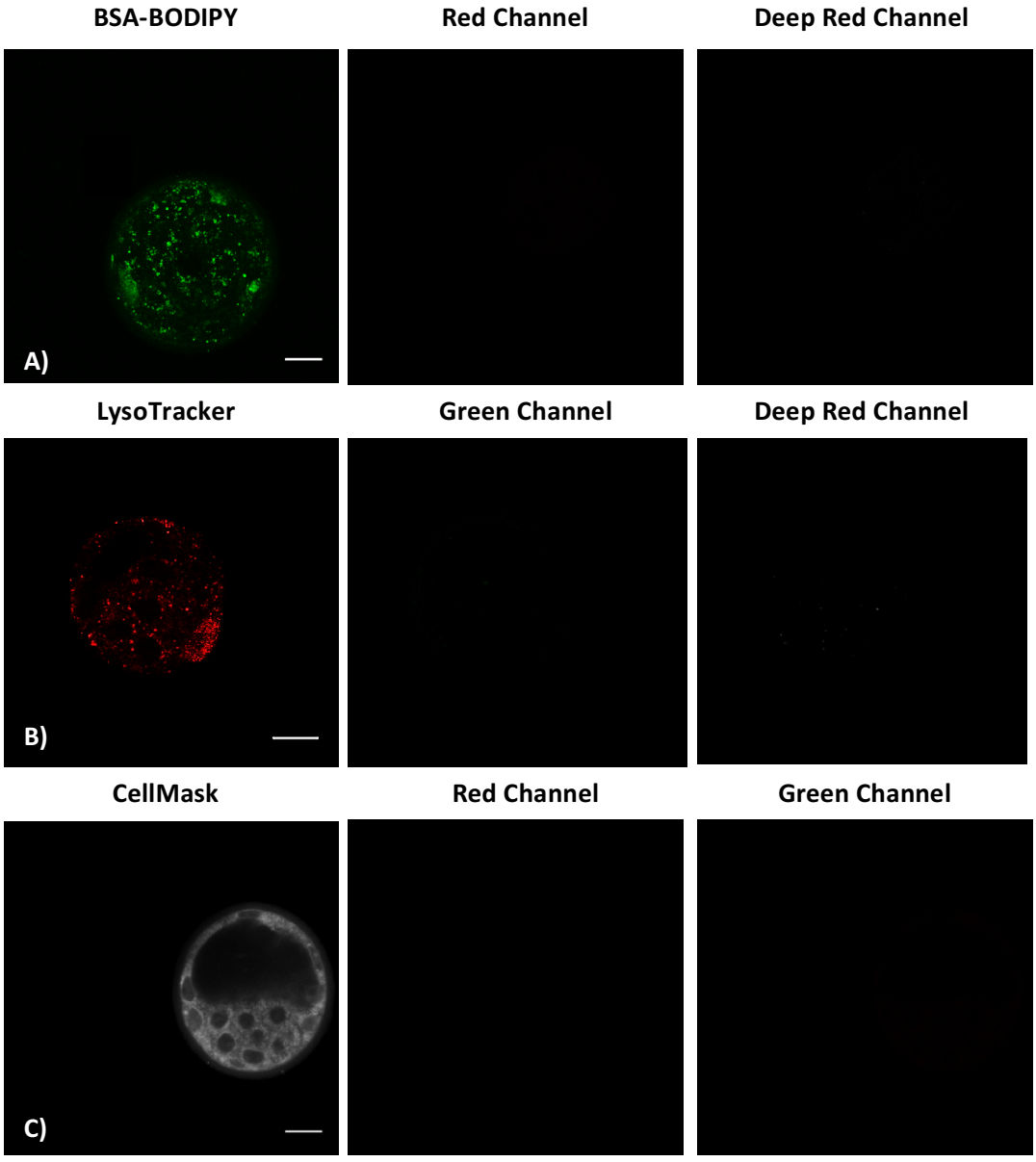

Figure 3.6 - Three blastocysts stained with A) BSA-BODIPY, B) LysoTracker or C) CellMask only. The other "empty" channels were imaged in order to verify if there was any signal bleaching (mid and right columns). There is no bleaching to any of the different channels. Scale bar = 20µm.

3.3.1.2 Zona pellucida removal vs non-removal

In previous studies made by our research group, using the BSA-BODIPY/LysoTracker assay, the ZP was removed with acid Tyrode's after the endocytosis assay and before immunocytochemistry (Sun et al., 2014) to allow labelling of the boundaries between TE cells. In a first approach, this method was repeated. However, endocytosis is highly sensitive to pH and the ZP removal with acid Tyrode's (pH 2.3) might interfere with the endocytosis. Thus, further protocols were tested in order to compare and verify if the acidic ZP removal had any effect on the endocytosis in E3.5 embryos. Although previous studies showed that the ZP removal has no effect on amino acid uptake by day 1 embryos (Epstein and Smith, 1973) and BSA-BODIPY detection is insensitive to pH, it is not known if these pH alterations might alter the endocytosis uptake in the embryo by affecting the lysosomes. The endocytosis assay was completed either before, after or without the ZP removal. The mouse ZP is permeable to substances of different molecular weight. Ferritin for example (480 to 1000 kD) can pass through the mouse zona as well as high molecular weight immunoglobins (Sellens and Jenkinson, 1975). Thus, albumin (66 kD) and Dextran (40 kD) are expected to penetrate the ZP. When the endocytosis was performed after the ZP removal, the embryos were then allowed to recover for 2 h in H6BSA at 37°C. As seen in *Figure 3.7,* the BSA-BODIPY and LysoTracker staining worked in the three approaches. However, the first 2 approaches mimic less *in vivo* conditions where the ZP is present. Thus, the third protocol (non-removal of ZP) was chosen to be used in future experiments.

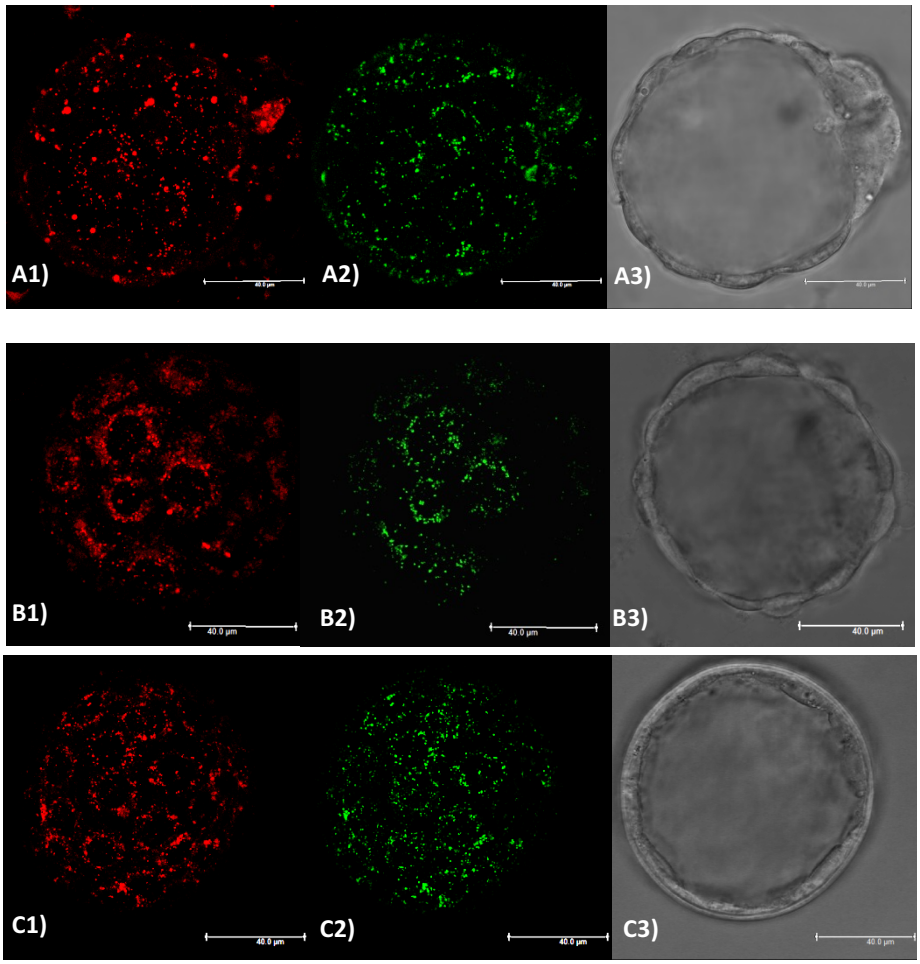

Figure 3.7 – Blastocysts stained with LysoTracker (1) and BSA-BODIPY (2) with the ZP removed after the endocytosis assay (A), before the assay (B) or without removing the ZP (C). A3, B3, C3 are brightfield images (one xy section from z-stack) where it is possible to see the embryo structure without the zona (A,B) and with the ZP on (C). Scale bar = 40 µm.

3.3.1.3 Cell membrane staining

E-Cadherin (E-Cad) antibody, generated in house to mouse E-cadherin GST fusion protein, was used as a first attempt to label the TE cell boundaries, as it is present in adherens junctions. In order to analyse individual TE cells (the cells closest to the coverslip) that were imaged with high resolution, these need to be cropped out using the VOLOCITY software. However, E-Cad staining was difficult to optimise. Although it seemed to work better with some secondary antibodies than others (Alexa 488 for instance), Alexa 647, which was theoretically ideal to use in combination with BSA-BODIPY and LysoTracker (since it has a different excitation/emission) did not work

consistently. Different embryos exposed to the same conditions did not always show immunostaining for E-cad (*Figure 3.8*). Although there is no apparent reason for this discrepancy, it was previously reported in our lab. Thus, CellMask Deep Red, a membrane stain, was chosen as a substitute for E-Cad to differentiate TE cells. From the three dilutions tested (1:200; 1:800 and 1:1000) over three different time points (30 min, 1 h and 1.5 h), 1:200 for 1 h showed optimal results, both in live embryos and after fixation (*Figure 3.9*), and was selected to be used in future experiments. Because it is a membrane stain, it will also label organelle membranes inside the cell. Using this method for cell membrane staining in subsequent experiments, for each embryo and depending on their precise orientation, 1 to 3 cells could be cropped out and analysed in VOLOCITY in the high resolution TE approach.

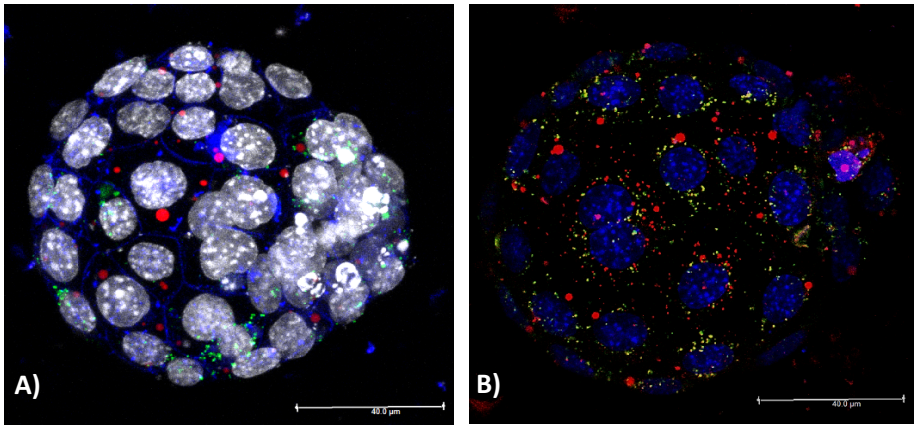

Figure 3.8 - E3.5 blastocysts stained with LysoTracker (red), BSA-BODIPY (green) and E-Cadherin (blue in figure A, absent in figure B) (1:250) secondary Ab goat anti-rabbit Alexa 647 (1:300). Both embryos were under the same conditions. In A) it is possible to distinguish individual cells (E-Cad in blue, DAPI in grey). In B), E-Cad did not work (DAPI in blue). Scale bar = 40 µm.

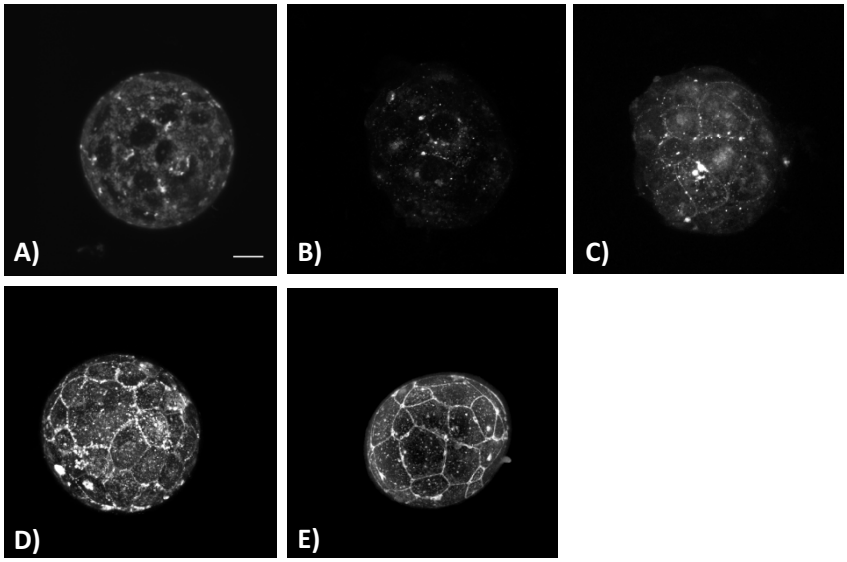

Figure 3.9 – E3.5 blastocysts fixed and with the ZP on, stained with CellMask Deep Red with different concentrations and with different incubation time points. A) CellMask diluted 1:800 in PBS and incubated for 1 h; B) CellMask diluted 1:1000 in PBS for 1 h; C) CellMask diluted 1:800 in PBS for 1.5h; D) CellMask diluted 1:200 in PBS for 30 min and E) CellMask diluted 1:200 in PBS for 1 h. Scale bar = 20 µm.

3.3.1.4 Live vs fixed embryos

Since CellMask can be used in live cells, it was a good opportunity to exclude the fixation step from the protocol, thus removing potential artefacts caused by fixation and reducing as much as possible the embryo manipulations. Although CellMask worked in live embryos, it is only stable for 30-90 minutes in live cells, depending on the cell type and experimental conditions, which makes it impossible to image a large number of embryos, thus compromising future experiments with large N numbers, as it takes approximately 20 minutes to image each embryo (using the two different approaches). Nevertheless, it was possible to compare live and fixed embryos after the endocytosis assay *(Figure 3.10),* which again confirmed the specificity of the assay even after fixation, as no differences were found between live and fixed embryos (*Appendix 8.6*). However, SYTO® dyes 40, 41, 42 and 45 staining, which were tested for nuclear staining in live embryos, could not be optimised.

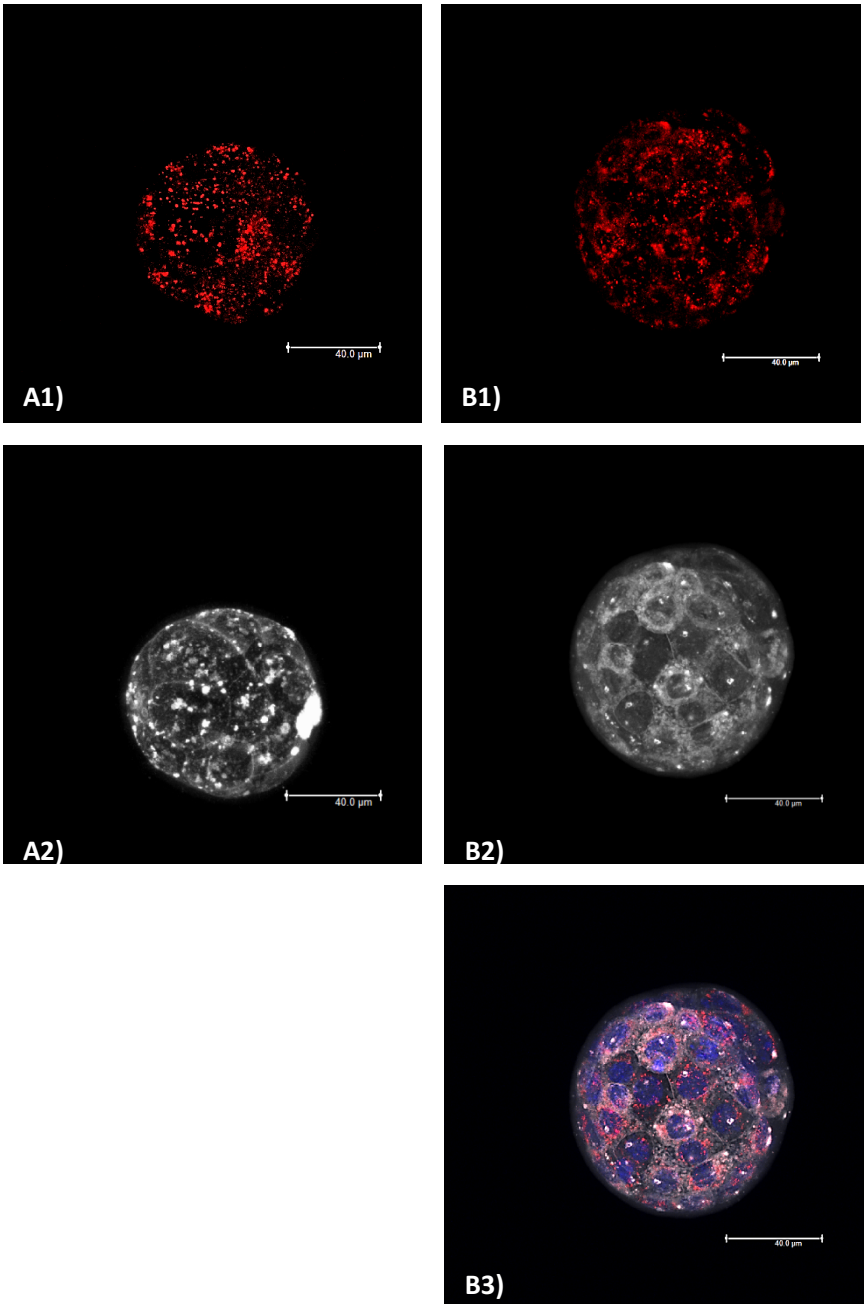

Figure 3.10 – Two E3.5 embryos stained with LysoTracker (A1 and B1), CellMask Deep Red (A2 and B2). A) was stained and imaged live and B) was fixed after the endocytosis assay and before CellMask incubation. B3 show the blastocysts with the LysoTracker (red), CellMask (grey) and DAPI (blue). SYTO® dyes 40, 41, 42, 45 were tested for nuclear staining in live embryos and did not work. A) is imaged with lower magnification and less Z stacks than B). Scale bar = 40 µm.

3.3.1.5 3D Analysis model with VOLOCITY software

VOLOCITY is a software system which analyses quantitatively 3D images. Each embryo was imaged twice, first using the system optimised option (**high resolution scan** – scanned at 0.15 μm intervals over z-series of 50-60 optical sections with no intervening spaces) where only the TE cells on the embryo surface closest to the coverslip were included, followed by a **half embryo scan** with z-series of 1 μm scans but with intervening spaces (*Figure 3.11*).

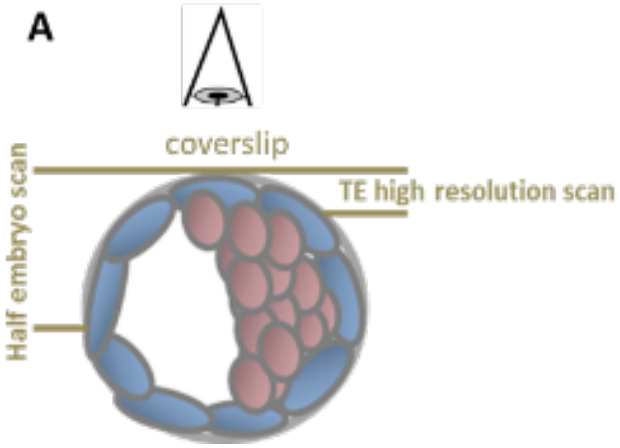

Figure 3.11 – Diagram showing the embryo TE high resolution (system optimised) and half embryo scan approaches. Each embryo was imaged twice, first using the system optimised option (high resolution – scanned at 0.15 μm intervals over a z-series of 50-60 optical sections) where only the TE cells on the embryo surface closest to the coverslip were included, followed by a half embryo scanning with z-series of 1 μm sections.

The first approach includes only the information about 1-3 cells (*Figure 3.12*), with the brightest staining intensity, since these cells are in the surface closest to the laser. In this scanning method, all the vesicles in the field are covered (*Figure 3.13*); however, the information is limited to 1-3 cells per embryo which are individually cropped using the VOLOCITY software.

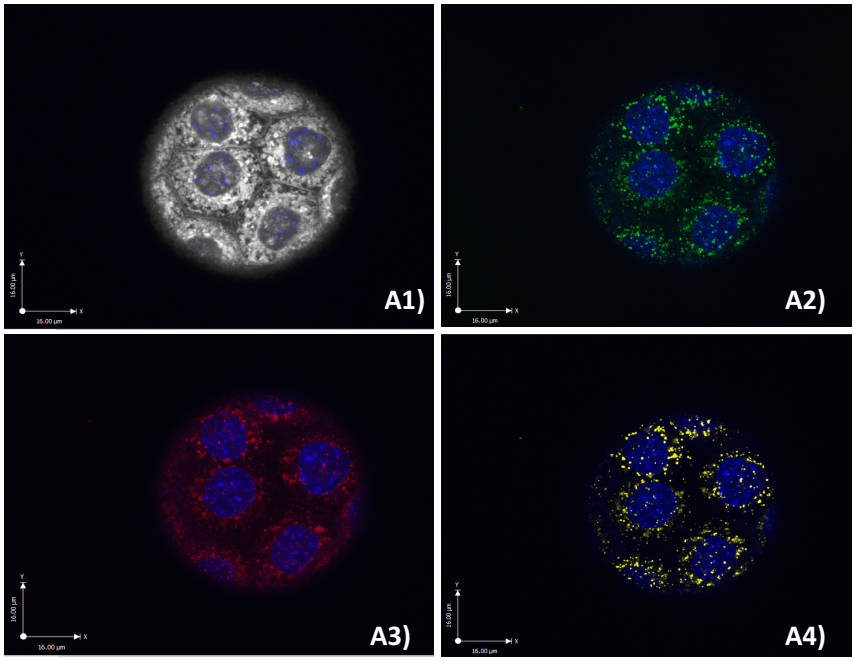

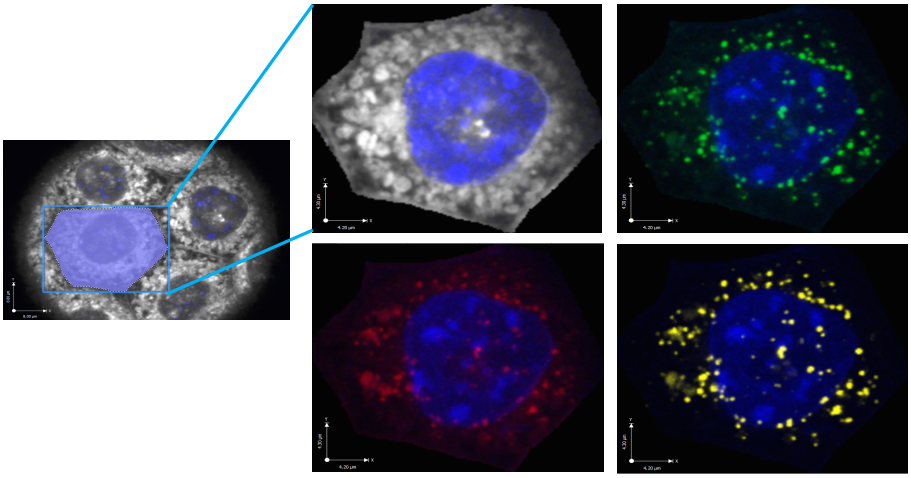

B)

Figure 3.12 – Blastocyst stained with CellMask Deep Red (grey), BSA-BODIPY (0.5 mg/ml) (green), LysoTracker (100 nM) (red) and DAPI (blue) and scanned using the TE high resolution approach in the confocal microscope. From each embryo, 1-3 cells can be analysed. A1) CellMask and DAPI. A2) BSA-BODIPY and DAPI; A3) LysoTracker and DAPI. A4) Colocalised BSA-BODIPY and LysoTracker vesicles (yellow) according to the VOLOCITY protocol set. B) shows a cropped cell from figure A) with nucleus, BSA-BODIPY vesicles and lysosomes detected by VOLOCITY software.

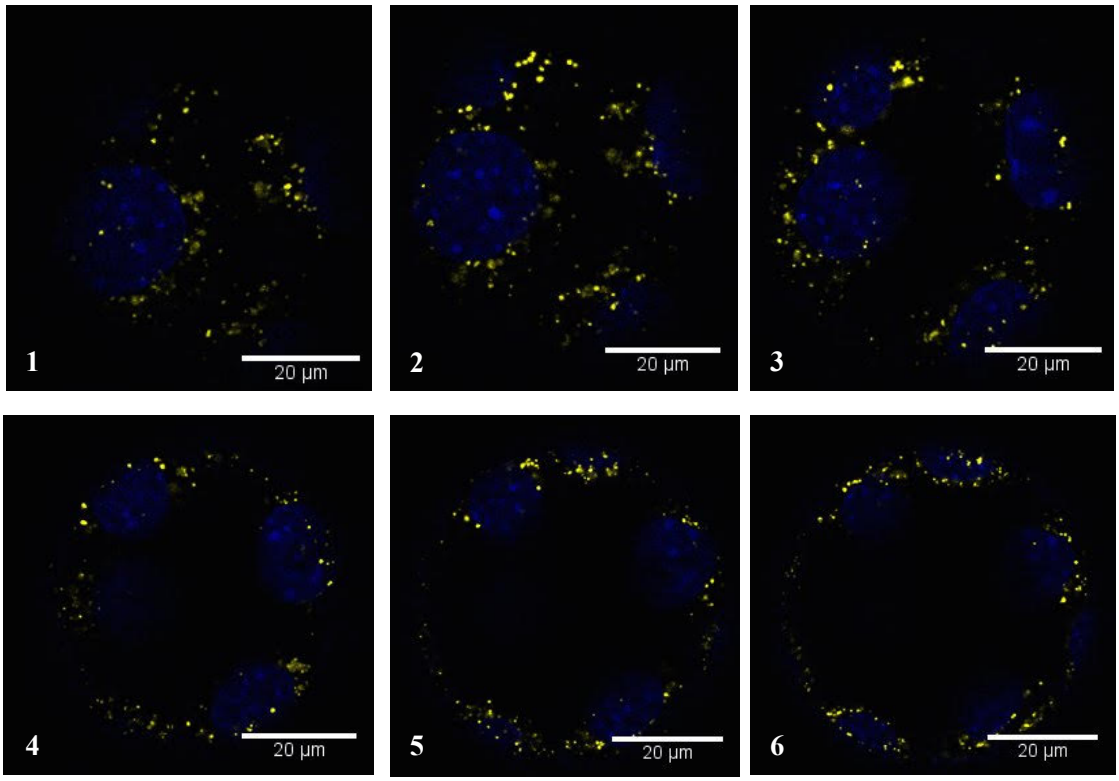

Figure 3.13 – Colocalised BSA-BODIPY and LysoTracker vesicles (yellow) shown in different sections of the z-stack in VOLOCITY (TE high resolution scan). In yellow are vesicles where green and red voxels are considered to be colocalised according to the VOLOCITY protocol developed. Scale bar = 20 µm.

In the half embryo method, the resolution is decreased, especially when the scanning comes closer to the mid part of the embryo (farthest from the laser). Moreover, in this method, the number and volume of the vesicles (combined total volume and mean individual vesicle volume per cell) is counted in all the half embryo cells – approximately half of which belong to the ICM – and is then divided by the number of total cells (identified by the total number of nuclei stained) (*Figure 3.14*).

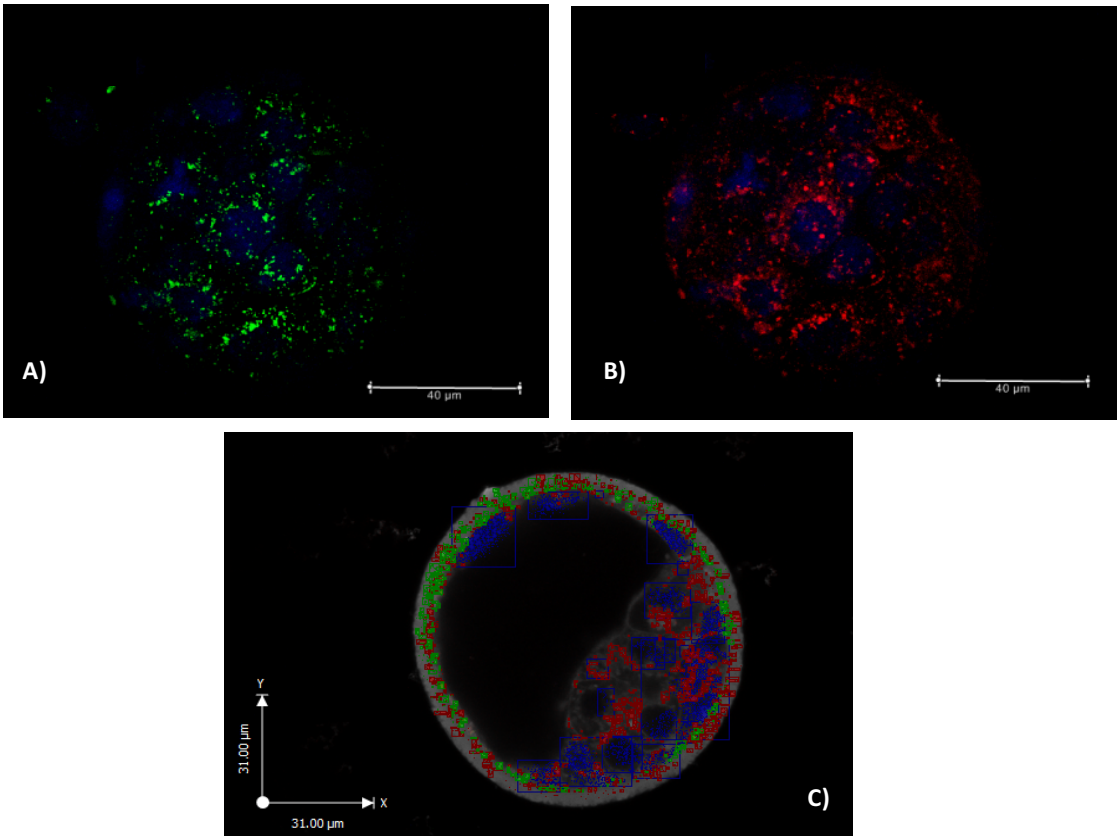

Figure 3.14 - Blastocyst stained with BSA-BODIPY (0.5 mg/ml) (A) and LysoTracker (100 nM) (B), CellMask Deep Red and DAPI and scanned using the half embryo scan approach in the confocal microscope. In this method, the number and volume of the vesicles per cell (combined total volume and mean individual vesicles volume) is counted in all the half embryo cells - half of which belong to the ICM – and is then divided by the total number of cells (identified by the total number of nuclei stained). Figure C) shows BSA-BODIPY vesicles and lysosomes detected by VOLOCITY. LysoTracker is present both in the TE cells and ICM, while BSA-BODIPY is only present in the TE (as shown in C) Scale bar = 40 µm (A, B), 31.00 µm (C).

As showed before (*Figure 3.5*) the BSA-BODIPY is not present in the ICM, which means that the total number and volume of BSA-BODIPY particles is not accurate. Furthermore, since the half embryo scan is imaged every 1 μm, information present in the gaps between scans might be lost. Consequently, the VOLOCITY programme combines vesicles that are close to each other counting them as being just one. This means that in this method, the total number of vesicles should be proportionally smaller compared to the TE high resolution method, although the total combined volume should be proportional, at least for the lysosomes (which are present in both ICM and TE, thus are divided by an accurate number of cells).

To test if this was the case, I analysed 7 blastocysts (each one scanned using both approaches) in order to compare the results obtained from both methods (*Figure 3.15)*. The number of BSA-BODDIPY vesicles per cell is significantly reduced ($P<0.05$) in the half embryo approach compared to the TE high resolution approach (*Figure 3.15a*), possibly due to VOLOCITY pitfalls in the half embryo approach as explained above. The lysosome number in the two methods was similar as anticipated and explained above, suggesting a similar number of lysosomes in ICM and TE. However, the combined vesicle volume (*Figure 3.15b*) is increased in the half embryo approach ($P<0.05$) and since individual vesicles are combined in this system this means that the real number of lysosomes is actually larger, suggesting increased labelling with LysoTracker in the ICM than TE (which is not accounted for in the TE scan method). The BSA-BODIPY volume is similar in both approaches, again suggesting that although vesicles are being combined in the half embryo method (difference seen in the BSA-BODIPY vesicle number) the total combined volume is still accurate. Moreover, the mean individual volume of vesicles – Lysosomes and BSA-BODIPY - is higher in the half embryo scanning approach than in the TE high resolution ($P<0.05$). The mean volume in the half embryo approach was 3.70 μm^3 while in the TE it was 1.67 μm^3 (*Figure 3.16*).

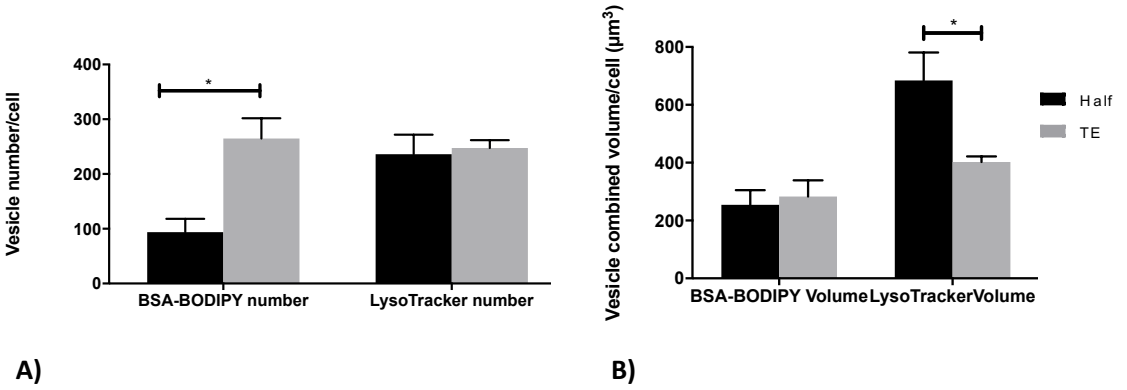

Figure 3.15 – Comparison between the half embryo scan approach and the TE high resolution approach. The same embryos were imaged first using the TE high resolution (TE) followed by the half embryo approach (Half). A) shows the number of vesicles (BSA-BODIPY and lysosomes) per cell. B) shows the collective volume of vesicles (BSA-BODIPY and lysosomes) per TE cell. N=7 embryos (from 3 mothers). * P value < 0.05.

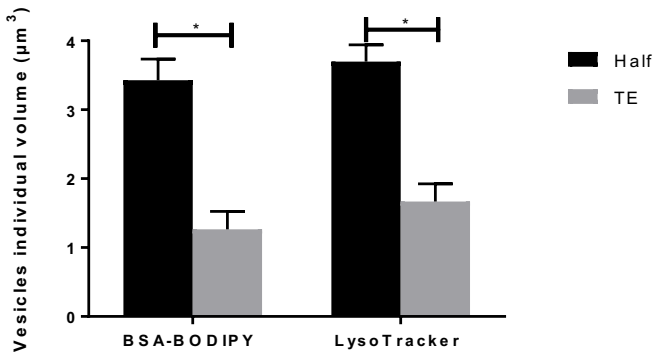

Figure 3.16 - Mean individual volume of vesicles –BSA-BODIPY and LysoTracker vesicles individual volume is higher in the half embryo scanning approach than in the TE high resolution. The mean volume in the half embryo approach was 3.70 μm^3 while in the TE it was 1.67 μm^3. N=7 embryos (from 3 mothers). * P value < 0.05.

3.3.1.6 Magic RedTM Cathepsin B – activated lysosomes – protocol optimisation

To the best of my knowledge, this is the first time Magic Red has been used to study lysosome activation in developing mouse embryos. The manufacture's protocol suggested for suspension cells was adapted and tested for embryo staining. Moreover, after staining, embryos were fixed in formaldehyde and further stained with CellMask and DAPI. Fixation after the staining was found to be compatible with Magic Red (MR) staining although the suppliers do not have current data on this (either empirical or from published papers). In order to test this, blastocysts were incubated for 1 h with MR according to the manufactures protocol and imaged immediately after or following fixation with formaldehyde at 1% for 20 minutes. As seen in *Figure 3.17* no apparent difference was found between MR staining with or without fixation. Thus, in the following experiments using MR, embryos were incubated with MR and LysoTracker green or BSA-BODIPY and, following fixation, with CellMask and DAPI staining.

In summary, MR was reconstituted to a concentrated stock solution at 260X: by adding DMSO and stored at -20°C. When ready to stain the embryos, MR stock was diluted 1:10 in distilled H_2O to form the staining solution at 26X and finally diluted 1:26 in KSOM. Drops of this final solution were pre-calibrated at 37°C covered with mineral oil.

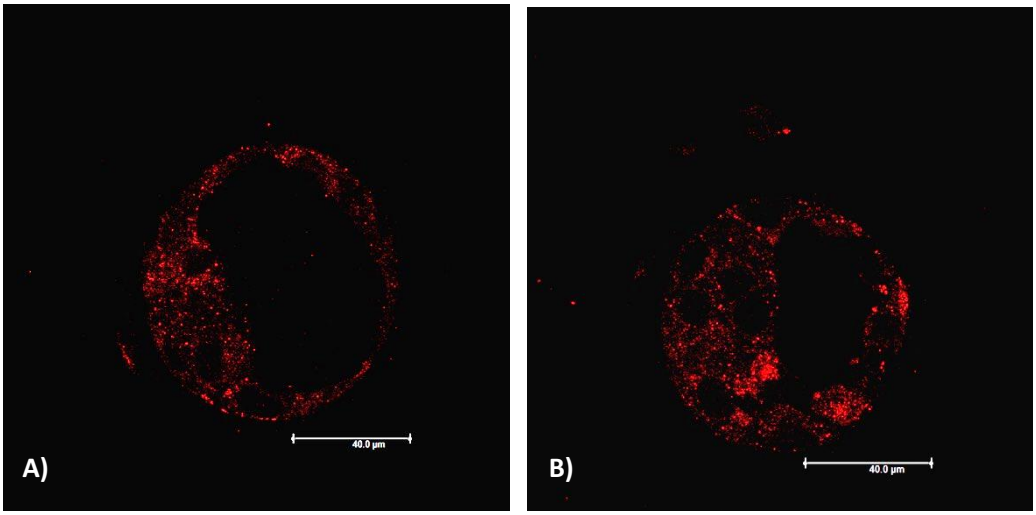

Figure 3.17 – Blastocysts stained with Magic Red after fixation (A) or imaged live (B). Transections of blastocysts stained with Magic Red (Cathepsin B) after (A) or before (B) fixation with 1% formaldehyde. In these images it is possible to see the ICM towards the left corner of both images and no staining in the blastocoel. Scale bar = 40 µm.

3.4 Discussion

Different studies have been conducted on the embryonic endocytic processing system by tracing the distribution of different molecules or complexes, using for example isotope-labelled proteins such as BSA (Pemble and Kaye, 1976) which is a common endocytic cargo, and which typically ends up being degraded by proteases in the lysosome. In contrast, the BSA-BODIPY used in this study consists of BSA heavily labelled with a fluorescence dye (BODIPY FL). The high local concentration of the fluorophore on BSA causes prominent self-quenching of the dye conjugate. However, when the protein is degraded, the BSA releases peptide fragments that carry the fluorophores, thereby releasing the dye from self-quenching (de-quenching), giving out light. BSA-BODIPY was used for the first time to evaluate the endocytosis in blastocysts in our lab (Sun et al., 2014) in combination with LysoTracker, which stains the lysosomes. The co-localisation of both dyes in the blastocyst TE confirmed the specificity of the assay. However, BSA was restricted to the TE lysosomes, while lysosomes were present both in the TE and ICM as the tight junction seal of the TE layer prevents diffusion of the BSA-BODIPY probe towards the ICM.

Not all lysosomes stained with LysoTracker are activated lysosomes, meaning that there might be lysosomes (red) without digested BSA (green) colocalised. Moreover, it seems that lysosomes are slightly larger compared to BSA digested fragments, suggesting that several fragments might be located (colocalised) in the same lysosome. This might also explain why the number of BSA fragments (but not the combined volume) in the TE high resolution approach might differ from the total number of lysosomes. Moreover, negative controls were included in order to confirm that the fluorescent vesicles comprised BSA being degraded. These consisted of 8-cell stage embryos (instead of blastocyst) in culture in the same conditions and blastocysts incubated with BSA-BODIPY at 4°C. These controls were included since endocytosis is inhibited at this temperature and because the receptor-mediated endocytosis system only matures at 32-cell stage (Assemat, 2005), meaning that BSA cannot be effectively endocytosed before that time.

During preimplantation development, the mammalian embryo remains enclosed in the zona pellucida, a glycoprotein coat, from which it hatches prior to implantation into the receptive maternal uterine endometrium (Enders and Schlafke, 1967). Hastings et al., (1972) have shown that the ZP of the mouse and rat embryos and the extracellular coats of rabbit embryos do not appear to screen molecules on the basis of size, within the range of molecular weights of compounds normally found in the female reproductive tract. It was previously shown that ferritin, with a molecular weight of over 480,000 could access the blastomeres of all preimplantation stages (Sellens and Jenkinson, 1975). In previous studies regarding blastocysts endocytosis uptake, acid Tyrode's was used to remove the zona after the assay (Sun et al., 2014). Endocytosis is a cellular process highly sensitive to pH. After entering the cell cytoplasm, vesicles fuse with early endosomes where the proton pump ATPase transforms it into an acidic environment (pH<5). These changes in pH induce ligands to segregate from the receptors and the early endosomes become late endosomes as the environment becomes more acidic (Mellman, et al., 1986). The low pH in endosomes thus regulates the sorting of ligand from the receptor (Mellman et al., 1986). However, the effect of potential pH changes on endocytosis was not considered before. Moreover, the fact that the modified assay worked without the need of removing the zona (not only LysoTracker and BSA-BODIPY but also CellMask and DAPI can penetrate the ZP) makes it more accurate and closer to what happens *in vivo*.

CellMask was used in order to stain the TE plasma membrane, so that individual cells could be seen and further cropped out using the VOLOCITY software. Initially, embryos were imaged live, so that possible artefacts caused by fixation could be avoided. However, CellMask is only stable for 30 to 90 minutes in live cells, depending on the cell type and experimental conditions, making it impossible to image a large number of embryos, thus compromising future experiments with large N numbers, as it takes approximately 20 minutes to image each embryo (using the two different imaging approaches – half embryo and high resolution TE). Nevertheless, it was possible to compare live and fixed embryos after the endocytosis assay, confirming the specificity and further validating the assay.

All data collected from the confocal microscopy was analysed by the VOLOCITY software, which converts fluorescent signals into 3D structures. Due to confocal microscopy limitations, the data obtained per embryo are limited. Samples are imaged layer by layer with an adjustable distance between each layer. Reducing the size of this distance produces images with higher resolution. Although more accurate information can be obtained with smaller distances between layers, it also takes much more time to image the same sample as compared to a lower resolution approach with higher spaces between scans, though more information can be lost between layers. To obtain the best embryo images, the researcher will always have to compromise, taking into account the quality of image versus the time and cost of the experiment. Thus, each embryo was imaged twice, the first with a high resolution (system optimised – every 0.15 μm) where only 1 to 3 TE cells are included, and the second where half embryo is imaged (with a separation of 1 μm between each layer). In the first approach only a few cells per embryo are included, but the higher resolution of the image allows a more accurate data analysis, while in the second approach we have access to more cells per embryo, giving a more general visual idea of the staining in the embryo, but analytically more compromised.

The data obtained from both approaches were analysed using the VOLOCITY software and further compared. The half embryo method proved to be less effective, as the VOLOCITY combines objects present in different layers as being one (even though they are separated by 1 μm spacing). Moreover, in the half embryo approach the total collective volume and number of vesicles is divided by the total number of cells present in the half embryo analysed, so as to estimate the result per cell. However, while this approach might be accurate for measuring lysosomes, it is not for the BSA-BODIPY which is not present in the ICM. Nevertheless, the collective LysoTracker volume per cell measured is actually increased in the half embryo compared to the TE approach, suggesting a higher expression of LysoTracker in the ICM (which is not included in the TE scan method). This is also suggested if we consider that vesicles are being combined in this method but the number of vesicles per cell is identical to the TE high resolution approach, suggesting that the real number of lysosomes may actually be increased. Comparing the lysosome individual mean volumes from the two approaches with the

literature, it is possible to verify that the VOLOCITY results in the TE high resolution approach is much closer to the reported lysosome mean size (between 0.1 – 1.2 µm diameter; (Kuehnel, 2003)). If we assume a spherical shape, it gives approximately 0.0005-0.9 μm^3 (volume = $4/3\pi r^3$). The mean volume in the half embryo approach was 3.70 μm^3 while in the TE 1.67 μm^3. The small difference found between the mean in the TE and the stipulated lysosomal size might be due to their shape, which is not a perfect sphere (Heuser, 1989) or due to possible pitfalls from the software – it is possible that even in the TE approach the VOLOCITY programme still combines some close vesicles, counting more than one vesicle as being just one, but to a lower extent than in the half embryo method.

Taking into account the two approaches and the significant differences in the results between them, the TE high resolution method was selected as the method to be used in all future data analysis as it shows to be superior (*Table 3.1*), with more accurate vesicle number and volume measurements.

		TE high resolution method	Half embryo scan method
Vesicles number	1. BSA-BODIPY	✓	✗
	2. LysoTracker	✓	?
Collective volume	3. BSA-BODIPY	✓	✗
	4. LysoTracker	✓	?
Individual volume	5. BSA-BODIPY	✓	✗
	6. LysoTracker	✓	✗
Data obtained per embryo		✗	✓

Table 3.1 – Schematic representation of results interpretation: comparison between TE high resolution and Half embryo scan methods. Data obtained using the TE method satisfies almost all parameters as analyses are made in individual TE cells. The individual size of lysosomes is similar to the size reported in the literature (Kuehnel, 2003). The disadvantage of using this method is the fact that only a small number of cells per embryo can be analysed. Using the Half embryo scan not all data obtained are accurate, due to its lower resolution and VOLOCITY pitfalls: not allowing the analysis of an accurate number of vesicles (combined vesicles as being just one) – 1, 2, 5, 6 - and no discrimination between TE and ICM cells when dividing by total number (in the TE high resolution method no ICM cells were analysed) – 1, 3 (BSA-BODIPY is not present in the ICM). The question mark in 2 and 4 represents the assumption made by dividing by total number of cells (ICM and TE) that these cells have the same expression of lysosomes. Considering that the increased individual volume of lysosomes in this method is due to the software pitfall of combining vesicles, it is suggested that the real number and collective volume of lysosomes is increased in the Half embryo method, which in turn suggests an increased proportion of lysosomes in the ICM compared to TE. However, the TE high resolution method does not provide data on ICM content and this cannot be compared. In the Half method we have access to an increased number of cells per embryo, giving a more general visual idea of the staining in the embryo, but analytically compromised.

Chapter 4 *In vitro* analysis of embryos exposed to different concentrations of BCAA and/or insulin in culture medium

4.1 Introduction

Embryo development requires an appropriate nutrient supply to support cell growth and proliferation. Consequently, maternal malnutrition is known to affect several cellular and physiological activities by inducing epigenetic and physiological modifications in the embryo that result in later adult disease risk. The mouse maternal Emb-LPD model has been widely used. Here, maternal protein restriction during preimplantation development leads to enhanced trophectoderm (TE) and primitive endoderm (PE) endocytosis in the embryo and embryoid body (EB), respectively (Sun et al., 2014). These early cellular responses are followed by increased foetal growth, birth weight and adult adiposity in female offspring, together with high blood pressure, increased locomotory behaviour and alterations in brain neuron proportion and short-term memory (Watkins et al., 2008a; Gould et al., 2018).

The endocytic system functions as a primary nutrient transport mechanism between embryo and maternal fluid, thus, this cellular response mediated by Emb-LPD treatment is seen as a compensatory mechanism to promote survival despite the deficient dietary environment. Emb-LPD was also shown to affect later gestation, by stimulating endocytosis in the mouse visceral yolk sac (VYS) endoderm, derived from PE, to support foetal growth (Watkins et al., 2008a). Such changes in cellular endocytosis included increased uptake of extracellular ligands and increased expression and activity of the major endocytic receptor, Megalin, both in the Emb-LPD VYS (Watkins et al., 2008) and blastocysts (Sun et al., 2014).

Studies comparing NPD and Emb-LPD maternal serum in rat and mouse models showed depleted levels of insulin and AAs, particularly the BCAAs - leucine, isoleucine and valine - within the Emb-LPD serum during the period of blastocyst morphogenesis (Eckert et al., 2012; Kwong, et al., 2000). Eckert et al., (2012) showed also BCAA depletion in the Emb-LPD uterine fluid by approximately 25 to 30% during the time of blastocyst

formation and expansion, coinciding with an increase in the blastocyst TE cell number. BCAAs and insulin are involved in the mTORC1 signal transduction pathway regulating cellular growth (Wang and Proud, 2009) and both have been shown to stimulate preimplantation embryo biosynthetic activity, cell proliferation and endocytosis, and promoting foetal growth (Kaye and Gardner, 1999; Lane and Gardner, 1997; Dunglison and Kaye, 1995; Dunglison et al., 1995). Moreover, blastocysts use mTORC1 signalling (through AA regulation) to regulate TE motility (Gonzalez et al., 2012; Martin and Sutherland, 2001).

In response to the Emb-LPD environment of low insulin and BCAA levels, blastocysts show a reduction in mTORC1 signalling (Eckert et al., 2012) accompanying increased proliferation, endocytosis and invasive phenotype in TE (Eckert et al., 2012; Sun et al., 2014). Interestingly, 2-cell stage mouse embryos cultured *in vitro* until blastocyst stage in media containing a 50% reduction of BCAA (as compared to the concentrations found in the NPD maternal uterine fluid), mimic the Emb-LPD environment and activate postnatal adverse health programming (Velazquez et al., 2017), suggesting a compensatory mechanism to safeguard nutrient provision but with critical long-term consequences as seen in embryos from the Emb-LPD model.

In this chapter I study which metabolite deficiencies precisely activate the stimulated endocytosis response *in vitro* using culture media with different concentrations and combinations of BCAAs and insulin, and also assess at what stage of embryo development this activation occurs. I have used BSA-BODIPY, LysoTracker and Magic Red™ Cathepsin B to study endocytosis, to compare lysosome numbers and lysosome activation in different groups as described in Chapter 3. Albumin, used in this study in the form of the dye BSA-BODIPY, is usually endocytosed by the Megalin-Cubilin complex. Thus, I assess the expression of the endocytic receptor Megalin and Clathrin (Megalin receptor mediated endocytosis is Clathrin-dependent) in blastocysts from our *in vitro* culture model. Finally, I study the role of BSA in early cleavage embryos and during the endocytosis assay in activating stimulated endocytosis.

4.2 Materials and Methods

4.2.1 Animals

MF1 females were derived and mated as described in *section 2.1 Animals.*

4.2.2 Embryo collection

E1.5 embryos were collected as described in *section 2.1.1.*

4.2.3 In vitro embryo culture

2-cell stage embryos (E1.5) collected from mice fed chow diet were cultured in KSOM medium with variable BCAA and/or insulin concentrations at 37°C in 5% CO_2 until reaching the blastocyst (or morula) stage.

4.2.3.1 Amino Acids Stocks

The KSOM medium frequently used in our laboratory is prepared with commercial solutions of essential and non-essential AAs. However, since in the following experiments the concentration of BCAAs (either the three together or each one individually) was changed in order to study the effect of low versus normal BCAA on blastocyst endocytosis, all AAs were prepared and stocked manually for up to 2 months at 4°C, in order to prepare the KSOM with the different AAs required. *Appendix 8.2.3.* reports the suppliers, molarity and concentrations to prepare each AA stock used for making KSOM.

4.2.3.2 KSOM media with altered BCAA concentration

Embryos from each mother were equally distributed in a random way across all treatment groups used in individual experiments. In all experiments control medium consisted of KSOM with 1 ng/ml insulin and the AA concentration found in E3.5 NPD uterine fluid (Eckert et al. 2012), including the three BCAA – leucine (0.32 mM), isoleucine (0.21 mM) and valine (0.46 mM) (*Appendix 8.2.3.)*. In the first experiment, one treatment included a 50% decreased BCAA concentration (LBCAA) and another where BCAAs were omitted (0BCAA), both compared to the control (NBCAA), and all

supplemented with 1 ng/ml insulin (*Figure 4.1*). In the second experiment, 2-cell stage embryos were cultured in 5 different groups. The same NBCAA as previously; a group with normal BCAA concentration but 50% decreased insulin concentration (0.5 ng/ml; L-INS); and three groups each with an individual BCAA decreased by 50% (L-LEU, 0.16 mM; L-ISO, 0.105 mM; and L-VAL, 0.23 mM) all with normal insulin (1 ng/ml). A third group of conditions tested included a single BCAA reduced by 50% as well as insulin compared to the NPD uterine fluid concentrations (L-ISO/L-INS or L-LEU/L-INS); two BCAA reduced by 50% as well as insulin, compared to the NPD uterine fluid concentrations (L-ISO/L-LEU/L-INS); or with all BCAA and insulin reduced by 50% (LBCAA/L-INS). All experiments were repeated at least four times.

After culture, embryos were incubated for 1 h at 37°C in 5% CO_2 in the same medium but containing BSA-BODIPY (0.5 mg/ml) and LysoTracker (100 nM) or Magic Red™ Cathepsin B.

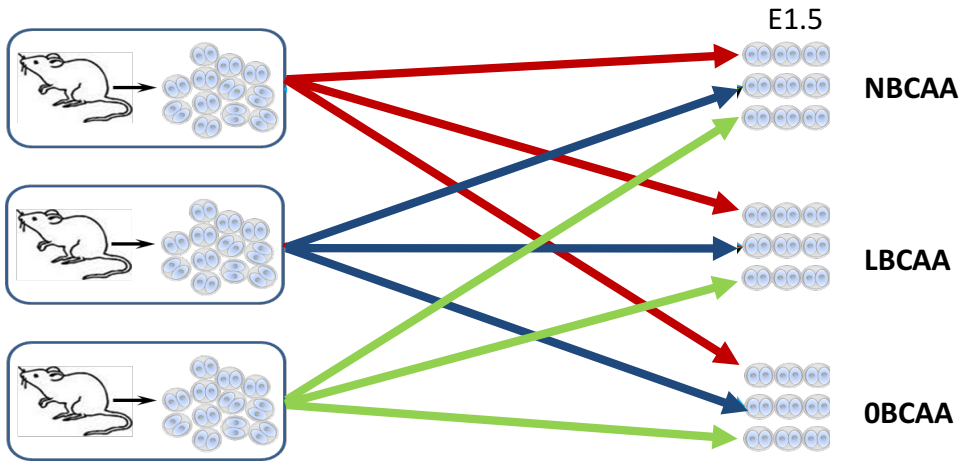

Figure 4.1 – Schematic representation of the experimental design for BCAAs experiments. Embryos collected from each mother (2-cell stage) are equally and randomly distributed across all treatment groups, shown here for Experiment 1 as described above.

4.2.4 Endocytosis Assays

The endocytosis assays used are described in detail as follows: BSA-BODIPY (*3.2.3.1. – Self-Quenched BODIPY FL Conjugate BSA BSA-BODIPY*), Lysotracker (*3.2.3.2. – Lysosome staining with LysoTracker Red DND-99*), Magic Red (*3.2.3.3. – Activated lysosomes activity – Magic RedTM Cathepsin B*).

4.2.5 Immunohistochemistry

After culture from 2-cell stage to blastocyst, embryos were fixed in 1% formaldehyde in PBS. Antibodies used for immunolabelling were: mouse monoclonal to megalin (Protein G purified, 1:400) (Meads and Wild, 1993) and rabbit polyclonal to clathrin (Cell Signaling P1663, 1:400). The protocol is described in *2.3*. For these experiments, the zona pellucida was not removed.

4.2.6 Image acquisition and data analysis

The VOLOCITY protocol for the endocytosis assay used to analyse data obtained from the confocal microscope is described in *3.2.7.* Statistical analysis was conducted with GraphPad Stats using One-way ANOVA test combined with Tukey's *post hoc* test for multi comparisons when data were normally distributed (or Student's t-test if only two groups analysed) or Kruskal-Wallis test with Dunn's multiple comparisons *post hoc* test when data were not normally distributed (or Mann-Whitney test if only two groups analysed). For all correlation analysis, correlation coefficient (R) was analysed as well as R^2 and P value. Significance was taken as $P < 0.05$ and a trend was assumed if P was between 0.1 and 0.051.

4.2.7 Single embryo RNA extraction and RT reaction

Described in *Methods 2.5*.

4.2.8 Single embryo qRT-PCR

Described in *Methods 2.6*.

4.2.9 Multiplex PCR and embryo genotyping

Described in *Methods 2.7*.

4.3 Results

4.3.1 Embryo culture with three depleted BCAAs does not alter the endocytosis rate in early blastocysts

Embryos from chow-fed mothers were collected at E1.5 (2-cell stage) and cultured until blastocyst stage (~48 h) either in KSOM medium with AAs and insulin at a concentration found in the NPD uterine fluid (Eckert et al., 2012); medium with low BCAAs (LBCAA) reduced by 50% compared to NPD uterine fluid concentrations; or absent (0BCAA) BCAAs. At the blastocyst stage, embryos were examined for endocytosis using the BSA-BODIPY and Lysotracker assay and imaged using the TE high resolution method.

No differences were found in embryo development in culture between groups *(Figure 4.2* and *Figure 4.3*) nor cell number in blastocysts used in the assays (*Figure 4.4)*. As expected from the results shown in *Chapter 3 – Protocol optimisation*, labelled vesicles (lysosomes and degraded protein) were mainly co-localised around the TE nucleus from all three groups. The collective vesicle volume and number were analysed in the TE high resolution approach, as well as the individual vesicle average volume and their mean distance to the cell nucleus. In the TE high resolution method, no significant difference was found between the groups in any of the experiments, although both the mean number and collective volume of lysosomes per cell were slightly increased (not statistically significant) in the LBCAA group compared to both the NBCAA and 0BCAA (*Figure 4.5).* In fact, when the lysosome individual volume was measured, the LBCAA mean value was slightly decreased (not statistically significant) which suggests that a possible increase in mean collective volume is due to an increase in mean number of vesicles and not an increase in mean vesicle size.

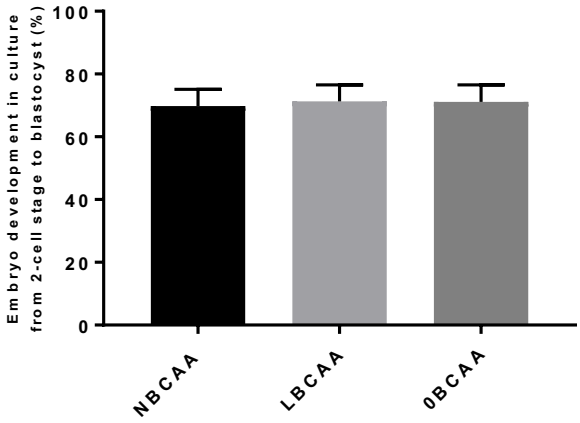

Figure 4.2 – Embryo development in culture from 2-cell stage until blastocyst. Percentage (%) of embryos that reached blastocyst stage in culture after 48 h. Morulae or arrested embryos at that time point were not used. 24-31 embryos per group (total number of cultured embryos) from 9 mothers in 7 experiment repeats.

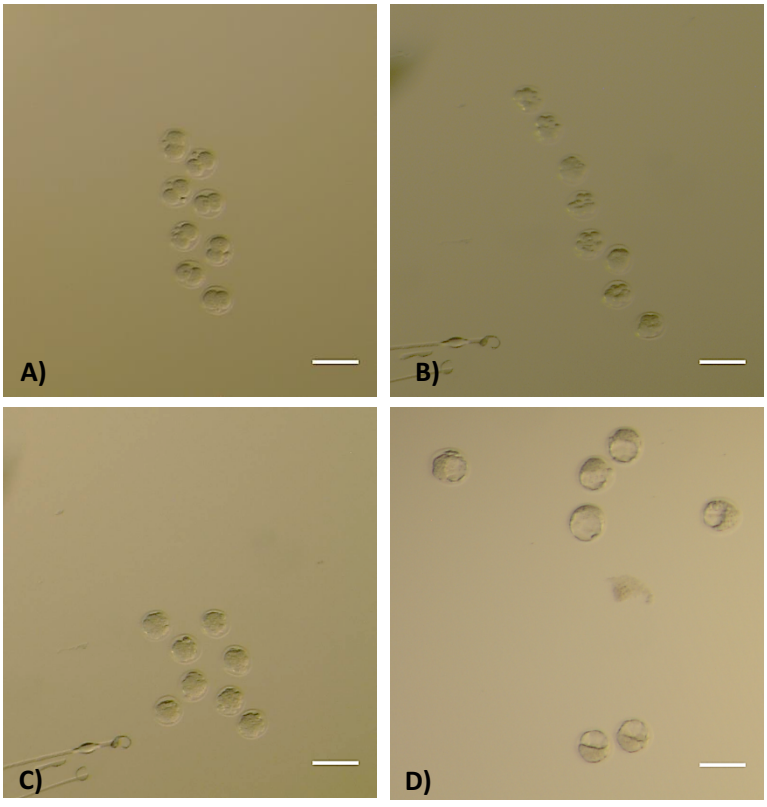

Figure 4.3 - Representative *in vitro*-derived blastocysts from the control group (NBCAA) (scale bar =100 µm). A) 2-cell embryos were *in vitro* cultured for 48 h up to the blastocyst stage (D); B) Embryos after 24 h in culture; C) Morulae after 36 h in culture.

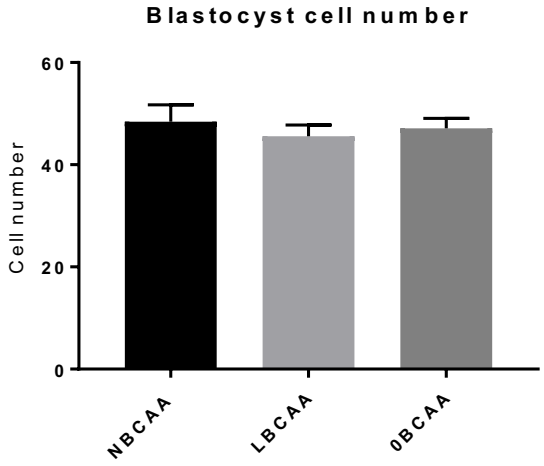

Figure 4.4 - Blastocyst cell number is not affected after culture in different media from 2-cell stage. Cells were counted based on DAPI positive staining. Values are mean ±SEM. 18-22 embryos per group from 9 mothers (in 7 replicates).

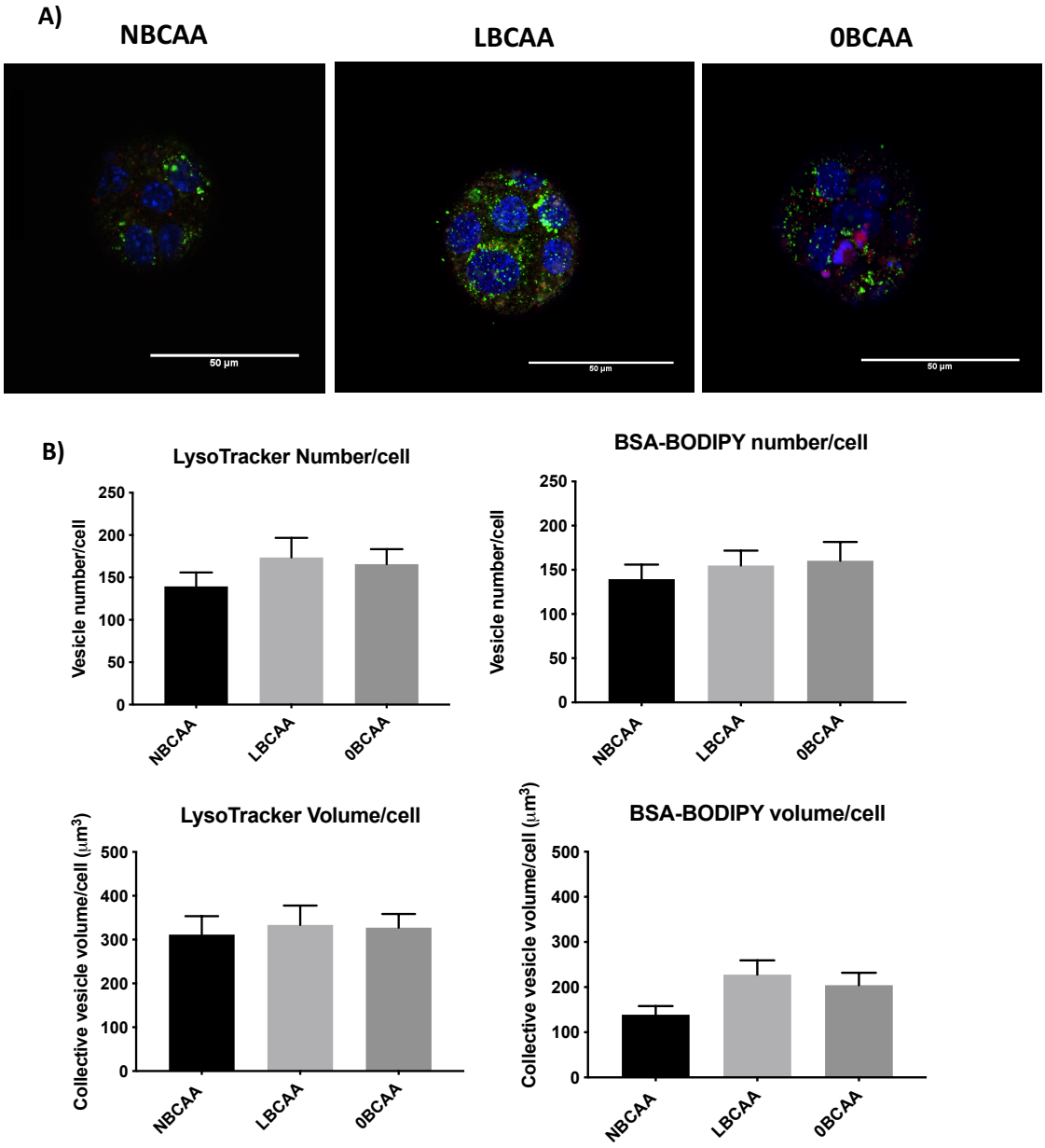

Figure 4.5 – Blastocysts cultured in vitro from 2-cell stage do not show altered endocytosis in response to depleted (50%, LBCAA) or absent (0BCAA) BCAAs in the culture medium compared to control (NBCAA). A) Representative blastocysts imaged for BSA-BODIPY (green), LysoTracker (red) endocytosis assays and nuclei (DAPI, blue) following culture in the three treatments using the TE high resolution scan. Scale bar = 50 µm. B) LysoTracker and BSA-BODIPY vesicle number and collective volume (μm^3) per TE cell. Values are presented as mean ±SEM. 18-22 embryos per group (37-58 cells per group) from 9 mothers (in 7 replicates).

To determine if vesicle size was changed, the average volume of individual vesicles (BSA-BODIPY and LysoTracker) was assessed. As shown in *Figure 4.6*, mean volume of both vesicles did not change significantly. The average size of the measured BSA-BODIPY fragments after digestion is approximately half that of LysoTracker vesicles.

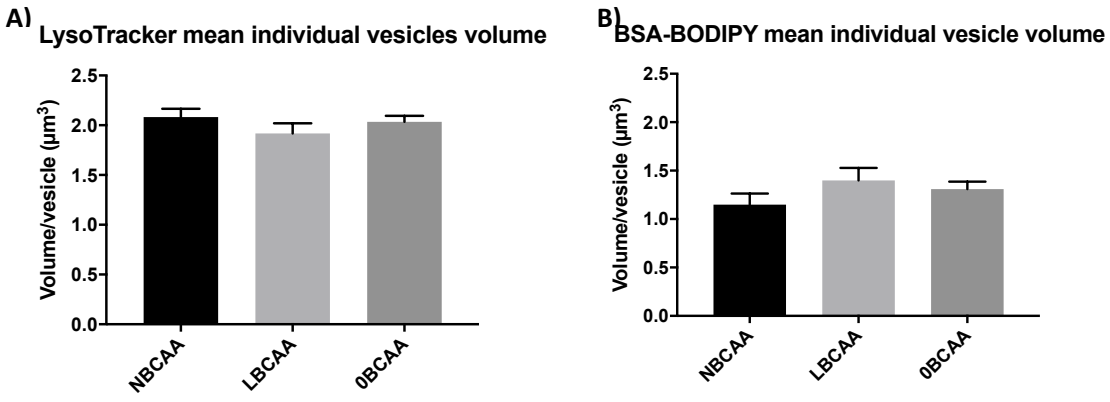

Figure 4.6 – Blastocyst mean individual vesicle volume of LysoTracker (A) and BSA-BODIPY (B) vesicles was not altered in response to 50% depletion (LBCAA) or absence (0BCAA) of BCAA from the culture medium (embryos cultured from 2-cell stage). In the TE high resolution approach, mean vesicle volume did not differ between treatments. The average size of BSA-BODIPY particles visualised after digestion is approximately half that of LysoTracker vesicles. Values are presented as mean ±SEM. 18-22 embryos per group (37-58 cells per group) from 9 mothers (in 7 replicates).

The distance between the centre of labelled vesicles (BSA-BODIPY and LysoTracker) and the edge of the nucleus was measured in each TE cell (*Figure 4.7*). No significant difference was found between the three culture treatments (NBCAA, LBCAA and 0BCAA).

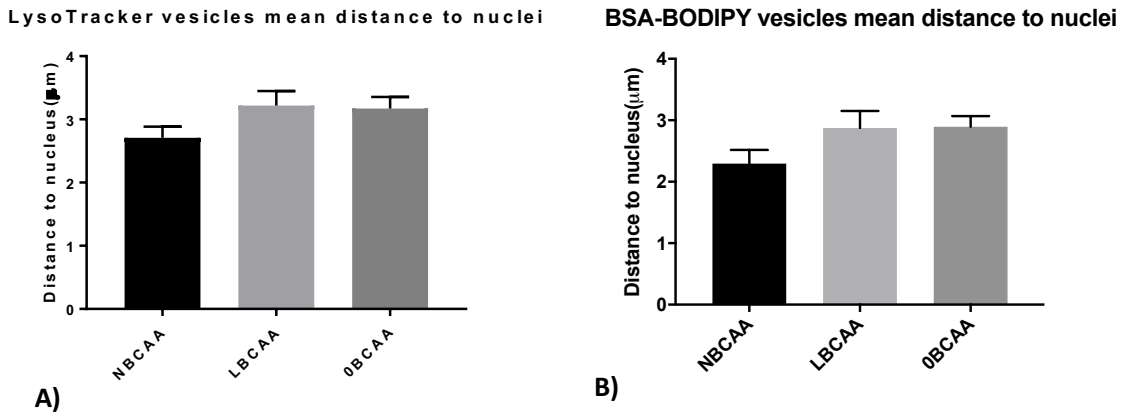

Figure 4.7 – Culture treatment had no effect on the distribution of labelled vesicles of LysoTracker (A) or BSA-BODIPY (B) within TE cells with respect to distance from nucleus. Values are presented as mean ±SEM. 18-22 embryos per group (37-58 cells per group) from 9 mothers (in 7 replicates).

4.3.2 Embryos cultured with Isoleucine depletion show increased endocytosis and increased expression of endocytic receptors

Embryos from chow-fed mothers were collected at E1.5 (2-cell stage) and cultured until blastocyst stage (~48 h) in five KSOM media with different BCAA and/or insulin concentrations. The control group consisted of AAs and insulin at a concentration found in the NPD uterine fluid and serum respectively (NBCAA/N-INS) (Eckert et al., 2012). Tested culture medium consisted of three groups with one BCAA individually reduced by 50% compared to the NPD uterine fluid concentrations and normal insulin (L-VAL/N-INS, L-LEU/N-INS and L-ISO/N-INS) and a fifth group with normal concentration of BCAAs but 50% decreased insulin (NBCAA/L-INS).

No differences were found in embryo development in culture between groups (*Figure 4.8*) nor in blastocyst cell number (*Figure 4.9*). At blastocyst stage, embryos were examined for endocytosis using the BSA-BODIPY and LysoTracker assays and imaged using the TE high resolution scan. The VOLOCITY analysis showed that in the L-ISO/N-INS group there was an increased mean number of lysosomes and significantly increased BSA-BODIPY positive vesicle number (*Figure 4.10*) compared to the control NBCAA/N-INS and also compared to L-VAL/N-INS and NBCAA/L-INS. LysoTracker collective volume in the TE cells was increased (1.5-fold) and BSA-BODIPY vesicle volume significantly increased (1.7-fold) in the L-ISO/N-INS group compared to the NBCAA/N-INS. No difference was found between L-VAL/N-INS, L-LEU/N-INS or NBCAA/L-INS and the control NBCAA/N-INS. However, L-LEU/N-INS consistently showed a non-significant increase in LysoTracker and BSA-BODIPY mean vesicle number and collective volume per TE cell compared with that of NBCAA/N-INS, appearing intermediary to the effects shown for L-ISO/N-INS (*Figure 4.10*). To determine if the collective volume change reflected an increase in total number of vesicles and/or an increase in the mean volume of individual vesicles, these factors were also analysed. As shown in *Figure 4.11*, the mean volume of individual BSA-BODIPY and LysoTracker vesicles did not differ between the five culture treatments. This indicates that the increase in vesicle number in the L-ISO/N-INS group explains the increase in collective volume in this group. Collectively, these data indicate embryo endocytosis was increased responding to reduced isoleucine alone in the culture medium.

The average distance of both vesicles (BSA-BODIPY and LysoTracker) to the nucleus was not altered (*Figure 4.12*). To determine if the changes found in LysoTracker vesicle number in the L-ISO/N-INS group was concordant with changes in lysosomal activation, MagicRed staining was used as a marker for Cathepsin B. In the L-ISO/N-INS group there was a significant increase in MagicRed staining as compared to the NBCAA/N-INS (*Figure 4.13).* MagicRed vesicle collective volume per cell was significantly increased and their number per cell increased at trend level ($P< 0.1$) in the L-ISO/N-INS group but their individual size per cell was not changed (*Figure 4.14*), indicating the increase seen in collective volume is due to an increase in their number. The total cell number from blastocysts analysed from both groups was not different (*Figure 4.15*) – this experiment was a repeat experiment and cell number analysis differs from *Figure 4.9* as different embryos from different mothers were used here, cultured in only two treatment conditions (control NBCAA/N-INS and L-ISO-N-INS) prior to MagicRed staining.

To investigate if the endocytosis upregulation seen in embryos cultured *in vitro* in L-ISO/N-INS from 2-cell to blastocyst stage coincides with increased expression of endocytic receptors, megalin was analysed by immunocytochemistry (*Figure 4.17*). Immunocytochemistry protocol was optimised using embryos collected at different developmental stages (*Figure 4.16*). Megalin was concentrated along the apical surface of TE cells as well as within vesicles in the apical cytoplasm (*Figure 4.17*). Its fluorescent intensity was analysed using the VOLOCITY software in voxel units (unit of pixel but in 3D) – top TE cells were analysed for total voxels in each fluorescent channel.

Clathrin facilitates endocytic vesicles containing receptors such as megalin to enter the cells by forming coated pits. Thus, I examined clathrin protein expression in the same blastocysts (double labelling – clathrin and megalin) cultured from 2-cell stage in either NBCAA/N-INS or L-ISO/N-INS. Clathrin is present mainly in the apical surface of TE cells (in the cell membrane) but it is also present in the cytoplasm (*Figure 4.17).* Megalin and clathrin signal intensity was increased in L-ISO/N-INS blastocysts TE (*Figure 4.17).*

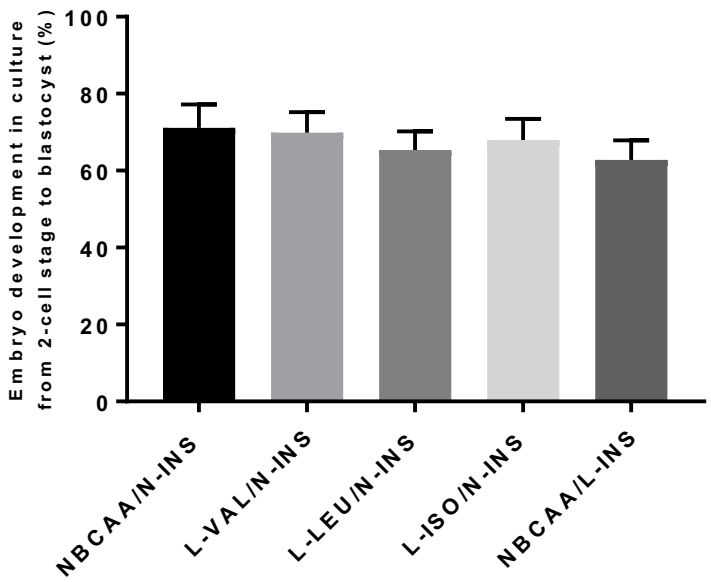

Figure 4.8 - Embryo development in culture from 2-cell stage until blastocyst. Percentage (%) of embryos that reached blastocyst stage in culture after 48 h. Morulae or arrested embryos at that time point were not used. 27-34 embryos per group (total number of cultured embryos) from 13 mothers in 10 replicates.

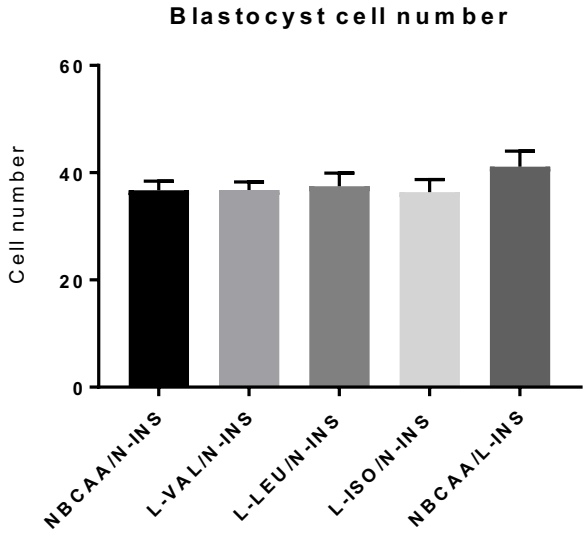

Figure 4.9 - BCAAs reduced individually by 50% (L-VAL/N-INS, L-LEU/N-INS and L-ISO/N-INS) and insulin reduced individually by 50% (NBCAA/L-INS) in the culture media had no effect on cell number of blastocysts in mice. In this experiment, cells were counted (DAPI positive

staining) only in the half embryo approach method, thus not representing the total number of cells in the blastocysts analysed. Values are presented as mean ±SEM. *P value <0.05; 17-24 embryos per group from 13 mothers (in 10 replicates).

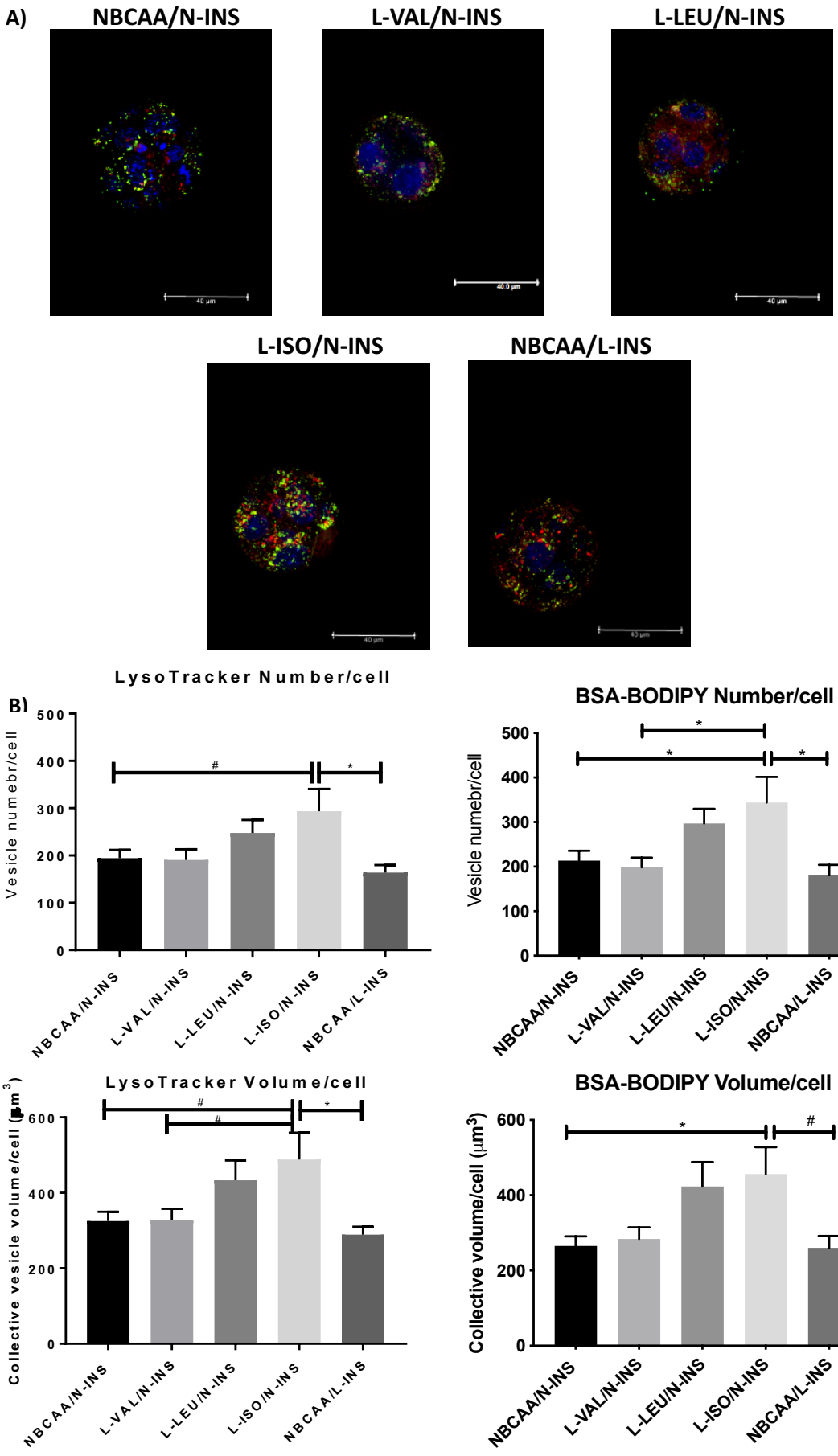
A)
NBCAA/N-INS
L-VAL/N-INS
L-LEU/N-INS
L-ISO/N-INS
NBCAA/L-INS
B)
LysoTracker Number/cell
Vesicle numebr/cell
BSA-BODIPY Number/cell
Vesicle numebr/cell
LysoTracker Volume/cell
Collective vesicle volume/cell (μm3)
BSA-BODIPY Volume/cell
Collective volume/cell (μm3)
NBCAA/N-INS
L-VAL/N-INS
L-LEU/N-INS
L-ISO/N-INS
NBCAA/L-INS

Figure 4.10 – Endocytosis is increased in blastocyst TE following culture from 2-cell stage in media with depleted Isoleucine alone and normal insulin (L-ISO/N-INS). A) Blastocysts after BSA-BODIPY (green) and LysoTracker (red) endocytosis assay and nuclei (DAPI, blue) staining following culture in different BCAAs concentrations - either at the level found in NPD uterine fluid (NBCAA), or with one BCAA individually reduced by 50% compared to NBCAA (L-VAL/N-INS, L-LEU/N-INS and L-ISO/N-INS) or with normal concentration of BCAAs but 50% decreased insulin (L-INS). Scale bar = 40 μm. B) LysoTracker and BSA-BODIPY vesicle number and collective volume (μm^3) per TE cell. Endocytosis is stimulated in the L-ISO/N-INS group but not in the other treatment groups. Values are mean ±SEM. *P <0.05; #P <0.1; 17-24 embryos per group (30-55 cells per group) from 13 mothers (in 10 replicates).

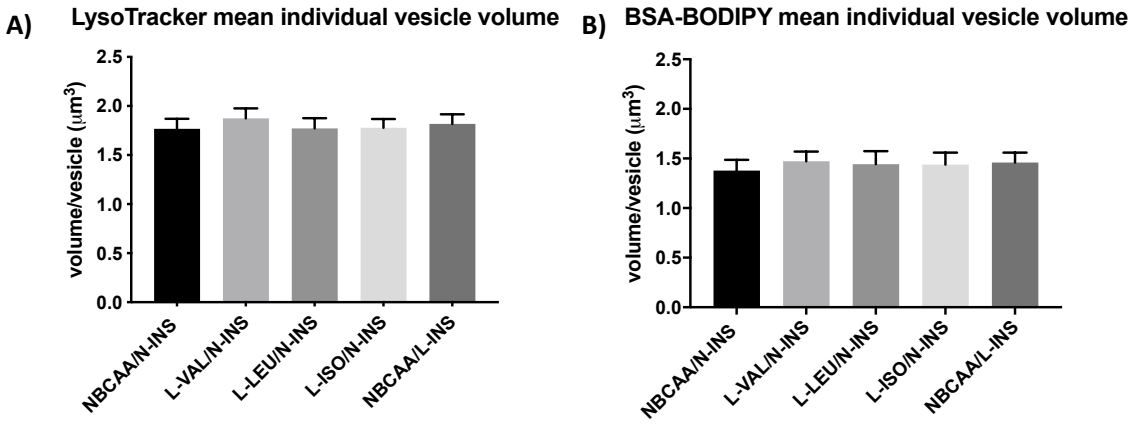

Figure 4.11 - Blastocyst individual LysoTracker (A) and BSA-BODIPY (B) vesicle volumes were not altered in response to different treatments. Embryos were cultured from 2-cell stage and analysed at blastocyst stage using the TE high resolution approach. Mean vesicle volume did not differ between groups. Values are mean ±SEM. 17-24 embryos per group (30-55 cells per group) from 13 mothers (in 10 replicates).

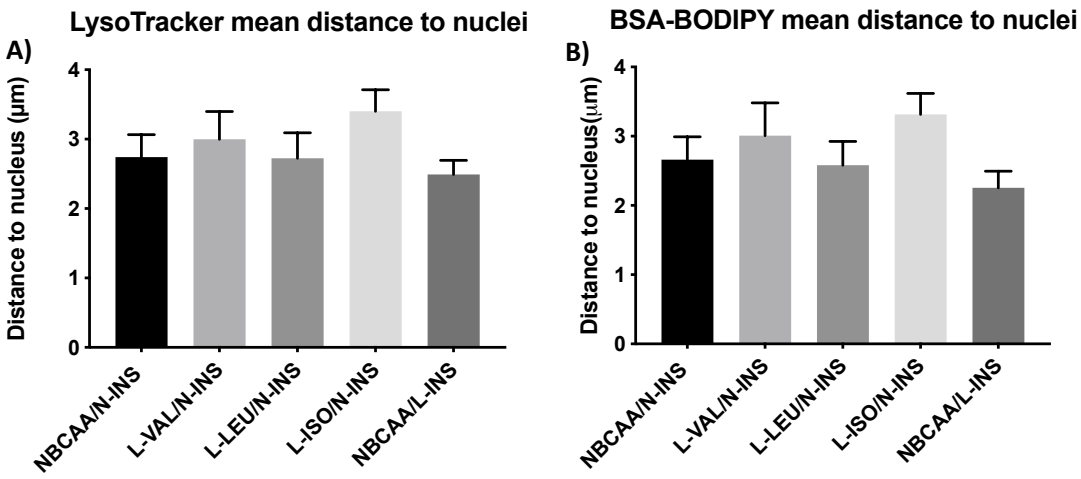

Figure 4.12 - Culture treatment had no effect on the distribution of labelled vesicles LysoTracker (A) or BSA-BODIPY (B) within TE cells with respect to distance from nucleus. Values are presented as mean ±SEM. *P value <0.05; 17-24 embryos per group (30-55 cells per group) from 13 mothers (in 10 replicates).

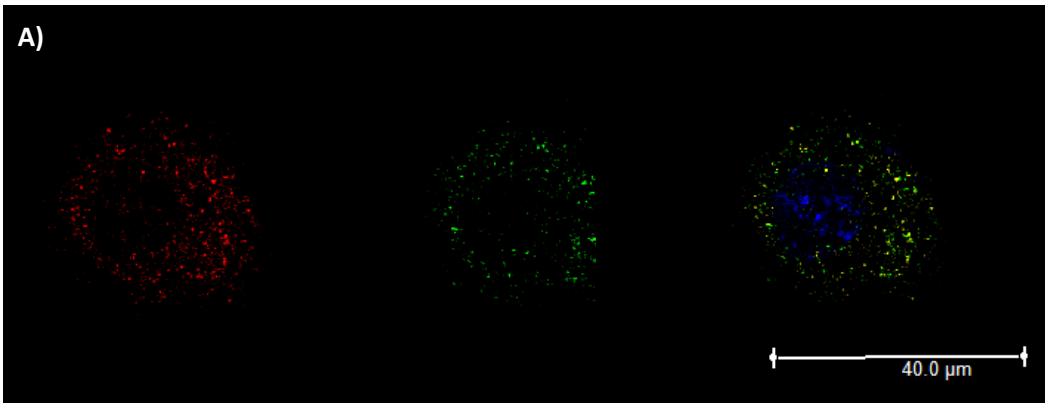

NBCAA/N-INS

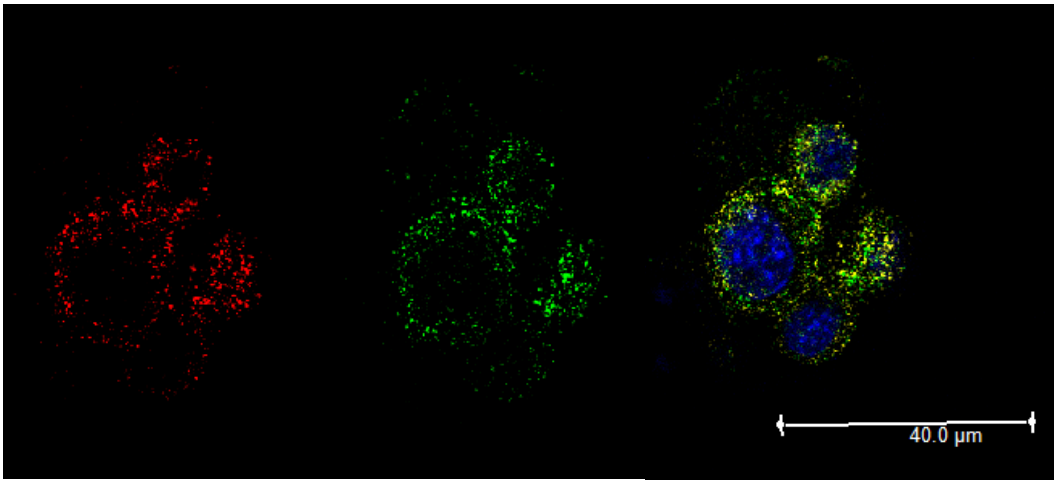

L-ISO/N-INS

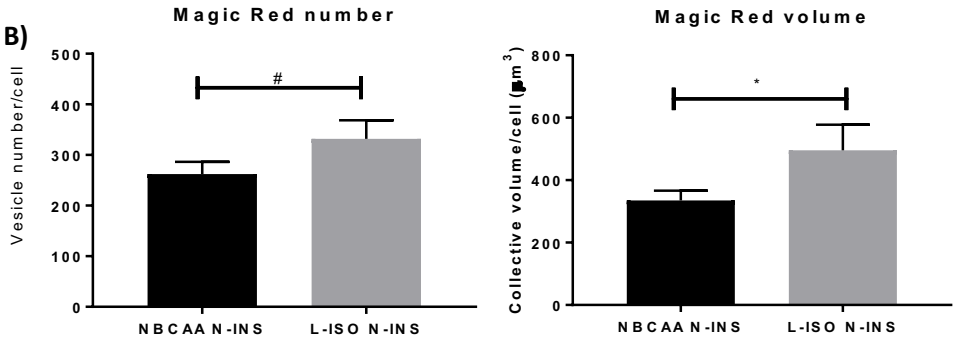

Figure 4.13 – Cathepsin B (MagicRed) expression is increased in blastocyst TE following culture from 2-cell stage in media with depleted Isoleucine A) Blastocysts after MagicRed (red) and LysoTracker (green) assay and nuclei (DAPI, blue) staining following culture in either the BCAA level found in NPD uterine fluid (NBCAA), or with less 50% of isoleucine (L-ISO). Scale bar = 40 µm. B) Cathepsin B per TE cell is increased in the L-ISO/N-INS group. Values are presented as mean ±SEM. *P value <0.05; #P value <0.1; 21-26 embryos per group from 7 mothers (in 4 replicates).

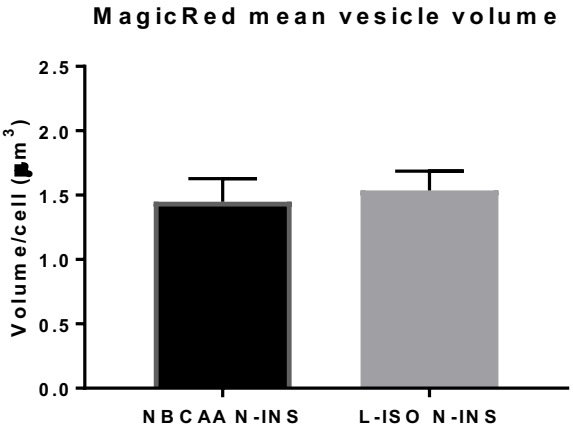

Figure 4.14 – MagicRed individual vesicle volume is not altered in response to different treatments. Embryos were cultured from 2-cell stage and analysed at blastocyst stage using the TE high resolution approach. Individual vesicle volume did not differ between groups. Values are presented as mean ±SEM. 21-26 embryos per group from 7 mothers (in 4 replicates).

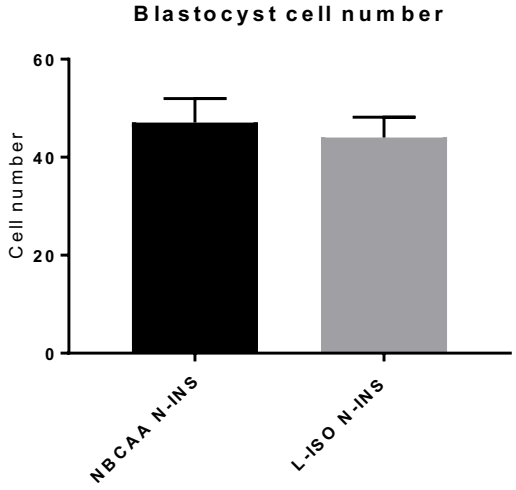

Figure 4.15 – Isoleucine reduced individually by 50% (L-ISO/N-INS) in the culture medium had no effect on cell number of blastocysts in mice. Values are presented as mean ±SEM. 21-26 embryos per group from 7 mothers (in 4 replicates).

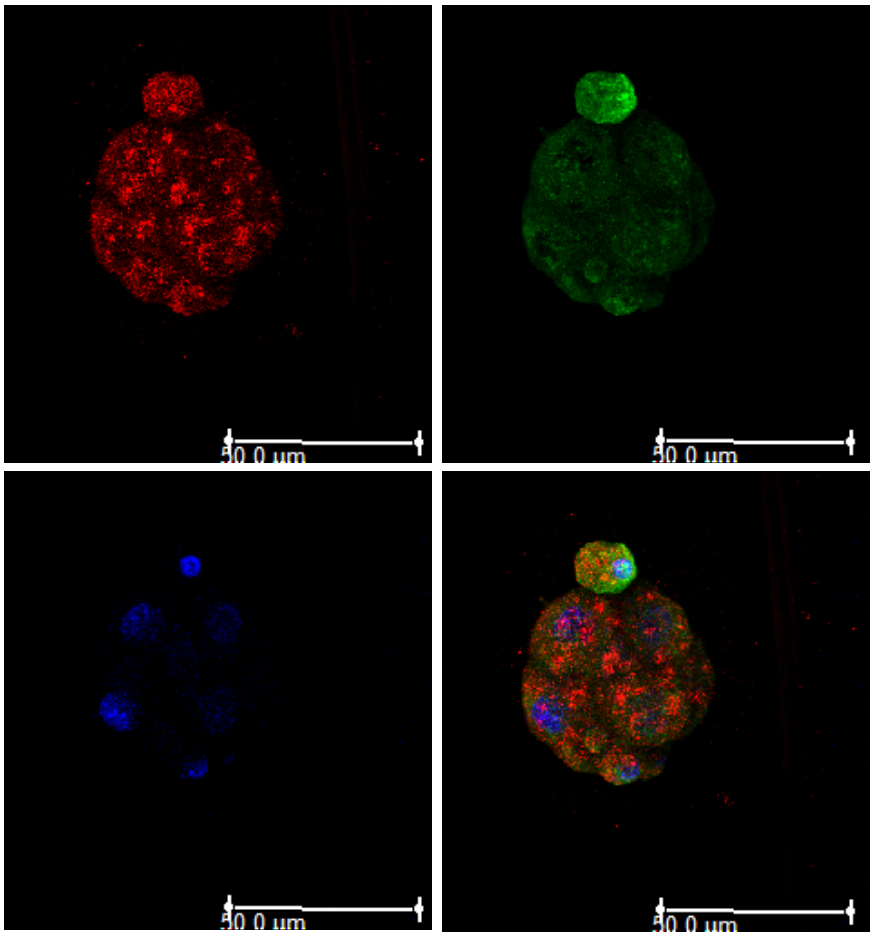

Figure 4.16 – Megalin (red) and Clathrin (green) immunohistochemistry protocol optimisation. The protocol was first optimised in embryos collected at different developmental stages. Here, a morula is shown stained with antibody concentrations used in the final experiment - Megalin (red) at 1:400, Clathrin (green) at 1:400 and secondary antibodies Alexa 568 and Alexa 488 at 1:300, respectively, and DAPI (blue). Scale bar = 40 μm.

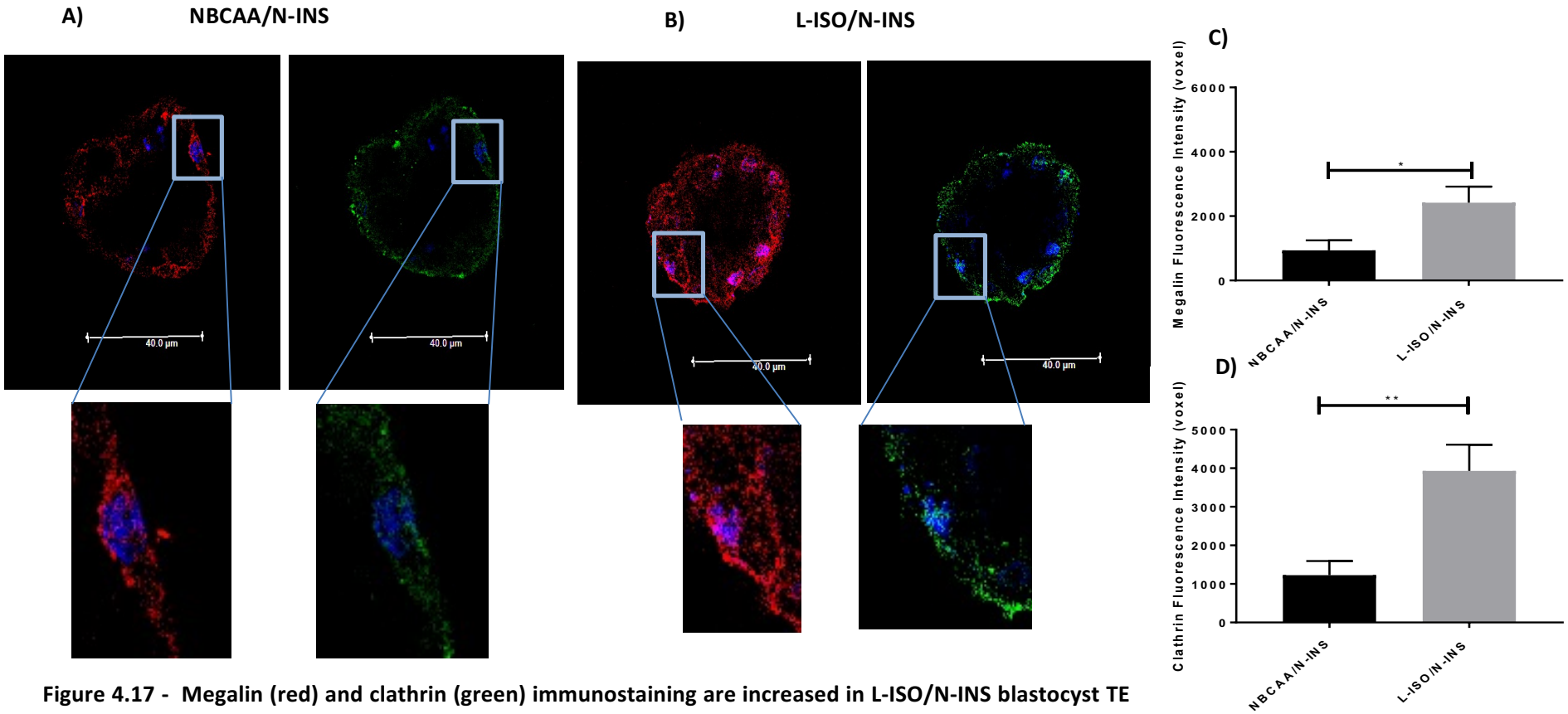

Figure 4.17 - Megalin (red) and clathrin (green) immunostaining are increased in L-ISO/N-INS blastocyst TE cells. NBCAA/N-INS (A) and L-ISO/N-INS (B) stained for megalin (red), clathrin (green) and nuclei (DAPI, blue). High magnification of TE layer is shown at the bottom, showing the markers localised to apical TE and cytoplasm. Megalin (C) and clathrin (D) staining intensity (voxels) is increased in L-ISO/N-INS blastocyst TE cells. Scale bar = 50 µm. Values are presented as mean ±SEM. *P value <0.05; **P value <0.01; 10-18 embryos per group from 6 mothers in 4 replicates.

To determine whether the increase in megalin protein was regulated at mRNA level, qRT-PCR was performed on blastocysts collected from both groups (NBCAA/N-INS and L-ISO/N-INS). Since previous studies have displayed Emb-LPD effects in a sex-dependent way (Watkins et al., 2008a), the sex of single blastocysts was identified using multiplex PCR (*see Methods 2.7.1*). However, due to the low number of female embryos identified, qRT-PCR was performed on male blastocysts only (see *Table 2.5*) (n = 10 mothers per group). Gene expression was normalised using H2afz and Sdha as reference genes previously selected by geNorm analysis (*See Methods 2.6.2*). qPCR was performed using primer assays previously optimised and verified beforehand using gel electrophoresis and melting curve analysis (*See Methods 2.6.1 and 2.6.3*). *Appendix 8.7* shows the gel electrophoresis for the qRT-PCR products.

Megalin mRNA expression did not show significant differences between culture treatments in male blastocysts (*Figure 4.18*).

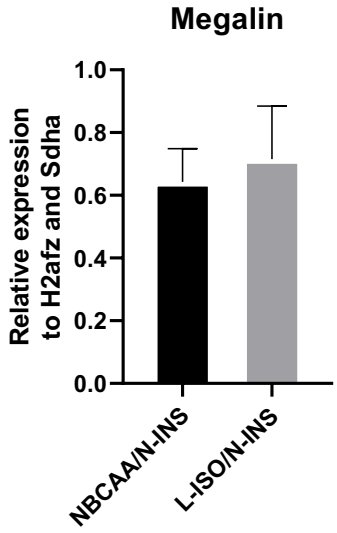

Figure 4.18 – Relative mRNA levels of Megalin in male blastocysts cultured in NBCAA/N-INS and L-ISO-N-INS from 2-cell until blastocyst stage (N = 10 embryos/group from 10 mothers). Values are presented as mean ± SEM.

4.3.3 Embryos cultured with a combination of Insulin and BCAA depletion show increased endocytosis

Embryos from chow-fed mothers were collected at E1.5 (2-cell stage) and cultured until blastocyst stage (~48 h) in six different KSOM media with different BCAA and/or insulin concentrations. The control group consisted of AAs and insulin at a concentration found in the NPD uterine fluid and serum respectively (NBCAA/N-INS) (Eckert et al., 2012). Tested culture media consisted of individual BCAA and insulin reduced by 50% compared to NBCAA/N-INS (L-ISO/L-INS or L-LEU/L-INS), a combination of two BCAA as well as insulin reduced by 50% compared to NBCAA/N-INS (L-ISO/L-LEU/L-INS) or with all BCAA and insulin reduced by 50% (LBCAA/L-INS). The group L-ISO/N-INS was used as a positive control, as in previous experiments this treatment induced a significant increase in endocytosis (*Figure 4.10*). As in the previous experiments, at the blastocyst stage, embryos were examined for endocytosis using the BSA-BODIPY and LysoTracker assay and imaged using the TE high resolution scan method. The different culture conditions tested did not affect blastocyst development (*Figure 4.19*) or blastocyst cell number (*Figure 4.20)*.

The VOLOCITY analysis showed that in the L-ISO/N-INS group, there was a trend for increased BSA-BODIPY vesicle number ($P = 0.06$) and a significant increase in BSA-BODIPY vesicle collective volume per cell ($P = 0.009$) compared with NBCAA/N-INS. In addition, a significant increase in BSA-BODIPY vesicle number was present in the L-ISO/L-LEU/L-INS group ($P = 0.04$) and a trend for increased collective volume for BSA-BODIPY vesicles per cell in this group ($P = 0.055$) (*Figure 4.21*). Similarly, a trend for increased collective volume for BSA-BODIPY vesicles per cell was also present in the LBCAA/L-INS group ($P=0.09$). However, other L-INS groups did show a consistent mean non-significant increase in vesicle number or collective volume compared with NBCAA/N-INS (*Figure 4.21*).

The apparent stimulation in BSA-BODIPY vesicle endocytosis in these treatment groups was broadly matched by the mean number and collective volume of LysoTracker vesicles per cell but not to statistical significance compared with control NBCAA/N-INS (*Figure 4.21)*. To determine if the collective volume changes reflected

an increase in total number of vesicles or if it reflected an increase in the mean individual vesicle volume, the individual vesicle volumes (LysoTracker and BSA-BODIPY) were analysed. As shown in *Figure 4.22*, the mean volume of both vesicles did not differ between the six culture treatments, indicating the changes in collective volume reflected an increase in number of vesicles in the L-ISO/N-INS and L-ISO/L-LEU/L-INS groups. Collectively, these data also indicate that embryo endocytosis was not altered in response to L-LEU/L-INS. The mean distance of both vesicles (LysoTracker and BSA-BODIPY) to the nucleus was not altered (*Figure 4.23*).

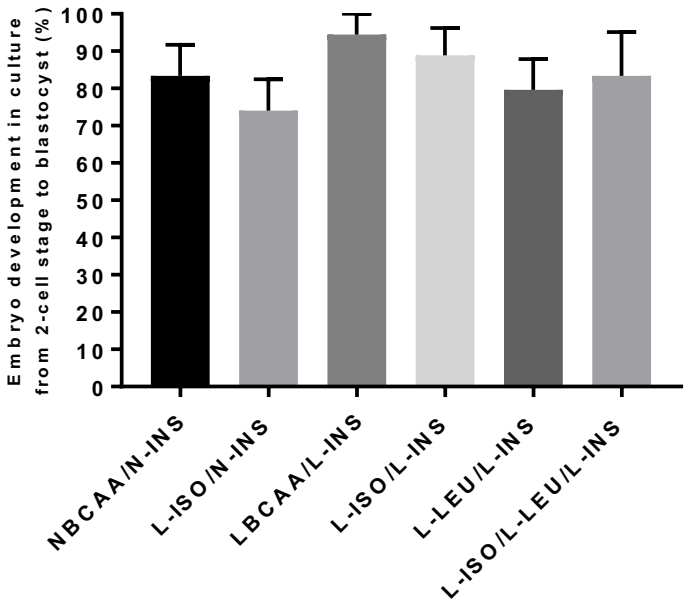

Figure 4.19 - Embryo development in culture from 2-cell stage until blastocyst. Percentage (%) of embryos that reached blastocyst stage in culture after 48 h. Morulae or arrested embryos at that time point were not used. 19-23 embryos per group (total number of cultured embryos) from 14 mothers in 8 replicates.

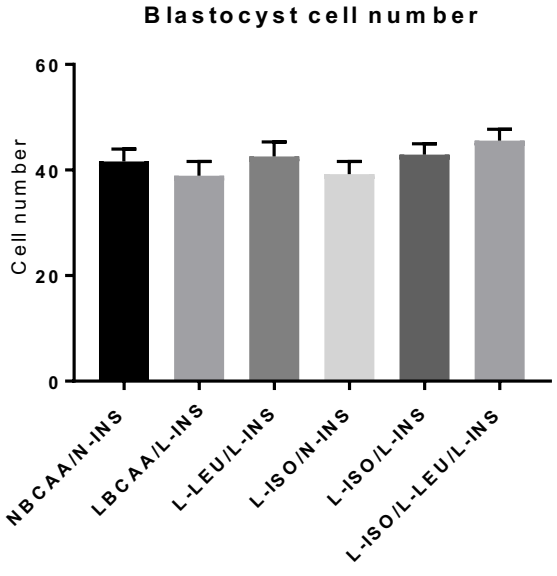

Figure 4.20 - Blastocyst cell number is not affected after culture in different media from 2-cell stage. Values are presented as mean±SEM. *P value <0.05; 13-19 embryos per group from 14 mothers (in 8 replicates).

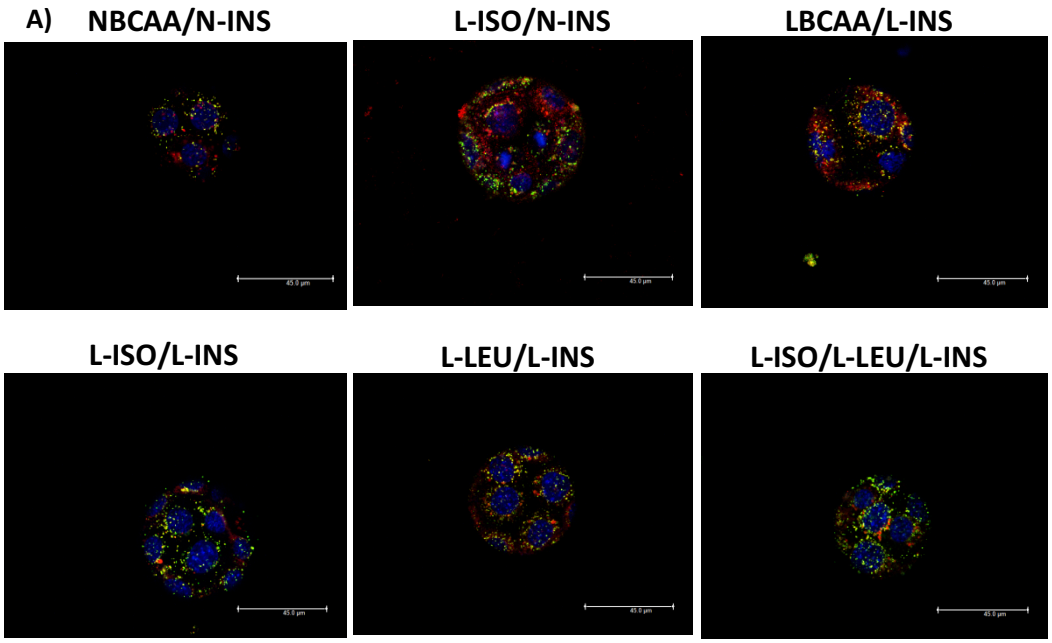
A)
NBCAA/N-INS
L-ISO/N-INS
LBCAA/L-INS
L-ISO/L-INS
L-LEU/L-INS
L-ISO/L-LEU/L-INS

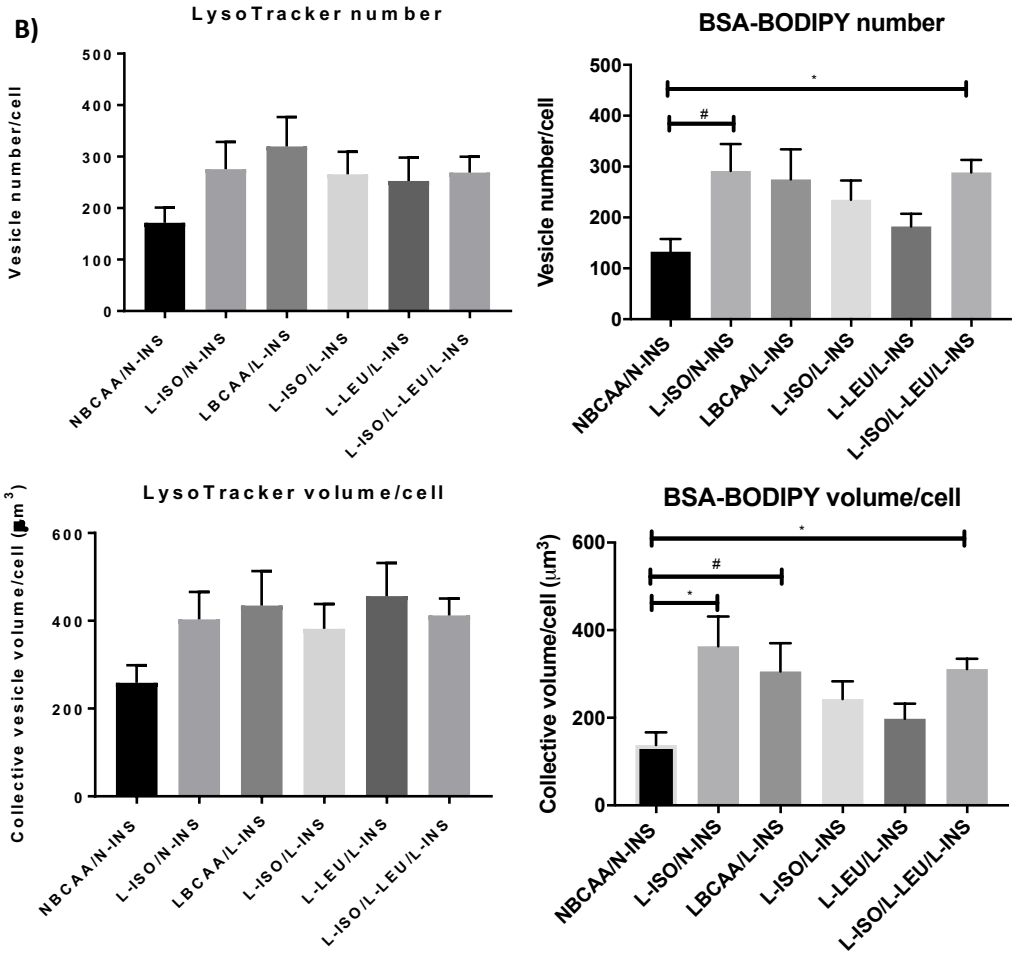
B)
LysoTracker number
Vesicle number/cell
BSA-BODIPY number
Vesicle number/cell
LysoTracker volume/cell
Collective vesicle volume/cell (μm3)
BSA-BODIPY volume/cell
Collective volume/cell (μm3)
NBCAA/N-INS
L-ISO/N-INS
LBCAA/L-INS
L-ISO/L-INS
L-LEU/L-INS
L-ISO/L-LEU/L-INS

Figure 4.21 – Endocytosis is increased in blastocyst TE following culture from 2-cell stage in media with L-ISO/N-INS and L-ISO/L-LEU/L-INS. Culture in LBCAA/L-INS increased endocytosis to a trend level. A) Representative blastocysts after BSA-BODIPY (green) and LysoTracker (red) endocytosis assay and nuclei (DAPI, blue) staining following culture in different combinations of BCAAs and insulin concentrations – BCAAs were either at the level found in NPD uterine fluid (NBCAA), with one BCAA individually reduced by 50% compared to the NPD uterine fluid concentrations (L-ISO or L-LEU), with two BCAA reduced by 50% compared to the NPD uterine fluid concentrations (L-ISO and L-LEU) or with all BCAA reduced by 50% (LBCAA) either with normal insulin (N-INS) or with 50% decreased insulin (L-INS). Scale bar = 45 μm. B) Lysosomes and BSA vesicles number and collective volume (μm^3) per TE cell. Endocytosis is stimulated in the L-ISO/N-INS and L-ISO/L-LEU groups but not significantly in the other depleted media. Embryos cultured in LBCAA/L-INS appeared to have a trend (not statistically significant) to increase endocytosis. Values are presented as mean ±SEM. *P value <0.05; #P value <0.1; 13-19 embryos per group (23-38 cells per group) from 14 mothers (in 8 replicates).

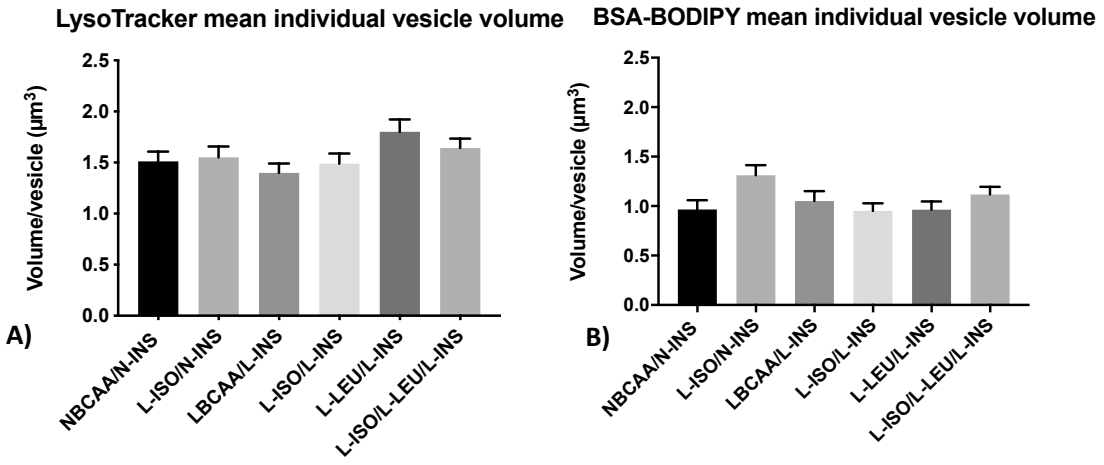

Figure 4.22 - Blastocyst individual LysoTracker (A) and BSA-BODIPY (B) vesicle volumes were not altered in response to different treatments. Embryos were cultured from 2-cell stage and analysed at blastocyst stage using the TE high resolution approach. Mean vesicle volume did not differ between groups. Values are presented as mean±SEM. 13-19 embryos per group (23-38 cells per group) from 14 mothers (in 8 replicates).

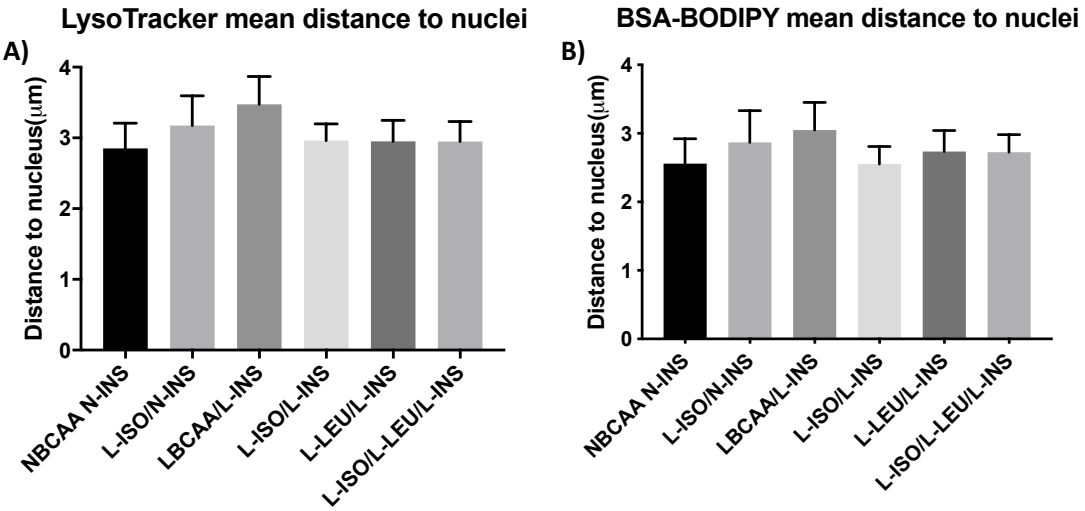

Figure 4.23 - Culture treatment had no effect on the distribution of labelled vesicles LysoTracker (A); BSA-BODIPY (B) within TE cells with respect to distance from nucleus. Values are presented as mean±SEM. 13-19 embryos per group (23-38 cells per group) from 14 mothers (in 8 replicates).

4.3.4 LysoTracker vesicle stimulation mediated by isoleucine depletion in vitro is not activated by the morula stage

Embryos from chow-fed mothers were collected at E1.5 (2-cell stage) and cultured until the morula stage (36 h) in KSOM medium with isoleucine depleted by 50% and with normal insulin concentration (L-ISO/N-INS) and compared with control (NBCAA/N-INS) group. At the morula stage some embryos were examined using the LysoTracker assay and imaged and analysed using the TE high resolution scan (or outer cell high resolution scan for this embryo stage) to determine whether the stimulation recorded at the blastocyst stage (see *4.3.2*) was induced during earlier development. This experiment was conducted alongside blastocyst analysis used as a positive control.

The VOLOCITY analysis showed that embryos cultured until the morula stage in L-ISO/N-INS group had no change in LysoTracker vesicle number or collective volume per cell compared to the NBCAA/N-INS control group (*Figure 4.24*). The individual vesicle volumes were also not altered (*Figure 4.25)* nor the mean distance of vesicles to the nucleus (*Figure 4.26*). Moreover, morulae analysed had no changes in cell number (*Figure 4.27*). Collectively, these data in combination with previous data indicate that the stimulation in LysoTracker vesicle number and collective volume per cell only occurs at the blastocyst stage.

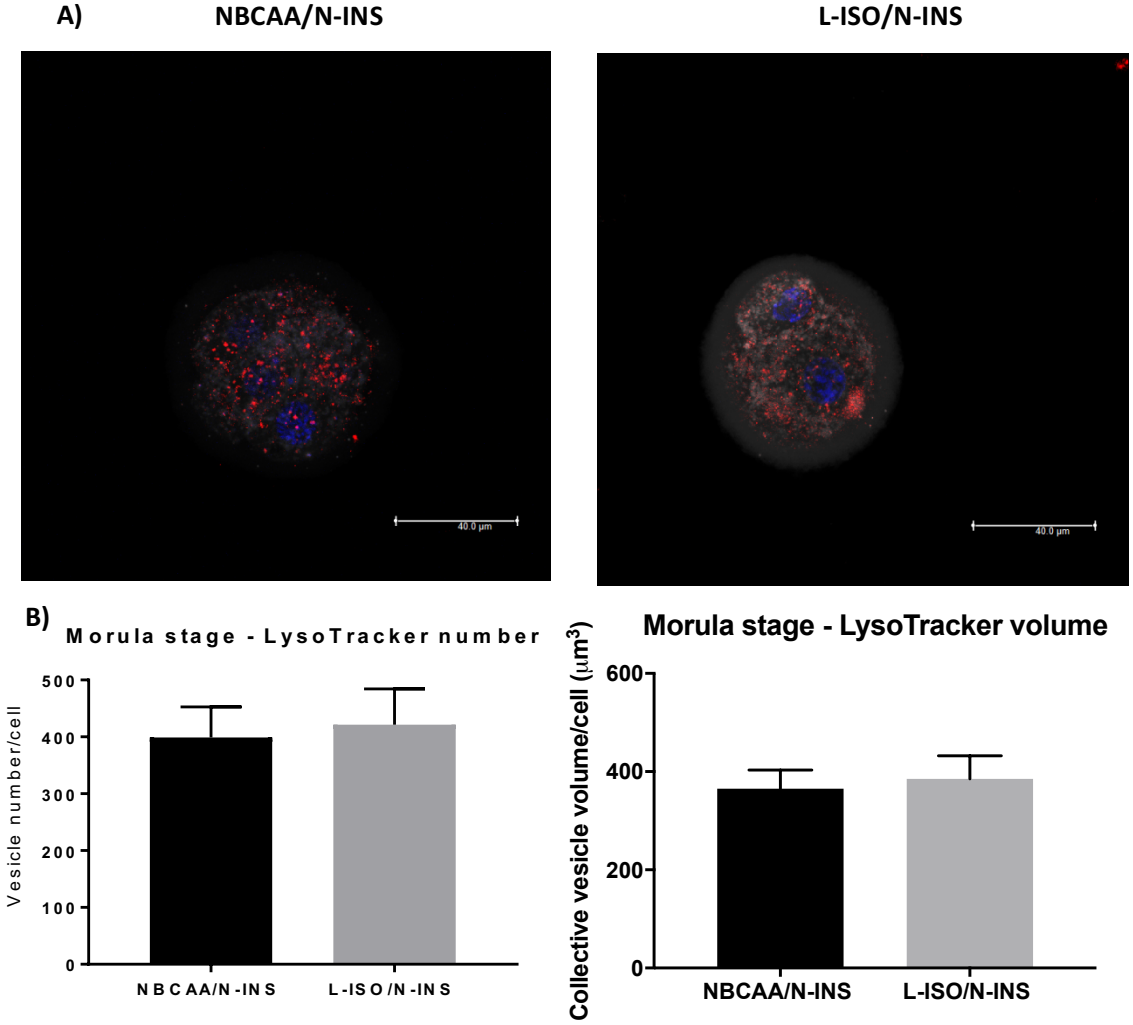

Figure 4.24 – Endocytosis is not increased in morulae TE following culture from 2-cell stage in media with depleted Isoleucine alone and normal insulin (L-ISO/N-INS). A) Morulae after LysoTracker (red) endocytosis assay, nuclei (DAPI, blue) and plasma membrane (CellMask, grey) staining following culture in different BCAAs concentrations - either at the level found in NPD uterine fluid (NBCAA), or with isoleucine individually reduced by 50% compared NBCAA (L-ISO/N-INS) Scale bar = 40 µm. B) LysoTracker vesicle number and collective volume (μm^3) per outer cell. Values are presented as mean ±SEM. 17-18 embryos per group (24-26 cells per group) from 5 mothers (in 4 replicates).

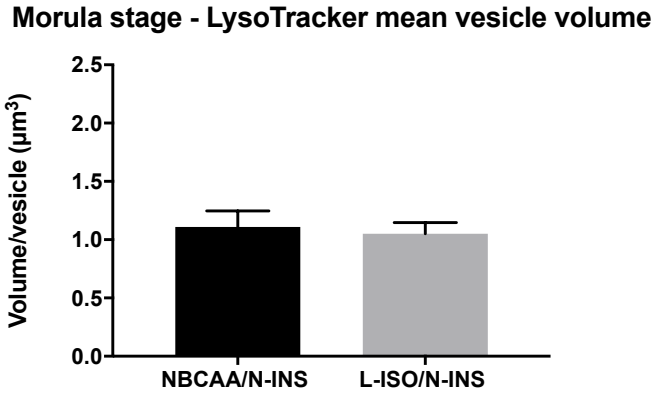

Figure 4.25 - Morula mean vesicle volume (LysoTracker) was not altered in response to L-ISO/N-INS (embryos cultured from 2-cell stage). In the outer cell high resolution approach mean vesicle volume did not differ between groups. Values are presented as mean±SEM. 17-18 embryos per group (24-26 cells per group) from 5 mothers (in 4 replicates).

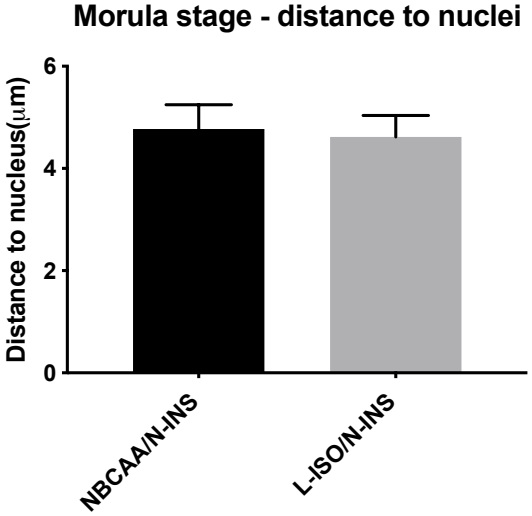

Figure 4.26 - L-ISO/N-INS in the culture media had no effect on the distribution of labelled lysosomes within TE cells with respect to distance from nucleus at morula stage. Values are presented as mean±SEM. 17-18 embryos per group (24-26 cells per group) from 5 mothers (in 4 replicates).

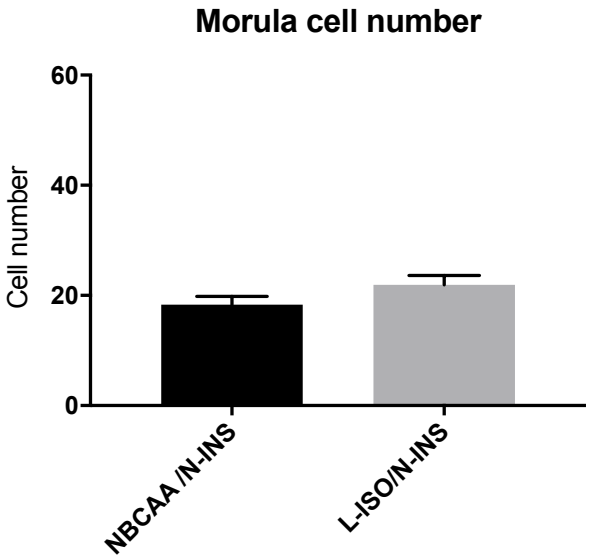

Figure 4.27 - Morula cell number is not affected after culture in L-ISO/N-INS compared to NBCAA/N-INS from 2-cell stage. Values are presented as mean±SEM. 17-18 embryos per group from 5 mothers (in 4 replicates).

4.3.5 BSA pulse exposure in early cleavage is required to 'prime' TE endocytosis responsiveness at the blastocyst stage

In all previous experiments, embryos were cultured in protein-free medium. However, embryos were briefly exposed to BSA (4 mg/ml) while flushing the oviduct with H6BSA. H6BSA is commonly used in laboratory practise for flushing embryos and several studies reporting the effects of culture medium composition, including amino acids and variations in protein concentration have used it to flush embryos from the ovidct/uterine horns (Velazquez et al., 2018; Sun et al., 2014). The aim of this experiment was to test if this short exposure to BSA had an effect on TE endocytosis. Embryos from chow-fed mothers were collected at E1.5 (2-cell stage). From each mother, one oviduct was flushed with H6BSA (4 mg/ml) as in previous experiments while the other was flushed with 6 mg/ml Polyvinylpyrrolidone (H6PVP), thus omitting the protein content, and cultured until blastocyst (~48 h) in L-ISO/N-INS or control NBCAA/N-INS or NBCAA/L-INS treatments, as described previously. Blastocysts were assessed using the BSA-BODIPY and LysoTracker assays and imaged and analysed using the TE high resolution scan.

The VOLOCITY analysis showed that the increased endocytosis previously seen in the L-ISO/N-INS group is only present when BSA is used to flush 2-cell embryos from the oviducts. When flushed with H6PVP, culture from 2-cell stage until blastocyst stage in L-ISO/N-INS medium had no effect on stimulating endocytosis either as vesicle number or collective volume per cell (*Figure 4.28*). Individual vesicle volumes were also not altered across treatment groups (*Figure 4.29*). Collectively, these data suggest that the compensatory response to this culture system requires an early short exposure to BSA.

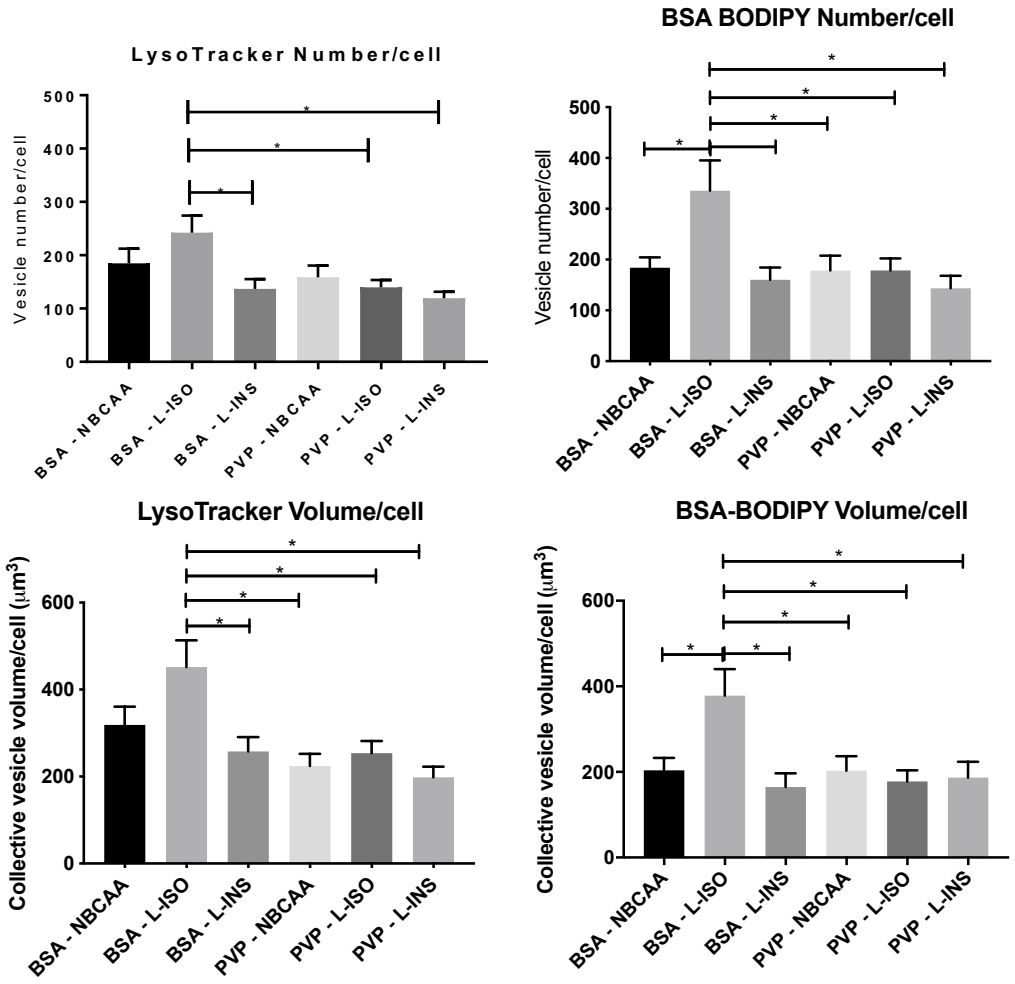

Figure 4.28 - LysoTracker and BSA-BODIPY vesicle number and collective volume (μm^3) per TE cell in embryos that were flushed from oviduct either with H6BSA or with H6PVP. Endocytosis is stimulated in the L-ISO/N-INS group only if a BSA exposure occurs early in embryo development (2-cell stage). The use of PVP in flushing medium at the 2-cell stage caused a decrease in endocytosis rate to baseline values at the blastocyst stage. Values are presented as mean ±SEM. *P value <0.05; 14-19 embryos per group (23-38 cells per group) from 12 mothers (in 9 replicates).

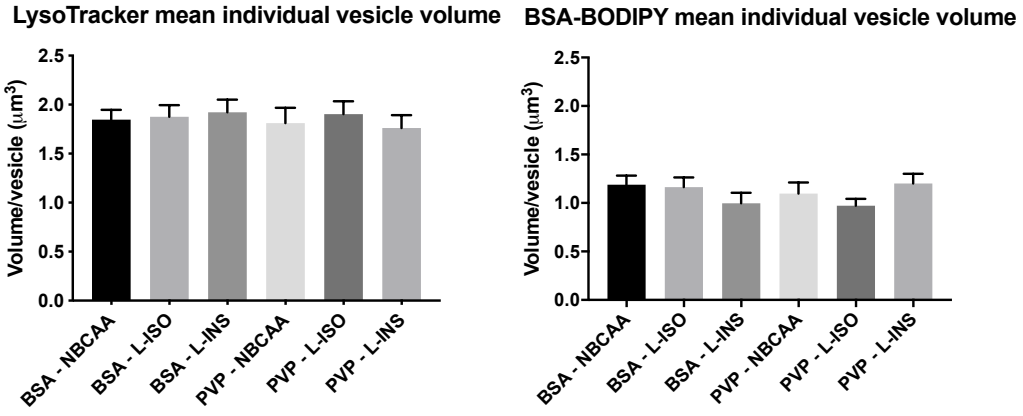

Figure 4.29 – Blastocyst individual LysoTracker (A) and BSA-BODIPY (B) vesicle volumes were not altered in response to different treatments. Embryos were cultured from 2-cell stage and analysed at blastocyst stage using the TE high resolution approach. Mean vesicle volume did not differ between groups. Values are presented as mean±SEM. 14-19 embryos per group (23-38 cells per group).

4.3.6 LysoTracker vesicle increase mediated by isoleucine depletion in vitro is independent of BSA concentration during the endocytosis assay

The BSA-BOPIDY endocytosis assay requires BSA protein provision during the 1 h incubation period which may be contributing to the stimulation seen in LysoTracker vesicle number and collective volume reported previously following L-ISO/N-INS treatment (showed in *4.3.2.)*. Here, we tested this possibility by modifying BSA concentration during the 1 h LysoTracker assay period (0-4 mg/ml). Embryos were cultured from 2-cell to blastocyst stages (~48 h) in L-ISO/N-INS or NBCAA/N-INS and in the last hour incubated in the same KSOM medium with LysoTracker and either 4, 0.5 or 0 mg/ml BSA included (0.5 mg/ml mimics the BSA concentration in BSA-BODIPY).

The VOLOCITY analysis revealed L-ISO/N-INS treatment caused an increase in mean LysoTracker vesicle number and collective volume per cell compared with NBCAA/N-INS control culture (although not always statistically significant) but independent of BSA concentration present in the final 1 h incubation (*Figure 4.30*). No changes were found between individual vesicle volume (*Figure 4.31*) nor lysosomal distance to nuclei (*Figure 4.32*) across treatment groups.

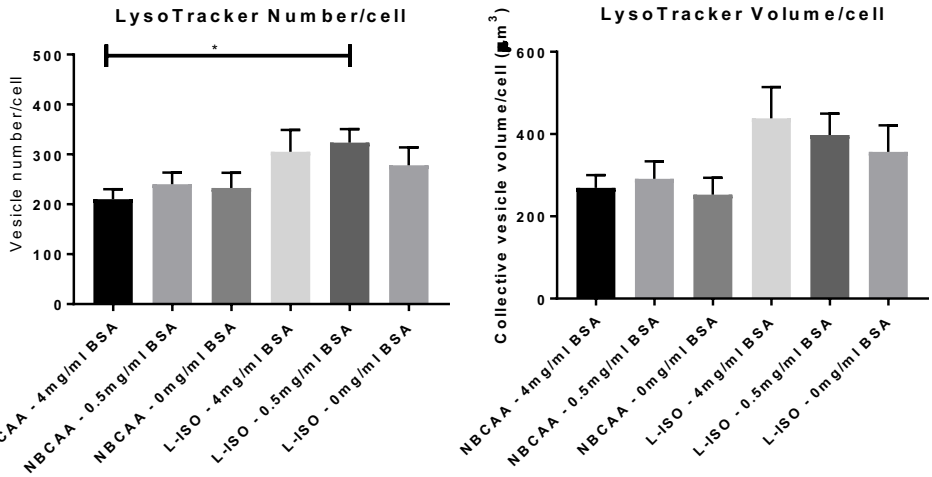

Figure 4.30 – LysoTracker vesicle number and collective volume per cell in blastocyst TE cultured from 2-cell stage in media with depleted Isoleucine and normal insulin (L-ISO) or control (NBCAA) followed by 1 h incubation with different concentrations of BSA (4mg/ml, 0.5mg/ml or 0mg/ml). Lysosome number and collective volume (μm^3) per TE cell. Values are presented as mean ±SEM. *P value <0.05; 13-21 embryos per group (17-29 cells per group) from 13 mothers (in 6 replicates).

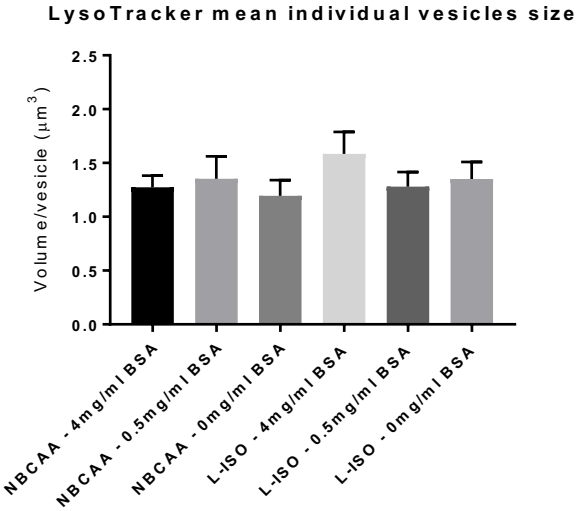

Figure 4.31 - Blastocysts mean LysoTracker vesicle volume was not altered in response to 1 h incubation in BSA at blastocyst stage (last hour in culture). Embryos cultured from 2-cell stage in either NBCAA/N-INS or L-ISO/N-INS. In the TE high resolution approach mean vesicle volume did not differ between groups. Values are presented as mean±SEM. 13-21 embryos per group (17-29 cells per group) from 13 mothers (in 6 replicates).

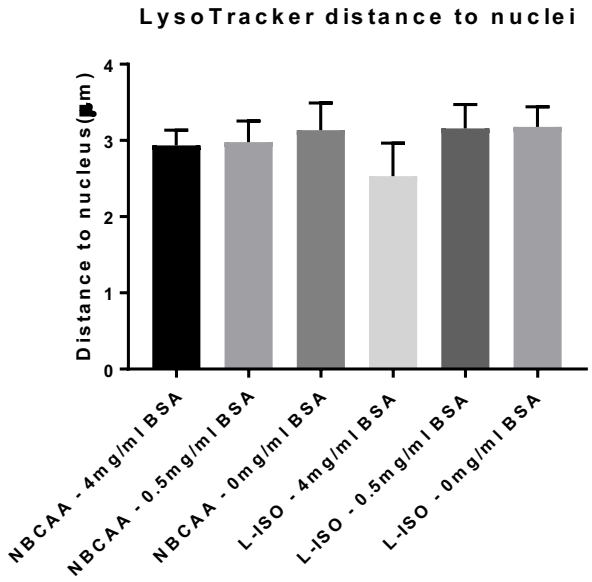

Figure 4.32 – 1 h incubation in BSA at the blastocyst stage (last hour in culture) after culture from 2-cell stage in either NBCAA/N-INS or L-ISO/N-INS had no effect on the distribution of labelled vesicles – Lysosomes within TE cell with respect to distance from nucleus. Values are presented as mean±SEM. 13-21 embryos per group (17-29 cells per group) from 13 mothers (in 6 replicates).

4.3.7 The cell volume of TE cells analysed in all previous experiments was not significantly changed between the different groups studied

After showing that some *in vitro* culture changes (i.e. L-ISO/N-INS) from the 2-cell stage altered the blastocyst phenotype in terms of LysoTracker/BSA-BODIPY number and/or collective volume per TE cell, I asked whether this increase is caused by cells becoming larger due to treatment and if so, whether this increase reflected a steady-state maintenance of lysosome density (number of lysosomes per unit volume cytoplasm). Thus, a VOLOCITY protocol was created to study if the cell volume of the TE cells analysed was altered by culture treatment and whether normalising endocytosis data against cell volume rather than per cell, affected the results obtained. By doing so, the relative effect of treatment and cell volume may be distinguished. Thus, here I studied 1) if TE cells were enlarged in those embryos where endocytosis increased, and 2) if an increase in LysoTracker/BSA-BODIPY number/volume in a TE cell was independent of cell volume.

For all previous experiments, using the entire sample number as reported, TE cell volume was not significantly changed in any group although the mean cell volume in L-ISO/N-INS and L-LEU/N-INS were higher than NBCAA/N-INS (*Figure 4.33*). In addition, total blastocyst volume was unchanged by treatment (graphs in *Appendix 8.8*). After normalising endocytosis data against cell volume, general effects induced by treatment seen previously following analysis per cell were maintained as were most cases where statistical differences were identified. However, in some cases, statistical significance was lost when data were normalised against cell volume (*Appendix 8.9*). *Figure 4.32* is an example of one experimental set (NBCAA/N-INS, L-VAL/N-INS, L-LEU/N-INS, L-ISO/N-INS and NBCAA/L-INS) where statistical significance of BSA-BODIPY was altered when data were normalised to cell volume.

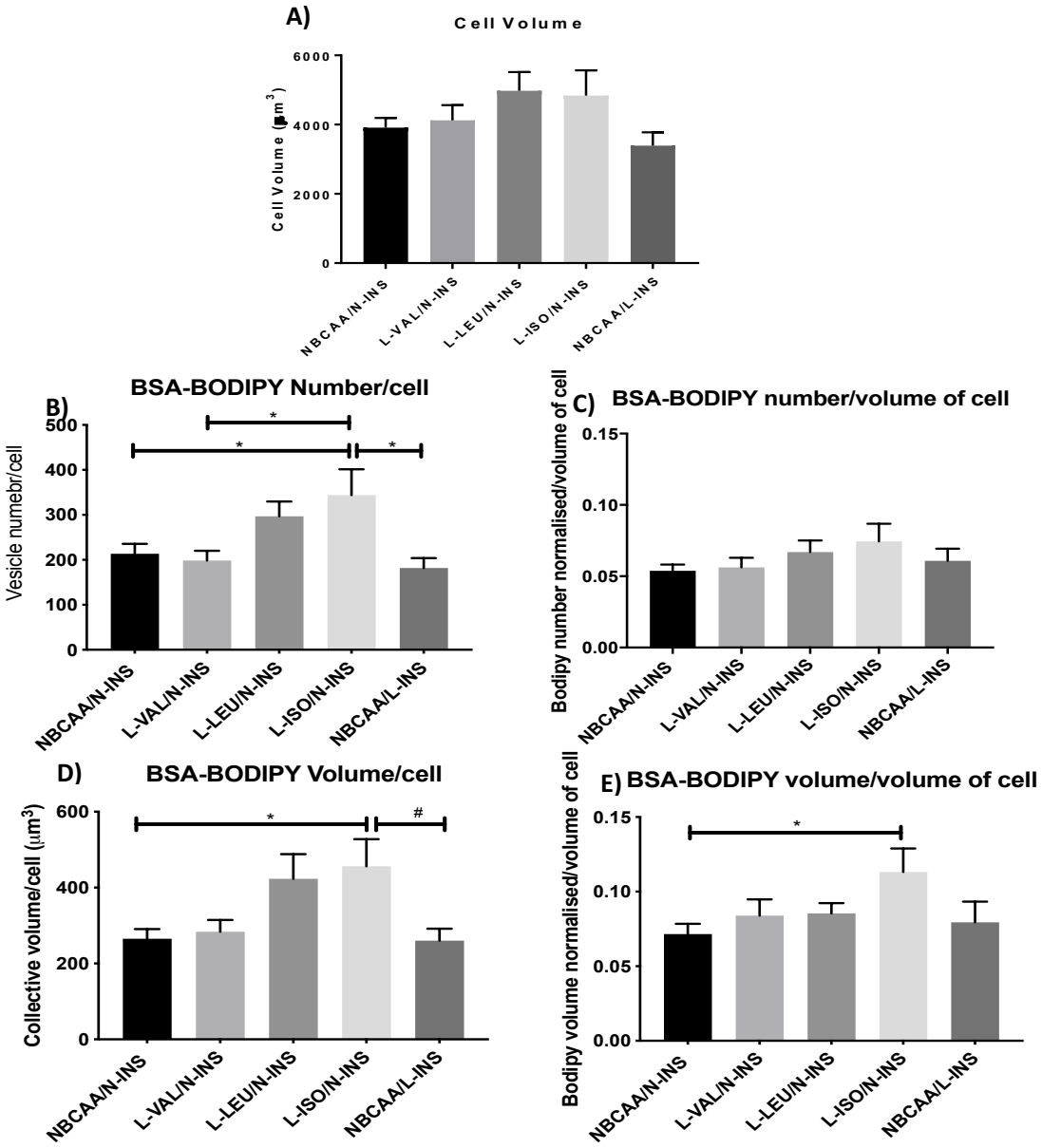

Figure 4.33 – Effect of culture treatments on cell volume and examples of effect of normalising cell volume on endocytosis data. Cell volume is not significantly changed between treatment groups (A). BSA-BODIPY number/cell and collective volume/cell (B,D) and BSA-BODIPY number and collective volume normalised to cell volume (C,E). Embryos cultured with Isoleucine depletion (L-ISO/N-INS) show increased BSA-BODIPY vesicle volume when data are normalised to volume of cell (E), also present without normalisation (D) – thus, both absolute volume of BSA-BODIPY in a cell and BSA-BODIPY volume per volume of cell were increased. However, although the general effects seen in the L-ISO/N-INS group is maintained in the BSA-BODIPY number/volume of cell (C) compared to the absolute number of BSA-BODIPY/cell (B), statistical significance is lost after normalising data to cell volume. Values are mean ±SEM. *P <0.05; #P <0.1; 17-24 embryos per group (30-55 cells per group) from 13 mothers (in 10 replicates).

4.3.8 A positive correlation exists between TE cell volume and the presence of lysosomes in the cell

Although all previous cell volume analyses were non-significant, I found some minor changes in cell volume between treatment groups. There was an increase in mean volume in the L-LEU/N-INS and L-ISO/N-INS treatments (*Figure 4.32*) which suggest cell volume effects may make a small contribution to the increased endocytosis previously studied per cell. To examine this possibility, correlation analysis was conducted between either lysosome number or collective volume per TE cell and cell volume for those same treatments as in *Figure 8.17* (*Appendix 8.10*). This will reveal whether it was specifically those cells with increased lysosomes (L-ISO/N-INS) that had increased volume or not, thereby revealing whether cell volume change might be contributing, either directly or indirectly, to the induction of increased vesicle number and volume observed, comprising part of the mechanism of endocytosis activation.

Correlation analysis revealed a positive relationship existed between cell volume and endocytosis *(Figure 4.34)* but this was not treatment-related. In general, it seems that cells with larger volumes have more lysosomes, independent of which *in vitro* treatment they derived from *(Figure 4.34*). *Appendix 8.10* shows all correlation graphs for each treatment group, while *Figure 4.34* shows the correlation between cell volume and BSA-BODIPY and LysoTracker number and volume for all treatments combined. We can see from *Figure 4.34* that there is a positive correlation in all four groups, with a significant P-value (<0.05) and moderately high correlation coefficient (R) – higher than 0.5. According to the statistical software used (GraphPad), correlation coefficient (R) reveals the strength of the relationship between variables (i.e., how strong do the variables correlate), and P-value clarifies if this correlation is significant.

In *Figure 4.35*, as an example, the individual treatment correlations between LysoTracker and BSA-BODIPY number/volume and cell volume are shown in different colours for the NBCAA/N-INS (blue) and L-ISO/N-INS (red) datasets. This shows a positive and significant correlation between cell volume and lysosomes number and volume in both treatment groups but with lysosomes number and volume significantly increased in the L-ISO/N-INS group compared to the control NBCAA/N-INS (data analysed in 4.3.2

– Figure 4.10). There is also a positive and significant correlation between cell volume and BSA-BODIPY number and volume in the L-ISO/N-INS group but not in the control NBCAA-N-INS, but again with a significantly increase in the L-ISO/N-INS BSA-BODIPY number and volume compared to NBCAA/N-INS (data analysed in 4.3.2 – Figure 4.10). Collectively, a more general mechanism of cell volume acting to increase lysosomes exists across treatments and in parallel a more specific AA-dependent mechanism acts to augment this relationship.

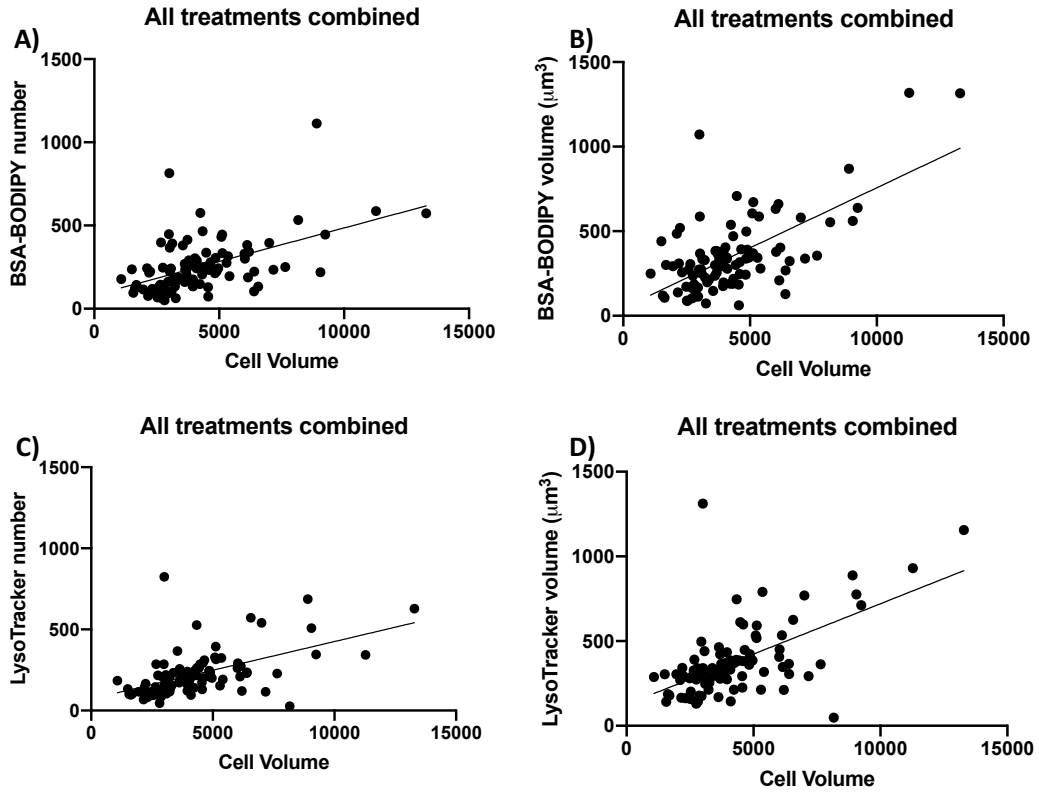

E)

Correlation	Cell Volume vs. BSA-BODIPY Number	Cell Volume vs. BSA-BODIPY volume	Cell Volume vs. LysoTracker number	Cell Volume vs. LysoTracker volume
	Y	Y	Y	Y
Pearson r				
r	0.5122	0.6430	0.5357	0.5840
95% confidence interval	0.3454 to 0.6476	0.5063 to 0.7481	0.3737 to 0.6661	0.4326 to 0.7034
R squared	0.2623	0.4134	0.2870	0.3411
P value				
P (two-tailed)	<0.0001	<0.0001	<0.0001	<0.0001
P value summary	****	****	****	****
Significant? (alpha = 0.05)	Yes	Yes	Yes	Yes
Number of XY Pairs	94	94	94	94

Figure 4.34 - Correlation between cell volume and BSA-BODIPY (A,B) and LysoTracker (C,D) number and volume for all treatments combined. All graphs show a positive correlation with R>0.5, with significant P value <0.05, showing that the model fits the data well.

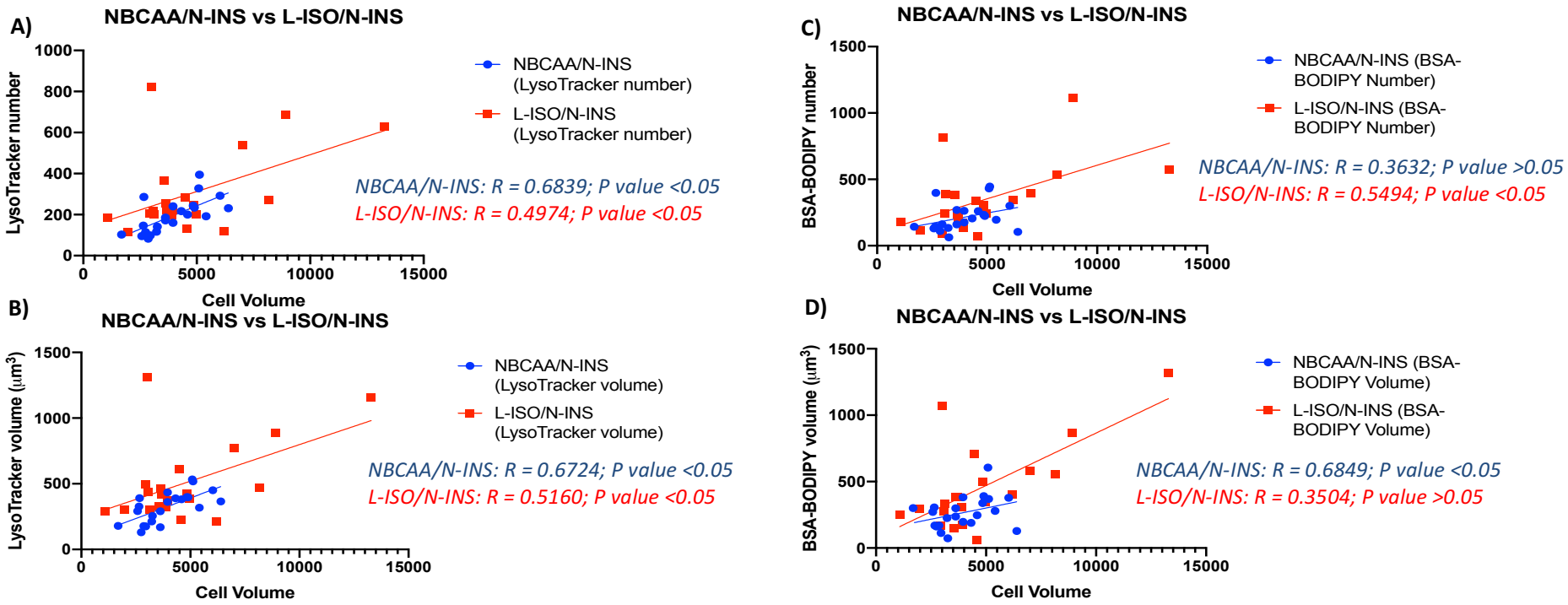

Figure 4.35 – **Correlation analysis between cell volume and endocytosis factors for NBCAA/N-INS (shown in blue) and L-ISO/N-INS treatments (red).** A) NBCAA/N-INS and L-ISO/N-INS show a positive and significant correlation between cell volume and lysosomes number but with lysosome number significantly increased in the L-ISO/N-INS group compared to the control NBCAA/N-INS. B) NBCAA/N-INS and L-ISO/N-INS show a positive and significant correlation between cell volume and lysosomes volume but with lysosomes volume significantly increased in the L-ISO/N-INS group compared to the control NBCAA/N-INS. C) L-ISO/N-INS show a positive and significant correlation between cell volume and BSA-BODIPY number while NBCAA-N-INS show a non-significant positive but weaker correlation, with BSA-BODIPY number significantly increased in the L-ISO/N-INS group compared to the control NBCAA/N-INS.D) L-ISO/N-INS show a positive and significant correlation between cell volume and BSA-BODIPY volume while NBCAA-N-INS show a non-significant positive but weaker correlation, with BSA-BODIPY number significantly increased in the L-ISO/N-INS group compared to the control NBCAA/N-INS.

4.4 Discussion

In this chapter we have shown that specific environmental conditions of depleted nutrient availability cause the mouse early embryo to alter its cellular metabolic phenotype in a way that is likely to be protective in nature, permitting the embryo to capture more nutrients by enhanced endocytosis, thereby helping subsequent growth and survival.

Mouse preimplantation embryos 'sense' nutrient availability in their immediate environment (here, from culture medium composition to mimic maternal tract fluids) via select amino acid and insulin concentrations. The most pertinent amino acid in this respect is isoleucine while leucine appears to have a lesser role. Thus, deficiencies in ISO alone (50% of normal tract concentration), or a combination of low ISO, LEU and insulin (all 50% level) during the period of cleavage (2-cell to 32-cell), signal to the embryo to activate enhanced endocytosis by the TE at the blastocyst stage but not before at morula stage.

Enhanced endocytosis has been quantified by measuring both the number of newly formed endocytic vesicles and the number of lysosomal vesicles in embryos using specific fluorescent markers with confocal microscopy and image analysis software, showing significantly increased endocytosed vesicles and lysosomes per TE cell in conditions of nutrient deficiency - L-ISO/N-INS. Both endocytosis and lysosome vesicles remain the same size, but their number and collective volume increases. The increased number of lysosomes detected per cell collectively contain increased levels of cathepsin B enzyme, hence are functional in their role. Moreover, key components of the endocytic pathway (cell surface endocytosis receptor, megalin; structural protein clathrin that enables vesicle formation) are similarly increased, confirming the stimulus to endocytosis is fully functional for nutrient uptake capacity.

4.4.1 Embryos cultured in media with the three BCAAs depleted maintain the endocytosis rate

In vitro studies have shown the influence of exogenous protein in the endocytosis uptake rate of preimplantation embryos and subsequent embryonic growth (Sun et al., 2014; Kaye and Gardner, 1999; Dunglison and Kaye, 1995). This suggests the importance of protein and AA availability as environmental factors sensed by early embryos with the capability of reprograming their development. Studies using the maternal LPD model showed that embryos exposed to mild malnutrition environment try to compensate by up-regulating its nutrient endocytosis ability to support growth (Sun et al., 2014; Watkins et al., 2008a). Therefore, the use of *in vitro* culture for early embryos is a useful model to study the pathways affected by the early environment as well as to study the appropriate conditions for embryo development. AAs have been reported as important for mTOR pathway and endocytosis. In fact, BCAAs were found to be depleted from the Emb-LPD uterine fluid (Eckert et al 2012), and the blastocysts from these mothers show a decreased mTOR signalling as well as some compensatory features such as increased TE cell number (Eckert et al., 2012) and increased TE endocytosis (Sun et al., 2014).

In my experiments, this environment was mimicked by culturing 2-cell stage embryos in media with depleted BCAAs until the blastocyst stage. The control group (NBCAA and N-INS) attempted to mimic the embryo compositional environment for both AAs detected in the maternal uterine fluid and the physiological level of serum insulin found in control diet mothers (NPD) at E3.5. This culture medium differs in composition to that found in normal KSOM+AA with multi-fold differences evident in the levels of many AAs (Eckert et al., 2012) but more closely resembling the *in vivo* conditions experienced by preimplantation embryos within the uterus. The two test culture treatments in my initial experiments were the same control medium but supplemented with either 50% the BCAA concentration (LBCAA) or with omitted BCAA (0BCAA). Embryo survival in culture was not altered between groups. BSA-BODIPY endocytosis was not altered in any of the culture conditions. However, previous studies using the same culture conditions reported an increased TE Dextran endocytosis uptake (Sun et al., 2014). Although the endocytic probes used in both

studies were different, and FITC-Dextran was used as a marker of fluid phase endocytosis, which might explain some of the difference with the current result but the lysosomes number and volume were also increased in Sun et al., (2014) study in the LBCAA/N-INS group compared to control which was not statistically significant in my study.

This discrepancy may be explained by technical improvements in the current assays used. In the earlier study, the ZP was removed after the assay using acid Tyrodes (pH 2.3), and it is known that endocytosis is highly sensitive to the pH. As discussed earlier, after entering the cell cytoplasm, vesicles fuse with early endosomes where the proton pump ATPase transforms it into an acidic environment (pH<5). These changes in pH induce ligands to segregate from the receptors regulating the sorting of ligand from the receptor (Mellman et al., 1986). Thus, it is possible that the acid treatment has a potential effect on endocytosis while such an artefact is avoided in my study by minimising live embryo manipulations and retaining the ZP. In fact, changes in the intracellular pH are known to be responsible for mTORC1 lysosomal translocation close to nuclei when AAs are depleted in the environment (Korolchuk et al., 2011). In the case of AA replenishment, lysosomes are translocated to peripheral areas (close to the upstream signalling modules) facilitating mTORC1 stimulation (Korolchuk et al., 2011). However, neither in this study nor in Sun et al., (2014) was any change found in the distance from the lysosome to the nuclei in response to BCAAs depletion. Moreover, the VOLOCITY protocol used in this study was optimised and improved from the previous one used by Sun et al (2014), by adding specific criteria such as: remove noise from objects (using a fine filter), separate touching objects, exclude objects by size (based on literature to the expected size/volume of lysosomes), and the application of this optimised protocol to all embryos without any further changes, thus avoiding any bias.

In this culture system, some features of the LPD uterine fluid were mimicked, however it is important to emphasize that only a small part of the elements that could be modified in the Emb-LPD fluid were studied (in this case the BCAAs concentration), and the compensatory mechanisms found in blastocysts from Emb-LPD mothers might be a result of a combination of factors that might not be included or might be

lost during *in vitro* culture. In fact, a recent study cultured 2-cell embryos until blastocyst stage in four different groups: NBCAA and normal insulin, LBCAA and normal insulin, NBCAA and low insulin and LBCAA and low insulin and then transferred to pseudopregnant recipients. This showed altered postnatal growth and cardiovascular physiology only in the group with both insulin and BCAA depletion (Velazquez et al., 2018). Thus, it is possible that the early compensatory mechanisms occurring in the Emb-LPD are caused by a combination of low insulin and BCAAs, which is further discussed. Moreover, the KSOM medium used might not reflect entirely the nutrient composition of the maternal uterine fluid (Summers and Biggers, 2003).

4.4.2 Embryos cultured with Isoleucine depletion show increased endocytosis and increased expression of endocytosis receptors

When membrane proteins are delivered to the lysosome for degradation, the resulting AAs are transported to the cytoplasm for reuse in protein synthesis. This recycling pathway might play an important role in the case of AA restriction. In fact, Jones et al., (2012) showed that a starvation model based on leucine depletion, using yeast cells, resulted in increased protein internalization and recycling pathway, thereby providing AAs through increased protein turnover, and showed that mTORC1 and a second, unknown nutrient-sensing system are responsible for the starvation-induced protein turnover. Similarly, blastocyst AA composition from the Emb-LPD model showed that despite the reduced maternal availability of BCAAs and the accompanying reduction in mTORC1 signalling, these AAs were nonetheless present within blastocysts at near normal concentrations (Eckert et al., 2012) and showed increased number and volume of lysosomes as well as degraded protein within the lysosomes (Sun et al., 2014) suggesting an increased uptake rate is occurring to compensate for the poor nutrient environment.

In my experiments, I focused on the potential role of insulin and BCAAs levels as signalling components involved in nutrient sensing. Both of these factors act to control proliferation and cellular phenotype during early development with long-lasting positive effects on foetal growth (Gonzalez et al., 2012; Martin and

Sutherland, 2001; Kaye and Gardner, 1999) and they also contribute to cellular growth through intracellular mTORC1 signalling. Five *in vitro* culture systems with BCAAs or insulin individually depleted by 50% and a control group with normal BCAA and insulin concentrations (as found in the NPD uterine fluid, Eckert et al., (2012)) were used to culture 2-cell stage embryos until blastocyst stage. Endocytosis was then assessed and compared between groups. VOLOCITY analysis showed that in the L-ISO/N-INS group – 50% depletion in Isoleucine - there is a higher number of lysosomes and significantly higher BSA-BODIPY positive vesicle number in the TE single cell analysis compared to the control group. Lysosome collective volume in the TE cells was increased (1.5-fold) and the BSA-BODIPY vesicles significantly increased (1.7-fold) in the L-ISO group compared to the NBCAA. Blastocyst formation *in vitro* was not altered in any group, which coincides with data from the Emb-LPD treatment (Eckert et al., 2012) and previous *in vitro* work in embryos cultured from 2-cell stage until blastocyst in a 50% reduction in insulin and/or the three BCAA concentrations (Velazquez et al., 2018). The total number of cells (counted by nuclei stained with DAPI) did not differ between the five groups. This had been previously reported in other *in vitro* culture models mimicking the Emb-LPD model (Velazquez et al., 2018) although the TE and total cells in the Emb-LPD blastocysts was actually increased (Eckert et al., 2012). The absence of effect on this particular blastocyst phenotype in the current study suggests that BCAA and insulin are not inductive for the increased TE proliferation seen in the Emb-LPD model and that different features of the compensatory response may be separately regulated. In fact, this is supported by the evidence that non-essential AAs rather than BCAAs may have a predominant effect on mouse embryo proliferation *in vitro* (Gardner and Lane, 1993).

Considering the results obtained in the L-ISO/N-INS group, I measured intracellular cathepsin B activity directly in lysosomes using an artificial commercial cathepsin-substrate peptide (MR), which is linked to the fluorophore cresyl violet and emits a red fluorescence signal after enzymatic cleavage. Using this substrate, I observed *in situ* an increase in cathepsin-activity, measured as the amount of red fluorescent signal, between NBCAA/N-INS and L-ISO/N-INS group. This shows that not only

lysosomes are increased in the L-ISO/N-INS but there is also an increase in lysosomal function (enzyme activity) as cathepsins are only present in activated lysosomes.

Albumin is normally endocytosed by the megalin-cubilin receptor complex. Because of the increased endocytosis (shown by increased BSA-BODIPY signal) in L-ISO/N-INS compared to control NBCAA/N-INS blastocysts, I looked at megalin expression in these embryos to study whether this increase was accompanied by increased expression of its main receptor. Megalin is first detected in the cytoplasm at the 8-cell stage and in some, but not all, outer cells of the morula. At the 32-cell stage, it is present in all outer cells of the embryo, which are at the origin of the TE, but not in the internal cells. During the blastocyst stage, megalin is predominantly localized at the apical membrane of the TE cells (Assémat et al., 2005), which separate the internal ICM cells from the maternal environment. As the embryo prepares for implantation, the PE is characterized by a high expression of both cubilin and megalin in membrane-coated pits and endosomes (Assémat et al., 2005). Thus, Albumin starts being internalised and degraded through the megalin-mediated pathway after the 32-cell stage, when megalin expression increases. Following internalisation via clathrin-coated pits, megalin localises in the early endosome before passing into pericentriolar recycling endosomes (Assémat et al., 2005; Verroust and Christensen, 2002). In my study, I found both megalin and clathrin mainly located in the TE cell apical membrane and within vesicles in the cytoplasm and with an increased expression in L-ISO/N-INS embryos compared to NBCAA/N-INS control embryos. This finding suggests that a larger quantity of the receptors could be the cause of the stimulated BSA uptake (increased BSA-BODIPY) in L-ISO/N-INS embryos.

The VYS endoderm contributes to foetal growth through endocytosis of maternal proteins, mainly via the megalin receptor and supply of released AAs. Watkins et al., (2008a) showed that LPD maintained throughout gestation stimulated VYS endoderm nutrient transport capacity and megalin expression in late pregnancy, with enhanced megalin expression evident even when LPD was limited to the preimplantation period. Similarly to our findings, Sun et al., (2014) showed also using immunohistochemistry increased presence of megalin and clathrin in LPD embryos. It is possible that clathrin as a crucial protein to form coated pits and invaginating

vesicles containing ligands and receptors, may change its expression to accommodate stimulated endocytosis in response to different depleted environments.

Nevertheless, megalin was not altered between both culture groups at mRNA level, suggesting the upregulation occurs at protein level. It is possible this increase in protein in the L-ISO/N-INS group is due to a transient upregulation of transcription, not present at the blastocyst stage, when just the raised protein level remains. Studying megalin mRNA in earlier embryonic stages could answer this question. Previous work from our group, showed the same upregulation in megalin protein followed Emb-LPD diet (Sun et al., 2014) but not at the mRNA level in blastocysts (Sun et al., unpublished), suggesting the same mechanism in both models. That research also looked at cubilin expression (which forms a complex with megalin), and found it to be increased both at mRNA and protein level. Since it takes more time for cubilin to reach the plasma membrane than megalin (cubilin needs to go through immature exposure to cellular membrane followed by recycling) (Moestrup and Verroust, 2001), it suggests that cubilin could be a rate-limiting factor in megalin activity and that more cubilin could further facilitate megalin endocytosis. Further work is needed to determine if cubilin is also upregulated in this *in vitro* culture system.

The increased endocytosis in response to isoleucine depletion (L-ISO/N-INS) could indicate altered mTORC1 activity. Despite the small number of studies looking at the effect of individual AAs in embryo development, there are some data supporting the importance of a role for isoleucine. Wallace et al., (2012) showed that increased concentrations of isoleucine, proline and leucine in ovarian follicular fluid is associated with successful pregnancy in women subjected to IVF cycles. Moreover, removal of isoleucine from medium used for human embryo culture from the zygote to 4/8 cells, causes a faster first cleavage division (Mortimer et al.1998), which might be an indicator of poor embryo quality (Burruel et al., 2014). The mechanism involved in the faster cleavage is not well understood, but might be seen as a very early compensatory mechanism to the adverse nutrient environment, similarly to later mechanisms in blastocysts such as increased TE cell proliferation and subsequent increased motility indicative of enhanced early trophoblast invasive capacity at

implantation (Eckert et al., 2012). In fact, other compensatory mechanisms have been reported as early as 2-cell stage. For instance, 2-cell stage embryos cultured in the absence of glucose are still able to form blastocysts by increasing their rate of consumption of pyruvate to meet the energy demands of cavitation (Martin and Leese, 1995), while fertilised zygotes do not have this capacity of compensation.

The role of individual AAs, particularly isoleucine, has also been studied in detail in different systems, namely in bovine mammary cells/tissue (Appuhamy et al., 2012; Arriola Apelo et al., 2014). Interestingly, in mammary epithelial cells and tissue, assessment of the correlation between intracellular concentrations of essential AA and mTOR phosphorylation indicated that isoleucine was a more potent regulator of phosphorylation than other AA studied, including leucine (Appuhamy et al., 2012). Supplementation with isoleucine alone revealed increased phosphorylation of mTOR and S6K1. Moreover, when this AA was individually omitted in the medium, its corresponding intracellular concentration was significantly reduced, not found for all other AAs upon their omission from the medium. This suggests that isoleucine is the primary driver in mTOR phosphorylation in this model (Appuhamy et al., 2012). This is particularly interesting considering that Eckert et al., (2012) showed that blastocysts from the LPD diet have a reduced mTORC1 signalling evident in reduced phosphorylation of effector S6 ribosomal protein and its ratio to total S6 protein but no change in effector 4E-BP1 phosphorylated.

The embryo sensing pathway to isoleucine depletion from the medium is not yet understood. It seems that when the three BCAAs concentration is kept constant (either all normal, all depleted by 50% or absent) the embryos do not respond to the depletion (data shown in 4.3.1) by changing the endocytosis rate. Moreover, if leucine or valine is depleted, the presence of isoleucine *in vitro* seems to assume a major role as embryos do not change endocytosis rate in response to the depletion. However, if isoleucine is depleted, the embryo does sense the nutrient depletion and increases the endocytosis rate. Interestingly, studies regarding diet supplementation in sows, showed that supplementation of isoleucine alone improves milk protein synthesis in lactating sows and litter weights, while a mixture of the three BCAA had no effect (Richert, et al., 1997).

More refined cultures could be used to determine the precise concentration at which the embryo becomes sensitive and starts to respond with increased endocytosis. Furthermore, when BCAAs are at normal concentration, 50% depletion in insulin alone does not alter the endocytosis rate in the blastocyst TE. This finding is supported by data from a recent study showing that 2-cell embryo cultured in LBCAA and low insulin until blastocyst stage and then transferred to pseudopregnant recipients presented altered postnatal growth and cardiovascular physiology (Velazquez et al., 2018) while no alterations were found when embryos were cultured with NBCAA and low insulin or LBCAA and normal insulin compared to the NBCAA/N-INS control. Thus, it is possible that the early compensatory mechanisms occurring in the Emb-LPD are caused by a combination of low insulin and low BCAAs. Therefore, I next evaluated the effect of a combination of low insulin with low BCAA (individually and combined) in the embryo endocytosis.

As mentioned before, isoleucine appears to have a higher impact as compared to the other BCAAs in embryo nutrient sensing *in vitro*, since its depletion, even in the presence of normal insulin concentration caused increased TE endocytosis, which might be seen as a mechanism to compensate for the poor nutrient environment.

4.4.3 Embryos cultured with a combination of Insulin and BCAA depletion show increased endocytosis

In the previous experiments I showed that isoleucine particularly has a major effect on preimplantation embryo adaptation to the environment, by causing increased endocytosis when this AA was reduced *in vitro*. However, when I considered the general effect of low BCAA, which is expected to mimic the Emb-LPD environment more closely, no changes were found. In fact, in an earlier study, a combined depletion of insulin and BCAA during embryo culture induced an increase in birth weight and body weight gain during early postnatal development, which did not happen when 2-cell stage embryos were cultured in LBCAA with normalised insulin or in low insulin with normalised BCAA (Velazquez et al., 2018). Furthermore, male offspring exposed to LBCAA/L-INS (and not in the other groups) displayed relative hypertension during early postnatal life and female offspring displayed reduced

heart/body weight, both characteristics of Emb-LPD offspring. Thus, I studied the combined effect of low insulin with low BCAA as well as the effect of low isoleucine and/or leucine combined with low insulin in order to better understand the role of these factors and their possible interaction and/or combined effect in regulating the maternal undernutrition response.

Interestingly, I found that the endocytosis is not only increased in response to L-ISO/N-INS but also to a combination of L-ISO/L-LEU/L-INS and a trend, although not statistically significant in the LBCAA/L-INS group when compared to the control NBCAA/N-INS. In this experiment, BSA-BODIPY vesicle number was not changed to a significant level (but to a trend level) in the L-ISO/N-INS differing from previous experiments. This change, as well as the trend showed in the LBCAA/L-INS group (and perhaps even L-ISO/L-INS) might account for the fact that this experiment had a large number of groups being tested and consequently a decreased number of embryos per group were included, even if having an increased number of females used. The trend seen in BSA-BODIPY positive vesicles number was similar in the lysosomes number, although no statistically significant differences were found between the groups. The mean individual volume of both vesicles did not differ between the six culture systems, showing an authentic increase in the BSA-BODIPY vesicles number in the L-ISO/N-INS and L-ISO/L-LEU/L-INS groups that in turn causes an increase in their collective volume per cell. However, the groups with increased collective volume but no increased numbers per cell cannot be explained by a change in their individual size, again reinforcing the idea that the reduced N number might cause the non-significant trend seen. Collectively, these data indicate that embryo endocytosis was not altered in response to low leucine combined with low insulin (and combined with normal insulin – as seen in 4.3.2) but there is at least a trend to an increased TE endocytosis when low insulin is combined with reduced BCAA that include isoleucine.

Once again, no differences were found in blastocyst total cell numbers after culture in the different media. These results are in accordance with our previous data where the cell number was not altered in blastocysts cultured in LBCAA/L-INS, LBCAA/N-INS and NBCAA/L-INS despite the postnatal changes seen in offspring from the LBCAA/L-INS group (Velazquez et al., 2018). This phenotype differs from the Emb-LPD

blastocyst phenotype, which had an increased proliferation of blastocyst TE and total number of cells (Eckert et al., 2012). Hence, alternative maternal environmental factors changing in response to Emb-LPD treatment should be assessed *in vitro* for evidence of their role in this early programming event. For instance, this could include glucose or other AAs, or other factors found to be altered in response to maternal undernutrition in other models, such as leptin, IGF-1 or nonesterified fatty acid (Velazquez, 2015).

Together, our results strongly support the notion that the composition of preimplantation culture medium can alter embryo responses to the environment which can in turn programme postnatal growth and cardiovascular phenotypes. Moreover, isoleucine has been implicated as the major mediator of increased endocytosis in this system. These data are not only relevant to better understand the preimplantation adaptive response to the maternal environment, namely in the LPD model, but it is also relevant to human ART practice since embryo culture composition might determine postnatal phenotype and yet commercial culture media compositions are undisclosed (Sunde et al., 2016).

4.4.4 LysoTracker vesicle stimulation mediated by isoleucine depletion in vitro is not activated by the morula stage

In order to study the embryonic stage when compensatory endocytosis initiates, embryos were cultured in L-ISO/N-INS or control (NBCAA/N-INS) medium only up to the morula stage (~36 hours) before analysis for lysosome number (LysoTracker Red). Here, unlike at the blastocyst stage, no increase in endocytosis was detected indicating initiation of response occurs at blastocyst stage.

Lysosome size, number and location change dynamically during early embryo development (Fleming and Pickering, 1985; Tsukamoto et al., 2013). Regarding lysosomal location, it is known that oocytes, eggs and embryos up to the early 8-cell stage contain clusters of endosomes (pre lysosomal vesicles) distributed randomly in the cortical cytoplasm and that from 8-cell stage until the early 16-cell stage, endosomes become progressively localized in the apical cytoplasm (polarization)

beneath the microvillous pole. The final maturation phase occurs at the late 16-cell stage when secondary lysosomes form and polarize in the basal cytoplasm (Fleming and Pickering, 1985), combined with a progressive increase in the rate of endocytosis occuring preferentially at the apical surface, and the differentiation of cytoplasmic endocytic pathways associated with transcytosis and membrane recycling (Fleming and Pickering, 1985; Fleming and Goodall, 1986; Pemble and Kaye, 1986). The timing of the maturation of the endocytic pathway appears to be relatively independent of environmental factors and therefore is likely to represent an integral stage in the temporally-regulated developmental programme (Fleming and Pickering, 1985).

Tsukamoto et al., (2013) showed that the number and size of lysosomes increase after fertilization and are abundant during mouse preimplantation development until the morula stage, but their numbers decrease slightly in blastocysts. Although our data also suggests a higher number of lysosomes at morula stage than at blastocyst stage (around 400 vs 150-200 lysosomes/cell in NBCAA), and distance of lysosomes to nuclei is also increased in morulae compared to blastocysts, the fact that morula cells are larger than blastocyst cells would explain this. In fact, I have collected data regarding cell volume and in *Appendix 8.9* I show number and collective volume of lysosomes normalised to cell volume in morulae and blastocysts, showing similar proportion of lysosomes per volume of cell. However, Tsukamoto et al., (2013) showed that the expression levels of mature cathepsins B and D were consistently high from the one-cell to morula stage but lower in the blastocyst stage, indicating that lysosomal function changes during this period.

The maturation of polarised TE lineage cells also relates to the fact that AA uptake and rates of protein synthesis are relatively low before the morula stage when cells obtain most of their AA substrates from degradation of existing proteins. It is only by the blastocyst stage that embryos acquire more extensive and sophisticated AA transport systems (DiZio and Tasca, 1977; Epstein and Edwards, 1975) which associates with an increasing dependence upon an exogenous source of AAs (Sellens and Sherman, 1981).

It is known that by the blastocyst stage, endocytic maturation is completed and is stimulated in response to *in vivo* LPD, low BSA or low BCAA *in vitro* (Sun et al., 2014). Although lysosome number and protein degradation through endocytosis are reported to be higher in early cleavage embryos until the morula stage than in blastocysts, BSA particularly is known to be taken up by the megalin-cubilin complex, which only appears in the outer cells around the morula stage (Assemat, 2005). In accordance, Pemble and Kaye, (1976) showed that BSA uptake rate is faster in blastocyst than morula and earlier stages. Moreover, as mentioned before, the AA transport system is not completely formed until the blastocyst stage, sugesting that the compensatory endocytosis is activated through AA sensing by this system. Together, my data suggest that the increased endocytosis and lysosome biosynthesis in response to depleted isoleucine in the culture medium (and possibly in response to LPD *in vivo*) is not activated at the morula stage and it is possibly regulated by the AA sensing system which appears at blastocyst stage.

4.4.5 BSA pulse exposure in early cleavage is required to 'prime' TE endocytosis responsiveness at the blastocyst stage

In all previous experiments, embryos were cultured in protein-free medium so that the role of exogenous AAs in activating endocytosis could be studied, as the effects of BSA could confound the actions of AAs added to the culture medium. The *in vitro* culture medium used was KSOM where BSA was omitted and BCAAs concentrations were altered. Embryo development *in vitro* in the absence of protein requires the use of a chelating agent, namely ethylene-diamine-tetra-acetic acid (EDTA), at non-toxic concentrations (0.02mM) to allow a chemically-defined milieu for embryo culture (Fissore et al., 1989). However, in all previous experiments, 2-cell stage embryos were briefly exposed to BSA (4 mg/ml) while flushed from the oviducts with H6BSA. The aim of this experiment was to test if this short exposure to BSA had an effect on TE endocytosis. Although different studies have used protein-free media to culture embryos to study the role of culture conditions *in vitro*, including the effect of AAs, H6BSA has been used to flush oviducts/uterine horns (Sun et al., 2014; Velazquez et al., 2018) and to the best of my knowledge this issue has never been addressed before.

Endocytosis rate at blastocyst stage increases in the absence of protein (Dunglison and Kaye, 1995) suggesting metabolic demand regulates protein supply to the embryo through endocytosis. Moreover, FITC-dextran labelled vesicles within blastocyst TE are increased after culture in 1 mg/ml BSA compared to 4 mg/ml. Moreover, when BSA in culture is switched from 1 mg/ml to 4 mg/ml BSA only for 1 hour before the FITC-dextran endocytosis assay, embryos retained a high level of endocytosis while culture in 4 mg/ml from the 2-cell stage but switching to a terminal 1 mg/ml BSA culture changed endocytosis pattern to a high level (Sun et al., 2014). These data indicate that low environmental protein during preimplantation development can activate compensatory endocytosis in a sustained way, mimicking the effects observed in the Emb-LPD *in vivo* model (Sun et al., 2014; Watkins et al., 2010).

These data may suggest that the use of BSA in embryo flushing at the 2-cell stage, and not used subsequently during culture, may influence endocytosis activation and rate at the blastocyst stage. To answer this question, pregnant females at E1.5 (2-cell stage) were flushed in one oviduct with H6BSA (4 mg/ml) and the other with H6PVP at 6 mg/ml. PVP facilitates handling of the embryos, presumably by influencing the physico-chemical properties of the medium (Biggers et al., 1997).

As mentioned before, embryos can develop *in vitro* in the absence of protein and BSA is mainly taken up by the megalin-cubilin complex, which only starts to appear in the outer cells around the morula stage (Assemat, 2005). So what is the role of albumin, which is present *in vivo* in the oviducts of early cleavage embryos? Gardner and Kaye, (1991) suggest that cell proliferation effects of BSA during culture to the blastocyst stage derive from a nutritional role (BSA is taken up through endocytosis) but that the effects on earlier stages, such as compaction, are from non-specific actions, possibly including osmotic or protective properties. Although it is not known the specific role of BSA in early stages, it seems that the short early exposure of 2-cell embryos to BSA (4 mg/ml) is sufficient to prime the increased endocytosis later at blastocyst stage in case of poor nutrient provision (i.e. L-ISO/N-INS) during the preimplantation culture. In contrast, no such increase in endocytosis occurred in blastocysts flushed in the absence of BSA at the 2-cell stage.

It is known that the purity of BSA preparations can determine developmental outcomes, as reported for hamster zygotes (Juetten and Bavister, 1983). Even higher-grade albumin preparations retain small, undefined molecules after purification (McKiernan and Bavister, 1992) which likely account for the variability in the embryotrophic effect observed with different batches of BSA (Biggers et al., 1997). It is possible although unlikely that such associated factors may promote the endocytosis outcomes reported. Conceivably, either the BSA itself or associated factors at early cleavage during flushing represent nutrient sufficiency, only to be followed by later nutrient deficiency, sensed through low isoleucine availability, act as a ‘mismatch’ in metabolic environment for the embryo between early and late cleavage, resulting in compensatory endocytosis, not found in response to PVP flushing. On the contrary, it could be that PVP is somehow preventing accurate

embryo sensing (i.e. unspecific binding to ZP) and further activation of compensatory response to poor environment.

Interestingly, embryos developing *in vitro* require a short exposure to glucose in order to "activate" embryo development. Embryos isolated from the maternal tract at the 2-cell stage can be cultured in the absence of glucose and can form blastocysts. However, if zygotes are collected and cultured without glucose, they do not progress beyond the morula stage, even though early stage embryos are unable to utilize glucose. These embryos do not develop the capacity to transport glucose should it become available, nor the adaptive capacity to cope with its absence (Martin and Leese, 1995). Remarkably, brief exposure to glucose prior to the morula stage (including 1-minute exposure at 4-cell stage) is sufficient to ''prime'' these naive embryos to develop to blastocyst stage (Chatot et al., 1994). Later, it was found that glucose acts as a signal via hexosamine biosynthesis to activate embryonic gene expression, differentiation, and development (Pantaleon et al., 2008). As in somatic cells, this glucose-sensing pathway provides the early embryo with a mechanism with which to tightly couple key cellular processes with nutrient availability. Similarly, it is possible that BSA "primes" early embryo sensing and adaptation indirectly, although not to the same extent as embryos do not block their development as happens with glucose absence.

Further studies are necessary to clarify how compensatory endocytosis is activated in early embryos and the role of BSA; if an early exposure to protein or molecules present in BSA are the main triggers of the endocytosis response; and the mechanisms behind it. Future work could include the use of a different protein source as flushing solution. Albumin is the main protein present in the maternal uterine fluid while transferrin, the second most present (Aitken, 1977a), might be a potential target to study if the same activation occurs with a different protein source. Moreover, a combination of BSA and PVP in the flushing solution might indicate if it is PVP preventing the early embryo programming in response to the culture conditions seen with BSA flushing.

4.4.6 LysoTracker vesicle stimulation mediated by isoleucine depletion in vitro is independent of BSA concentration during the endocytosis assay

Although the culture medium used in all previous experiments was designed to be protein-free so that the role of exogenous AAs in culture in activating endocytosis could be studied, without protein turnover (protein degradation into AA followed by new synthesis), BSA was provided in the form of BSA-BODIPY during the last hour of culture in order to be taken up and digested through endocytosis. Thus, I wanted to test if the increased endocytosis and lysosome formation seen in deprived culture environments, such as decreased isoleucine (L-ISO/N-INS), was a compensatory response to the 48 h culture (from 2-cell to blastocyst) and independent of the amount of BSA provided during the assay; that is, if the final hour in culture in the presence of BSA (0.5 mg/ml in BSA-BODIPY), or the switch from protein-free to BSA in culture, had any effect in stimulating lysosome formation to promote endocytosis. It is known that embryos cultured from 2-cell stage until blastocyst stage in low BSA (1 mg/ml) changed to 4 mg/ml in the final hour (at blastocyst stage) have increased endocytosis and lysosome number compared to culture in 1 mg/ml or 4 mg/ml without any change (Sun et al., 2014). To study if the change in the protein content in culture affected lysosome number in blastocysts, I cultured 2-cell embryos in protein-free medium with L-ISO/N-INS as this group has demonstrated before to stimulate BSA endocytosis and lysosome biosynthesis (see 4.3.2 and 4.3.3.) or control NBCAA/N-INS for 48 h until reaching blastocyst stage. Subsequently, embryos were randomly assigned to 3 different culture subgroups: 4 mg/ml BSA, 0.5 mg/ml BSA (mimicking the amount present in BSA-BODIPY) or without BSA all with 100 nM LysoTracker for 1 hour.

No differences in lysosomes number and collective volume per TE cell were seen between the three NBCAA/N-INS subgroups or L-ISO/N-INS subgroups, although L-ISO/N-INS groups had increased (though not all statistically significant) values compared to the NBCAA/N-INS controls. This indicates that the increased lysosome formation in the L-ISO/N-INS group is a response to the culture medium environment and it is independent of the BSA provided in the last hour to study endocytosis uptake. Together, our data suggests that early embryos interact with their environment and are particularly susceptible to low isoleucine *in vitro*, which is able to modulate the inherent

developmental programme by blastocyst stage and to confer plasticity to support survival in these challenging conditions.

4.4.7 The influence of TE cell volume on the effects mediated by culture treatment on endocytosis profile

Even though I did not find significant changes in TE cell volume from all different treatment groups analysed, some groups showed a small non-significant increase in cell volume, which in some cases was responsible for the loss of significance when data was normalised to cell volume. For instance, L-ISO/N-INS showed a slight increase in cell volume (*Figure 4.33*), causing a loss of significance when BSA-BODIPY was normalised to cell volume (previously significantly different compared to control group NBCAA/N-INS). However, the fact that L-LEU/N-INS cell volume was also increased (non-significant) and even higher than L-ISO/N-INS cell volume with the latter showing increased endocytosis activation as opposed to L-LEU/N-INS, is not consistent with a cell volume driven mechanism, suggesting this would only be a partial contributor.

This loss of significance when data are normalised to cell volume suggests that even though endocytosis is increased in some groups (i.e. L-ISO/N-INS) – absolute number or collective volume of lysosomes and/or BSA-BODIPY – that alteration is not proportional to cell volume increase, thus when divided by higher cell volumes (normalisation to cell volume), statistical significance is lost (even though the pattern of response was always maintained).

Early embryos have mechanisms for maintaining their normal cell volumes. Early preimplantation embryos are particularly sensitive to osmolarity (Xie et al., 2007; Ruane et al., 2018) and require the importation of the AA glycine to regulate their cell volumes using a mechanism unique to early embryos (Baltz and Tartia, 2010). In addition to accumulating glycine, early embryos also need to release intracellular glycine (and other osmolytes), particularly when cell volume increases above the normal level. Mammalian cells, including oocytes and preimplantation embryos, express a volume-sensitive anion channel that is permeable to a number of organic osmolytes and that opens upon cell swelling to allow the efflux of intracellular osmolytes - swelling-activated channel activity (Kolajova and Baltz, 1999; Strange, et al., 1996). If their ability to use glycine for cell volume control is disrupted, fertilized oocytes fail to develop to blastocysts,

becoming blocked, even at normal *in vivo* osmolarities. Thus, cell volume is fundamental in determining whether embryos develop from fertilized oocytes. Other AAs such as glutamine, betaine, proline and β-alanine are also known to have osmoprotective effects (Dawson and Baltz, 1997). However, in my experiments where the concentrations of AAs, particularly BCAAs, were manipulated *in vitro*, all the other AAs were included at the same concentration in each treatment group and the osmolarity was always checked after medium preparation and only used if comprised in the perfect range - 250-260 mOsm. Moreover, the total embryo cell number and blastocysts total volume (*Appendix 8.8*) were not altered, reinforcing the insignificance of the slight increase in cell volume. However, even though I found that there is not a direct significant change in cell volume dependent upon treatment, the graph shape indicated a sizeable (non-significant) increase in cell volume for those treatments where endocytosis was increased (ie. L-ISO/N-INS) but also for some treatments where endocytosis response was weaker (ie. L-LEU/N-INS). Thus, I thought the next step would be a direct analysis by correlation (between cell volume versus BSA-BODIPY and LysoTracker number and volume) – in order to verify if perhaps AA composition to change endocytosis rate may act partially through cell volume change.

Endosomes and lysosomes are maintained during cell division and do not fragment or fuse (Bergeland et al., 2001). Moreover, it is known that the endocytosis process is arrested upon the entry into mitosis (Warren, 1993). Bergeland, et al., (2001) found no evidence for a strict mechanism assuring an equal division of endosomes/lysosomes into the two daughter cells and that these organelles were approximately halved after cell division, being then increased in the daughter cells after division – most likely as a result of endocytosis being reinitiated. Here, I found a positive relationship between cell volume and endocytosis (*Figure 4.34*) which was not treatment-related. In general, from my study it seems that cells with larger volumes have more lysosomes, which is presumably part of cell cycle dynamics. When the cell divides into two daughter cells, lysosomes are shared - smaller cell volume and fewer lysosomes each - then cell growth (and endocytosis reactivation) increases both lysosomes and cell volume. However, where a specific *in vitro* AA treatment provokes an increased response in lysosome production when another treatment does not (i.e. L-ISO/N-INS vs. NBCAA/N-INS – *Figure 4.10*), this may still require cell volume to increase to enact lysosomes to increase.

Together, these findings suggest a more general mechanism of cell volume increase across treatments, and a more specific AA-dependent mechanism that adds to that, as shown in *Figure 4.35* where L-ISO/N-INS correlation line is higher than control NBCAA/N-INS (we previously shown that to be significantly different) but where both lines show a positive and significant correlation between cell volume and LysoTracker/BSA-BODIPY number/volume. The nature of the association between culture treatment and the activation of increased lysosome production is the subject of the next Chapter of my studies.

Chapter 5 Lysosome regulation via mTOR and TFEB

5.1 Introduction

Lysosomes have several roles, including maintaining cellular homeostasis and mediating different physiological processes, such as cellular clearance, lipid homeostasis, energy metabolism, plasma membrane repair, bone remodelling, and pathogen defence (Settembre et al., 2012). These processes require an adaptive and dynamic response of the lysosome to the environment. However, the mechanisms that regulate lysosomal function and underlying lysosomal adaptation are still not fully understood. "Lysosomal gene network" — the coordinated lysosomal expression and regulation (CLEAR) network and its master gene transcription factor EB (TFEB) - were first discovered ten years ago and found to regulate lysosomal function and biogenesis as a response to environmental cues (Sardiello et al., 2009). Under basal conditions, TFEB is located in the cytoplasm, however, under specific conditions, such as starvation or lysosomal dysfunction, TFEB translocates from the cytoplasm to the nucleus (Sardiello et al., 2009; Settembre et al., 2012).

The nuclear translocation of TFEB is regulated by its phosphorylation status. Phosphorylated TFEB is located predominantly in the cytoplasm, while its dephosphorylated form is found in the nucleus (Settembre et al., 2012). TFEB interacts with mTOR on the lysosomal membrane and, through this interaction, it senses the lysosomal content. When mTOR is downregulated (i.e. through nutrient deprivation) TFEB is translocated to the nucleus. When in the nucleus, TFEB induces generation of new lysosomes, increases number of autophagosomes and autophagic flux, leading to clearance of storage material by promoting lysosomal secretion (Medina et al., 2011; Palmieri et al., 2011) and it is involved in lipid catabolism (as a form to generate energy) (*Figure 5.1*). Therefore, TFEB acts both as a sensor of lysosomal state, when on the lysosomal surface, and as an effector of lysosomal function when in the nucleus. This unique lysosome-to-nucleus signalling mechanism allows the lysosome to regulate its own function.

A 'sensing device' also referred to as LYNUS machinery (lysosome nutrient sensing), which is responsive to the lysosomal amino acid content and involves both the vacuolar

H^+–adenosine triphosphatase (v-ATPase) and mTORC1, was identified on the lysosomal surface (Zoncu, 2012). In the presence of adequate nutrition, TFEB interacts with LYNUS machinery, sensing lysosomal nutrient content via the v-ATPase complex, and it is phosphorylated by mTORC1 on the lysosomal surface. When phosphorylated, TFEB remains inactive by cytosolic sequestration, with the majority being diffused in the cytoplasm and a smaller fraction being found on lysosomes through its ability to physically bind mTORC1 (Settembre et al., 2012).

Nutrient withdrawal, v-ATPase inhibition, and lysosomal stress inactivate the Rag guanosine triphosphatases (GTPases), causing mTORC1 to be released from the LYNUS machinery and becoming inactive, thus resulting in failure to re-phosphorylate TFEB. Rag GTPases are activated by amino acids and promote the translocation of mTORC1 to the lysosomal surface where it is activated (Kim et al., 2008). Unphosphorylated TFEB progressively accumulates in the nucleus, where it induces its own transcription, activating lysosomal gene expression directed to correct the nutrient deficiency in the lysosome. If nutrition is restored, amino acids and v-ATPase regulate Rag GTPases, which in turn activate mTORC1 by translocating it to the lysosomal surface (Sancak et al., 2008; Zoncu, 2012). In fact, constitutively active Rags rescued nuclear translocation of TFEB caused by starvation and lysosomal stress, while inactive Rag mutants caused TFEB accumulation in the nucleus even in fully fed cells (Martina and Puertollano, 2013). These results imply that, among the many regulatory inputs to mTORC1, the amino acid pathway is particularly important in controlling TFEB activity.

Since lysosome number is increased in the L-ISO/N-INS embryo group (see 4.3.2.), in this chapter I investigate TFEB as a possible candidate stimulating lysosome biosynthesis as a response to poor amino acid lysosomal content. Through immunocytochemistry, I have compared the location (nuclear/cytoplasmic) of TFEB in L-ISO/N-INS and control NBCAA/N-INS, and using qRT-PCR I studied the gene expression of lysosomal genes known to be direct targets of TFEB. Furthermore, it is well stablished that mTORC1 is inhibited by rapamycin. Thus, because there are currently no studies regarding TFEB expression in embryos, I tested different concentrations of rapamycin in culture, used as an mTORC1 inhibitor, in order to study TFEB expression and localisation when mTORC1 is fully or partially inhibited in mouse embryos.

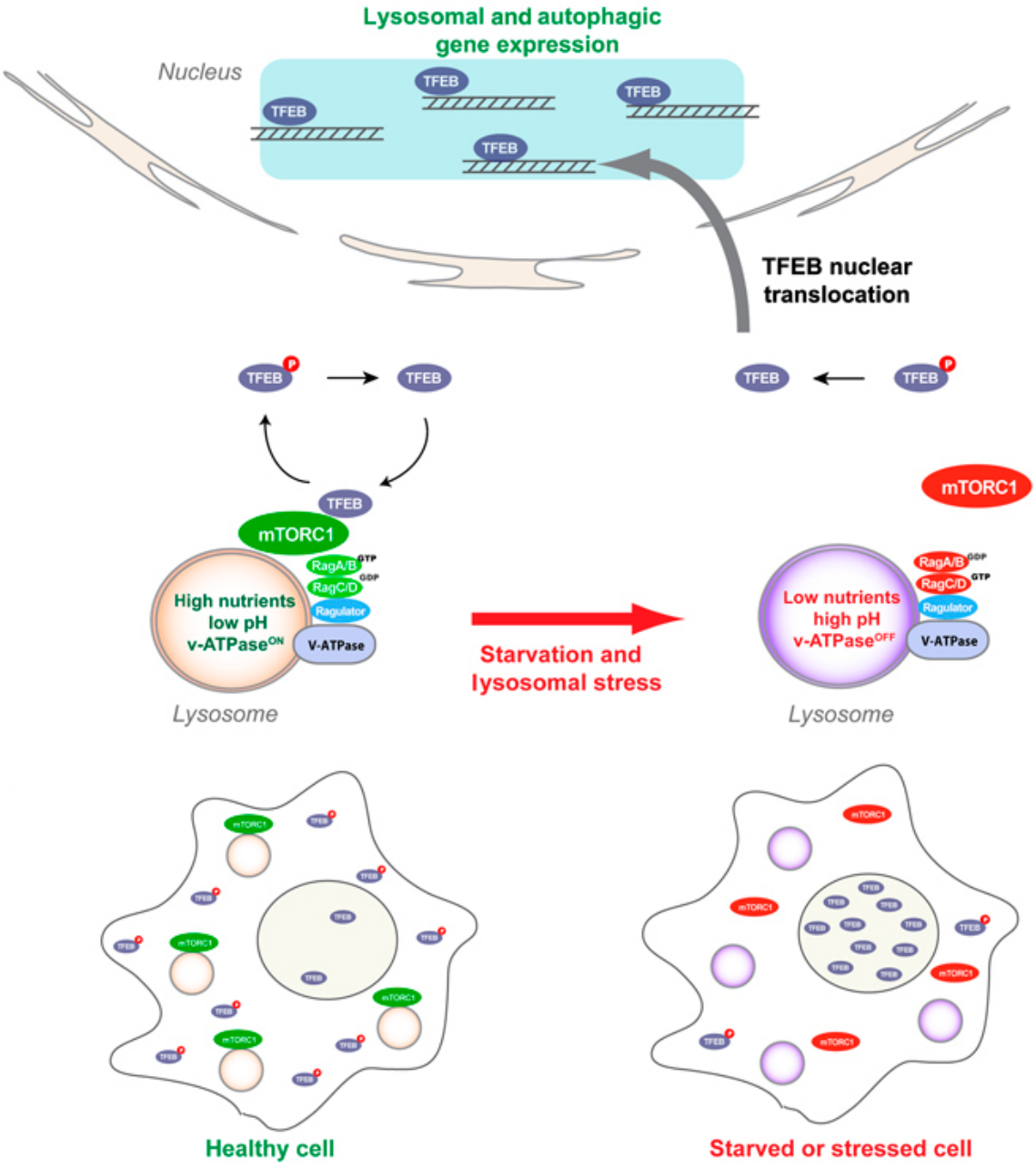

Figure 5.1 - Model of lysosomal sensing and lysosome-to-nucleus signalling by TFEB and mTOR under full nutrients (left) and starvation models (right) (from Settembre et al., 2012).

5.2 Materials and Methods

5.2.1 Animals

Described in section *2.1.*

5.2.2 Embryos collection

E1.5 embryos were collected as described in *section 2.1.1.*

5.2.3 In vitro embryo culture

2-cell stage embryos (E1.5) collected from mice fed chow diet were cultured in KSOM medium with variable BCAA concentration (NBCAA/N-INS or L-ISO/N-INS) at 37°C in 5% CO_2 until reaching the blastocyst stage. At that point embryos were fixed and used for immunocytochemistry with TFEB.

5.2.3.1 Amino Acids Stocks

Described in section *4.2.3.1.*

5.2.3.2 KSOM media with BCAAs concentration change

From each mother, the same number of embryos was randomly distributed to the treatment groups. In all *in vitro* experiments, control medium consisted of KSOM with 1ng/ml insulin and the amino acids concentration found in E3.5 NPD uterine fluid (Eckert et al. 2012), including the three BCAA – leucine (0.32mM), isoleucine (0.21mM) and valine (0.46mM). 2-cell stage embryos were cultured in NBCAA/N-INS or with 50% decreased Isoleucine (L-ISO/N-INS) and normal insulin concentration (1ng/ml). *Appendix 8.2.3.* shows the components and respective concentrations used to prepare the different KSOM media.

5.2.4 Immunocytochemistry

After culture from 2-cell stage to blastocyst, embryos were fixed in 1% formaldehyde. For these experiments the zona pellucida was not removed. The protocol is described in *2.3*.

5.2.5 Image acquisition and data analysis

VOLOCITY software used to analyse data obtained from the confocal microscope is described. A new protocol was designed to measure the localization of TFEB (nuclear or cytoplasmic) in TE cells. Using the designed settings, VOLOCITY was used to calculate the volume of TFEB present in the cell nucleus and cytoplasm. *Appendix 8.11* contains print-screens "step-by-step" to perform the optimised protocol in VOLOCITY 6.3.

Statistical analysis was conducted with GraphPad Stats using t test when data were normally distributed or Mann-Whitney test when data were not normally distributed. Significance was taken as $P < 0.05$ and a trend was assumed if P was between 0.1 and 0.051.

The protocol consisted of:

1. Crop cell

2. Find object (based on channel) – blue channel (DAPI – nucleus) and green channel for TFEB

3. Remove noise from objects (fine filter)

4. Separate touching objects (by 2 µm)

5. Exclude objects by size: chosen based on the literature, according to Tsichlaki and Fitzharris, (2016) the blastocyst nuclei size is 690±20 μm^3

   5.1. nuclei < 150 μm^3Nuclei – fill holes in objects

6. Objects of interest were selected by automatic threshold using an offset of 50%.

7. Define cytoplasm: subtract nucleus from ROIs (cell)

8. Find TFEB in nucleus: intersect nucleus with TFEB

   a) Remove noise from objects (fine filter)

   b) Separate touching objects (by 2 µm)

9. Find TFEB in cytoplasm: intersect cytoplasm with TFEB

   a) Remove noise from objects (fine filter)

b) Separate touching objects (by 2 μm)

10. Colocalization: automatic threshold (Costes) – Costes Pearson correlation

11. Object data were exported to Excel for analysis.

In the VOLOCITY programme, the automatic Costes method was used to identify threshold values for each TE cell analysed. This method automatically identifies the threshold value to be used to identify background based on an analysis that determines the range of pixel values for which a positive Pearson correlation value is obtained (Dunn et al., 2011). In this approach, Pearson correlation coefficient is measured for all pixels on the regression line, until reaching pixel values with Pearson correlation of zero or below (Dunn et al., 2011). The blue channel (nuclei) and green channel (TFEB) intensity values on the regression line at this point are then used as the threshold values for identifying background levels in each channel. Only pixels whose blue and green intensity values are both above their respective thresholds are considered to be pixels with colocalized probes (Dunn et al., 2011). This method for estimating thresholds eliminates user bias.

5.2.6 Single embryo RNA extraction and RT reaction

Described in *Methods 2.5*.

5.2.7 Single embryo qRT-PCR

Described in *Methods 2.6*.

5.2.8 Multiplex PCR and embryo genotyping

Described in *Methods 2.7*.

5.2.9 Rapamycin treatment – mTORC1 inhibition

2-cell stage embryos (E1.5) were collected from mice fed chow diet and cultured in NBCAA/N-INS medium supplemented with rapamycin (LC laboratories, Woburn, USA) at final concentrations of 100 nM, 1 μM or 20 μM at 37°C in 5% CO_2. After 36 hours in culture, embryos were transferred to fresh medium containing the same concentration

of rapamycin until reaching the blastocyst stage. Control embryos were cultured in KSOM without rapamycin but complemented with DMSO at 1:1000 since rapamycin was first diluted in DMSO (same amount of solvent). At that point embryos were stained with LysoTracker (see 3.2.3.2), fixed and imaged before immunocytochemistry with TFEB (see 5.2.4).

5.3 Results

5.3.1 TFEB protocol optimization

Rabbit polyclonal antibody to TFEB, gene 7942 (A303-673A-T Bethyl Laboratories) reacts with human and mouse and the epitope recognized by A303-673A-T maps to a region between residue 426 and 476 of human TFEB. In order to optimise the protocol and because no other published data regarding TFEB expression in mouse blastocysts were available, the protocol used was based on the manufacture's information, using the same incubation time (overnight) and temperature (4°C) and testing different concentrations of the primary antibody within the suggested range (1:25 – 1:100) to determine when an optimal signal is achieved with low background noise. These were: 1:100 (*Figure 5.2 A*), 1:50 *(Figure 5.2B)* and 1:25 (*Figure 5.2C)* and negative controls *(Figure 5.2D,E*) by omitting primary antibody. Based on signal strength and low background, 1:50 was selected as the best concentration and was used in the further experiments. 1:25 showed some non-specific and higher background while 1:100 staining was weak.

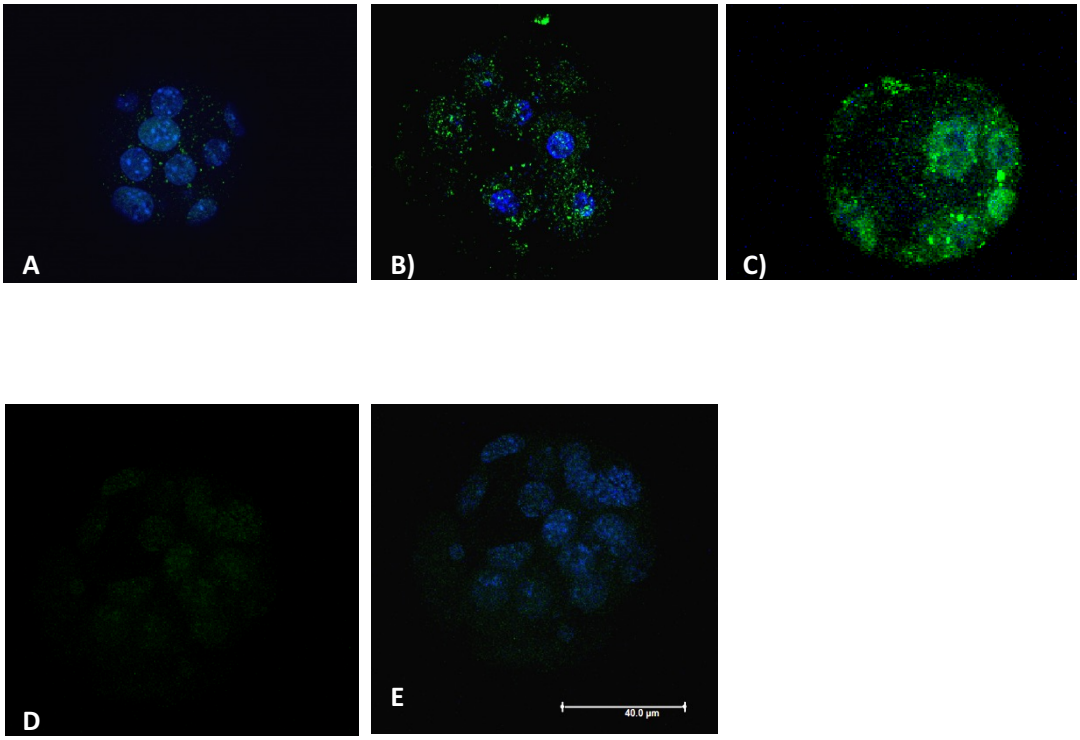

Figure 5.2 – TFEB immunocytochemistry protocol optimisation in mouse blastocysts. Fixed embryos were incubated overnight with TFEB antibody at 4°C at different concentrations: 1:100 (A), 1:50 (B) and 1:25 (C). Negative controls (D,E) were included by omitting the primary antibody (incubation overnight with PBS-Tween). D) TFEB E) TFEB and DAPI (blue). Scale bar = 40 µm.

5.3.2 TFEB nuclear translocation occurs in blastocyst TE following culture from 2-cell stage in L-ISO/N-INS culture medium

Because embryos cultured in L-ISO/N-INS showed an increased number of lysosomes and increased endocytosis, I tested whether this treatment affected TFEB cellular localisation. TFEB subcellular localization was analysed in blastocysts after culture from 2-cell stage in either L-ISO/N-INS or NBCAA/N-INS control. To quantify cellular localisation, the volume of TFEB in the cytoplasm and nucleus was divided by total volume of TFEB in the cell (*Figure 5.3)*. Immunofluorescence analysis showed that isoleucine depletion (L-ISO/N-INS) induced nuclear translocation of TFEB (*Figure 5.2)*. The statistical Pearson Correlation was calculated by VOLOCITY software to measure the statistical relationship/association between the two channels (green – TFEB and blue – DAPI) (*Figure 5.4*). Preliminary data suggest that approximately 80% of TFEB is located in the nucleus in the L-ISO/N-INS group against 40% in the control NBCAA/N-INS (*Figure 5.2).* Pearson Correlation test for nucleus and TFEB colocalization is also increased in the L-ISO/N-INS group (*Figure 5.4*). This test interprets both the intensity and position of different fluorophores in one-pixel field. This means that a significantly higher proportion of the total TFEB is localised in the nucleus (or is co-labelled with DAPI) in the L-ISO/N-INS group compared to NBCAA/N-INS. There were no differences in the cell numbers of the blastocysts analysed (*Figure 5.5*).

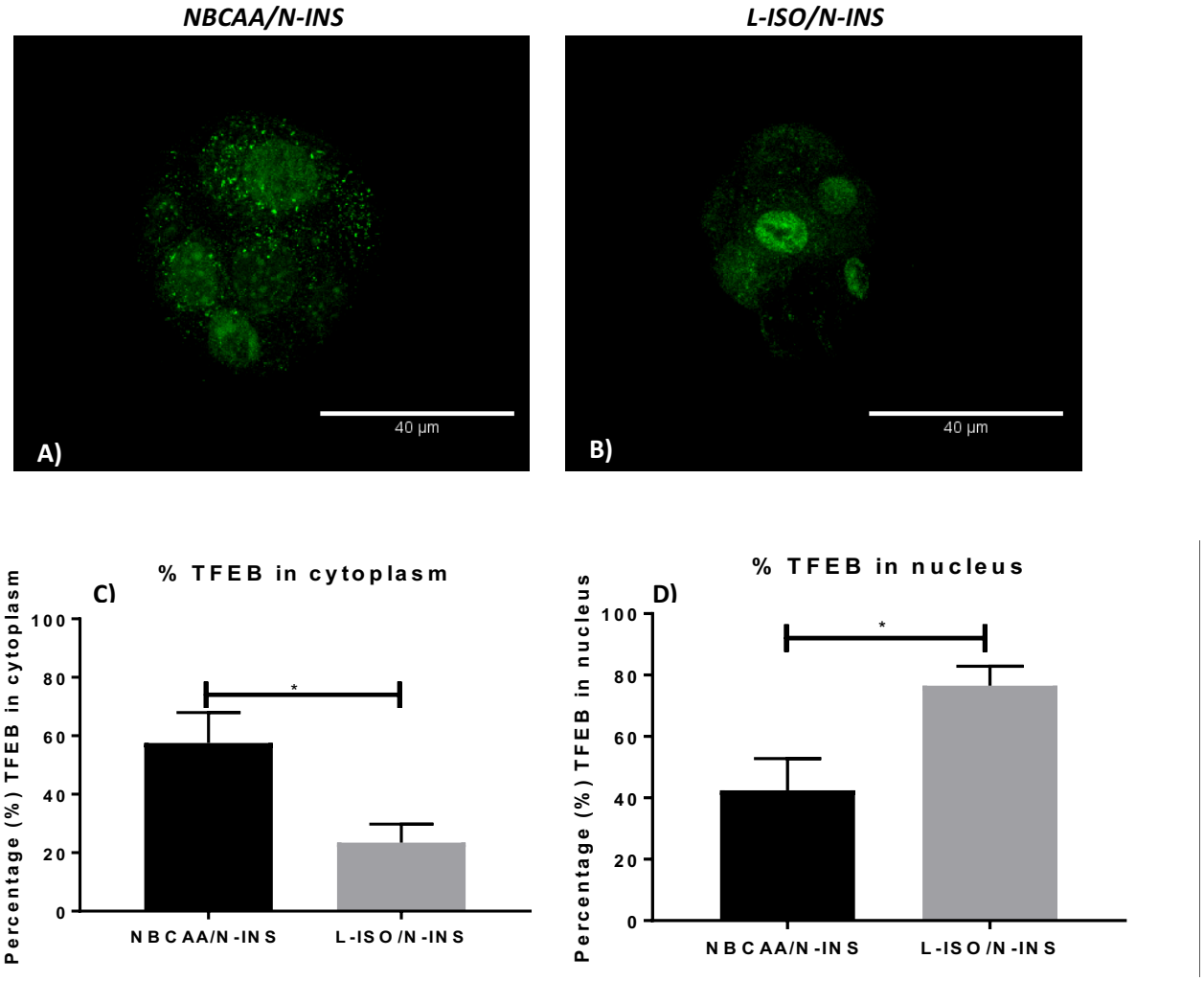

Figure 5.3 – TFEB staining in NBCAA/N-INS (A) and in L-ISO/N-INS (B). Percentage (%) of TFEB localised in the cytoplasm (C) and in the nucleus (D). TFEB nuclear translocation occurs in blastocyst TE following culture from 2-cell stage in medium with depleted Isoleucine alone and normal insulin (L-ISO/N-INS) while TFEB in NBCAA/N-INS is mainly located in the cytoplasm (C,D). Values are mean ±SEM. * P <0.05; 7-8 embryos per group (9-10 cells per group) from 4 mothers (in 4 replicates). Scale bar = 40 µm.

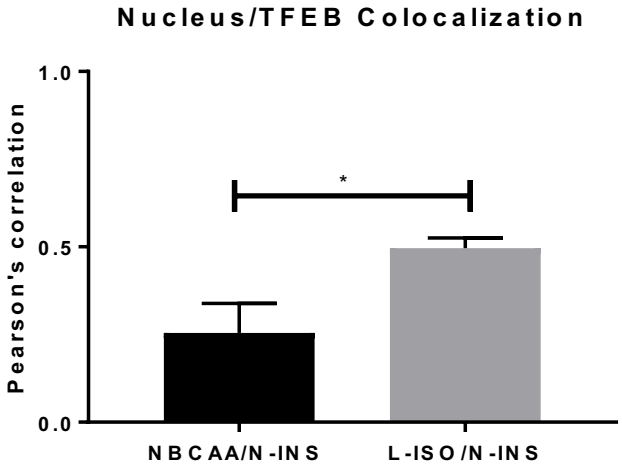

Figure 5.4 – L-ISO/N-INS TE cells have a significantly increased proportion of the TFEB (green channel) co-labelled with the nucleus (DAPI – blue channel). Values are mean ±SEM. * P <0.05; 7-8 embryos per group (9-10 cells per group) from 4 mothers (in 4 replicates).

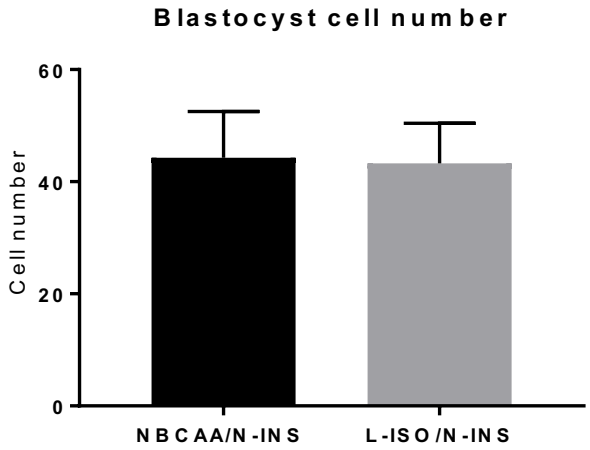

Figure 5.5 – No difference was found in the blastocyst number of cells analysed between the L-ISO/N-INS and NBCAA/N-INS groups. Values are mean ±SEM. 7-8 embryos per group (9-10 cells per group) from 4 mothers (in 4 replicates).

5.3.3 Gene expression of TFEB direct targets

Palmieri et al., (2011) performed transient TFEB overexpression in HeLa cells and profiled gene expression by using microarray technologies deep sequencing of TFEB chromatin immunoprecipitate (ChIP-seq) and unbiased genomic and expression meta-analysis to obtain a more comprehensive map of the TFEB targetome. Among the most likely lysosomal direct targets of TFEB are genes that encode for proteins that can be grouped in several distinct categories, including hydrolases and accessory proteins, lysosomal membrane proteins, subunits of the proton pump (lysosomal acidification), proteins participating in autophagy and non-lysosomal proteins involved in lysosomal biogenesis. Moreover, Sardiello et al (2009) also observed an increase in the mRNA levels of lysosomal genes (22 out of 23 genes tested) after TFEB overexpression and identified 291 upregulated and 7 downregulated genes responsive to TFEB on a genomic scale, using microarray analysis of the HeLa transcriptome after TFEB over-expression. Based on those genes described in both papers, I have selected the genes with highest fold change differences in each different category related to lysosomal function. Cathepsin B (Ctsb), a lysosomal hydrolase which I have shown to be significantly increased in L-ISO/N-INS blastocysts at protein level (*see 4.3.2*); lysosomal-associated membrane protein 1 (Lamp1) responsible for maintaining lysosomal integrity, pH and catabolism; vacuolar protein sorting 18 homolog (Vps18), a protein involved in autophagy, and ATPase, H+ transporting, lysosomal 38kDA, V0 subunit d2 (Atp6v0d2) responsible for lysosomal acidification.

Due to the low number of female embryos identified, qRT-PCR was performed on male blastocysts only (*see Table 2.5*) (n = 10 mothers per group). Gene expression was normalised using H2afz and Sdha as reference genes previously selected by geNorm analysis (*See Methods 2.6.2*). qPCR was performed using primer assays previously optimised and verified beforehand using gel electrophoresis and melting curve analysis (*See Methods 2.6.3*). *Appendix 8.7* shows the gel electrophoresis for the qRT-PCR products.

L-ISO/N-INS treatment did not alter the mRNA expression of Ctsb, Lamp1 and Vps18

in male blastocysts (*Figure 5.6*). Moreover, Atp6v0d2 was not amplified in blastocysts. Since positive control (liver sample) showed amplification, this suggests that Atp6v0d2 is not expressed or it is expressed at non-detectable low levels in mouse embryos at blastocyst stage.

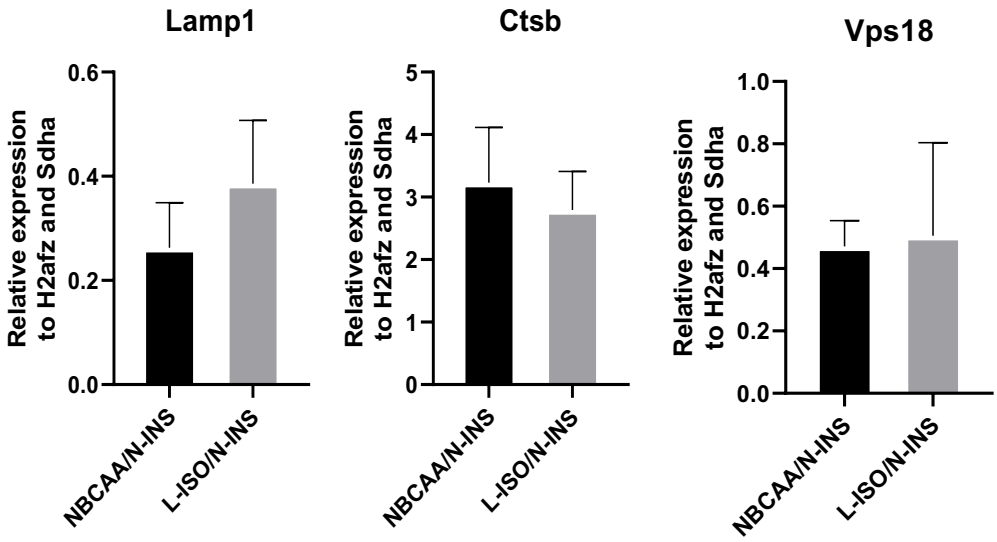

Figure 5.6 - Relative mRNA levels of Lamp1 (A), Ctsb (B) and Vps18 (C) in male blastocysts cultured in NBCAA/N-INS and L-ISO-N-INS from 2-cell until blastocyst stage (N = 10 embryos/group from 10 mothers). Values are presented as mean ± SEM.

5.3.4 TFEB expression and localisation in blastocysts with mTORC1 inhibited by Rapamycin

2-cell stage embryos were collected and cultured in NBCAA/N-INS medium supplemented with rapamycin at different concentrations (100 nM, 1 μM or 20 μM) or without rapamycin. Rapamycin concentrations tested in this study were selected based on studies where the drug was used as an mTORC1 inhibitor in mouse preimplantation embryos (Eckert et al., 2012; Murakami and Ichisaka, 2004; Lee et al., 2016).

At the blastocyst stage, embryos were cultured in the same medium but with LysoTracker Red for 1 h, fixed and imaged in the confocal microscope, followed by immunohistochemistry analysis using TFEB antibody. No significant difference was

found in LysoTracker staining between the four groups (*Figure 5.7*), even though embryos cultured in 20 μM rapamycin showed a trend of increased volume of lysosomes in the TE cells. Furthermore, a proportional increase in TFEB localisation within the nucleus was found in embryos cultured in higher concentrations of rapamycin (*Figure 5.8*).

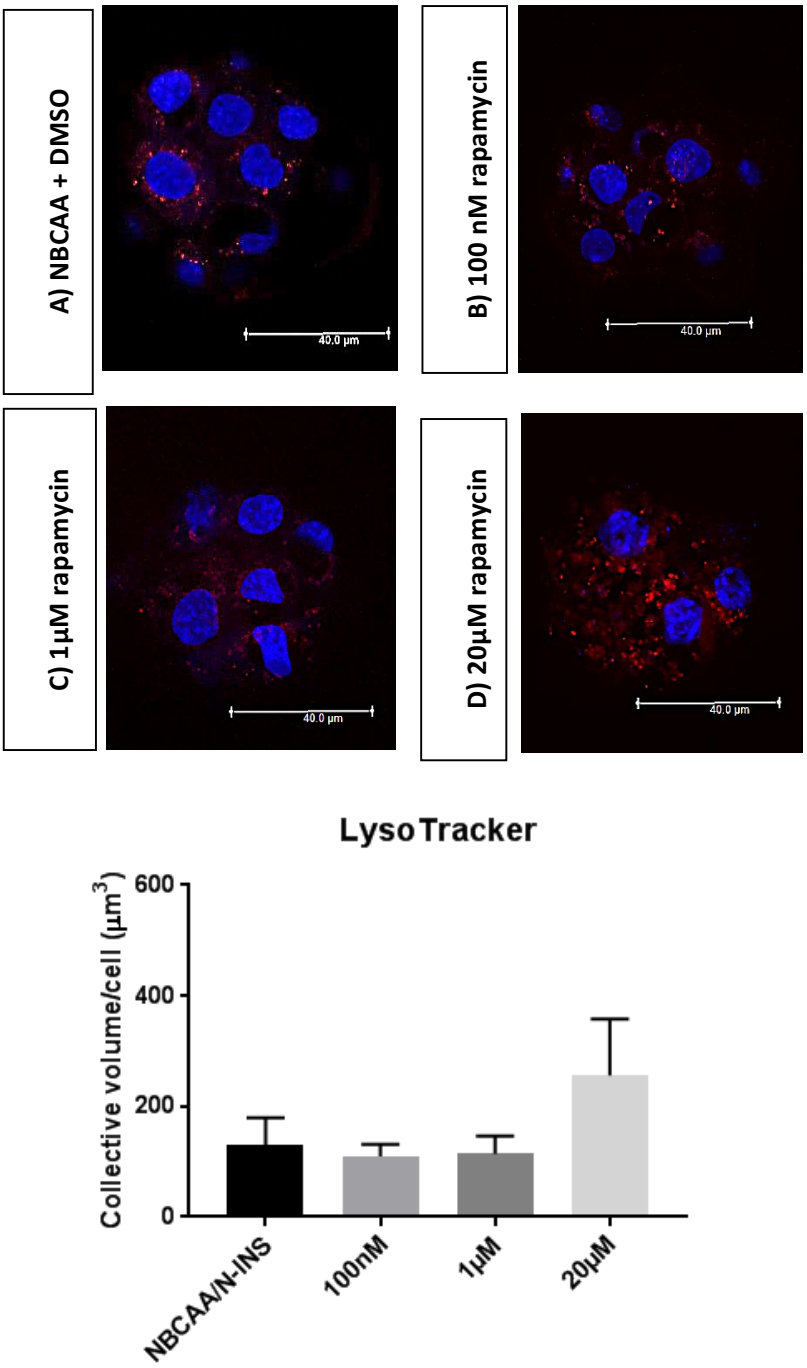

Figure 5.7 – LysoTracker staining is not altered in 2-cell stage embryos collected and cultured until blastocyst stage in NBCAA/N-INS medium supplemented with rapamycin at different concentrations – 0 (A), 100 nM (B), 1 µM (C) or 20 µM (D). At blastocyst stage, embryos were analysed for lysosome collective volume/cell (LysoTracker Red) and no significant changes were observed, even though embryos in the 20 µM group showed a slightly increase. Blue – nuclear staining (DAPI). Values are presented as mean ±SEM; 6-13 embryos per group from 5 mothers (in 4 replicates). Scale bar = 40 µm.

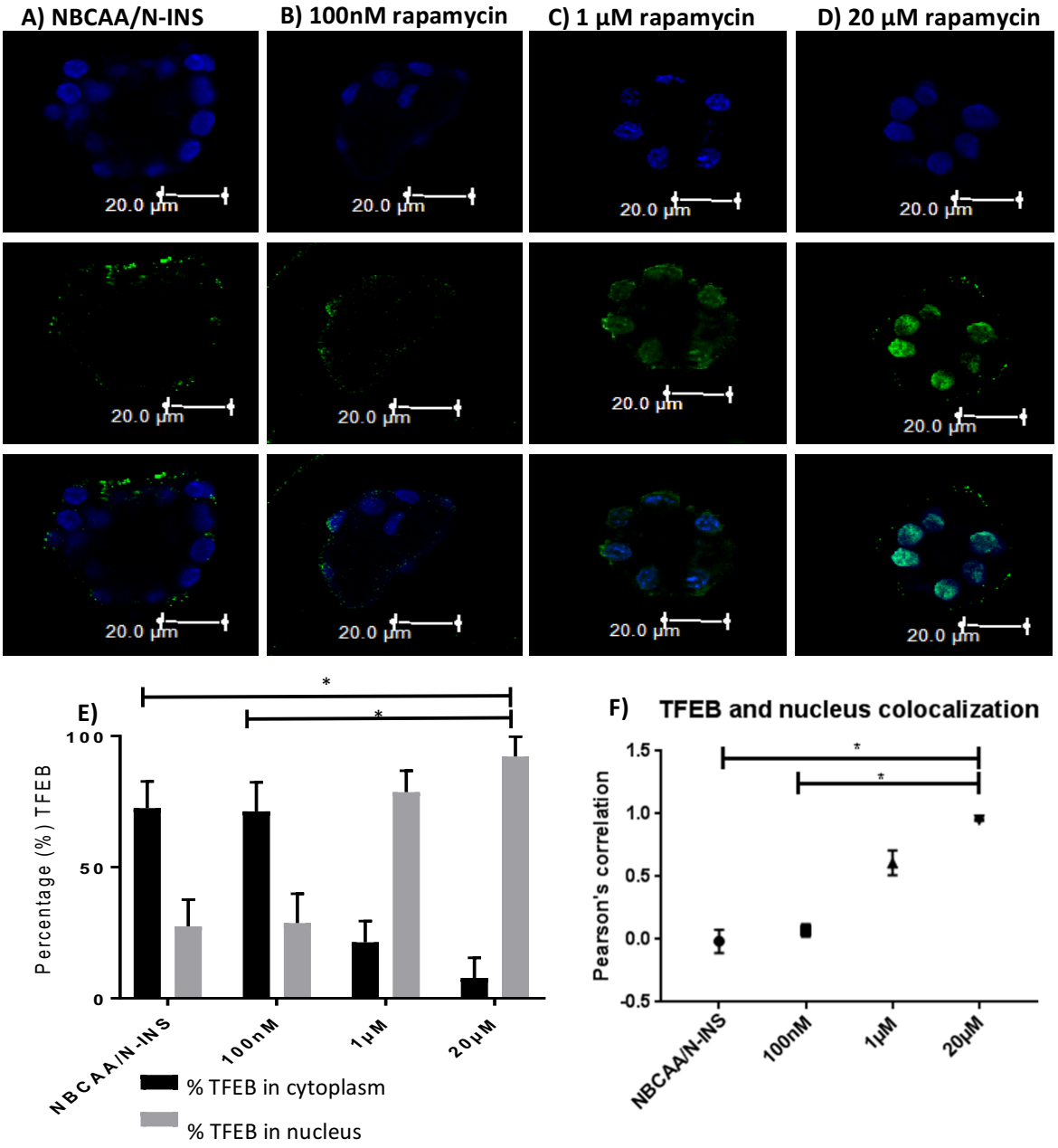

Figure 5.8 – TFEB staining and localisation in 2-cell stage embryos cultured until blastocyst stage in NBCAA/N-INS medium supplemented with rapamycin at different concentrations – 0 (A), 100 nM (B), 1 µM (C) or 20 µM (D). At blastocyst stage, embryos were fixed and analysed by immunohistochemistry for TFEB (green). In A-D, top is blue channel (nuclei), middle green channel (TFEB) and lower combined. Embryos cultured in 20 µM rapamycin showed increased percentage of TFEB in the nucleus compared to the control NBCAA/N-INS and 100 nM groups (E). Pearson correlation values show very high colocalisation between TFEB and DAPI (nuclear staining) as rapamycin concentration increases (F). Values are presented as Mean with SEM, * P value <0.05; 6-13 embryos per group from 5 mothers (in 4 replicates). Scale bar = 20 µm.

5.3.5 There is no correlation between TE cell volume and TFEB nuclear location

In Chapter 4 (see 4.3.7), I found a positive relationship between cell volume and endocytosis but not treatment related. In general, cells with larger volumes have more lysosomes, independently of which *in vitro* treatment they were submitted to. This means a more general mechanism of cell volume increase in lysosomes across treatments, and a more specific AA-dependent mechanism that adds to that. Thus, to assess whether cell volume was contributing to the switch in TFEB localisation upon L-ISO/N-INS treatment, both cell volume in relation to treatment and correlation of cell volume with TFEB nuclear localisation were determined. Cell volume was found not to change between treatments (*Figure 5.9A*) and no correlation was found between cell volume and nuclear TFEB in treatments (*Figure 5.9B*) with low R^2 values and high P values present (*Figure 5.8C*). However, the line of best fit was higher in the L-ISO/N-INS than the NBCAA/N-INS correlation graph reflecting the increased percentage nuclear TFEB per unit cell volume in this group (*Figure 5.9B*).

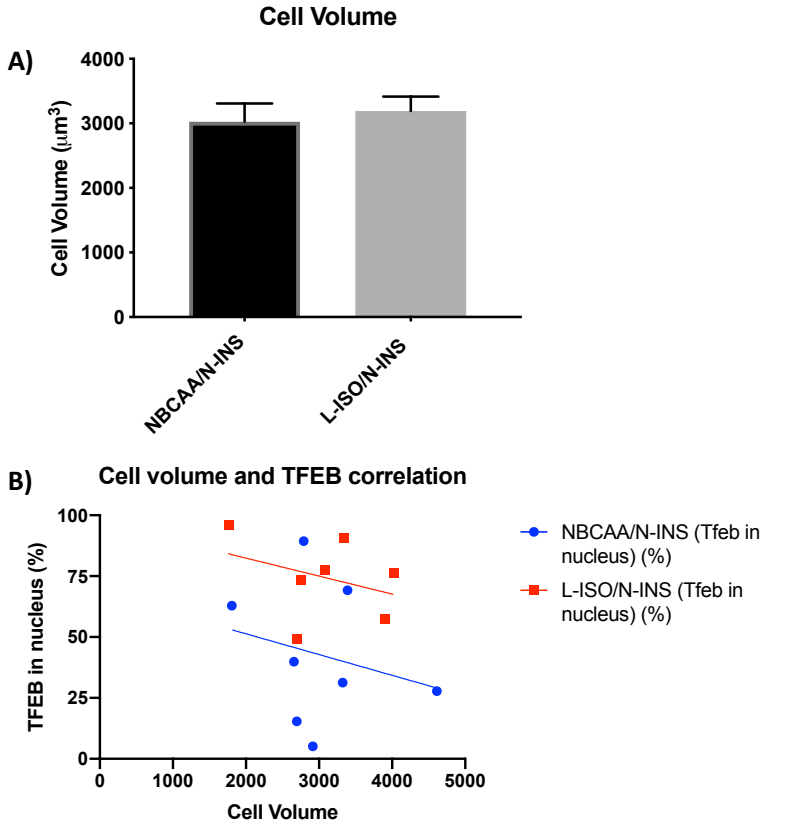

C)

Correlation	Cell Volume vs. NBCAA/N-INS (Tfeb in nucleus) (%)	Cell Volume vs. L-ISO/N-INS (Tfeb in nucleus) (%)
	Y	Y
Pearson r		
r	-0.2381	-0.3451
95% confidence interval	-0.8073 to 0.5606	-0.8716 to 0.5512
R squared	0.05669	0.1191
P value		
P (two-tailed)	0.5702	0.4483
P value summary	ns	ns
Significant? (alpha = 0.05)	No	No
Number of XY Pairs	8	7

Figure 5.9 - Cell volume analysis and correlation between cell volume and TFEB in nucleus in treatments NBCAA/N-INS and L-INS/N-INS. Cell volume was not altered between treatments (A). There is no correlation between cell volume and the percentage of TFEB in the nucleus in both groups (B) – NBCAA/N-INS (blue) and L-ISO/N-INS (red). Statistics from the correlation analysis show low R^2 values and high P values (C) suggesting no correlation between the two factors. Values are mean ±SEM. 7-8 embryos per group (9-10 cells per group) from 4 mothers (in 4 replicates).

To confirm results, the same cell volume and correlation analysis was carried out in embryos treated with different concentrations of rapamycin which inhibits mTORC1. Higher concentrations of rapamycin (20 μM) had been found to have no effect on lysosome number per cell but contributed to TFEB activation, shown by increased proportion of TFEB nuclear staining. Again, as in *Chapter 4* (4.3.8), a positive correlation was found between cell volume and lysosome number and volume (*Figure 5.10A* and *Figure 5.10B*) when all treatments were combined. However, no correlation existed between cell volume and percentage of TFEB in the nucleus when all treatments are combined (*Figure 5.10C*) with low R^2 values and high P values (*Figure 5.9D*). Moreover, no correlation was found between cell volume and TFEB percentage of nuclear localisation when compared across treatments (*Figure 5.11A*). However, treatments with higher rapamycin concentration occur in the top of the graph (1 μM green and 20 μM purple) and lower concentrations at the bottom (100 nM red and no rapamycin blue) showing higher and lower percentages of TFEB in the nucleus per unit cell volume due to rapamycin treatment and not cell volume (*Figure 5.11B*). In summary, contrary to what we observed in the lysosome response, we found no relationship between cell volume and TFEB localisation.

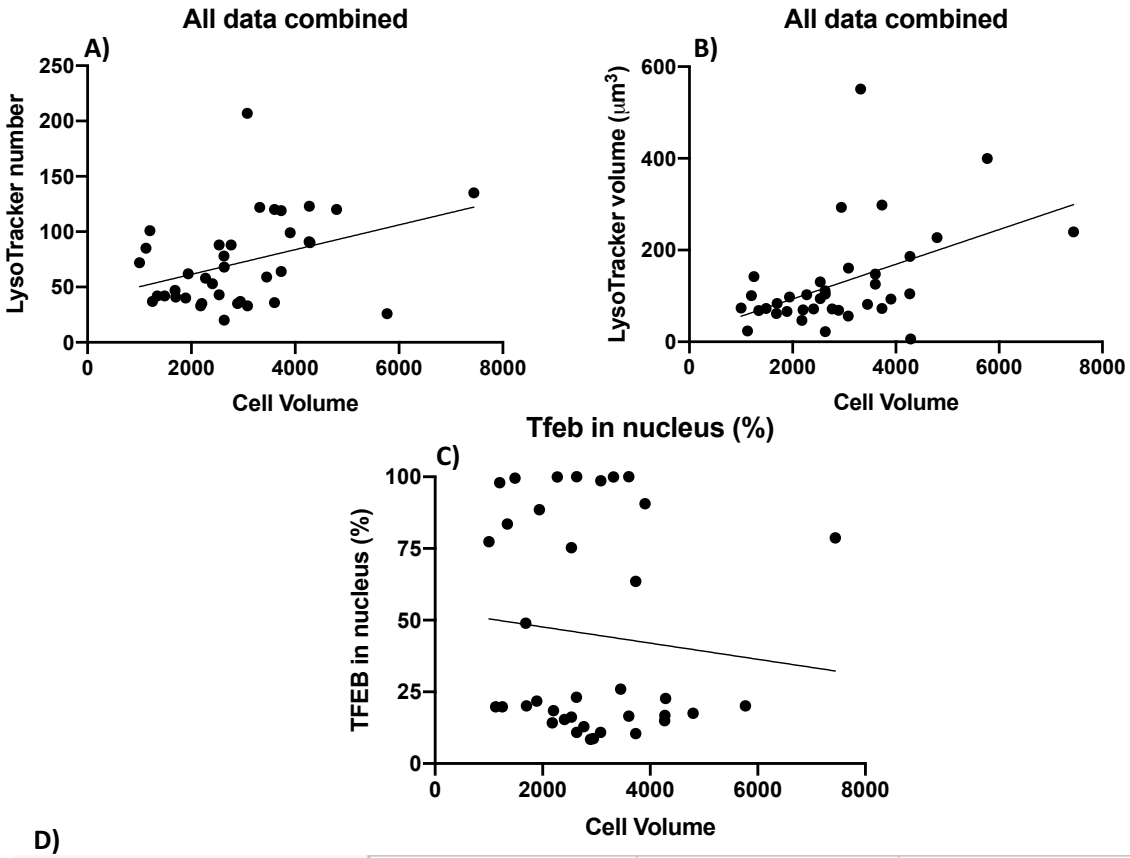

D)

Correlation	Cell Volume vs. LysoTracker number	Cell Volume vs. LysoTracker volume	Cell Volume vs. Tfeb in nucleus (%)
	Y	Y	Y
Pearson r			
r	0.3777	0.4682	-0.1046
95% confidence interval	0.06120 to 0.6252	0.1699 to 0.6879	-0.4145 to 0.2271
R squared	0.1427	0.2192	0.01094
P value			
P (two-tailed)	0.0212	0.0035	0.5379
P value summary	*	**	ns
Significant? (alpha = 0.05)	Yes	Yes	No
Number of XY Pairs	37	37	37

Figure 5.10 – Correlation between cell volume and lysosome number (A), lysosome collective volume (B) and percentage of TFEB in nucleus (C) in embryos cultured in different concentrations of rapamycin - 0, 100 nM, 1 µM and 20 µM - from 2-cell stage to blastocyst stage (data from 4 treatment groups combined). There is a positive correlation between cell volume and lysosome number and volume (A and B) but no correlation between cell volume and percentage of TFEB in the nucleus (C) – as shown by statistics in D. * P value <0.05 ** P value < 0.01; 37 embryos combined (from 5 mothers, in 4 replicates) .

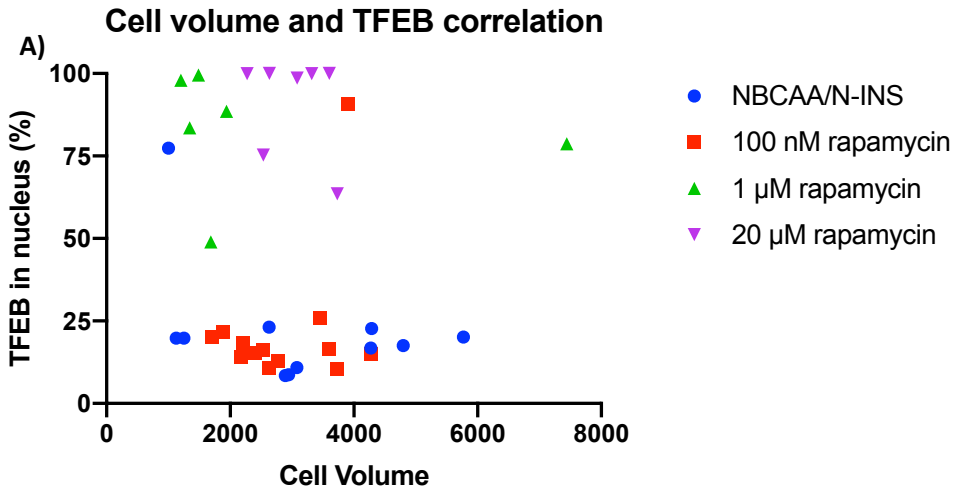

B)

Correlation	Cell Volume vs. NBCAA/N-INS	Cell Volume vs. 100 nM rapamycin	Cell Volume vs. 1 µM rapamycin	Cell Volume vs. 20 µM rapamycin
	Y	Y	Y	Y
Pearson r				
r	-0.4042	0.3249	-0.1493	-0.2687
95% confidence interval	-0.8081 to 0.2583	-0.2754 to 0.7429	-0.8570 to 0.7536	-0.8498 to 0.6072
R squared	0.1634	0.1055	0.02228	0.07220
P value				
P (two-tailed)	0.2175	0.2788	0.7778	0.5601
P value summary	ns	ns	ns	ns
Significant? (alpha = 0.05)	No	No	No	No
Number of XY Pairs	11	13	6	7

Figure 5.11 – Correlation between cell volume and percentage TFEB in the nucleus (A) in embryos cultured in different concentrations of rapamycin – NBCAA/N-INS with no rapamycin (blue), 100 nM (red), 1 µM (green) and 20 µM (purple) - from 2-cell stage to blastocyst stage. There is no correlation between cell volume and TFEB (B). 6-13 embryos per group, from 5 mothers (in 4 replicates).

5.4 Discussion

5.4.1 TFEB activation occurs in blastocyst TE following culture from 2-cell stage in L-ISO/N-INS culture medium and in embryos with mTORC1 inhibited by rapamycin

TFEB is tightly controlled by nutrient status, with energy-rich conditions leading to hyperphosphorylation and cytoplasmic retention and low-energy stores promoting hypophosphorylation and nuclear localization (Settembre et al., 2012). TFEB interacts with mTOR on the lysosomal membrane sensing the lysosomal content. When mTOR is downregulated (i.e. decreased lysosomal nutrients) TFEB is translocated to the nucleus increasing the transcription of multiple genes implicated in lysosomal biosynthesis and function and autophagy.

We previously found that endocytosis and lysosome number were increased in blastocyst TE cells cultured from 2-cell stage in L-ISO/N-INS (see *4.3.2*). Similarly, Emb-LPD blastocysts showed increased compensatory endocytosis and lysosome number (Sun et al., 2014) and have reduced mTORC1 signalling (Eckert et al., 2012). Thus, TFEB emerged as a potential target regulating lysosome formation in this model. We used immunofluorescence to study TFEB localisation/nuclear translocation in L-ISO/N-INS and control NBCAA/N-INS.

I found that almost 80% of total TFEB volume in TE cells is located in the nucleus in L-ISO/N-INS as opposed to approximately 40% in the control NBCAA/N-INS group. Moreover, Pearson correlation analysis was used to validate this outcome by quantifying the colocalization between nucleus (blue channel – DAPI) and TFEB (green channel). This showed a moderately high correlation in the L-ISO/N-INS significantly higher than the weak correlation found in NBCAA/N-INS.

Settembre et al., (2012) showed that in fully fed cells, the majority of TFEB appeared to freely diffuse in the cytoplasm while a small fraction of TFEB could always be found on lysosomes, due to its ability to physically bind mTORC1. At any given time, a fraction of TFEB rapidly and transiently binds to the lysosomal surface, where it is phosphorylated by mTORC1 and thus kept in the cytoplasm. However, TFEB clustered

on lysosomes shortly after mTORC drug inhibition and progressively appeared in the nucleus. Martina et al., (2012) suggested that TFEB might shuttle continuously between the cytosol and late endosomes/lysosomes as a means to constantly monitor mTORC1 activity. Alternatively, additional modifications or hetero-oligomerization of TFEB may occur at lysosomes, thus providing further checkpoints for the activation of this transcription factor. In the current study, the identity of the specific cytoplasmic location of TFEB (~20% in L-ISO/N-INS and ~60% in NBCAA/N-INS) has not yet been determined. However, as future work, TFEB and a lysosome marker colocalisation in this model could be studied to see if a higher fraction of TFEB is interacting with lysosomes before being translocated to the nucleus.

Despite the TFEB activation seen in L-ISO/N-INS blastocysts, mRNA levels of three TFEB direct targets with known roles in lysosomal function (Lamp1, Ctsb and Vps18) were not altered. These genes (and several other lysosomal genes) were previously shown to be upregulated following TFEB transient overexpression – HeLa cells transfected with plasmids carrying TFEB cDNA - which showed how TFEB is able to modulate the expression of lysosomal genes (Sardiello et al., 2009). Due to high variability in embryos it is possible that a larger n number would be necessary to detect any statistically significant difference, especially for Lamp1. Ctsb (Cathepsin B) was increased at protein level (see *Chapter 4 – 4.3.2.*) but not at mRNA level. This increase in protein could be due to transient upregulation of transcription which might have disappeared at the end of experiment, remaining the raised protein level. Previous work done using a widely used marker for the autophagosome (LC3) showed that autophagy was not altered in the Emb-LPD blastocysts (Sun et al., 2014). Here, Vps18 (a protein involved in autophagy) was not altered at mRNA level but further work is necessary to confirm if autophagy is altered in this *in vitro* culture model.

Although mTORC1 downregulation was seen in Emb-LPD blastocysts (Eckert et al., 2012), mTORC1 regulation has not been studied directly in our *in vitro* model. Nevertheless, we found that TFEB is activated under specific *in vitro* conditions (L-ISO/N-INS) and since TFEB is triggered in response to lysosomal status (low nutrients) through downregulated mTORC1, we then used the mTORC1 inhibitor rapamycin at different concentrations *in vitro* (from 2-cell to blastocyst stage) to determine

whether mTOR regulation of TFEB occurs in our model. Interestingly, we found that higher concentrations of rapamycin (20 μM) caused TFEB activation, shown by increased nuclear staining compared to lower concentrations of the drug (control NBCAA/N-INS, 100 nM and 1 μM) where TFEB was mainly cytoplasmic. However, even though in our model, embryo culture in L-ISO/N-INS was sufficient to cause not only TFEB activation but also subsequent increased lysosome formation (when in the nucleus, TFEB induces generation of new lysosomes), rapamycin treatment only partially increased lysosome number and only at the highest concentration used (20 μm; *Figure 5.7*). A possible explanation for these results is that rapamycin is actually only a partial inhibitor of mTOR, as some substrates are still efficiently phosphorylated in the presence of this drug (Thoreen et al., 2009). In Settembre et al., (2012) study, the combined use of Rapamycin at 2.5 μM and amino acid rich medium in starved cells resulted in a partial TFEB molecular weight shift but did not affect its subcellular location as opposed to stimulation with amino acids alone which induced both TFEB molecular weight shift and re-localisation to the cytoplasm. However, the use of kinase inhibitors Torin 1 and 2, which belong to a class of molecules that target mTOR catalytic site, thus completely inhibiting mTOR activity (mTORC1 and mTORC2), entirely prevented the molecular weight shift induced by nutrients and resulted in a substantial TFEB nuclear accumulation. Even though this could suggest an mTORC2 contribution to TFEB regulation, that is not the case, since 1) stimulation of starved cells with AA only, which activates mTORC1 but not mTORC2, induces TFEB activation, and 2) cells with disrupted mTORC2 signalling show TFEB activation upon Torin1 treatment, similar results to control cells (Settembre et al., 2012), suggesting that Torin1 action is occuring in mTORC1 and not mTORC2. Additionally, even though a previous study which showed that rapamycin-treated cells causes a shift in TFEB localisation (Pena-Llopis et al., 2011), Settembre et al., (2012) tested different concentrations of rapamycin, ranged from 10 nM to 10 μM, and showed no effect on nuclear translocation. This might explain why the lower concentrations we tested did not affect TFEB localisation, and only higher concentration (25μM) did. However, even the treatment with the highest concentration only induced a partial lysosomal response, whereas deprived AA

environment (L-ISO/N-INS) showed both TFEB activation and increased lysosome number. Together, these data suggest that rapamycin is actually only a partial inhibitor of mTOR, as suggested by Thoreen et al., (2009), and that even high concentrations of this drug might be sufficient to cause TFEB activation but not to show new lysosome formation yet (upon TFEB translocation, transcription of target genes for new lysosome formation are induced). It is also possible that the low number of embryos was not sufficient to show statistical differences between the groups in the lysosome number and volume analysis, even though in the TFEB analysis the difference was much more clear to pick up the significance. Nevertheless, these data reinforce the importance of isoleucine for preimplantation embryo development and how strong its effects are – a single AA reduction by 50% *in vitro* is sufficient to cause a stronger response than the use of a drug (rapamycin) that inhibits mTORC1.

Moreover, mTOR downregulation and TFEB activation are highly correlated with increased autophagy, as TFEB controls autophagy by positively regulating autophagosome formation and autophagosome–lysosome fusion (Settembre et al., 2011). Despite the fact Emb-LPD blastocysts had decreased mTOR (Eckert et al., 2012), autophagy was not activated in these embryos (Sun et al., 2014), suggesting the response was focused on retrieving more extracellular nutrients present in the uterine fluid rather than increasing cellular catabolism. However, pre-implantation murine blastocyst TE cells are known to respond to some environmental stressors, such as hyperglycemic environment, by increasing activation of autophagy in a differential pattern within the embryo (Adastra et al., 2011). Thus, considering our results showing increased TFEB activation and lysosome formation, future work should include autophagy and more detailed mTOR regulation studies in blastocysts in response to L-ISO/N-INS *in vitro* culture, to identify if in this model TFEB is not responsible for regulating autophagy as opposed to the cellular starvation models used by Settembre et al., (2011). Moreover, TFEB regulation could also be examined in the Emb-LPD *in vivo* model, to study whether the *in vivo* environment causes TFEB activation in the same way as the *in vitro* conditions studied here.

The participation of TFEB in cellular adaptation to starvation is now well established (reviewed in Puertollano et al., 2018). In conditions in which nutrients are scarce, TFEB activates the coordinated lysosomal expression and regulation response. More recently, a novel role for TFEB was identified in cellular response to endoplasmic reticulum (ER) stress. After treatment with ER stress inducers, TFEB translocated to the nucleus where it upregulated expression of activating transcriptional factor 4 (ATF4) and other regulators of the cellular stress response (Martina et al., 2016). ATF4 promotes cell survival by inducing transcriptional upregulation of genes required for autophagy, redox homeostasis, and amino acid import and synthesis (Ameri and Harris, 2008). Our work also indicates that TFEB may have a more general role in cellular adaptation to stress than previously recognized, as not only starvation but also mild amino acid restriction (L-ISO/N-INS) *in vitro* induces TFEB nuclear translocation. Moreover, it was the first time TFEB expression and activation was identified in preimplantation embryos, giving new insights regarding compensatory mechanisms (including increased lysosome formation and autophagy) in response to potentially different environmental stressors.

5.4.2 There is no correlation between TE cell volume and TFEB nuclear location

We have previously demonstrated in *Chapter 4* a positive correlation between cell volume and the total lysosomes in TE cells (see *4.4.8.*) which we showed was not treatment related. In general, we observed that cells with larger volumes have more lysosomes, which is presumably part of the cell cycle dynamics. During cell division, lysosomes are shared between daughter cells which have less cell volume and fewer lysosomes each than the original cell – which is then followed by cell growth and endocytosis reactivation. We also reported that a specific *in vitro* AA treatment provokes an increased response in lysosome production when another treatment does not (i.e. L-ISO/N-INS), which may still require cell volume to increase to enact lysosomes to increase.

In this chapter we demonstrated that embryos cultured in L-ISO/N-INS also showed increased TFEB activation. Based on these results, we analysed whether the same correlation between cell volume and lysosomes seen across treatments acts with or separate from the TFEB mechanism. Interestingly, we found no correlation between cell volume and TFEB in nucleus in both treatment groups as opposed to the lysosome/cell volume relationship, suggesting an independent process where TFEB activation occurs as a response to environmental challenges such as deprived AA conditions (L-ISO/N-INS) but not to physiological changes regarding cell division and consequent cell volume alterations. The best-studied mechanism that regulates TFEB subcellular localisation involves the phosphorylation of specific serine residues in the TFEB protein, and so far several phosphorylation sites have been directly evaluated, with the mTOR kinase being the most studied and shown to play major role in the regulation of TFEB subcellular localisation (Puertollano et al., 2018) - the nutrient dependence of mTOR-mediated TFEB phosphorylation indicates that mTORC1 is the complex involved (Settembre et al., 2011, 2012; Martina et al., 2012; Vega-Rubin-de-Celisa et al., 2017) with serine 211 (S211) being particularly relevant because its phosphorylation creates a binding site for cytosolic chaperone 14-3-3. Interaction with 14-3-3 results in sequestration of this transcription factor in the cytosol (Martina et al. 2012, 2014; Settembre et al. 2012). Conversely, when nutrients are scarce, inactivation of mTORC1, together with dephosphorylation of S211, prevents binding to 14-3-3, causing a rapid accumulation of

TFEB in the nucleus. Other kinases including ERK, GSK3, and AKT were more recently found to be also responsible for TFEB protein phosphorylation at different sites (Li et al., 2016; Nezich et al., 2015; Palmieri et al., 2017), although the relationship and interdependence of these phosphorylation events are still unclear (reviewed in Puertollano et al., 2018).

To confirm our results, we studied the same correlation in embryos that were treated with different concentrations of rapamycin, which inhibits mTORC1. We previously found that higher concentrations of rapamycin (20 μM) had no significant effect on lysosomes number but it contributed to TFEB activation, shown by increased nuclear staining (TFEB nuclear translocation). Again, we showed a positive correlation between cell volume and lysosome number and volume, independent of treatment, but no correlation between cell volume and percentage of TFEB in the nucleus, suggesting that TFEB activation responds to specific conditions affecting mTORC1 such as starvation models or in this particular case high concentrations of rapamycin sufficient to inhibit mTORC1 or specific AAs – such as low isoleucine - depleted from culture.

In conclusion, the current chapter demonstrated that contrary to lysosome abundancy and endocytosis in a cell, that are positively correlated to cell volume in a non-treatment related way, TFEB activation is independent of cell volume changes that occur as part of the normal cell cycle dynamics. The increased TFEB activation in response to L-ISO/N-INS culture reinforces the concept of embryo vulnerability to the preimplantation environment and its adaptation to non-optimal conditions.

Chapter 6 Endocytosis in human embryos – Maternal high BMI versus normal BMI

6.1 Introduction

The mammalian embryo has been shown to be able to respond and adapt to the environment it encounters. A period of developmental plasticity enables the embryo, and later the foetus, to alter intrauterine 'programming' for later life, as first enunciated by Professor David Barker (Barker, 2004). This environment can be altered by maternal diet and has been shown to have significant implications for development and health in later life. For instance, The Dutch Famine cohort studies emphasised that exposure to suboptimal conditions in early development leads to increased risk of chronic diseases later in life (Roseboom, et al 2011).

Uterine fluid represents the preimplantation milieu of the embryo but its nutritional contents have not been fully characterized in the human, specifically during early pregnancy due to obvious ethical reasons, and it remains unclear how these contents may be altered by factors such as maternal diet and disease. The amino acid composition of uterine fluid is significantly influenced by a woman's diet, with a healthier diet being associated with a significant reduction in asparagine, histidine, serine, glutamine, valine, phenylalanine, isoleucine and leucine (Kermack et al., 2015). These findings are comparable to what has previously been observed in the mouse LPD model, where reductions in the BCAAs were also observed (Eckert et al., 2012), suggesting that the nutritional environment of human uterine fluid is sensitive to female diet. However, no alterations in the uterine fluid composition were found in response to BMI or age (Kermack et al., 2015) despite the fact these women are more likely to experience reduced ovulation and subfertility linked to obesity and polycystic ovarian syndrome (PCOS) (Lintsen et al., 2005; Roupa et al., 2009). Increased BMI is also recognised to promote risk of offspring congenital abnormalities (Basatemur et al., 2013; Grindler and Moley, 2013) and increased risk of embryo arrest, miscarriage and preterm birth (Kulie et al., 2011; Robker, 2008). Similarly, the success of assisted conception is inversely

proportional to maternal BMI (Carrell, 2001). Thus, identifying the major inductive factors that may initiate adverse embryo programming and potential compensatory responses occurring at this time will permit a preventative strategy to protect future health.

The impact of maternal obesity on the preimplantation embryo is less well characterised than its long term programming and postnatal effects, possibly due to technical challenges. However, different animal models have been used to identify the metabolic defects in oocytes and early embryos caused by maternal overnutrition (reviewed in Eckert et al., 2016). Women with high BMI have higher circulating concentrations of hormones and metabolites, such as insulin, triglycerides, leptin and lactate, which accumulate within the ovarian follicular fluid and can adversely affect oocyte maturation and its potential (Yang et al., 2012). This rich follicular fluid coincides with increased inflammatory mediators that may contribute to the reduced potential of embryos from obese mothers (Gonzalez et al., 2018). Moreover, oocytes from high BMI mothers are smaller and produce blastocysts with increased triglycerides and reduced glucose consumption, markers of poorer potential (Leary et al., 2015). In addition, maternal obesity in mice induces defects in the mitochondrial phenotype of oocytes, including abnormal morphology and cristae structure, altered membrane potential and distribution and increased mitochondrial DNA content (Luzzo et al., 2012; Igosheva et al., 2010), all markers of disturbed mitochondrial function and energy homeostasis (reviewed in Fleming et al., 2018). Oocytes from obese dams also exhibit increased oxidative stress, impairing developmental potential and increasing aneuploidy (Luzzo et al., 2012; Igosheva et al., 2010; Hou et al., 2016). The combination of metabolic, mitochondrial and chromosomal alterations in oocytes and embryos from obese mothers has important implications for subsequent development. In mice, obese mothers have smaller foetuses and pups which develop overgrowth, adiposity and glucose intolerance after birth (Jungheim et al., 2010). Transfer of mouse blastocysts from obese mothers to normal recipients produces similarly growth-restricted foetuses with associated brain developmental malformations despite the absence of gestational maternal obesity (Luzzo et al., 2012), showing the importance of the preimplantation period for embryo programming. Similarly, in a sheep model, female offspring from

embryos of obese natural mothers transferred to non-obese recipients exhibit increased adiposity, with dysregulation in liver and muscle insulin signalling and hepatic fatty acid oxidation (Nicholas et al., 2013). These changes are associated with epigenetic perturbations in the liver, including upregulation of microRNAs regulating insulin signalling (Nicholas et al., 2013).

Since we found that increased compensatory endocytosis is associated with later risk of developing chronic diseases in mouse offspring in response to Emb-LPD (Sun et al., 2014; Watkins et al., 2007; Watkins et al., 2010), I wanted to study if the same type of enhanced endocytosis mechanism occurs in human embryos and if it is associated with maternal demographic factors known to be related with higher risk of chronic disease in the offspring, such as high BMI.

Furthermore, several studies have suggested that the composition of the medium used in ART for embryo culture may have an impact on the quality of embryos generated in IVF/ICSI cycles thereby influencing implantation and pregnancy rates (Mantikou et al., 2013). However, knowledge regarding the potential effects of the culture medium composition is still scarce, even though it has now been established that this has a significant effect on treatment efficacy and birth weight (Kleijkers et al., 2016). Medium used for human embryo culture was first developed based on data extrapolated from mouse embryo development (Gardner and Lane, 1998) whereby the nutritional content may not reflect the nutritive requirement of the developing human embryo (Kermack et al., 2015). Moreover, different culture systems used in IVF laboratories have different compositions and commercial companies do not divulge the exact composition of their media which may condition early embryonic development, making it difficult to study what might be responsible for different embryonic development outcomes (Zollner et al., 2004). Although most culture media share the same basic components such as a buffer system, mineral salts, carbohydrates and amino acids and most of them have albumin and antioxidants (Zandstra et al., 2015), the addition of extra supplementation, alterations in amino acids or carbohydrate compositions and/or concentrations and the lack of information on the exact amount of each component makes it difficult to compare different studies (Zandstra et al., 2015). Moreover, it is also difficult to

differentiate between effects mediated through parental infertility and the actual ART conditions.

Using mouse models for embryo *in vitro* culture I found that amino acid changes in culture, particularly low isoleucine from 2-cell stage, alter the endocytosis activation in blastocysts. Thus, studying if identical endocytosis activation response occurs in human embryos cultured *in vitro* from early stages in response to amino acid and/or insulin alterations could give us new insights into embryo development and adaptation and possible development of more suitable culture media for human embryos. However, it is important to reinforce the idea that this kind of experimental design is extremely complex since we would need to make new culture medium suitable for human embryo culture taking into account the lack of information from the current commercially available media used in IVF clinics. Also, the diverse maternal characteristics of human patients plus their infertility, in contrast to the normalised profiles of fertile mouse dams and culture environment as used in my previous chapters, makes it impossible to just replicate the design used in the earlier experiments.

In this chapter, we compare human embryo development *in vitro* from at least embryonic day 3 (D3) to blastocyst stage (D5) and endocytosis-related features (lysosome volume per TE cell; TFEB cellular location) in response to maternal demographic features, in this case high versus normal BMI, as a measure of normal or dysfunctional physiological/nutritional states. Thus, my aim is to determine whether human maternal phenotype influences embryo endocytosis profile as in the mouse model. Although this contrasts with the undernutrition focus of the mouse LPD and BCAA culture model I have used previously, most ART patients have either normal or high BMI rather than low BMI, reflecting the link with overweight and infertility, so to ensure sufficient replicates for a meaningful study, normal and high BMI were assessed here. Since periconceptional embryo programming occurs in response to both maternal over- and under-nutrition (reviewed in Fleming et al., 2018), this approach should meet my aim.

6.2 Materials and Methods

6.2.1 Patients

Described in section *2.2*.

6.2.1.1 Patients selection for the study

Frozen donated human embryos are stored in the University of Southampton - Institute of Developmental Sciences, in liquid nitrogen. They were frozen at the Wessex Fertility Clinic using either slow freezing or vitrification methods. These embryos must be used by the time of their "expiry" date (10 years after freezing) as stated by the HFEA. Embryos used for the optimisation and validation of the thawing, culture and endocytosis assays in human embryos were due to expire in the same year of usage. After optimisation, donors were selected for this study based on the following criteria: 1) maternal BMI (normal/control – 18.5-24.9; High BMI >25); 2) number of embryos per patient (each patient must have at least 3 embryos stored); 3) freezing method (all embryos selected were vitrified); 4) embryonic developmental stage (all embryos selected were frozen at least at D3 or later stage of development); 5) All patients age was less than 38 by the time they had embryos collected; 6) For each group of patients (high or normal BMI) half had gone through ICSI. We considered the reduction in fertility at age 38 based on the decay rate of non-growing follicles (Hansen et al., 2008) and a BMI over 25 as overweight (obese patients, with BMI > 30 were included in this group). BMI (kg/m^2) was calculated by dividing the weight (kg) by squared height (m). *Table 6.3* and *Table 6.4* show the selected patients for this study and relevant demographic data from each one.

6.2.2 Embryo Culture

Protocols for thawing and culture of frozen embryos from both methods are described in sections *2.2.1 (slow frozen embryos)* and *2.2.2 (vitrified embryos)*.

For embryo culture up to blastocyst stage, I used Sage 1-step with human serum albumin (Origio, 67010010) continuous culture medium, which was the same used in

the Wessex Fertility Clinic. This type of medium allows uninterrupted culture following IVF or ICSI insemination through to the blastocyst stage. Even though Origio does not discriminate the full composition and concentration of each component of the medium, they disclose its basic composition:

- Magnesium sulphate
- Potassium chloride
- Potassium phosphate
- Sodium chloride
- Amino acids
- L-alanyl-L-glutamine
- Calcium-L-lactate
- Glucose · Sodium pyruvate
- Sodium bicarbonate
- EDTA · Gentamicin
- Phenol red
- Sodium hyaluronate
- Human Serum Albumin

6.2.3 Endocytosis Assays

The endocytosis assay (BSA-BODIPY and LysoTracker – protocol in *Appendix 8.4*) as used for mouse embryos was optimised for human embryos for the first time. In summary, embryos that reached the blastocyst stage *in vitro* were washed 3 times in 40 μl drops of BSA-BODIPY (0.5 mg/ml) and LysoTracker (100 nM) in culture medium (Origio, 67010010) pre-equilibrated overnight and cultured in the same medium in a 6 cm dish covered with mineral oil for 1h at 37℃. Embryos were then washed 3 times in pre-equilibrated medium and fixed in 1% formaldehyde in PBS at room temperature for 20 min followed by washing 3 times in PBS. After the washings, embryos were incubated in CellMask Deep red in PBS (1:200) for 1 h at room temperature, and again washed 3 times in PBS and incubated in DAPI (2 μg/ml) in PBS for 20 min at room temperature, washed in PBS and transferred to a chamber to be imaged on the confocal microscope on the same day.

6.2.4 Immunohistochemistry

The protocol is described in *2.3*.

6.2.5 Image acquisition and data analysis

The VOLOCITY protocol used for mouse embryos described in *Appendix 8.4* was also used for human embryo TE cells.

6.2.6 Statistical analysis

Immunofluorescence and endocytosis data were analysed using a multilevel linear regression model using IBM SPSS statistics version 25 (SPSS), in which there was a random effect assigned to each blastocyst cell volume; cell number; whether a pregnancy resulted from the same cycle that the embryos under study were retrieved; as well as patient ID to account for mother effect (data was corrected for these factors). ICSI procedure was not included as a cofactor as ICSI-patients were represented equally in both BMI-groups and because they are ordinal binary data (ICSI or Non-ICSI). However, treatment (BMI values) was also included as a cofactor in the ICSI vs conventional IVF (non-ICSI) study. After analysis with the multilevel linear regression model, each fixed factor has its own p-value in the results, which show if a factor is or is not a significantly influencing cofactor *(Appendix 8.12)*.

6.3 Results

6.3.1 Endocytosis assay optimisation

From a total of 27 embryos thawed at different stages, 10 embryos reached blastocyst stage *in vitro*. From these, 2 were thawed at day 1 (2-cell stage) and 8 were thawed at 2 pronuclei stage (2PN); each pronucleus comes from the reformed nucleus of either the sperm or the egg and, as day 1 passes, the pronuclei break down and cell division begins. From the total embryos thawed, the majority were lysed upon thawing, while 3 reached morula stage and arrested. *Table 6.1* shows patient and embryo information regarding the successful thawed embryos that reached blastocyst stage, including thawing method, maternal BMI, age, reason for infertility and if pregnancy was achieved from this cycle.

After reaching the blastocyst stage *in vitro*, I used the same endocytosis protocol as used for mouse blastocysts and found that despite intracellular staining, the ZP was substantially labelled by BSA-BODIPY probe, forming a halo around the embryo (*Figure 6.1*). DAPI (nuclear staining) and LysoTracker were specific and were not retained in the ZP (*Figure 6.2*). Human embryos are larger than mouse embryos and have a thicker ZP visible in *Figure 6.1B*. Thus, it is uncertain if BSA-BODIPY intracellular staining is specific or if this dye is captured and retained inside the embryos due to the density of the ZP with part of the staining being trapped by it. Although embryos were washed several times upon thawing and after the endocytosis assay, this ZP binding is strong and difficult to remove. For instance, *Figure 6.3* shows an arrested embryo at 4-cell stage, stained with DAPI and CellMask with several sperm attached to the ZP even after incubation in thawing solutions, washings in culture medium and 24 h culture. Removing the ZP of these embryos before the endocytosis assay would be challenging as these are more fragile and intolerable to manipulation than mouse embryos, with lysing during the process much more likely.

Embryos used in these optimisation steps were due to expire and had to be used before the stated date. Thus, some of these do not provide enough information to interpret

associations between maternal demographics and endocytosis rates and could only be used as part of the optimisation process. Moreover, it is important to refer that several embryos were initially thawed and only a total of 10 reached the blastocyst stage – slow-frozen embryos have a lower survival rate *in vitro* than vitrified embryos (data acquired from Wessex Fertility Clinic). Some of these embryos showed increased fragmentation early in cell division, even though they reached the blastocyst stage. *Table 6.2* and *Figure 6.4* show endocytosis data collected from embryos that reached the blastocyst stage *in vitro* and an example of a TE cell with BSA-BODIPY and LysoTracker colocalised using the VOLOCITY protocol, respectively. Because of the high variability of BSA-BODIPY staining within embryos and because for some embryos where LysoTracker worked and BSA-BODIPY did not (*Table 6.2* – embryos 350 and 352) we decided not to continue studying BSA-BODIPY in human embryos and instead study TFEB cellular localisation within blastocyst TE, based on the interesting results found in our L-ISO/N-INS mouse embryo dataset (see *Chapter 5*).

Embryo ID	Stage	Method	BMI	Age	Reason	Pregnancy from this cycle
366	D1	slow	<25	35	oncology	no
357	D1	slow	21.5	32	PCOS+male	yes
350	2PN	slow	unknown	unknown	unknown	unknown
351						
352						
486	2PN	slow	unknown	unknown	unknown	unknown
487						
488						
371	2PN	slow	26.78	35	endometriosis	yes
372						

Table 6.1 - Patient and embryo information for each human embryo used in the optimisation of endocytosis assay for those embryos that reached blastocyst stage in vitro, including the stage when thawed, freezing method, patient age, reason for infertility and if pregnancy occurred from this cycle. 2PN – 2 pronuclei; D1 – day1 (2-cell stage); PCOS – polycystic ovarian syndrome; male – male infertility factors, slow – slow-frozen.

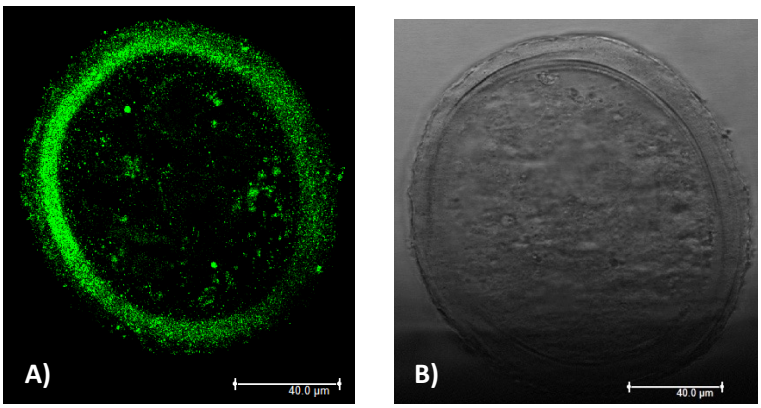

Figure 6.1 - **Human Embryo (ID 371) endocytosis assay with BSA-BODIPY (A) and phase contrast (B).** This embryo was cultured from 2PN (pronuclear). This embryo had high fragmentation from day 1 in culture when one cell lysed. Cells continued to divide and it formed a blastocyst at day 5 although with some visible dead cells. Human embryos have a thick ZP – and part of the staining is retained by the ZP forming a halo around the embryo.

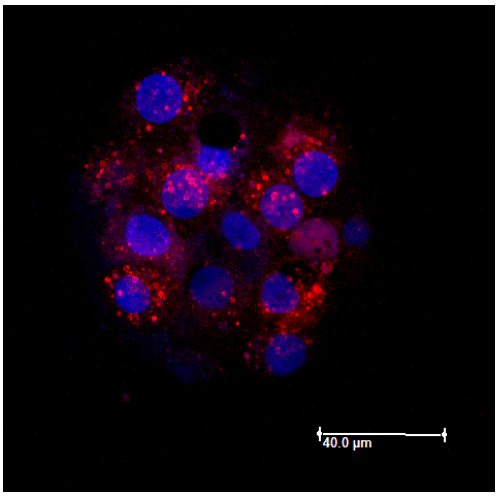

Figure 6.2 - **Human Embryo (ID 371) endocytosis assay with LysoTracker.** Top TE cells stained with LysoTracker Red, showing lysosomes around the cell nucleus (DAPI, blue).

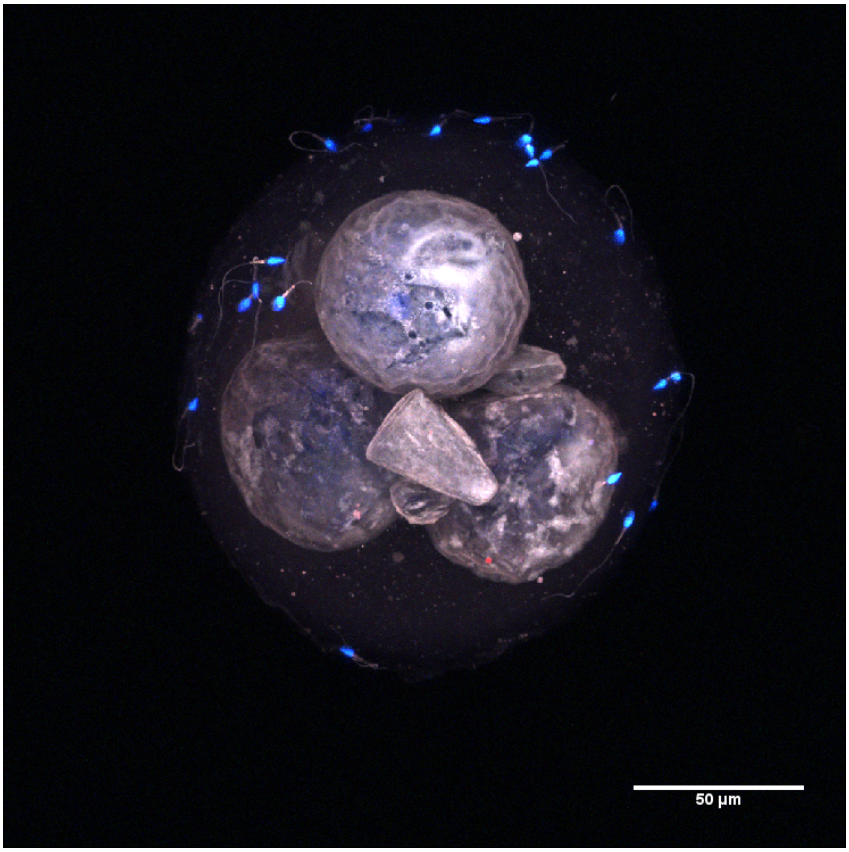

Figure 6.3 - **4-cell human embryo arrested after 24 h in culture and stained with DAPI (blue) and CellMask (grey) (extended focus/z-series view) with sperm attached to the embryo ZP (sperm head stained with DAPI – blue)**

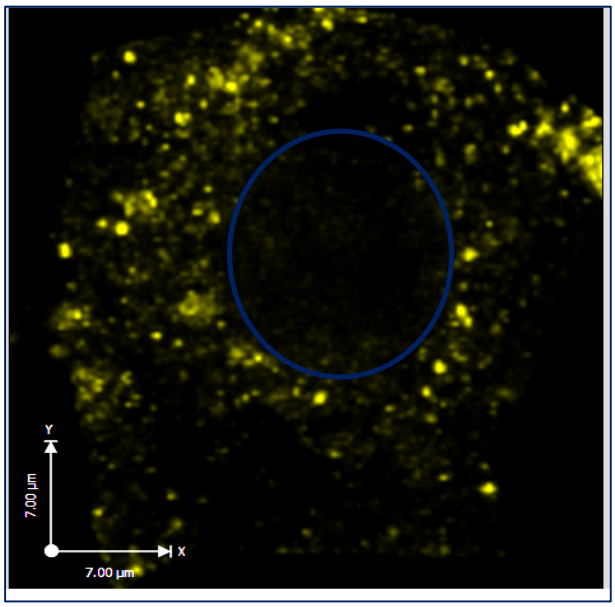

Figure 6.4 - VOLOCITY image of TE cell from embryo (ID 371) stained with BSA-BODIPY and LysoTracker. In yellow are Lysosomes and digested BSA colocalisation. The blue line represents the nucleus location

Embryo ID	BSA-BODIPY Volume (μm^3)	BSA-BODIPY mean volume (μm^3)	LysoTracker volume (μm^3)	LysoTracker mean volume (μm^3)
366	167.55	0.298	181.55	2.3
350	-	-	153.52	2.17
352	-	-	176.815	1.46
486	668.74	2.27	1133.71	2.31
487	263.4	0.451	506.75	0.85
488	1160.99	0.164	1779.85	0.616
371	255.93	0.499	332.40	0.524
372	186.21	0.273	548.84	0.681

Table 6.2 - **Endocytosis results obtained using VOLOCITY software** – BSA-BODIPY and LysoTracker number, collective volume and mean volume in embryos thawed and used for endocytosis optimisation protocol. Empty cells show cases where no staining or VOLOCITY data were obtained.

6.3.1.1 TFEB expression in human embryos – optimisation

For TFEB staining in human embryos, I tested the same protocol used for mouse embryos (see 5.3.1) and also included negative controls by omitting primary antibody (*Figure 6.5 and 6.6*). In *Figure 6.5-B2*, a small green halo around the embryo can be seen in the ZP, even though no primary antibody was used, suggesting that the halo seen in *Figure 6.6* is a combination of ZP auto-fluorescence and antibody attached to the ZP.

To conclude, in the optimisation study I decided not to continue with the BSA-BODIPY study because of its high variability in human embryos, in order to exclude the inclusion of false-positive and/or false-negative data. Instead, TFEB will be studied in combination with LysoTracker in human embryos from different maternal demographics.

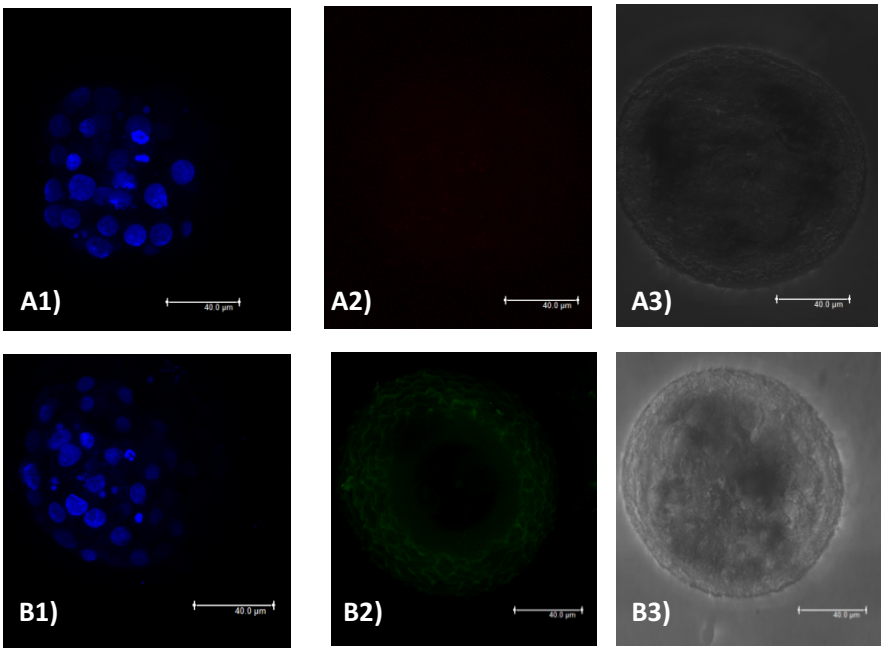

Figure 6.5 – Negative controls for LysoTracker (A) and TFEB (B). Three blastocysts stained without A) LysoTracker and B) TFEB (omitting primary antibody). (1 - Dapi staining, 2 – incubation without primary antibody (TFEB) and LysoTracker; 3 – phase contrast). The red channel A2 did not show any signal while green channel B2 showed some non-specific signal around the ZP. Scale bar = 40 µm.

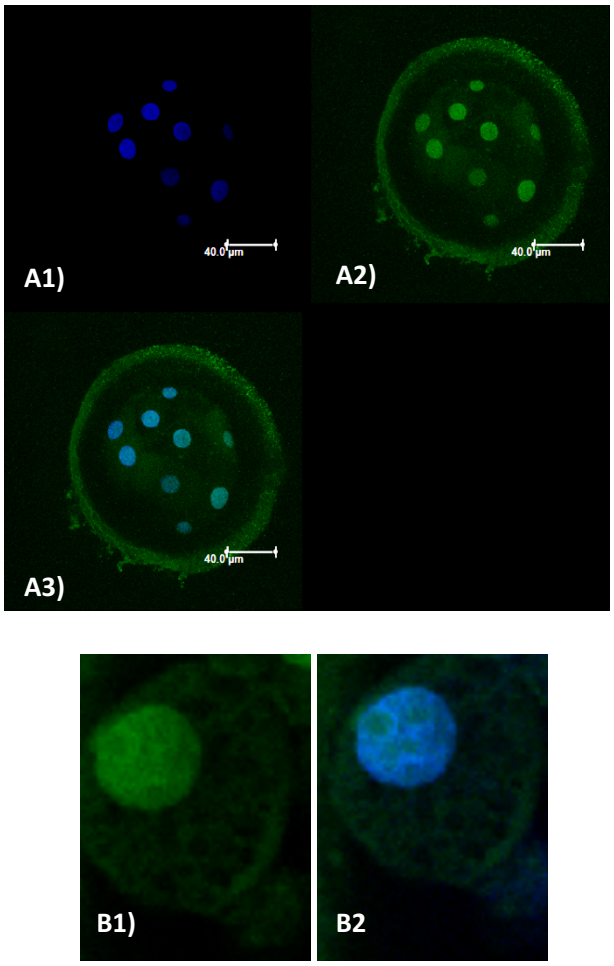

Figure 6.6 – Embryo stained with DAPI (A1) and TFEB (A2) and combined (A3). Figure B shows a zoom in of a cropped cell showing TFEB staining only (B1) and TFEB with DAPI (B2). Scale bar = 40 µm.

6.3.2 Endocytosis analysis with optimised protocol

Tables 6.3 and 6.4 show the selected patients (embryo donors) for this study and relevant demographic data from each one. At the end, patients were selected whose embryos reached the blastocyst stage in culture, thus, used for this study, had a BMI range from 18.9 to 23 in the normal BMI group and 27 to 33 in the high BMI group. Embryos donated from a total of 17 patients (8 in the normal BMI group and 9 in the high BMI group) were cultured (total of 94 embryos, 45 in the normal BMI group and 49 in the high BMI group). From these, 36% and 32%, respectively, reached the blastocyst stage *in vitro (Figure 6.7)*. The embryo total volume of the analysed blastocysts did not differ between groups (*Figure 6.8*). Patient 1 (normal BMI) had one embryo that reached blastocyst stage but that was lost during the endocytosis assay. This means that it was included in the survival analysis but not for further studies. Patients 9 and 14 (high BMI) had one embryo each that was lost between the LysoTracker and TFEB analysis. These embryos were included in the survival, blastocyst volume and number of cells analysed as well as LysoTracker study, but not in the TFEB study. This means that for the TFEB analysis, we included two embryos less than the previous LysoTracker analysis. Moreover, we found after confocal imaging and VOLOCITY analysis for LysoTracker that 3 embryos (2 from the normal BMI and 1 from the high BMI group) could not be used due to unspecific staining / lack of nuclear (DAPI) staining. This means that for the survival study we had 16 viable blastocysts in each group (from 7 mothers per group); in the LysoTracker analysis we ended up with 13 blastocysts in the normal BMI group and 15 in the high BMI group; and finally in the TFEB/DAPI colocalisation we used 13 embryos in the normal BMI and 14 in the high BMI group.

	Normal BMI								
	Patient 1	**Patient 2**	**Patient 3**	**Patient 4**	**Patient 5**	**Patient 6**	**Patient 7**	**Patient 8**	**Mean**
Patient ID	582-589	529-531	452-461	430-432	411-417	341-344	618-623	594-597	
BMI	18.97	21.72	22.94	21.97	21.91	23.1	22.48	22.14	21.90
Age	31	35	27	36	38	33	35	35	33.75
Number embryos	8	3	10	3	7	4	6	4	Total = 45
Stage	D3	D3 (2) D5 (1)	D3	D3	D5	D3	D3 (3) D5 (3)	D5	
Method	Vitrified	Vitrified	Vitrified	Vitrified	Vitrified	Vitrified	Vitrified	Vitrified	
Reason	PCOS	Low sperm count + low ovarian reserve	Male	Endometriosis /tubal blockage	Unexplained	Male	Tubal	Unexplained	
ICSI	NO	YES	YES	NO	NO	YES	NO	NO	5 NO 3 YES
Born (pregnancy resulted from that IVF cycle)	YES	NO	NO	YES	YES	YES	NO	YES	3 NO 5 YES
Expiry date	18/06/20	19/09/23	03/05/24	25/04/23	14/11/22	30/10/20	08/07/23	17/01/25	
Thawed on	10/08/18	16/10/18	26/11/18	08/10/18	21/08/18	13/08/18	09/01/19	22/10/18	
In culture	6 in culture + 2 lost upon thawing	3 in culture	8 in culture	3	4 in culture + 3 lost upon thawing	4 in culture + 1 lost upon thawing	6 in culture	4 early blasts in culture	
Final number	3 good blasts (+ 1 blast lost during assay)	1 blast	3 blasts	2 arrested 1 lysed	3 blasts (+ 1 lysed)	1 blast	2 blasts	2 blasts (good) + 2 dead	Final number embryos that reached blastocyst = 16 (15 for endocytosis analysis)

Table 6.3 – List of patient information (Normal BMI patients) used in the study. Blast = blastocyst.

	High BMI									
	Patient 7	**Patient 8**	**Patient 9**	**Patient 10**	**Patient 11**	**Patient 12**	**Patient 13**	**Patient 14**	**Patient 15**	**Mean**
Patient ID	578-581	482-485	402-405	512-518	377-385	532-535	264-269	610-617	509-511	
BMI	32.39	31.25	31.16	30.12	27.25	28.13	28.69	27.15	29.76	29.54
Age	36	35	34	35	34	30	38	36	35	34.7
Number embryos	4	4	4	7	9	4	6	8	3	Total = 49
Stage	D4 (2) D5 (2)	D3	D3	D3	D3 (7) D5(2)	D3	D3	D3 (6) D5 (2)	D3	
Method	Vitrified	Vitrified	Vitrified	Vitrified	Vitrified	Vitrified	Vitrified	Vitrified	Vitrified	
Reason	Male + PCOS	Unexplained	Tubal damage + Male factor	Unexplained	PCOS	Unexplained	Unexplained	Tubal	PCOS	
ICSI	YES	YES	YES	YES	NO	NO	NO	NO	YES	4 NO 5 YES
Born (pregnancy resulted from that IVF cycle)	YES	YES	YES	NO	YES	YES	YES	YES	NO	7 YES 2 NO
Expiry date	09/09/21	30/08/20	08/04/21	30/07/20	25/04/20	24/03/24	18/03/20	23/06/24	21/06/20	
Thawed on	21/08/18	29/08/18	07/09/18	8/10/18	10/10/18	03/09/18	13/08/18	30/01/19	03/12/18	
In culture	3 in culture + 1 lost upon thawing	3 in culture + 1 lost upon thawing	5 in culture	7 in culture	9 in culture	4 in culture	5 in culture + 1 lost upon thawing	8 in culture	3 in culture	
Final number	1 blast	1 blast	2 blasts (1 lost before TFEB)	3 blasts 4 arrested	4 blasts	0 (all arrested)	0 (all arrested)	3 blasts (1 from D5, 2 from D3) – 1 lost before TFEB	2 blasts	Final number of blastocysts analysed = 16 (14 for TFEB)

Table 6.4 – List of patient information (High BMI patients) used in the study. Blast = blastocyst.

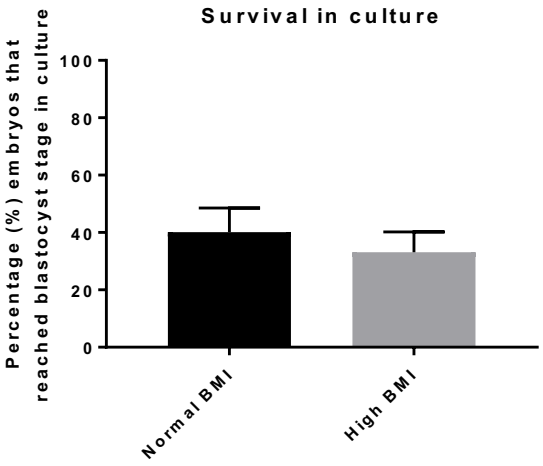

Figure 6.7 - Percentage (%) of embryos in culture that reached blastocyst stage / survived in culture without arresting (as evidenced by presence of blastocoel). Embryos were initially at D3-D5. Morulae or arrested embryos at that time point were not used. Normal BMI – 16 blastocysts from total 45 initial embryos cultured (36% survival); High BMI – 16 blastocysts from total 49 initial embryos cultured (32% survival).

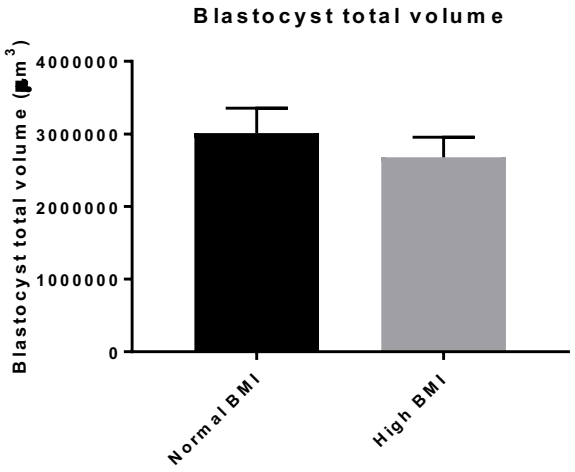

Figure 6.8 - The total volume of blastocysts (volume includes cavity) analysed did not differ between embryos from normal and high BMI donors. Values are presented as mean±SEM. 15-16 embryos per group from 7 mothers per group.

6.3.2.1 Effect of maternal BMI on human blastocyst endocytosis profile

The final number of blastocysts analysed from the normal BMI group was 13 from 7 patients; and for the high BMI group, 15 blastocysts from 7 patients (*Tables 6.3 and 6.4*). Blastocyst data from same or different patients was accounted for in the statistical analysis. Embryos from patients within the high BMI group exhibited an enhanced endocytosis phenotype similar to that previously seen in mouse embryos cultured *in vitro* in medium with deprived amino acids (specifically reduced isoleucine) as well as in blastocysts collected from mothers on a poor diet (LPD) using the same marker LysoTracker Red. Moreover, scores were highly variable in the high BMI group (*Figure 6.9D*) which did not occur in the embryos from the normal BMI group. In the statistical analysis performed here, cell volume and cell number were significantly influencing cofactors but not pregnancy from that cycle as the first two were significantly changed and contributing to the final p-value (*Figure 6.9E,F*). Furthermore, using the same cofactors, examination of human embryos for TFEB localisation revealed increased nuclear versus cytoplasmic location for the high BMI group, but not quite at significance level (*Figure 6.10*). However, in this analysis none of the cofactors were significantly contributing to the final p-value.

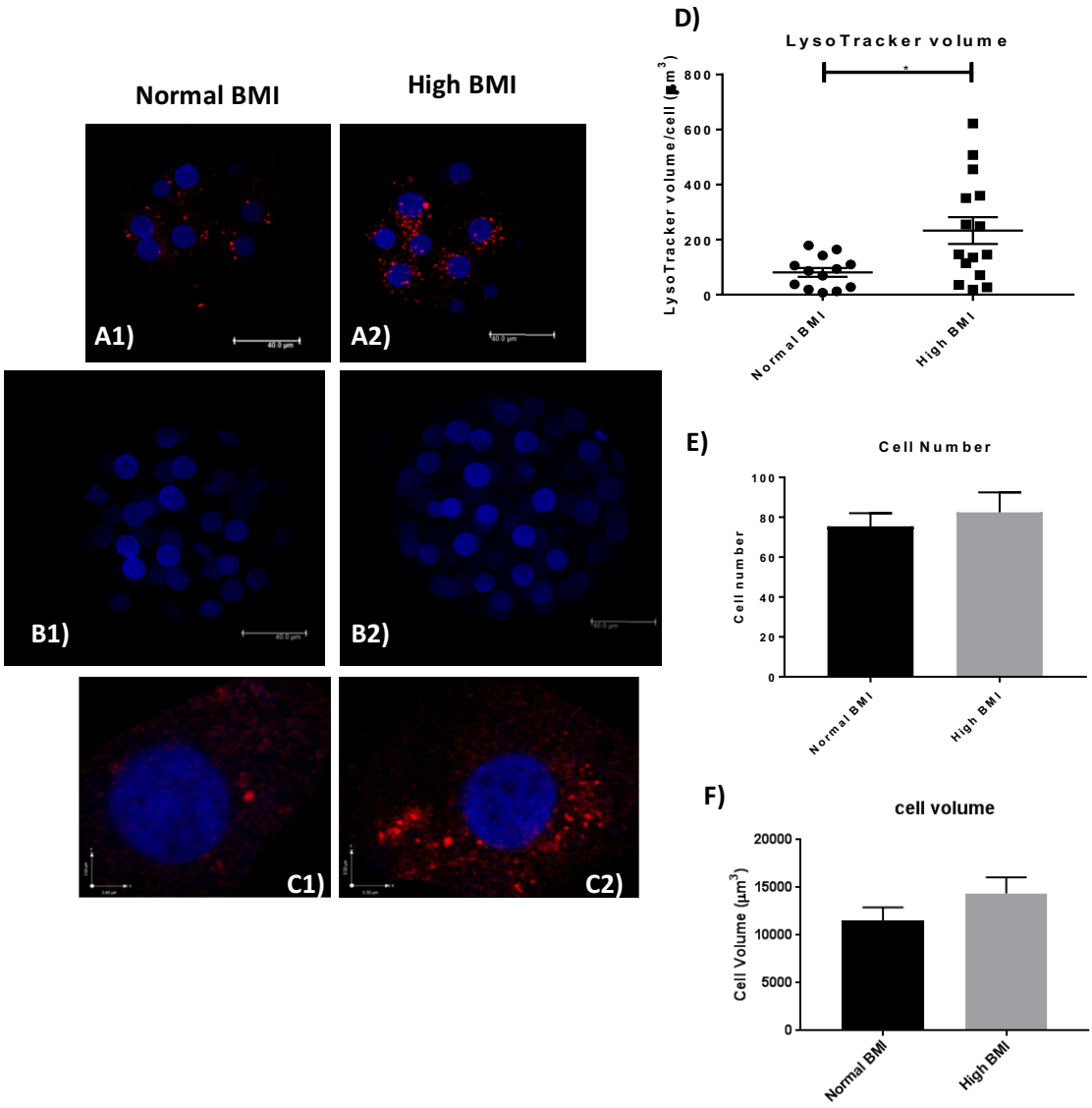

Figure 6.9 – Lysosomes collective volume per cell in blastocyst TE from normal (1) and high BMI (2) patients. A) Top TE cells with DAPI and LysoTracker, B) whole embryo stained with DAPI, C) single TE cell analysed in VOLOCITY software. Scale bar = 40 µm. D) Each point is a single blastocyst. The average for blastocysts from each patient was then taken into account as a cofactor (patient ID) to account for mother effect (possible similarity in embryos from the same mother). Values are presented as mean ±SEM. E, F) Cell number and cell volume distribution between the two groups. In the statistical analysis performed (multilevel linear regression model), cell volume and cell number were significantly influencing cofactors, contributing to the final p-value *P value <0.05; 13-15 embryos per group from 7 mothers per group.

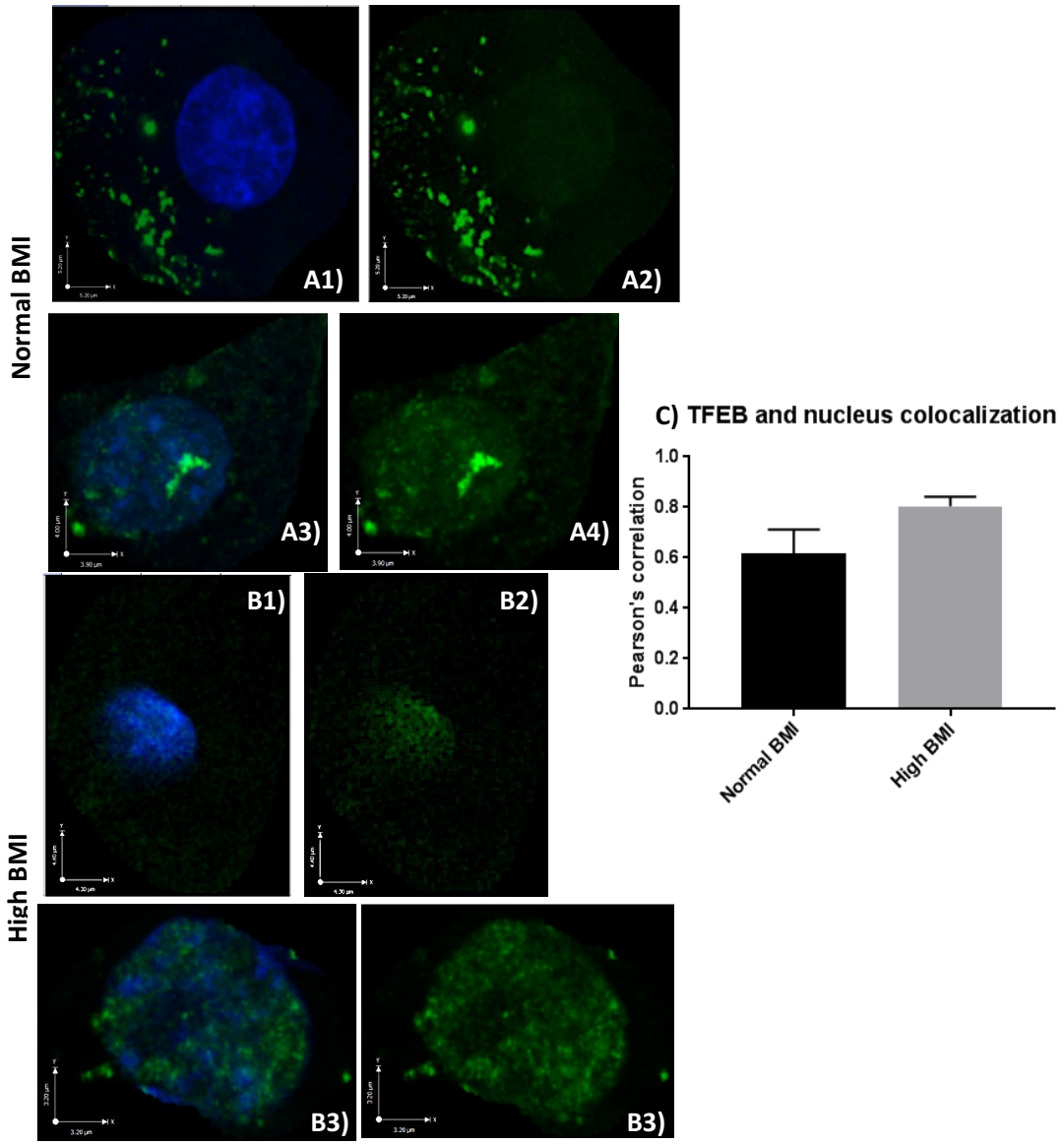

Figure 6.10 – TE cells stained with TFEB (green) and DAPI (blue) from normal (A) and high BMI (B) patients. TFEB is mainly located in the cytoplasm in embryos from normal BMI mothers (A) while the nucleus from high BMI mothers (B) has more green staining (although not statistically significant - C). Values are presented as mean ±SEM. * P value <0.05 (statistical analysis using a multilevel linear regression model); 13-14 embryos per group from 7 mothers per group.

6.3.2.2 The effect of ICSI vs conventional IVF on endocytosis profile

The final number of blastocysts analysed in the ICSI group was 11 from 7 patients; and 17 blastocysts from 7 patients in the conventional IVF group (*Tables 6.3 and 6.4*).

Here, the effect of ICSI or conventional IVF on endocytosis is analysed and corrected for the same fixed factors as before but also for patient BMI (ICSI and IFV data include high and normal BMI in both groups). ICSI procedure did not affect LysoTracker volume in blastocysts cultured *in vitro* (*Figure 6.11*) as well as it did not alter the TFEB subcellular localization (*Figure 6.12*), suggesting that embryos are vulnerable to maternal features such as BMI but not the later procedure in the IVF clinic that consists of sperm intracytoplasmic injection in the egg. However, the same high variability seen in the high BMI group (*Figure 6.9D*) is also seen in the ICSI group (*Figure 6.11*) such that the highest values in the ICSI group belong to the high BMI mothers (*Figure 8.31* - *Appendix 8.13*). In the statistical analysis performed here, the BMI, cell volume and cell number (but not pregnancy from that cycle) are significantly changed suggesting that these are influencing cofactors contributing to the result (effect of ICSI = non-significant).

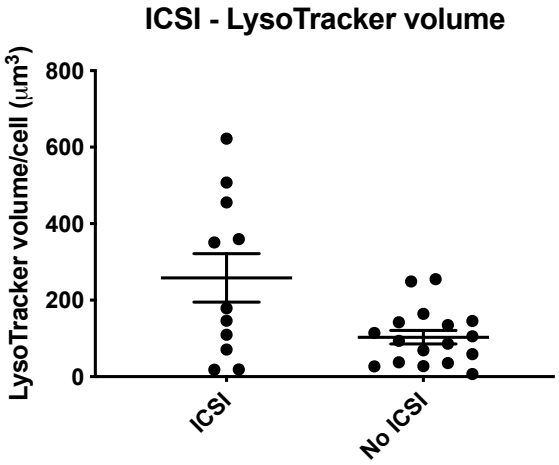

Figure 6.11 - Lysosome collective volume per cell in blastocyst TE from ICSI and non-ICSI embryos. Values are presented as mean±SEM. *P value <0.05 (statistical analysis using a multilevel linear regression model); 11-17 embryos per group from 7 mothers per group.

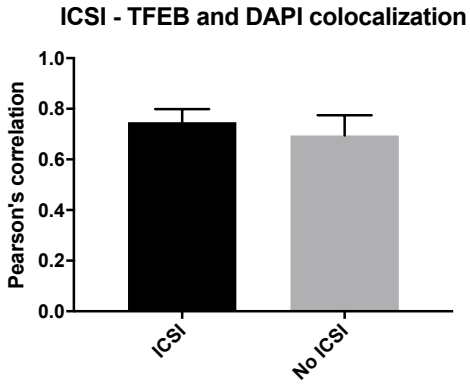

Figure 6.12 – Pearson correlation for TFEB and DAPI channels in blastocyst TE from ICSI and non-ICSI embryos. Values are presented as mean±SEM. *P value <0.05 (statistical analysis using a multilevel linear regression model); 11-16 embryos per group from 7 mothers per group.

6.4 Discussion

Since the first report on human pregnancy using a frozen embryo in 1983 (Trounson and Mohr, 1983), embryo cryopreservation has become a widespread and reliable routine procedure in ART. An efficient embryo cryopreservation method offers the advantage of increasing pregnancy rate for a single ovarian stimulation cycle while minimizing the risk of multiple pregnancies. In cases where ovarian hyperstimulation may be anticipated or where embryo transfer may be considered inadvisable, embryo cryopreservation offers the option of freezing all embryos for thawing and transfer in subsequent, more favourable cycles (Zheng et al., 2008). It is well known that only some cryopreserved embryos remain fully intact after thawing even if only the embryos with the best morphological appearance have been frozen. Other embryos lose one or more blastomeres after thawing and are referred to as partially damaged though they might still be used for transfer. However, there are conflicting results regarding the developmental potential of partially damaged frozen and thawed embryos. Some studies have reported that damaged embryos have the same capacity to produce pregnancies as fully intact embryos (Hartshorne, et al., 1990), while others have reported a harmful effect of embryo damage on their implantation potential (Burns et al., 1999). The reason for lower viability remains unclear. A potential toxic effect from damaged blastomeres on their neighbour blastomeres has been proposed as a mechanism. More recently, it was found that the developmental potential of partially damaged cryopreserved human embryos with below 25% cells lost is comparable to that of fully intact embryos (Zheng et al., 2008). Thus, the presence of one or two lysed blastomeres in the thawed day 3 embryo does not appear to have a negative influence on the further development of the sibling intact cells. During the process of embryo thawing I experienced severe embryo lysis and fragmentation. However, some embryos developed until blastocyst stage even when one or two blastomeres were lysed early in development (2-cell stage), as previously reported.

After the endocytosis assay in the optimisation stage, a halo of staining formed around the embryos on the ZP from BSA-BODIPY incubation. The ZP of human embryos is thicker than mouse embryos and, according to Bertrand et al., (1995), this thickness appears to be an additional factor that should be taken into account when interpreting the

fertilization rate. ZP thickness influences sperm penetration, even when the spermatozoa are considered normal, and although intracellular and specific staining was present in the TE cells of these embryos, it is possible that some dye becomes trapped inside the embryo by the ZP staining, thus possibly causing non-specific staining and influencing the VOLOCITY data analysis. For instance, it was possible to see embryo nuclei stained or non-specific punctate staining in some embryos. Although embryos were washed several times upon thawing and after the endocytosis assay, the BSA-BODIPY ZP binding is strong and difficult to remove, similar to sperm remaining attached to the ZP after incubation in thawing solutions despite washings in culture medium and 24h culture (*Figure 6.3*). Removing the ZP of these embryos before the endocytosis assay would be very challenging as these are more fragile and intolerant to manipulation than mouse embryos, and lysis during the process is likely. However, because for the optimisation steps we used embryos that were initially at different developmental stages with different scores in terms of viability and ability to implant (i.e. cell number and fragmentation), it is possible that the staining would work better using superior quality embryos, as were used for the experiment after optimisation. In these embryos the ZP was usually thinner than those less healthy embryos used in the optimisation steps.

To analyse all human embryo data, we used a multilevel linear regression model in which there was a random effect assigned to patient ID to account for mother effect, embryo cell number, cell volume and if there was a pregnancy from that same cycle (cofactors - data corrected for these factors). In all the analyses made, pregnancy from the same cycle showed no influence, suggesting that whether the patient became pregnant with an embryo from the same batch as used here did not influence the results obtained. Because I analysed raw lysosome volume and did not normalise this value against cell volume (by diving lysosome volume by TE cell volume) the use of cell volume as a cofactor is highly justifiable. However, if that normalisation was done instead, cell volume would be included twice in the analysis, potentially over-emphasizing its effect. Thinking further, cell volume and cell number can be closely related in early embryos, thus, one can argue that by including both cofactors the cell-effect might be overemphasized. However, these were both included in the analysis given the method of confocal analysis (selected cells from the TE only) and the nature of human embryos

(highly variable cell volumes) so cell number is a proxy for developmental stage of the entire embryo whilst cell volume is specific for the particular cell examined.

Using this regression model, I found that embryos from the high BMI group exhibited increased lysosomes compared to the normal BMI group. Another interesting feature found was that the range of scores of LysoTracker volume per cell varied across the high BMI group (*Figure 6.11D*) showing individual embryo variation, which did not happen in the embryos from the normal BMI group. This preliminary work suggests that human embryos exhibit a similar mechanism to mouse embryos in regulating endocytosis in response to maternal nutritional status, particularly maternal BMI. Furthermore, TFEB, an mTOR-associated transcription factor for lysosome expression that I previously found to be translocated from the cytoplasm to the nucleus in cases where lysosomes were increased (namely, in response to deprived amino acids *in vitro* culture) in the mouse model, was also increased in the nuclear versus cytoplasmic location for the high BMI group, but not quite at significance level.

Despite these differences found in embryos from normal versus high BMI, there were no differences found in embryo survival in culture or embryo total volume. This supports the idea that even though embryos might be scored the same in the clinic, even using the most recent technology of time-lapse microscopy to select the best embryos to be transferred and/or frozen, differences do exist at the cellular and molecular level as evidenced by the endocytosis data. Thus, there are features that embryologists and researchers would not be able to account for in embryo selection. This novel study indicates the validity of endocytosis as a marker in human embryos more explicitly, thus enabling testing of intervention-effectiveness in humans but with a big limitation of turning the studied embryos unviable for transfer. This emphasises the importance of discovering new non-invasive techniques to study this feature in human embryos. Some non-invasive studies have been done based on the embryo culture media metabolites. These included analysis of blastocysts from the same patient with the same scores which revealed a wide spread of metabolic activities as determined through the measurement of glucose consumption (Gardner et al., 2001) as well as discreet differences in the proteome, in alignment with subsequent differences in physiology (Katz-jaffe et al., 2006). Hence, the incorporation of non-invasive embryo physiology analysis in IVF clinics will be of great value in the prospective selection of the most viable embryos, even

though the technology for such work is not readily available to date (Gardner and Balaban, 2016). However, we cannot forget the importance of these new technologies to be assessed for risk as well as potential benefit (reviewed in Brison et al., 2013) before being introduced in a safe and controlled manner.

Since we had access to the parental and endocytosis data and because it was the first time endocytosis assays were performed in human embryos, we also analysed our data in respect to ICSI versus conventional IVF embryos. Embryos were divided in two groups (ICSI or NO-ICSI) and treatment (BMI values) as well as the same previous cofactors were applied as before. In each BMI group (normal / high BMI) half of the patients selected donated embryos generated through ICSI and the other half by conventional IVF. I found that LysoTracker collective volume and TFEB localisation were not significantly changed between groups. However, we did see a vast variability in the results in the ICSI group compared to the non-ICSI conventional IVF, as seen in the high BMI group, showing individual embryo variation. This might be explained by comparing both studies, since the higher values in the ICSI group are the same top values in high BMI mothers, explaining how in the SPSS analysis, high BMI appears as a significant highly contributing cofactor in this analysis (*Appendix 8.12*).

ICSI treatment is usually performed when male or both male and female infertility causes are the reason(s) for ART treatment. Retrospective data suggests that IVF and the combination of IVF with ICSI procedures are safe and the majority of the resulting pregnancies lead to the birth of healthy babies. The long term follow-up of the first IVF/ICSI generation offers a clearer picture of the safety of these technologies, however, there is still only an incomplete picture of all the risks associated with these techniques (Alukal and Lamb, 2008). Recent meta-analysis suggested that the risk of developing congenital defects can be increased by IVF and ICSI (Zhao et al., 2018) and that children conceived by IVF and ICSI showed a lower weight during the first 4 years of age, with the difference disappearing afterwards (Bay et al. 2019). This rapid growth during early development is associated with increased risk of developing obesity (Baird et al., 2005; Monteiro and Victora, 2005), hypertension (Bansal et al., 2008; Lei et al., 2015) and diabetes later in life (Dunger et al., 2019). Moreover, reproductive potential seems to be affected as well, since young adults conceived through ICSI showed low sperm

concentration and motile sperm count compared to men born after spontaneous conception (Belva et al., 2016).

Giving the reported adverse effects associated with ART, there is an active effort to ensure a safe application of human ART, including monitoring the health status of the resultant offspring (reviewed in Velazquez et al., 2019) and to continue to study the impact of new technologies on human embryo development using human embryos donated to research (Brison et al., 2013). However, it is challenging to establish the nature of these risks since they might be related to the technology itself and/or the parental genetic defects, thus the ideal study design to answer the question of whether or not ART is safe is nearly impossible to achieve (Alukal and Lamb, 2008). Standard statistics cannot be used to compare fertility, as it is the combined fertility potential of the couple that ultimately determines whether a couple is fertile or not and it is nearly impossible to include an appropriate control population for infertile couples.

Although our results are very preliminary we acknowledge the limitations of this type of study not only by the reduced number of patients and embryos analysed per patient (from a total of 94 embryos thawed, 32 blastocysts were included in the study) but also the low chances to remain fully intact after thawing and culture. Moreover, considering the high variability of these embryos and parental demographics, it is difficult to account for every factor that might influence the results seen. For example, these may include different infertility reasons (maternal, paternal, both or unexplained) and treatments as well as the culture medium used at the time of freezing in the clinic, the number of years embryos were frozen and possible differences in conditions and practices used over this time since freezing. Furthermore, the commercial culture medium composition used (Sage 1-Step^{TM}, Origio) is undisclosed, as no information regarding the concentrations of amino acids is revealed. Even though we used the same medium to culture all embryos, some may be more vulnerable to this composition than others, depending for example if they were initially cultured in the same medium in the clinic before cryopreservation.

Due to all the limitations of this study, we acknowledge the difficulty of drawing any final conclusions. Nevertheless, we have supportive evidence from this preliminary work that human embryos exhibit a similar mechanism to mouse embryos in regulating endocytosis in response to adverse maternal features, in this case high BMI, though

more studies are required to substantiate the activation and signalling pathways involved.

In the wider context of research on peri-conceptional environment in both animal and human species it is clear that the early embryonic period is sensitive to a diverse range of external stimuli (i.e., from parental nutrition or assisted reproduction culture conditions, immunological status and alcohol consumption) that affect later life health through cellular, physiological and epigenetic mechanisms (reviewed in Fleming et al., 2018). These significant risks argue for couples to prepare for pregnancy before conception, which might include changing their diet and health habits for the wellbeing of the next generation (Barker et al., 2018; Stepheson et al., 2018). Moreover, this study also reinforces the importance of the composition of IVF culture medium to ensure sufficient inclusion of metabolites to prevent activation of altered embryo phenotype as a forerunner of later life disease risk, a strategy we have recently achieved in a mouse model (Velazquez et al., 2018 and *chapter 4*).

Chapter 7 General Discussion

7.1 General Conclusions

In the past two decades, our group has been studying and developing models to understand how maternal malnutrition restricted to the preimplantation period affects embryo development and adaptation and its effects later in life. We found that maternal LPD from time of conception to blastocyst formation – Emb-LPD (before implantation) is sufficient to predispose offspring to cardiovascular and neurological diseases (Watkins et al., 2007, 2008a, 2010; Gould et al., 2018). During embryo development, extraembryonic lineages such as TE provide support for embryo growth by mediating nutrient delivery of essential nutrients from the maternal environment. In the same Emb-LPD model we found that endocytosis was increased in TE cells as a compensatory mechanism which might allow the embryo to get sufficient nutrients and survive in a deprived environment (Sun et al., 2014). The endocytosis system in TE cells of preimplantation embryos serves as the first contact between embryo and maternal environment. Moreover, the maternal uterine fluid composition is also altered in response to Emb-LPD with decreased concentrations of BCAAs as well as decreased plasma insulin (Eckert et al., 2012). Thus, in this study I wanted to define the exact signals sensed by early embryos to which they respond and adapt by comparing different *in vitro* conditions, with different combinations and concentrations of BCAAs and insulin, as well as to define the mechanisms leading to this activation and when in the preimplantation window this activation occurs. Moreover, we studied if the same activation of endocytosis occurs in the human in response to maternal demographics known to be related with offspring chronic disease, including BMI as well as ART procedure ICSI, in embryos cultured from early stages to blastocyst.

In *Chapter 3*, I designed and optimised a protocol to study endocytosis in early embryos, using different markers for endocytosis and lysosomes, including LysoTracker, BSA-BODIPY and MagicRed (cathepsin B). I also developed a protocol in VOLOCITY software in order to measure the total number and volume of endocytic vesicles and endocytosed BSA in 3D blastocysts.

Blastocyst formation *in vitro* was not altered in any culture condition investigated in this work, which coincides with data from the *in vivo* Emb-LPD model (Eckert et al., 2012) and previous *in vitro* work conducted in embryos cultured from 2-cell stage until blastocyst in a 50% reduction in insulin and/or the three BCAA concentrations (Velazquez et al., 2018). In all our experiments, no differences were found in blastocyst total cell number after 48 h in culture in all different medium conditions tested. These results are in accordance with previous data where the cell number was not altered in blastocysts cultured from 2-cell stage in LBCAA/L-INS, LBCAA/N-INS and NBCAA/L-INS despite the postnatal changes seen in offspring from the LBCAA/L-INS group (Velazquez et al., 2018). This phenotype differs from the Emb-LPD blastocyst phenotype, which had an increased total number of cells (Eckert et al., 2012), suggesting that alternative maternal environmental factors changed in response to Emb-LPD treatment might be responsible for this change and should be assessed *in vitro* for evidence of their role in this early programming event. This could include glucose or other amino acid(s), or other factors found to be altered in response to maternal undernutrition in other models, such as leptin, IGF-1 or nonesterified fatty acid (Velazquez, 2015).

In the first experiment of *Chapter 4* I cultured 2-cell stage embryos in medium with depleted BCAAs until the blastocyst stage, mimicking the Emb-LPD environment. The control group (NBCAA/N-INS) attempted to mimic the embryo compositional environment for both amino acids detected in the maternal uterine fluid and the physiological level of serum insulin found in control diet mothers (NPD) at E3.5 (Eckert et al., 2012). The two experimental culture treatments were the same medium supplemented with normal insulin and either 50% the BCAA concentration (LBCAA/N-INS) or with omitted BCAA (0BCAA/N-INS). BSA-BODIPY endocytosis was not altered in any of the altered culture conditions. However, previous studies using the same culture conditions reported an increased TE Dextran fluid phase endocytosis uptake (Sun et al., 2014) as well as increased lysosome number in the LBCAA/N-INS group, which was not statistically significant in this present study. This can be explained by the fact that the ZP was removed after the assay in Sun et al (2014) using acid tyrode's (pH 2.3), and it is known that endocytosis is highly sensitive to pH alterations. Thus, it is possible that the acid treatment has a potential effect on endocytosis. Changes in the intracellular pH are known to be responsible for mTORC1 lysosomal translocation close to nuclei when

amino acids are depleted in the environment (Korolchuk et al., 2011). When amino acids are replenished, lysosomes are translocated to peripheral areas (close to the upstream signalling modules) facilitating mTORC1 stimulation (Korolchuk et al., 2011). However, we did not see any changes in the distance from the lysosome to the nuclei in response to any BCAA and/or insulin depletion in all our experimental groups and neither has Sun et al., (2014).

VOLOCITY analysis showed that embryos cultured in L-ISO/N-INS have a higher number of lysosomes and significantly higher BSA-BODIPY positive vesicles compared to the control group NBCAA/N-INS as well as increased collective volume of lysosomes and BSA-BODIPY vesicles. Considering these results obtained in the L-ISO/N-INS group, I measured intracellular cathepsin B activity directly in lysosomes using MagicRed fluorescent staining. Using this substrate, I observed *in situ* an increase in cathepsin-activity in the L-ISO/N-INS group. This shows that not only lysosomes are increased in these blastocysts but there is also an increase in the lysosomal function (enzyme activity) as cathepsins are only present in activated lysosomes.

Albumin is normally endocytosed by the megalin-cubilin receptor complex. Because of the increased endocytosis in L-ISO/N-INS compared to control NBCAA/N-INS blastocysts, I looked at megalin expression in these embryos to study whether this increase was accompanied by increased expression of its main receptor. Albumin starts being internalised and degraded through the megalin-mediated pathway after the 32-cell stage, when its expression increases. Following internalisation via clathrin coated pits, megalin localises in the early endosome before passing into pericentriolar recycling endosomes (Assémat et al., 2005; Verroust and Christensen, 2002). In my study, I found both megalin and clathrin mainly located in the TE cell apical membrane and within vesicles in the cytoplasm, with an increased expression in L-ISO/N-INS embryos compared to NBCAA/N-INS control embryos. This finding suggests that a larger quantity of the receptors could be the cause of the stimulated BSA uptake (increased BSA-BODIPY) in L-ISO/N-INS embryos. However, megalin gene expression was not altered, suggesting the upregulation occurs at protein level. It is possible this increase in the L-ISO/N-INS group is due to a transient upregulation of transcription, not seen at the blastocyst stage.

The embryo sensing pathway to these *in vitro* conditions is not yet understood. It seems that when the three BCAAs concentrations are kept constant (either all normal, all depleted by 50% or absent), the embryos do not respond to the depletion *in vitro* at least by altering the endocytosis rate. Moreover, if leucine or valine are depleted by 50% (L-LEU or L-VAL) in the culture medium, the presence of normal concentration of isoleucine *in vitro* seems to assume a major role as embryos do not change endocytosis rate in response to the depletion. If isoleucine is depleted (L-ISO), the embryo does sense the nutrient depletion and increases the endocytosis rate. Although we do not know exactly why this sensibility to isoleucine depletion occurs and current data regarding this amino acid supplementation *in vitro* is scarce, studies regarding diet supplementation in sows, showed that supplementation of isoleucine alone improves milk protein synthesis in lactating sows and litter weights, while a mixture of the three BCAA had no effect (Richert et al., 1997).

Moreover, in a previous study we found that a combined depletion of insulin and BCAA (LBCAA/L-INS) during embryo culture induced an increase in birth weight and body weight gain during early postnatal development, which did not happen when 2-cell stage embryos were cultured in LBCAAs with normalised insulin (LBCAA/N-INS) or in low insulin with normalised BCAA (NBCAA/L-INS) (Velazquez et al., 2018). Furthermore, male offspring exposed to LBCAA/L-INS (and not in the other groups) displayed relative hypertension during early postnatal life and female offspring displayed reduced heart/body weight, both characteristics of Emb-LPD offspring. Interestingly, we found that endocytosis is not only increased in response to L-ISO/N-INS but also to a combination of L-ISO/L-LEU/L-INS and a trend, although not statistically significant, in the LBCAA/L-INS group when compared to the control NBCAA/N-INS. These data indicate that embryo endocytosis was not altered in response to low leucine combined with either low or normal insulin but there is at least a trend to an increased TE endocytosis when low insulin is combined with reduced BCAA that include isoleucine, reinforcing the importance of this amino acid in regulating the blastocyst compensatory endocytosis. The importance of isoleucine over leucine has been reported in regulating mTOR signalling and protein synthesis in bovine mammary cells tissue (Appuhamy et al., 2012).

Interestingly, the compensatory endocytosis previously reported in blastocysts cultured

from 2-cell stage in L-ISO/N-INS only starts to occur after the morula stage as after 36 h of culture, morulae with approximately 20 cells had no change in lysosome number compared to control morulae cultured in NBCAA/N-INS. This response after the morula stage coincides with the timing of the maturation of the endocytic pathway (Fleming and Pickering, 1985) which may be permissive for the phenotype change in my experiments.

In all previous experiments, embryos were cultured in protein-free medium so that the role of exogenous amino acids in activating endocytosis could be studied, since the effects of BSA could confound the actions of amino acids added to the culture medium. The *in vitro* culture medium used was KSOM where BSA was omitted and BCAAs concentrations were altered. However, in all previous experiments, 2-cell stage embryos were briefly exposed to BSA (4 mg/ml) while flushed from the oviducts with H6BSA. Although different studies have used protein-free media to culture embryos in order to study the role of different culture conditions *in vitro*, including the effect of amino acids, H6BSA has been used to flush oviducts/uterine horns (Sun et al., 2014; Velazquez et al., 2018) and to the best of my knowledge this issue was never addressed before. Gardner and Kaye, (1991) suggest that cell proliferation effects of BSA during culture to the blastocyst stage derive from a nutritional role (BSA is taken up through endocytosis) but that the effects on earlier stages, such as compaction, are from non-specific actions, possibly including osmotic or protective properties.

Although the specific role of BSA in early stages is not known, we found that the short early exposure of 2-cell embryos to 4 mg/ml BSA is sufficient to 'prime' the increased endocytosis seen later at the blastocyst stage in the case of poor nutrient provision (i.e. L-ISO/N-INS) during the preimplantation culture. Interestingly, the effects of L-ISO/N-INS in blastocyst endocytosis came down to baseline values (as seen in control NBCAA/N-INS group) when 2-cell embryos were flushed from oviducts with PVP instead of BSA. It is known that the purity of BSA preparations can determine developmental outcomes, as reported for hamster zygotes (Juetten and Bavister, 1983) and that even higher-grade albumin preparations retain small, undefined molecules after purification (McKiernan and Bavister, 1992) which likely account for the variability in the embryotrophic effect observed with different batches of BSA (Biggers et al., 1997). A possible explanation for the effects seen with BSA but not with PVP might be due to a

combination of a deprived environment (L-ISO/N-INS) with the effects of undefined molecules in BSA, which might represent a challenge for embryo development. On the contrary, it could be that PVP is somehow (i.e. unspecific binding to ZP) preventing accurate embryo sensing and further activation of compensatory response to poor environment. Future work is required in order to investigate how this activation is primed early in development and the exact role of BSA as a trigger for that activation later in development.

Although, as mentioned earlier, the culture medium used in all previous experiments was designed to be protein-free, BSA was provided in the form of BSA-BODIPY during the last hour of culture in order to be taken up and digested through endocytosis and then quantified using VOLOCITY. Thus, we tested if the increased endocytosis and lysosome formation seen in deprived culture environments, such as L-ISO/N-INS, was a compensatory response to the 48 h culture and fully independent of the amount of BSA provided during the assay or if the final hour in culture (the assay itself) with the presence of BSA (0.5 mg/ml in BSA-BODIPY) or the switch from protein-free to BSA in culture had any effect in stimulating lysosome formation to promote endocytosis. We found that increased lysosome formation in the L-ISO/N-INS group is a response to the culture medium environment and it is independent of the BSA provided in the last hour to study endocytosis uptake. This suggests that early embryos interact with their environment and are particularly susceptible to L-ISO/N-INS *in vitro*, which is able to modulate the inherent developmental programme by the blastocyst stage and to confer plasticity to support survival in these challenging conditions.

Because we found this activation of endocytosis and lysosome number in blastocysts cultured from 2-cell stage in L-ISO/N-INS, and since Emb-LPD blastocysts showed not only similar endocytosis response (Sun et al., 2014) but also reduced mTORC1 signalling (Eckert et al., 2012), TFEB emerged as a potential target regulating lysosome formation in this model. TFEB is tightly controlled by nutrient status, with energy-rich conditions leading to cytoplasmic retention and lysosomal low-energy stores promoting hypophosphorylation and nuclear localization (Settembre et al., 2012), through TFEB interaction with mTORC1 on the lysosomal membrane. When mTORC1 is downregulated, TFEB is translocated to the nucleus increasing the transcription of genes implicated in lysosomal biosynthesis and function. We found that approximately 80% of

total TFEB volume in TE cells is located in the nucleus in L-ISO/N-INS blastocysts as opposed to approximately 40% in the control NBCAA/N-INS group. These data were further validated by statistical Pearson correlation test between nucleus and TFEB colocalisation, suggesting that TFEB regulates lysosomal formation through its activation and translocation to the nucleus by promoting the transcription of genes involved in lysosome biosynthesis. However, despite the TFEB activation seen in L-ISO/N-INS blastocysts, mRNA levels of three TFEB direct targets with known roles in lysosomal function (Lamp1, Ctsb and Vps18) were not altered. Due to the high variability between embryos it is possible that a larger n number would be necessary to detect any statistically significant difference. Further investigation, including studying the gene expression of other known lysosomal direct targets of TFEB, is required.

Since TFEB is triggered in response to lysosomal status through downregulated mTORC1 we then used the mTORC1 inhibitor, rapamycin, at different concentrations *in vitro* (from 2-cell to blastocyst stage) to study if the L-ISO/N-INS effects on lysosome formation and TFEB activation are comparable to this drug treatment effect. Interestingly, we found that higher concentrations of rapamycin (20 μM) caused TFEB activation, shown by increased nuclear staining compared to lower concentrations of the drug where TFEB was mainly cytoplasmic. However, even though in our model, embryo culture in L-ISO/N-INS was sufficient to cause not only TFEB activation but also its response to increase lysosomes formation, rapamycin treatment, even at the highest concentration, did not affect lysosome formation to a significant level. A possible explanation for these results is that rapamycin is a partial inhibitor of mTOR, as some substrates are still efficiently phosphorylated in the presence of this drug (Thoreen et al., 2009). Nevertheless, it was the first time TFEB expression and activation was identified in preimplantation embryos and our work indicates that TFEB may have a more general role in cellular adaptation to stress than previously recognized, as not only starvation but also mild amino acid restriction (L-ISO/N-INS) *in vitro* induces TFEB nuclear translocation.

Furthermore, I found a positive relationship between cell volume and endocytosis, which was not treatment-related. In general, it seems that cells with larger volumes have more lysosomes, which is presumably part of cell cycle dynamics. However, a specific *in vitro* AA treatment provokes an increased response in lysosome production when

another treatment does not (i.e. L-ISO/N-INS vs. NBCAA/N-INS). These findings suggest a more general mechanism of cell volume increase and a more specific AA-dependent mechanism that adds to that. Interestingly, we found no correlation between cell volume and TFEB translocation to nucleus in both treatment groups as opposed to the lysosome/cell volume relationship, suggesting an independent process where TFEB activation occurs as a response to environmental challenges such as deprived AA conditions (L-ISO/N-INS) but not to cell volume alterations. To confirm these results, we studied the same correlation in embryos that were treated with different concentrations of the mTORC1 inhibitor, rapamycin. Again, we showed a positive correlation between cell volume and lysosome number and volume independent of treatment but no correlation between cell volume and percentage of TFEB in the nucleus. Thus, we confirmed that there is no relationship between cell volume and TFEB, suggesting that its activation responds to specific challenging conditions affecting mTORC1 (i.e. starvation models, rapamycin inhibited mTORC1 and specific AAs – such as low isoleucine - depleted from culture).

In chapter 6, we have compared the cellular characteristics of human embryos, donated for research within our HFEA licence, based upon the BMI of maternal donors as a marker reflecting maternal nutritional quality. Whilst no difference was found between blastocysts in terms of embryo survival and cell number, those from the high BMI group exhibited the enhanced endocytosis phenotype seen in mouse embryos cultured *in vitro* in L-ISO/N-INS and the range of scores varied across the high BMI but not the control group showing individual embryo variation. Moreover, blastocysts from high BMI mothers have increased TFEB in the nucleus and reduced in the cytoplasm compared to blastocysts from normal BMI mothers, but not quite at significance level. Thus, we have supportive evidence from this preliminary work that human embryos exhibit a similar mechanism to mouse embryos in regulating endocytosis in response to maternal nutritional status, however, more studies are required to validate the activation and signalling pathway involved.

Additionally, using the same patient and embryo information, I studied endocytosis activation in response to ICSI procedure vs. conventional IVF. Here I found that LysoTracker collective volume and TFEB localisation were not significantly changed between both groups. However, we did see a vast variability in the results in the ICSI

group compared to the non-ICSI conventional IVF, as seen in the high BMI group, showing individual embryo variation.

Our limited data on human embryos suggest a similar metabolic phenotype may be activated in the human in response to a dysfunctional maternal nutritional profile. In the wider context of research on peri-conceptional environment in both animal and human species, it is clear that the early embryonic period is sensitive to a diverse range of external stimuli (i.e., parental nutrition, immunological status and alcohol consumption, assisted reproduction techniques and culture conditions) that affect later life health through cellular, physiological and epigenetic mechanisms (reviewed in Fleming et al 2018). Putting mouse and human results together, we could argue that a) endocytosis is a potential biomarker in a relevant setting for humans (BMI as more relevant proxy for malnutrition) and b) developing an *in vitro* environment that can rectify the process of endocytosis during culture safely (i.e. sufficient inclusion of metabolites in the composition of IVF culture media) may help prevent long-term consequences in human IVF in the future. However, more preliminary studies are needed, in both models, including studying refined culture conditions in order to determine the precise metabolites and its concentrations to which the embryo becomes sensitive and starts to respond with increased endocytosis and lysosome formation to promote adaptation and survival to the environment.

7.2 Work implications

This study further confirms in general terms the critical relevance of the mammalian preimplantation period as a developmental window where programming with long-term consequences for health and disease risk are evident in both rodent and human models. Amino acids' concentration in culture, specifically decreased isoleucine concentrations, were recognised to have a significant impact in mouse embryo *in vitro* development, by changing their TE endocytosis levels. Here, increased endocytosis is seen as a compensatory response to poor nutrient environment, and was previously linked to programming of DOHaD-type diseases, including increased risk of developing postnatal cardiomatabolic disease in our mouse LPD model (Sun et al., 2014).

In a broader perspective, this periconceptional window where embryo culture conditions may affect postnatal phenotype is pertinent to the human ART. ART children

display increased risk of cardiovascular dysfunction likely to derive from their *in vitro* treatments rather than factors associated with parental infertility, including relative hypertension (Venezuela-Alcaraz et al., 2013; Guo et al., 2017) together with cardiovascular remodelling during pregnancy resulting in alterations in heart shape and chamber size (Venezuela-Alcaraz et al., 2013; Zhou et al., 2014). Thus, embryo culture conditions and composition are critical factors determining postnatal phenotype both in animal models and in human ART. Studies using our *in vitro* culture system of decreased amino acids concentrations are required to confirm whether isoleucine plays a similar role in human embryos. Nevertheless, I have confirmed that human embryos show similar metabolic alterations in response to a dysfunctional maternal nutritional status (high BMI). Improving the methods used here in order to study metabolic variations (i.e. endocytosis level; lysosome numbers) in live embryos without disturbing their *in vitro* development, would probably have a massive impact in the IVF embryo selection and quality assessment procedures and further disease programming. This would allow embryologists to select the best embryo for transfer not only by morphological features but also by metabolic status. Thus, it may be pertinent in future clinical embryology to screen for metabolic criteria such as endocytosis level or numbers of lysosomes through advanced non-invasive light microscopy technologies and imaging (i.e, optical coherence microscopy; Karnowski et al., (2017)).

A further, wider implication of my work, coupled with that of related past studies from colleagues, has been on biological mechanisms of preimplantation development. The concept has emerged that phenotypic selection may be occurring in the early embryo to optimise survival dependent upon maternal condition, an example of the epigenetic model first proposed by Conrad Waddington in the 1940s (Tronick and Hunter, 2016). Denisenko et al., (2016) showed that characteristics that determine adult rDNA transcription rates (i.e. DNA methylation profile and Rrn3 protein levels) are set during the preimplantation period of mouse development. Specifically, maternal Emb-LPD triggered a decreased rDNA methylation and increased rDNA transcription together with Rrn3 expression during both foetal and adult life, demonstrating the prolonged legacy of the preimplantation nutrient experience.

7.3 Limitations

It is important to reflect on some factors that could have influenced our results. Our *in vitro* mouse (but not human) embryo culture was carried out under atmospheric O_2 conditions (~20%), and it is known that a low O_2 environment (5%) promotes a better utilization of amino acids in mouse preimplantation embryos (Wale and Gardner, 2012). Furthermore, unlike microfluidic systems where a constant flow of medium can be regulated (Wheeler and Rubessa, 2017), in our static *in vitro* system, consumption and degradation of culture medium components took place without renewal, hindering a constant exposure of nutrients tested in our study. Although it remains to be determined if these refinements could alter the blastocyst phenotype observed, we believe our data come from a robust *in vitro* embryo culture model.

Due to confocal microscopy limitations, data obtained per embryo is limited, as the quality of image acquired decreases with the distance away from the coverslip within the 3D embryo sample. Moreover, VOLOCITY software pitfalls combine vesicles that are close to each other, giving incorrect data analysis, especially when the image quality is poor. For that reason, we used TE high resolution scan only – top cells closest to the coverslip imaged with high resolution - (and not half embryo scan method) during confocal image acquisition to analyse our data which reduces drastically the amount of information acquired per embryo.

In this study we used natural mating and not superovulation to collect 2-cell embryos for our *in vitro* experiments in order to reduce external factors that could influence embryo quality. Some evidence suggest that superovulation in the mouse causes a delayed embryonic development *in vitro* and *in vivo*, an increased abnormal blastocyst formation and a pronounced foetal growth retardation (Van der Auwera and D'Hooghe, 2001). However, natural mating reduces the number of embryos obtained per female, imposing the need of using more females to obtain a reliable N number in each replicate of experiment, particularly when comparing a large number of experimental groups.

qRT-PCR was performed in male embryos only, due to the lack of female embryos acquired to study both sexes. All endocytosis and immunohistochemistry data was done without genotyping embryos, which makes it impossible to study any sex-dependent effects.

Research in human embryos is very limited, especially considering that we have frozen embryos that were collected many years ago (up to 10 years) using different methods at different stages of development. This means that techniques used by then have evolved, including culture media used, type of incubators, embryo selection using time-lapse or not. The commercial culture medium (Sage 1-Step™, Origio) composition used is undisclosed, as no information regarding the concentrations of amino acids is revealed. Moreover, the number of embryos per patient varies, sometimes being very low to make accurate comparisons. In culture, the percentage of embryos that reach blastocyst stage and/or that can be classified/graded as good (no or minor fragmentation and cells mostly or of equal size) is very reduced compared to mouse embryo culture. We acknowledge the difficulty of drawing any final conclusions for this type of study considering the high variability of these embryos and parental demographics, it is difficult to account for every factor that might influence the results seen. Even though we accounted for several factors using a multilevel regression model in which data was corrected (random effect assigned) to each blastocyst cell volume; cell number; whether a pregnancy resulted from the same cycle that the embryos under study were retrieved; as well as patient ID to account for mother effect; several other factors were not accounted for, including different infertility reasons (maternal, paternal, both or unexplained) and treatments as well as the culture medium used at the time of freezing in the clinic, the number of years embryos were frozen and possible differences in conditions and practices used over time since freezing.

7.4 Future work

In order to extend our understanding of the endocytosis response seen following depleted BCAA (isoleucine) culture *in vitro*, studies regarding autophagy and mTOR in blastocysts in response to this culture condition could be done. We found in this study that TFEB is activated in these conditions (L-ISO/N-INS) and mTORC1 was downregulated in Emb-LPD blastocysts (Eckert et al., 2012). Since TFEB is activated in response to lysosomal status (low nutrients) through downregulated mTORC1, studies to access whether mTORC1 is also downregulated in these *in vitro* cultured embryos could be done. This could include the use of quantitative immunoblotting of mTORC1 downstream targets S6 and 4E-BP1 proteins. Moreover, since TFEB activation

(translocation to nucleus) is known to induce transcriptional upregulation of genes implicated in autophagy regulation through promoting autophagosome formation and autophagosome-lysosome fusion (Settembre et al., 2012), autophagy could be further studied in these embryos. Even though I did not find changes in the gene expression of Vps18 (a protein involved in autophagy), LC3, a fluorescent marker for autophagosomes, could be used in embryos to detect autophagy activity. Moreover, other downstream genes differentially expressed followed TFEB overexpression could be looked at and the gene expression experiments done could be repeated using a larger n number and including both male and female embryos.

System A amino acid transport activity is known to be upregulated in response to amino acid withdrawal, as an "adaptive regulation" and it is linked with increased expression of SNAT 2 (Ling et al., 2001). Since we are depleting isoleucine (BCAA) concentration *in vitro*, and BCAAs are one of system A preferred substrates we could investigate if this particular amino acid transporter is upregulated in these embryos. Moreover, SNAT2 is expressed in blastocysts and not earlier, and the endocytosis response seen in this model was not present before the blastocyst stage.

Finally, we are very intrigued with the activation of the endocytosis seen as a response to BSA pulse early in development at 2-cell stage during flushing from oviduct as opposed to PVP in the flushing solution. Future work could include the use of a different protein source as flushing solution, namely transferrin, the second most present protein in the oviduct after albumin (Aitken, 1977b), in order to clarify if an early exposure to a protein source or BSA particularly (either albumin or unspecific molecules from BSA) are the causes for priming early embryos to respond later in development. Moreover, flushing the oviducts with a combination of BSA and PVP might indicate if it is PVP instead preventing the early embryo programming later in development.

Chapter 8 Appendix

8.1 LPD/NPD diet composition

	NPD (18% casein)	LPD (9% casein)
Casein	180	90
Corn starch	425	485
Fibre	50	50
Sucrose	213	243
Choline Chloride	2	2
DL-Methionine	5	5
AIN-76 mineral mix	20	20
AIN-76 vitamin mix	5	5
Corn oil	100	100

Table 8.1 - Composition of synthetic casein diet in grams per kilograms (g/Kg) of diet (Langley and Jackson, 1994).

8.2 Embryo Culture Media

8.2.1 H6BSA composition

	Amount added
H_2O	78 ml
Solution F	10 ml
Solution B	1.6 ml
Solution G	1.0 ml
Solution H	1.0 ml
Solution E	8.4 ml
BSA	0.400 g
20% NaCl	0.600 ml

Table 8.2 – H6BSA media composition. The following tables describe the composition of each solution F, B, G, H and E used for this media preparation.

8.2.1.1 Solution F (per 100ml, osmolarity 2555+/-20mOsm)

	Amount added
Sodium Chloride	4.720 g
Potassium Chloride	0.11 g
Sodium dihydrogen orthophosphate	0.06 g
Magnesium chloride	0.1 g

D-Glucose	1.0 g
DL-lactic acid (60%)	3.4 ml

Table 8.3 – Solution F composition.

8.2.1.2 Solution G (per 10ml, osmolarity 60+/-10mOsm)

	Amount added
Pyruvic	0.03 g
Penicillin	0.06 g
Streptomycin	0.05 g

Table 8.4 - Solution G composition.

8.2.1.3 Solution B (per 10ml, osmolarity 444+/-20mOsm)

	Amount added
Sodium hydroge carbone	0.2106

Table 8.5 - **Solution B composition.**

8.2.1.4 Solution H (per 10ml, osmolarity 415+/-20mOs

	Amount added
Calcium Chloride 2-hydate	0.26 g

Table 8.6 - Solution H composition.

8.2.1.5 Solution E (per 10ml, osmolarity 444+/-20mOsm)

	Amount added
Hepes (pH to 7.4 with 5M NaOH before checking mOsm)	2.9785 g
Phenolred	6 mg/ml
Sodium Chloride	20%

Table 8.7 - Solution E composition.

8.2.2 KSOM media Composition

	Concentration (mM)
Sodium Chloride (NaCl)	190
Potassium Chloride (KCl)	5
Potassium Dihydrogen Orthophosphate (KH_2PO_4)	0.7
Magnesium Sulphate 7-hydrate ($MgSO_47H_2O$)	0.4
Lactic Acid	20
Sodium Pyruvate	0.4
Glucose	0.4
Sodium Bicarbonate ($NaHCO_3$)	50
Penicillin	
Strep Sulphate (Stock = 0.100g/ml – make up with sterile H_2O)	(1ml stock)
EDTA (Stock 0.5mM)	0.02

Table 8.8 – KSOM 2x Stock composition (Store at -80°C – Two-month shelf life)

	Amount added to 2x KSOM
$CaCl_2$	100 µl
NEAA	50 µl
Essential AA	100 µl
L-Glutamine	50 µl
Sterile H_2O	4.75 ml
BSA	0.040 g

Table 8.9 – KSOM 1x composition – Components added to KSOM 2x stocks. After adding all the components, the solution is filtered through a 0.22 µm syringe filter and the osmolarity is checked and adjusted to 250-260 mOsm using 20% NaCl or H_2O.

8.2.3 Amino Acids

Amino Acid	Supplier	Catalogue/product no
L-Cysteine	BDH	372183X
L-Lysine monohydrochloride, minimum 98% TLC	Sigma	L5626-100G
L-Tyrosine	Sigma	T-8566 25g
L-LEUcine, minimum 98% TLC	Sigma	L8000-100G
L-Tryptophan, minimum 98% TLC	Sigma	T0254-25G
L-Arginine monohydrochloride, minimum 98% TLC	Sigma	A5131-100G
L-Proline, minimum 99% TLC	Sigma	P0380-100G
L-Methionine, minimum 98% TLC	Sigma	M9625-25G
Glycine, Biotechnology Performance Certified	Sigma	G8790-100G

L-ISOleucine	Sigma	I-2877 10g
L-Phenilalanine, >=98%	Sigma	P2126-100G
L-Alanine, minimum 98% TLC	Sigma	A7627-100G
V-Valine, Minimum 98% (TLC)	Sigma	V0500-25G
L-Histidine monohydrochloride monohydrate, minimum 98% TLC	Sigma	H8125-100G
L-Serine, minimum 99% TLC	Sigma	S4500-100G
L-Threonine, minimum 98% TLC	Sigma	T8625-25G
L-Glutamic acid, minimum 99% (TLC)	Sigma	G1251-100G
L-Asparagine monohydrate	Sigma	A4284-25G
L-Aspartic acid, minimum 98% TLC	Sigma	A9256-100G
Taurine	Sigma	T-8691 100g

Table 8.10 – List of Amino acids used and suppliers

8.2.3.1 Amino Acids in vivo concentration

AMINO ACID	*In vivo* concentration (mM)
Alanine	3.8
Arginine	0.16
Asparagine	0.14
Aspartic acid	1.83
Glutamic acid	4.72
Glutamine	1.41
Glycine	2.68
Histidine	0.14
Isoleucine	0.21
Leucine	0.32
Lysine	0.5
Methionine	0.18
Phenylalanine	0.14
Serine	0.97
Taurine	14.74
Threonine	0.72
Tryptophan	0.06
Tyrosine	0.18

Valine	0.45
Cystine	0.2
Proline	0.1

Table 8.11 - Amino Acids in vivo concentration in the NPD mother at E3.5 (Eckert et al., 2012)

8.2.3.2 Amino Acids Stocks preparation

		Stock concentration (mM)	
1	Aspartic acid	33.3	0.02216 g/5ml
2	Glutamic acid	50	0.03678 g/5ml
3	Asparagine	100	0.07507 g/5ml
4	Serine	100	0.052545 g/5ml
5	Histidine	100	0.104815 g/5ml
6	Glutamine	200	Commercial Stock
7	Glycine	100	0.037535 g/5ml
8	Threonine	100	0.05956 g/5ml
9	Arginine	100	0.105335 g/5ml
10	Taurine	73.5	0.0919485g/10ml
11	Tyrosine	1	0.001812g/10ml
12	Alanine	100	0.044545 g/5ml
13	Tryptophan	50	0.0510575 g/ml
14	Methionine	100	0.074605 g/5ml
15	Valine	100	0.058575 g/5ml
16	Phenylalanine	100	0.082595 g/5ml
17	Isoleucine	100	0.0656 g/5ml
18	Leucine	100	0.06559 g/5ml

19 Lysine	100	0.091325 g/5ml
20 Proline	100	0.057565 g/5ml
21 Cystine	100	0.06058 g/5ml

Table 8.12 – Concentrations used to prepare the amino acids stocks solutions.

8.2.3.3 KSOM with different BCAA concentration

		Dilution for 1 ml of medium (µl)
1	**Aspartic ac id**	54
2	**Glutamic acid**	94
3	**Asparagine**	1
4	**Serine**	10
5	**Histidine**	1
6	**Glutamine**	7
7	**Glycine**	27
8	**threonine**	7
9	**Arginine**	2
10	**Taurine**	200
11	**Tyrosine**	
12	**Alanine**	38
13	**Tryptophan**	1.2
14	**Methionine**	2
15	**Valine**	**5**
16	**Phenylalanine**	1
17	**Isoleucine**	**2**
18	**Leucine**	**3**
19	**Lysine**	5

20	**Proline**	1
21	**Cystine**	2
	Total	463.2

Table 8.14 – Amino acids amount added (from stocks – table 8.12) to prepare the KSOM media used in the BCAA in vitro culture experiments (for NBCAA group). For treatment groups BCAAs (15, 17 and 18) were decreased by 50% (individually or combined) or omitted in experimental groups.

AA volume (µl)	463.2
KSOM volume (µl)	500
CaCl volume (µl)	10
Insulin (µl)	10 (final concentration = 1ng/ml)
H_20 volume (µl)	16.8
TOTAL	1000

Table 8.13 – KSOM media preparation (used in BCAAs in vitro culture experiments) - for NBCAA. In the treatment groups the AA volume was decreased (by changes in BCAAs) and adjusted with H_2O.

8.3 Immunocytochemistry

8.3.1 Acid Tyrode's Solution (per 100 ml, pH 2.3)

	Amount added
NaCl	0.8 g
KCl	0.02 g
$CaCl_2.2H_2O$	0.0265 g
$MgCl_2.2H_2O$	0.01 g
D-Glucose	0.1 g
PVP	0.4 g
or	
$CaCl_2$	0.02 g

Table 8.15 – Reagents used to prepare Acid Tyrode's Solution

8.3.2 Chambers preparation

1. File down the inner ring of the washer to ensure the surface is flat.

2. Wash the washers in detergent and rinse and dry thoroughly.

3. When washers are dry place superglue around the middle of the washer in a circle.

4. Carefully drop a dried 22mm coverslip previously treated with 1M HCl followed by several washes in dH_2O onto the glue and watch to see if the glue spreads. It is important that there are no gaps around the hole in the washer and the glass coverslip. The glue should spread to cover the washer under the coverslip.

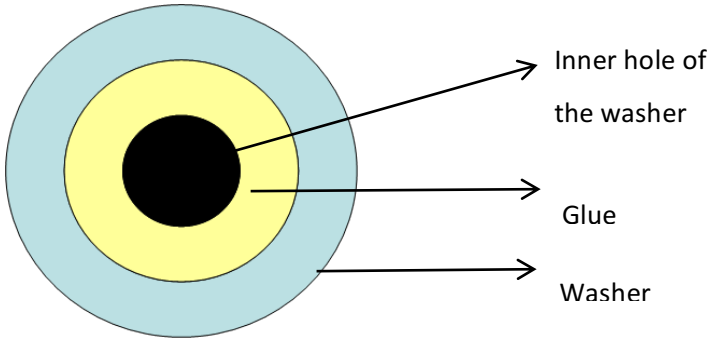

Figure 8.1 – Making chambers using M6 x 40 mm steel penny washers

8.3.3 Embryo Immunocytochemistry Protocol

1. Fixation in cavity block – 1% formaldehyde
2. 0.25% Triton-X-100 in PBS – 15min
3. Wash in PBS-Tween-20
4. 2.6mg/ml NH4CL – 10min
5. Wash 3 times (5min each) in PBS-Tween
6. Incubate with primary antibody diluted in PBS-Tween overnight at 4°C
7. Wash 3 times (10min each) in PBS-Tween
8. Incubate secondary antibody (diluted in PBS-Tween) for 1h at room temperature
9. Wash 3 times (10min each) in PBS-Tween
10. Incubate with DAPI (2 μg/ml) diluted in PBS-Tween for 20min
11. Prepare Poly-L-Lysine 2.5mg/ml in PBS (Poly-L-Lysine should be removed from freezer previously and allow to warm up at room temperature before opening). Wash chambers 3 times in PBS and replace the last PBS with the Poly-L-Lysine and leave for 30minutes in a hot plate
12. Remove Poly-L-Lysine with syringe without touching the coverslip on the button of the chamber and replace with PBS
13. Transfer embryo to chamber
14. Add citifluor and a 18mm coverslip
15. Seal with nail varnishing.

8.4 VOLOCITY protocol

1. Crop cell (for TE high resolution approach only)
2. Find object (based on channel) – red channel for LysoTracker Red; green channel for BSA-BODIPY and FITC-Dextran
3. Remove noise from objects (fine filter)
4. Separate touching objects (by 2 µm)
    a. Exclude objects by size:
        i. vesicles <0.01 μm^3 and > 20 μm^3
        ii. nuclei < 150 μm^3
5. Nuclei – fill holes in objects
6. Offset/Intensity – 50%
7. Measure distance to nuclei edge (TE)

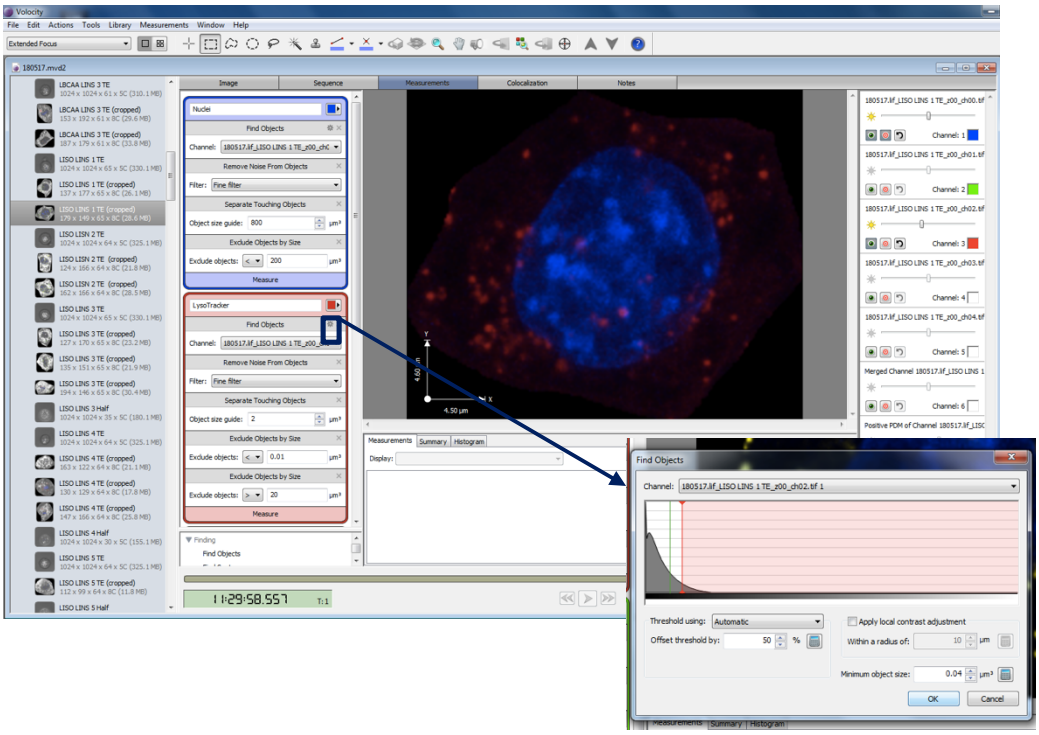

Figure 8.2 – After being cropped, one cell is displayed and the VOLOCITY protocol designed for BSA-BODIPY and LysoTracker vesicle counting in TE high resolution applied. On the right the channels used can be turn on/off (in this example blue channel – DAPI and red channel – Lysotracker are on. On the left side of the figure there is a part of the set protocol with the definitions used to analyse the nucleus and lysotracker. By clicking in settings for each channel the offset threshold can be changed (in this case it was set as 50% for all channels).

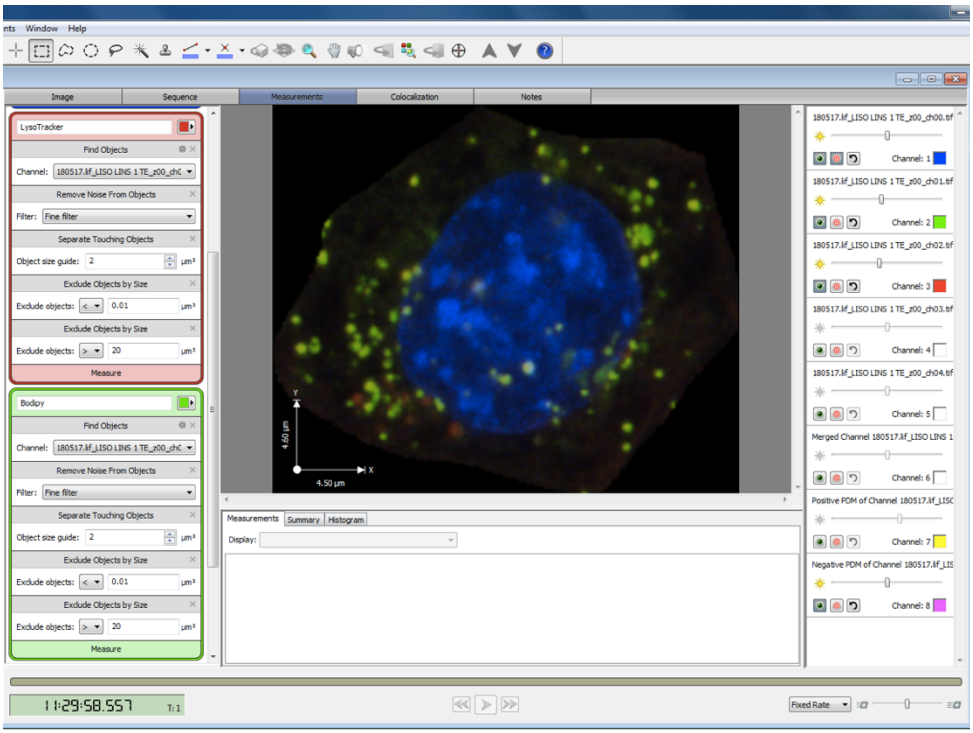

Figure 8.3– Cell with blue channel (DAPI), green (BSA-BODIPY) and red (LysoTracker) turned on (right side). On the left there is the protocol setting for the red and green channels.

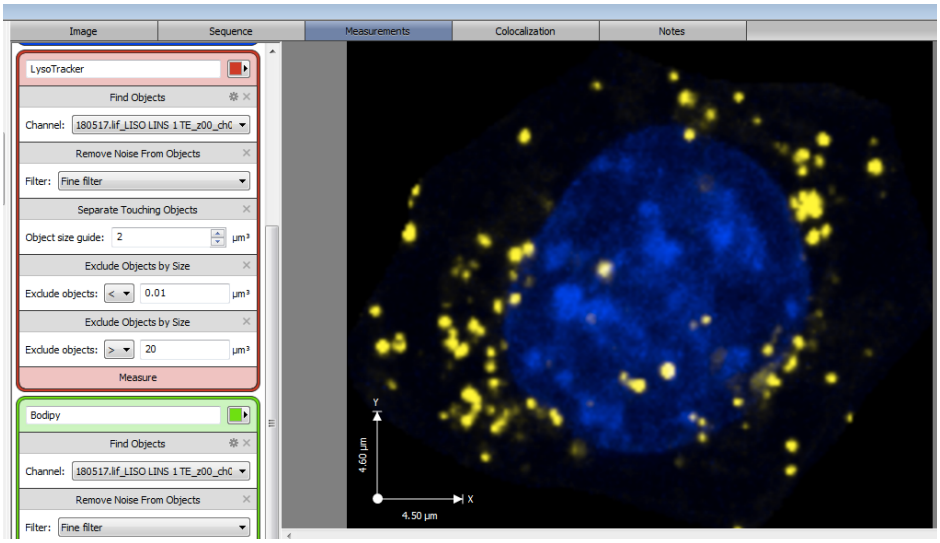

Figure 8.4 – Cell with blue channel (DAPI) and the colocalised vesicles (yellow) (green and red vesicles – BSA-BODIPY and LysoTracker) according with the designed protocol. Unspecific staining and/or stained particles that did not fit the designed protocol (i.e. did not fit the size range selected) were excluded

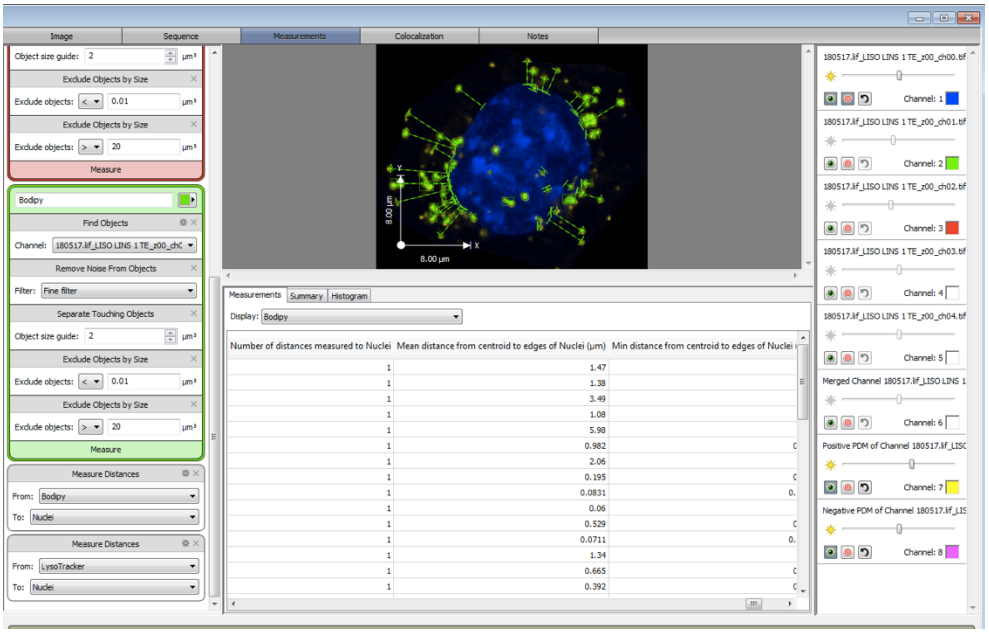

Figure 8.5 – BSA-BODIPY particles distance to nucleus. On the left there is the protocol setting for the green channel and distance from centre of vesicles to nucleus edge. In measurements the software displays the individual measurements analysed.

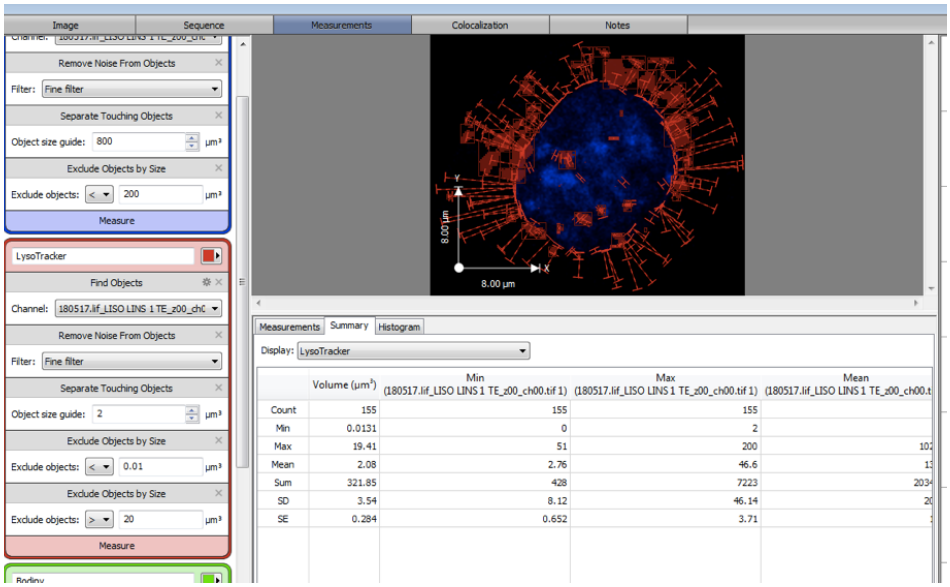

Figure 8.6 - LysoTracaker vesicles distance to nucleus (distance from centre of red vesicles to nucleus edge). In measurements the software displays the summary of all measured items.

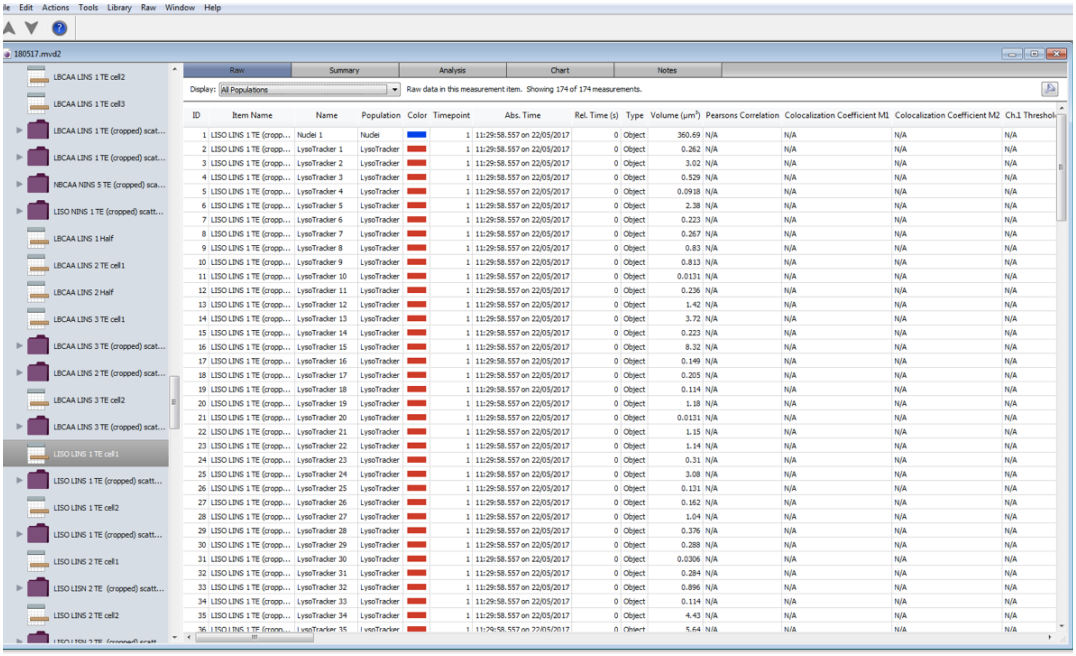

Figure 8.7 – After analysing the cells using the previously defined protocols, data is saved in sheets that can be opened and saved as excel files. Data can be either saved as raw data (individual data for all measured vesicles, including volumes and distances to nuclei) or as a summary of the data (including total number of vesicles counted and combined volume) – see *Figure 8.8*.

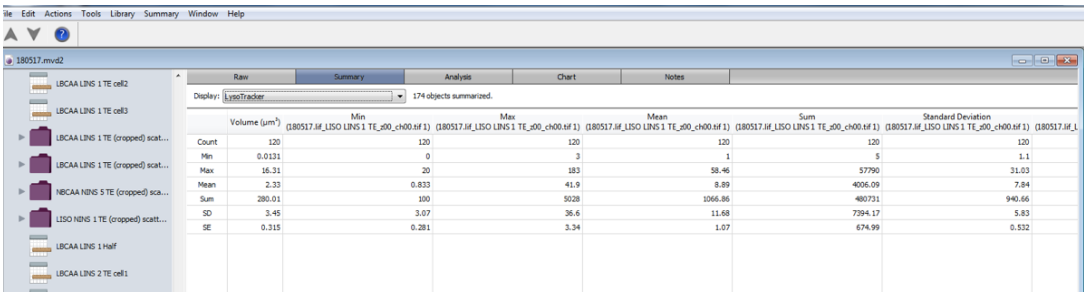

Figure 8.8 – After analysing the cells using the previously defined protocols, a summary of the data obtained can be saved as an excel files.

8.5 Endocytosis Assay

1. Mouse dissection - oviducts/uterine horns collected and placed in pre-warmed (37℃) saline
2. Transfer the oviducts/uterine horns to a drop of H6BSA or H6PVP
3. Under the dissection microscope inject pre-warmed H6BSA/PVP in the infumdibulum (part of oviduct closest to the ovary) for 2-cell stage embryo collection or in the uterine horn (closest of the oviduct) for blastocyst stage and flush
4. Collect embryos by pipetting under the microscope and place them in a drop of H6 media (H6 - BSA or PVP, depending on the experiment)
5. Wash embryos three times in H6 drops
6. Wash embryos in a drop of BSA-BODIPY (0.5mg/ml) or 40kD FITC-Dextran (5mg/ml)+ LysoTracker (100nM)
7. Incubate embryos in a drop of BSA-BODIPY (0.5mg/ml) or 40kD FITC-Dextran (5mg/ml) + LysoTracker (100nM) in KSOM, covered with mineral oil for 1h at 37℃
8. Wash 3 times in H6 (H6 - BSA or PVP, depending on the experiment)
9. Fixation in 1% formaldehyde at room temperature for 20 min.
10. Wash 3 times in PBS
11. Incubate embryos in CellMask Deep red in PBS (1:200) for 1h at RT
12. Wash 3 times in PBS
13. Incubate in DAPI (2 μg/ml) in PBS for 20 minutes at RT
14. During DAPI incubation, prepare Poly-L-Lysine 2.5mg/ml in PBS (Poly-L-Lysine should be removed from freezer previously and allow to warm up at room temperature before opening). Wash chambers 3 times in PBS and replace the last PBS with the Poly-L-Lysine and leave for 30minutes in a hot plate
15. Remove Poly-L-Lysine with syringe without touching the coverslip on the button of the chamber and replace with PBS
16. After DAPI incubation, wash embryos 3 times in PBS
17. Transfer embryos to chamber by pipetting and allow it to stick to the bottom
18. Remove the excess PBS
19. Add citifluor in PBS and a 18mm coverslip
20. Seal with nail varnishing

8.6 Endocytosis results in fixed Vs. live embryos

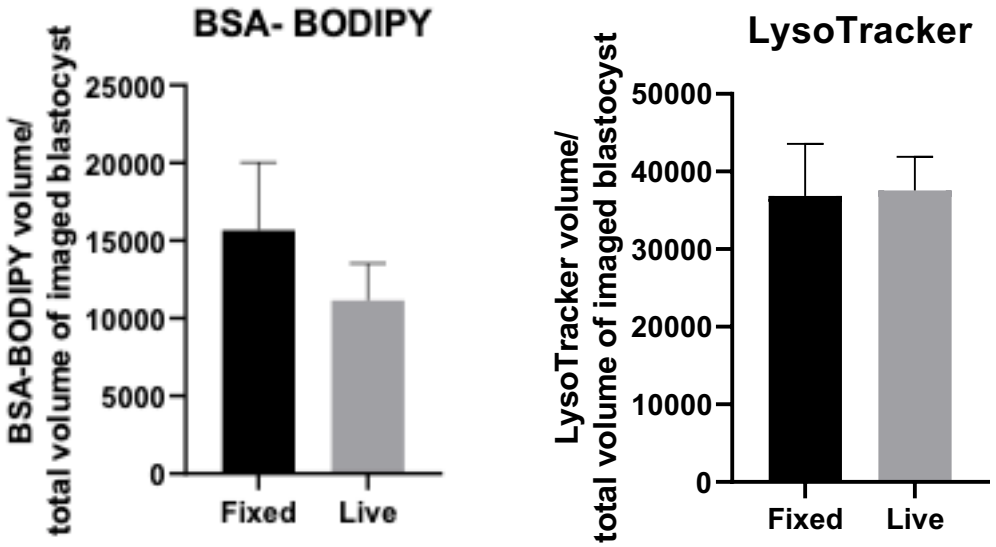

Figure 8.9 –BSA-BODIPY and LysoTracker collective volume per blastocyst volume. Blastocysts were imaged using the half embryo scan method (thus, approximately half embryo was imaged). BSA-BODIPY and LysoTracker volume was not normalised to the number of blastocyst cells present since the nuclear staining in live embryos (using SYTO blue dye) did not work. Values are presented as mean ±SEM. 4-5 embryos per group from 2 mothers.

8.7 Gel electrophoresis for the qRT-PCR products

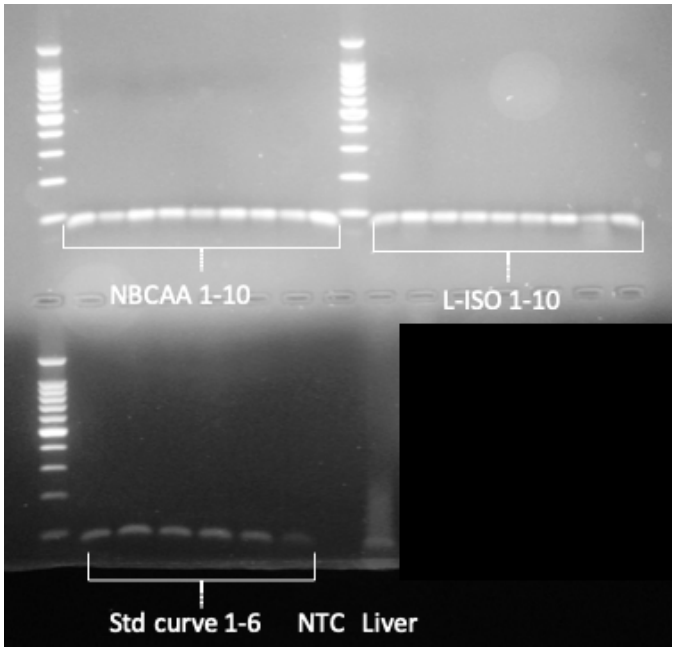

Figure 8.10 – 2% gel electrophoresis for the qRT-PCR products – Megalin expression (64 bp) in NBCAA/N-INS (NBCAA 1-10) and L-ISO/N-INS (L-ISO 1-10) (n = 10 embryos/group), standard curve, NTC control and liver sample as positive control.

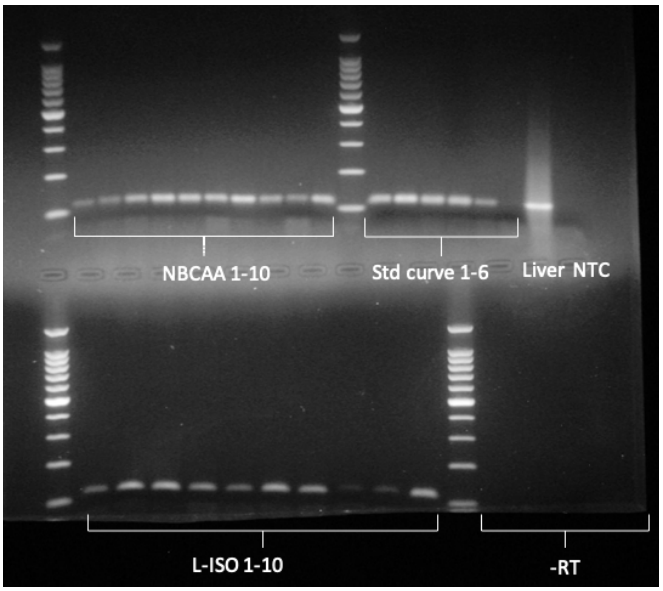

Figure 8.11 – 2% gel electrophoresis for the qRT-PCR products – Lamp1 expression in NBCAA/N-INS (NBCAA 1-10) and L-ISO/N-INS (L-ISO 1-10) (n = 10 embryos/group), standard curve, liver sample as positive control, NTC control and RT- controls.

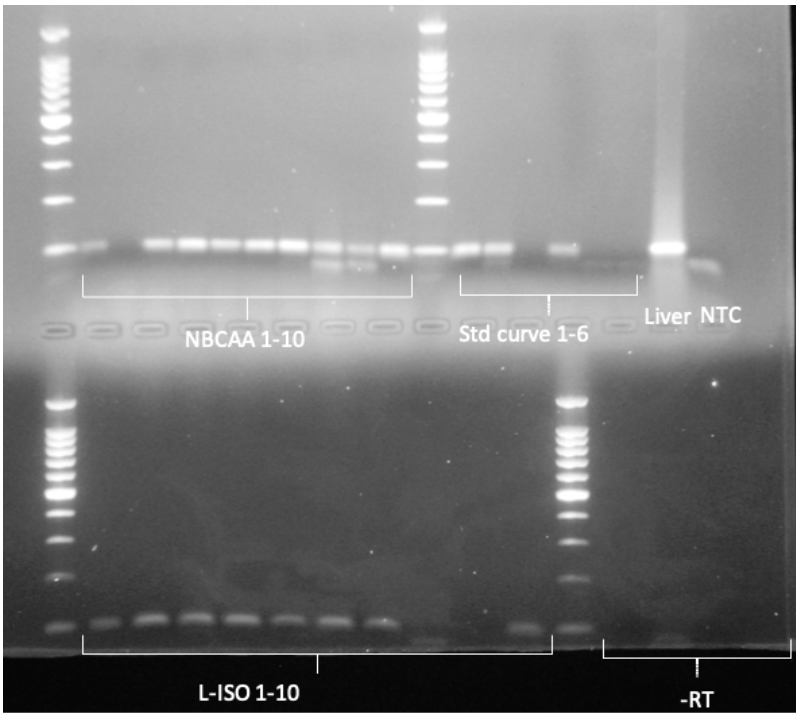

Figure 8.12 – 2% gel electrophoresis for the qRT-PCR products – Ctsb expression in NBCAA/N-INS (NBCAA 1-10) and L-ISO/N-INS (L-ISO 1-10) (n = 10 embryos/group), standard curve, liver sample as positive control, NTC control and RT- controls.

8.8 Embryo total volume

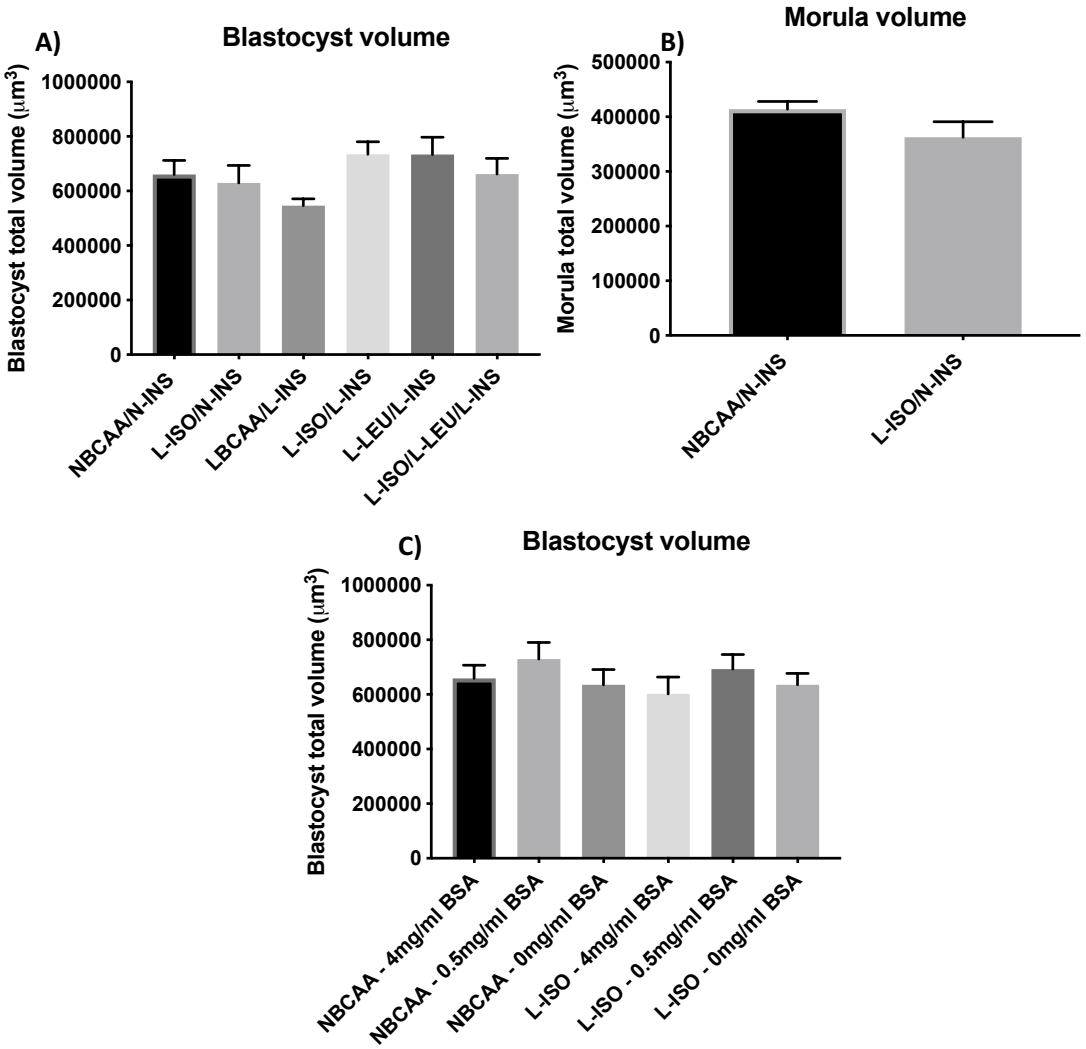

Figure 8.13 –Embryo total volume. Blastocyst (A,C) and morula (B) volumes is not significantly changed between groups. The first two experiments (NBCAA/N-INS, LBCAA/N-INS, 0BCAA/N-INS and NBCAA/N-INS, L-VAL/N-INS, L-LEU/N-INS, L-ISO/N-INS, NBCAA/L-INS) were not included since confocal imaging was acquired in half embryo only and not total blastocyst. Values are presented as mean ±SEM. A) 13-19 embryos per group (23-38 cells per group) from 14 mothers (in 8 replicates). B) 17-18 embryos per group (24-26 cells per group) from 5 mothers (in 4 replicates). C) 13-21 embryos per group (17-29 cells per group) from 13 mothers (in 6 replicates).

8.9 Cell volume and data normalised to cell volume

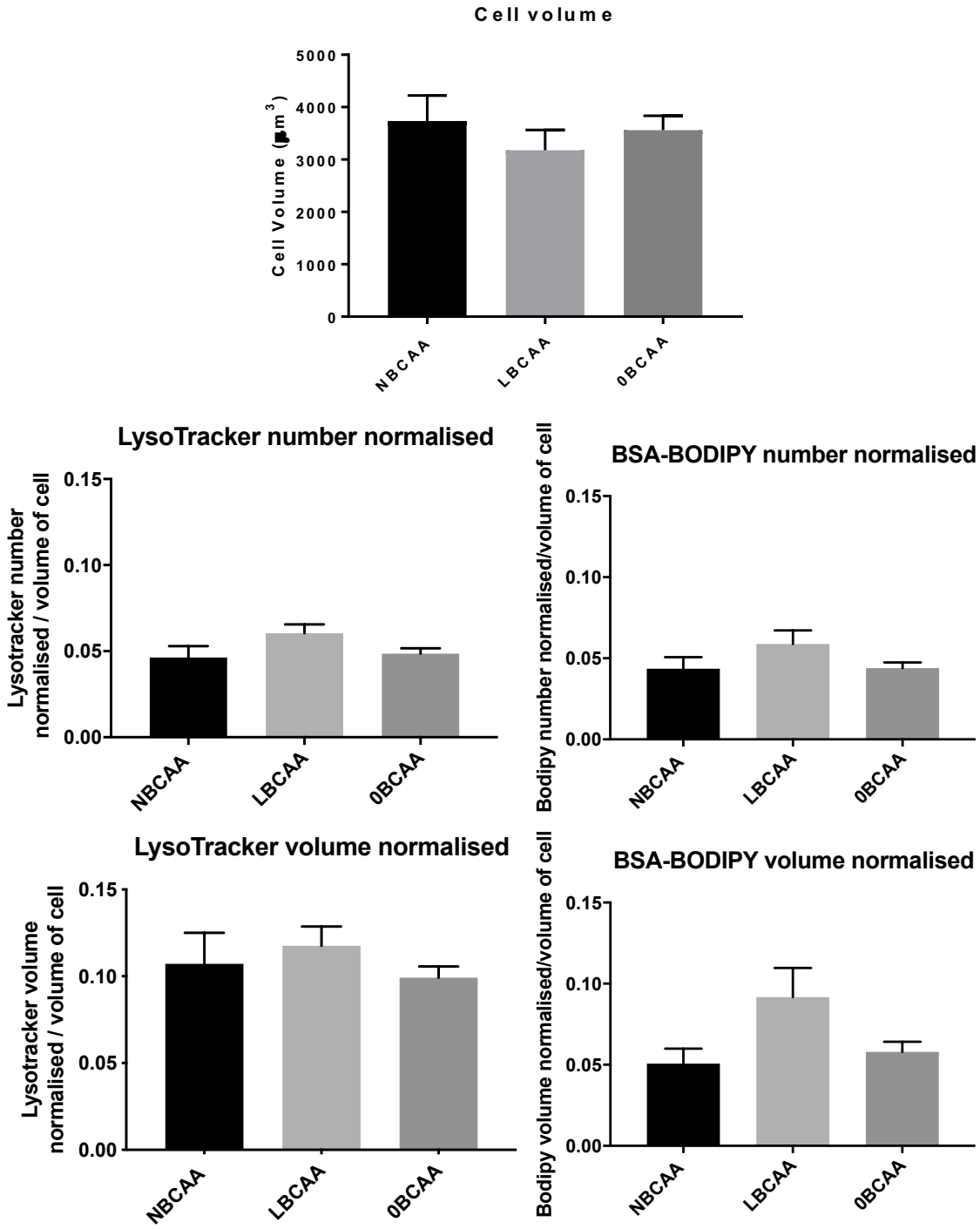

Figure 8.14 - LysoTracker number and volume and BSA-BODIPY number and volume normalised to cell volume. Cell volume is not changed between groups. Embryo culture with depleted (LBCAA) or absent BCAAs (0BCAA) did not affect embryo endocytosis to a statistically significant level. Values are presented as mean ±SEM. 18-22 embryos per group (37-58 cells per group) from 9 mothers (in 7 replicates).

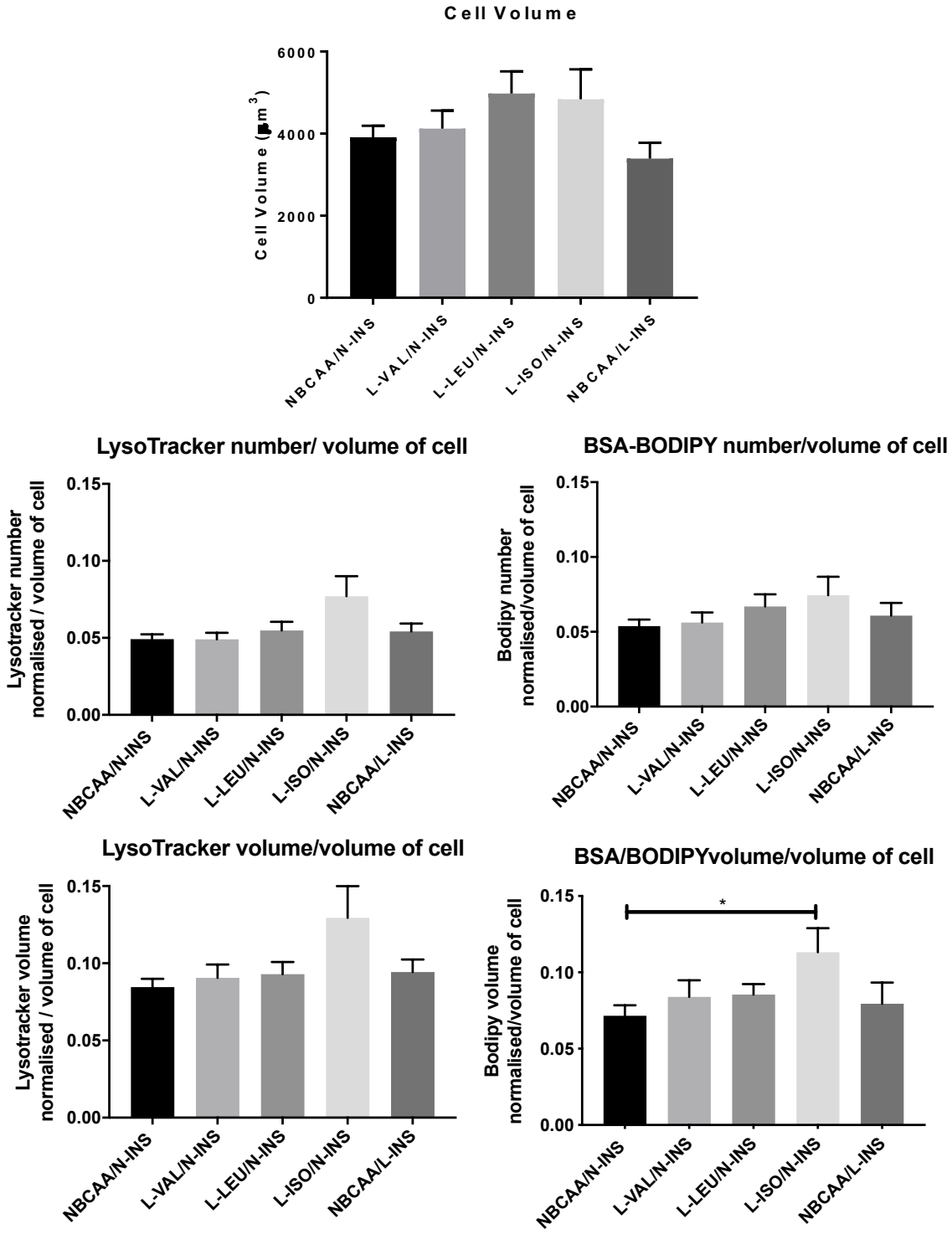

Figure 8.15 – LysoTracker number and volume and BSA-BODIPY number and volume normalised to cell volume. Cell volume is not changed between groups. Embryos cultured with Isoleucine depletion (L-ISO/N-INS) show increased BSA-BODIPY volume when data are normalised to volume of cell. In other graphs significance was lost after normalising data, even though the trend seen in the L-ISO/N-INS group is maintained. Values are mean ±SEM. *P <0.05; 17-24 embryos per group (30-55 cells per group) from 13 mothers (in 10 replicates).

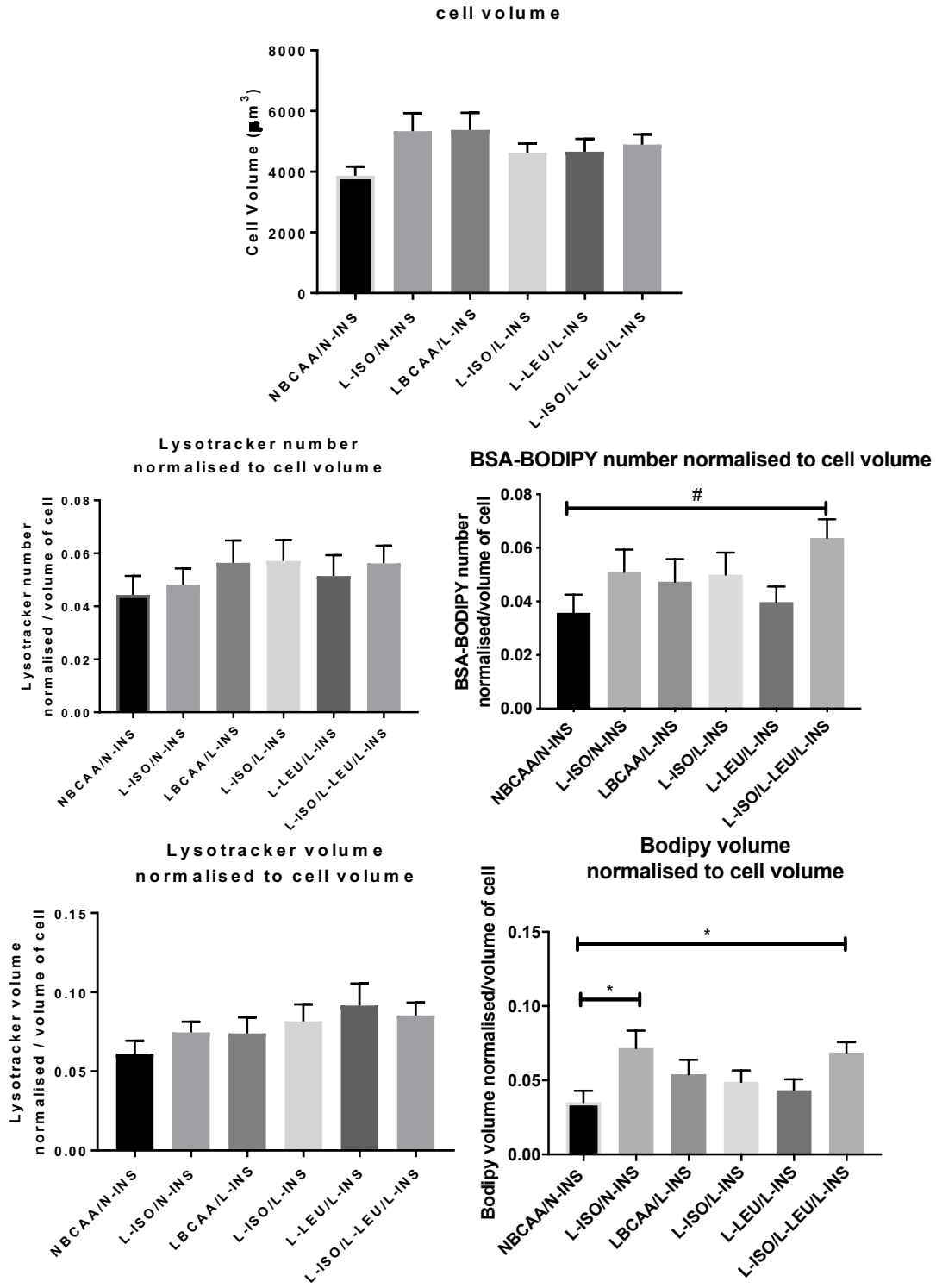

Figure 8.16 – LysoTracker number and volume and BSA-BODIPY number and volume normalised to cell volume. Cell volume is not changed between groups. Embryos cultured with Isoleucine depletion (L-ISO/N-INS) and a combination of low isoleucine, low leucine and low insulin (L-ISO/L-LEU/L-INS) show increased BSA-BODIPY volume when data is normalised per volume of cell. Values are presented as mean ±SEM. *P value <0.05; 13-19 embryos per group (23-38 cells per group) from 14 mothers (in 8 replicates).

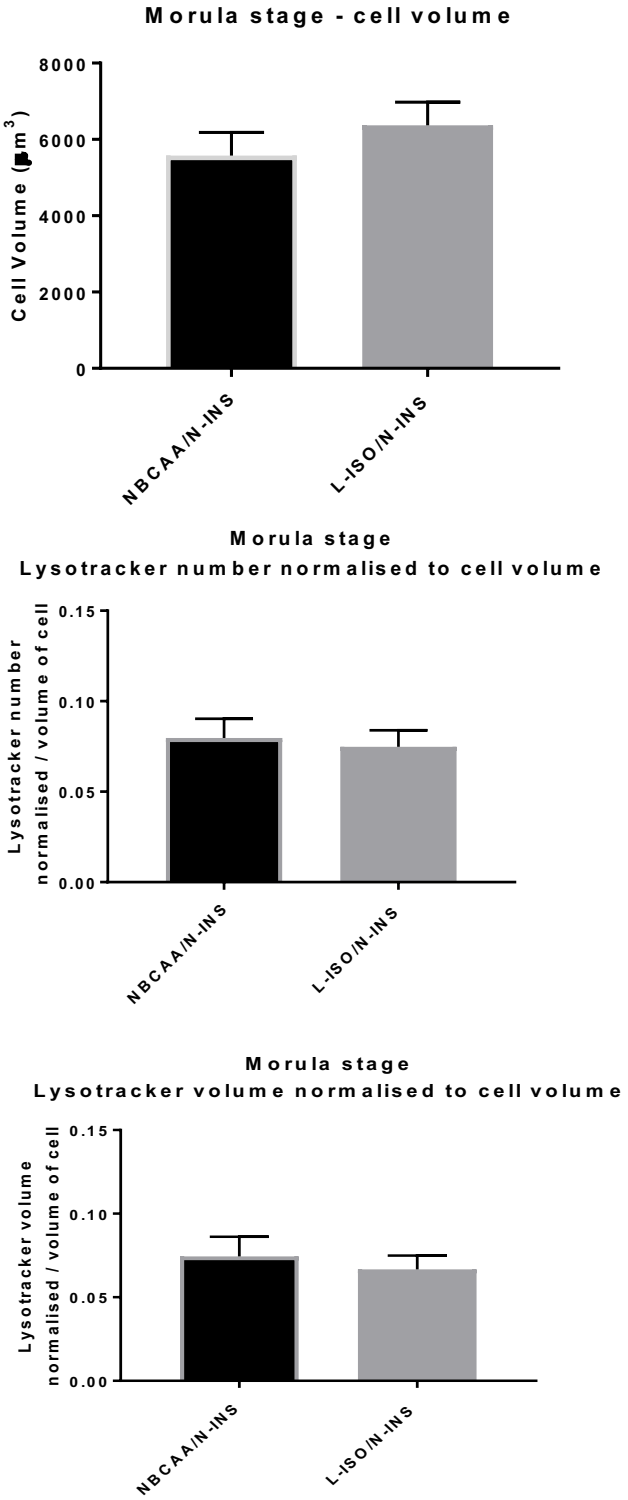

Figure 8.17 –Cell volume of morulae cultured in L-ISO/N-INS was not altered nor LysoTracker number and volume either with or without normalisation to cell volume. Values are presented as mean ±SEM. 17-18 embryos per group (24-26 cells per group) from 5 mothers (in 4 replicates).

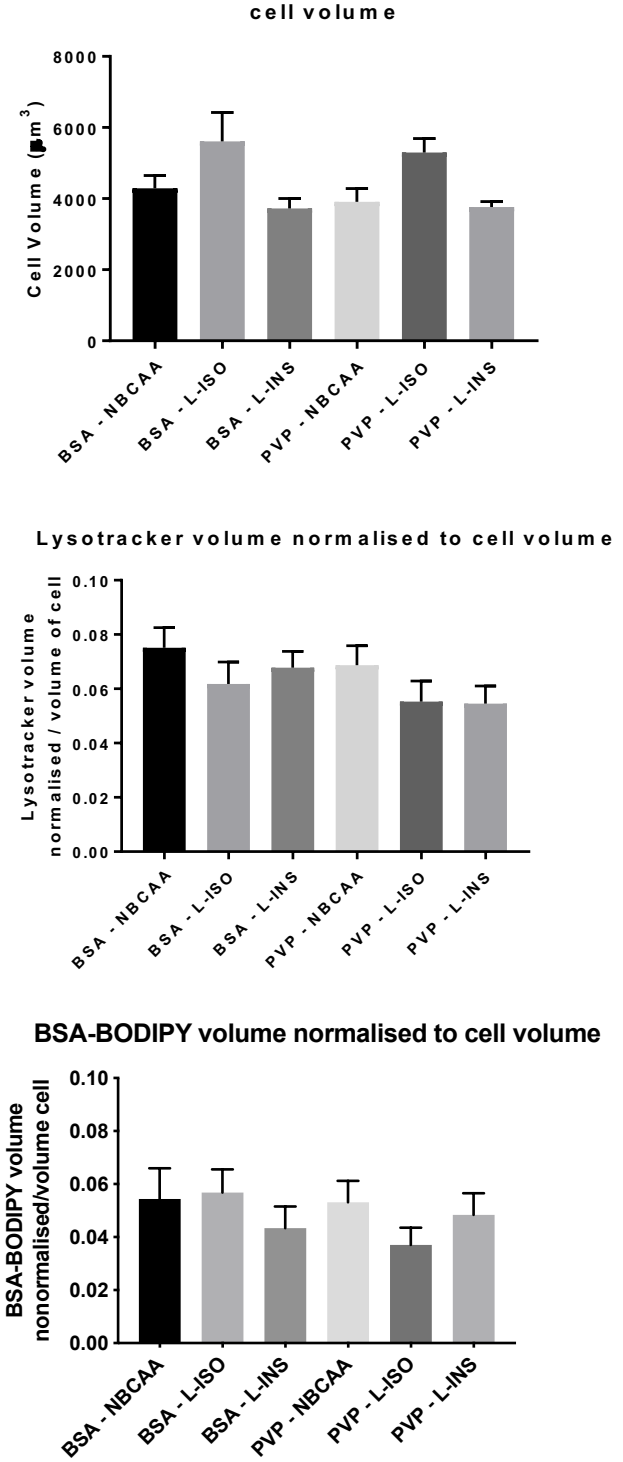

Figure 8.18 –LysoTracker volume and BODIPY volume normalised to cell volume. Cell volume is not significantly changed between groups. However, embryos flushed with BSA and cultured with L-ISO show a slight increase in cell volume which explains the loss of significance with normalisation from without normalisation (Figure 4.25). Values are presented as mean ±SEM. 14-19 embryos per group (23-38 cells per group) from 12 mothers (in 9 replicates).

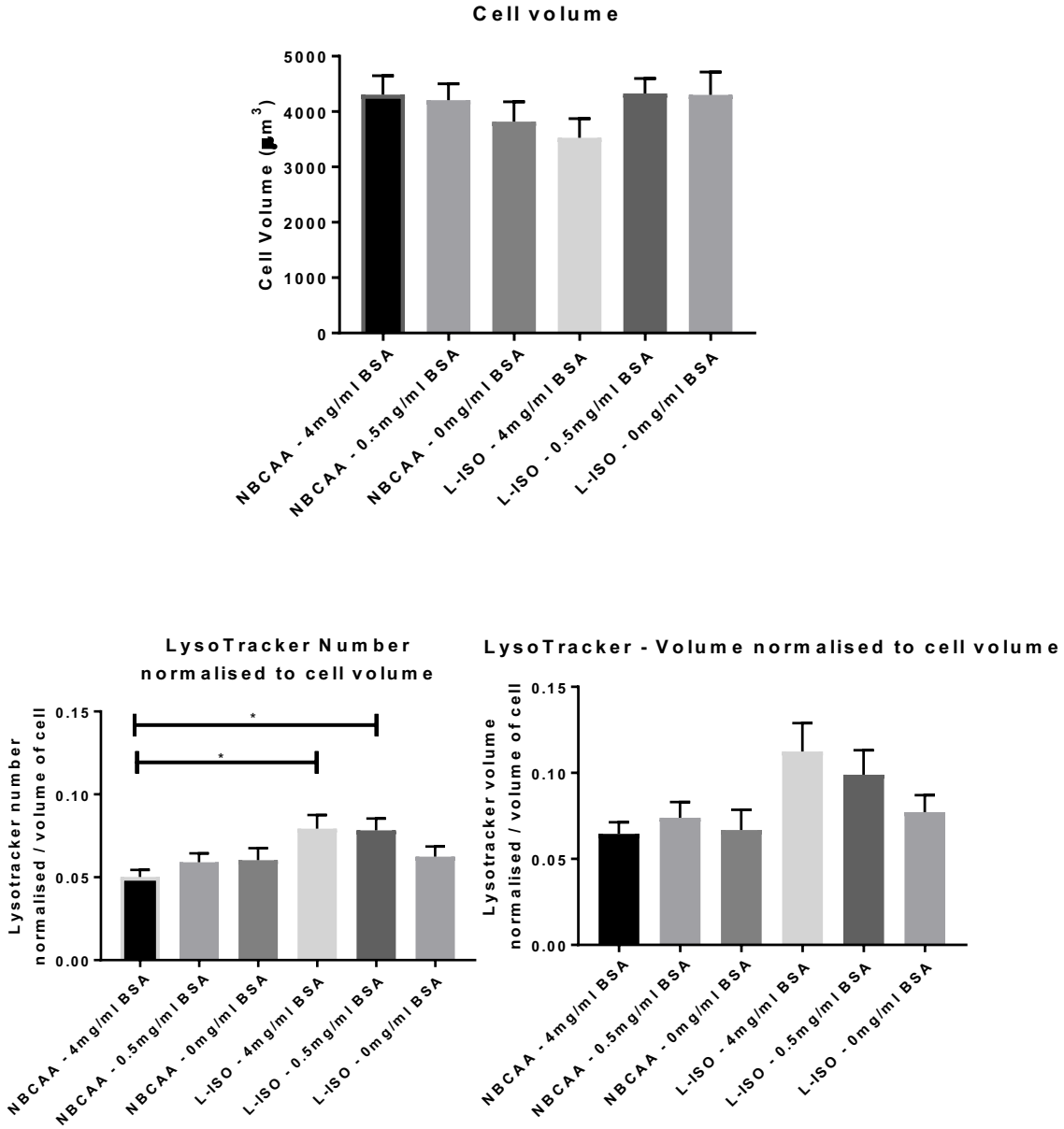

Figure 8.19 –LysoTracker number and volume normalised to cell volume. Cell volume is not significantly changed between groups. Data normalised to cell volume show the same changes in the L-ISO – 0.5 mg/ml BSA as previously seen without normalisation. Values are presented as mean ±SEM. *P value <0.05; 13-21 embryos per group (17-29 cells per group) from 13 mothers (in 6 replicates).

8.10 Cell volume and endocytosis correlation

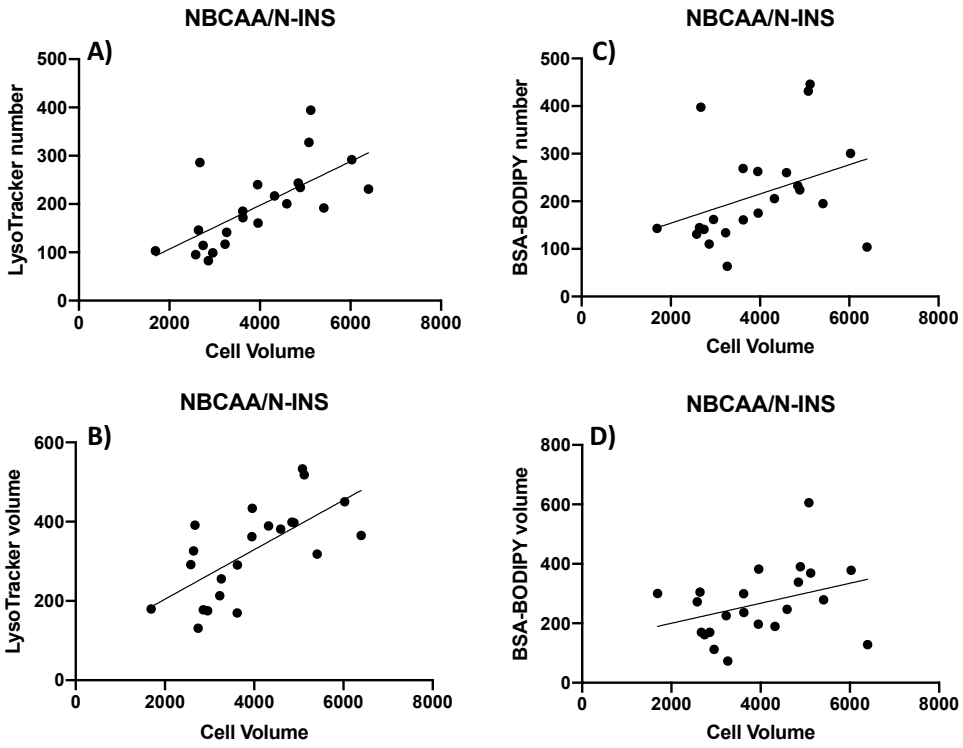

E)

Correlation	Cell Volume vs. BSA-BODIPY Number	Cell Volume vs. BSA-BODIPY volume	Cell Volume vs. LysoTracker number	Cell Volume vs. LysoTracker volume
	Y	Y	Y	Y
Pearson r				
r	0.3632	0.3504	0.6839	0.6724
95% confidence interval	-0.06897 to 0.6806	-0.08353 to 0.6727	0.3686 to 0.8581	0.3501 to 0.8524
R squared	0.1319	0.1228	0.4678	0.4522
P value				
P (two-tailed)	0.0966	0.1099	0.0004	0.0006
P value summary	ns	ns	***	***
Significant? (alpha = 0.05)	No	No	Yes	Yes
Number of XY Pairs	22	22	22	22

Figure 8.20 – Correlation between cell volume and lysoTracker number (A) and volume (B) and BSA-BODIPY number (C) and volume (D) in blastocysts that were cultured from 2-cell stage in NBCAA/N-INS medium. Table E shows the Pearson correlation values (R and R2) as well as P values for each graph.

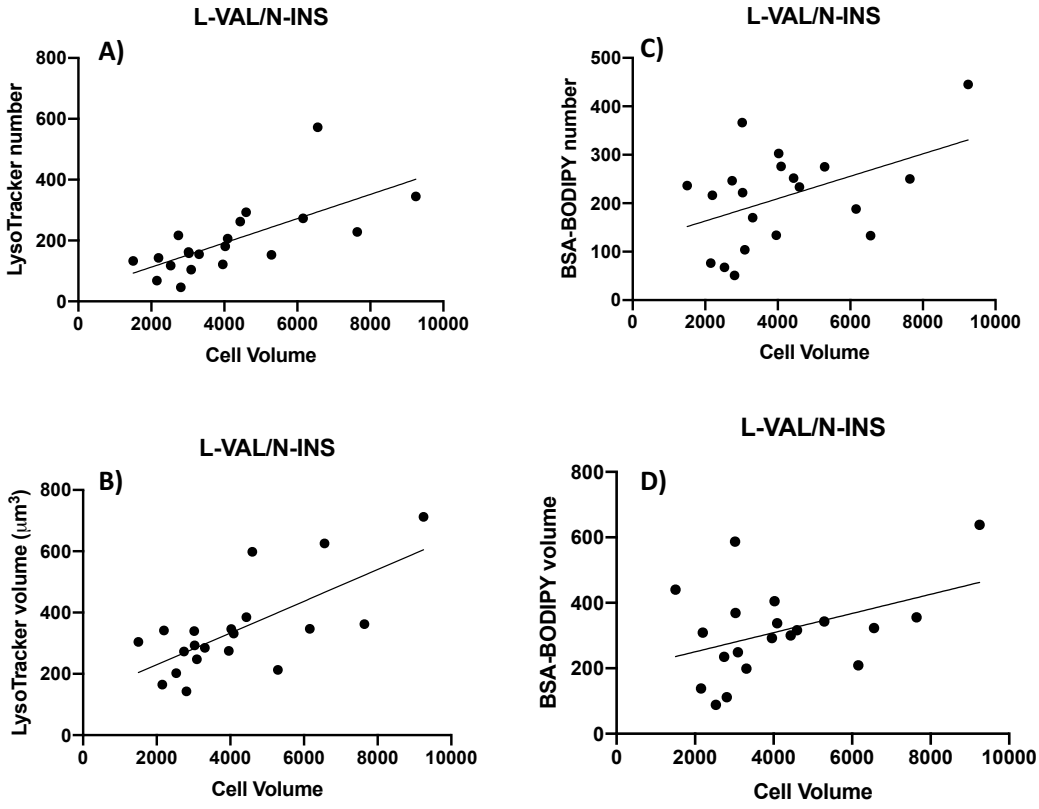

E)

Correlation	Cell Volume vs. BSA-BODIPY Number	Cell Volume vs. BSA-BODIPY volume	Cell Volume vs. LysoTracker number	Cell Volume vs. LysoTracker volume
	Y	Y	Y	Y
Pearson r				
r	0.4290	0.8193	0.5491	0.7386
95% confidence interval	-0.04729 to 0.7464	0.5707 to 0.9303	0.1105 to 0.8086	0.4147 to 0.8964
R squared	0.1841	0.6712	0.3015	0.5455
P value				
P (two-tailed)	0.0756	<0.0001	0.0183	0.0005
P value summary	ns	****	*	***
Significant? (alpha = 0.05)	No	Yes	Yes	Yes
Number of XY Pairs	18	18	18	18

Figure 8.21 – Correlation between cell volume and LysoTracker number (A) and volume (B) and BSA-BODIPY number (C) and volume (D) in blastocysts that were cultured from 2-cell stage in L-VAL/N-INS medium. Table E shows the Pearson correlation values (R and R2) as well as P values for each graph.

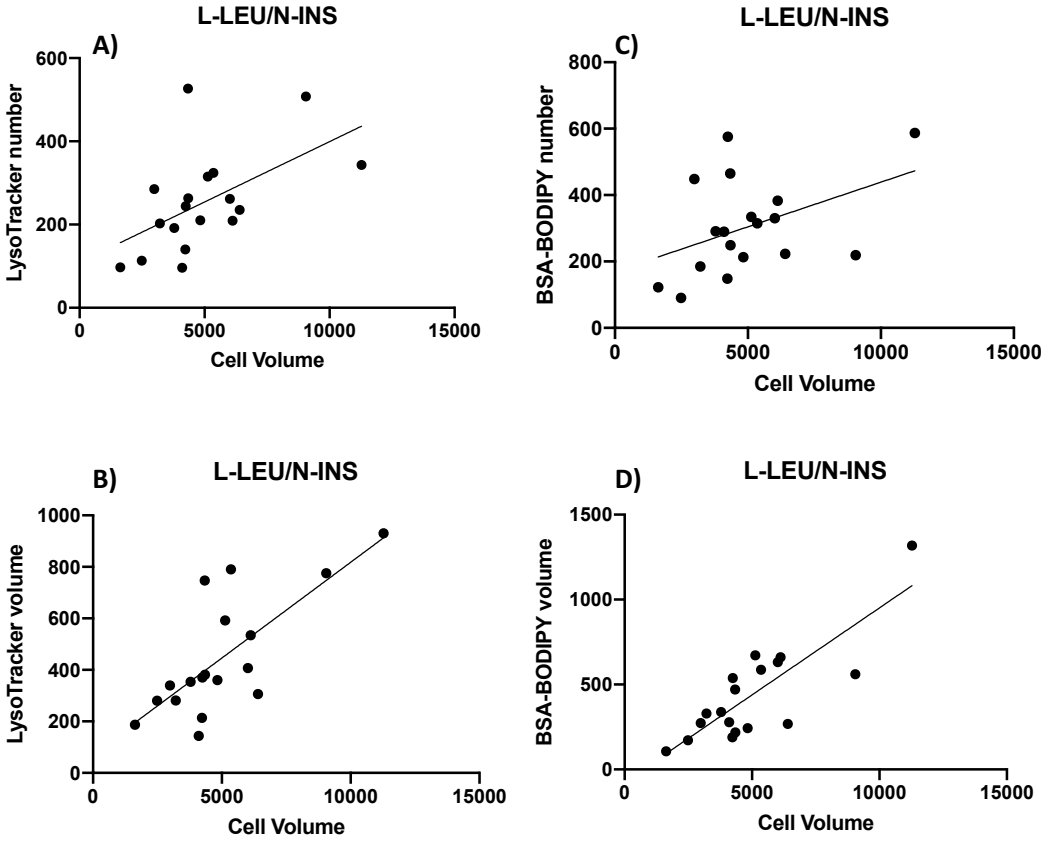

E)

Correlation	Cell Volume vs. BSA-BODIPY Number	Cell Volume vs. BSA-BODIPY volume	Cell Volume vs. LysoTracker number	Cell Volume vs. LysoTracker volume
	Y	Y	Y	Y
Pearson r				
r	0.4581	0.4185	0.6816	0.6943
95% confidence interval	0.01960 to 0.7488	-0.02950 to 0.7265	0.3423 to 0.8636	0.3634 to 0.8696
R squared	0.2099	0.1751	0.4645	0.4820
P value				
P (two-tailed)	0.0422	0.0663	0.0009	0.0007
P value summary	*	ns	***	***
Significant? (alpha = 0.05)	Yes	No	Yes	Yes
Number of XY Pairs	20	20	20	20

Figure 8.22 – Correlation between cell volume and lysoTracker number (A) and volume (B) and BSA-BODIPY number (C) and volume (D) in blastocysts that were cultured from 2-cell stage in L-LEU/N-INS medium. Table E shows the Pearson correlation values (R and R2) as well as P values for each graph.

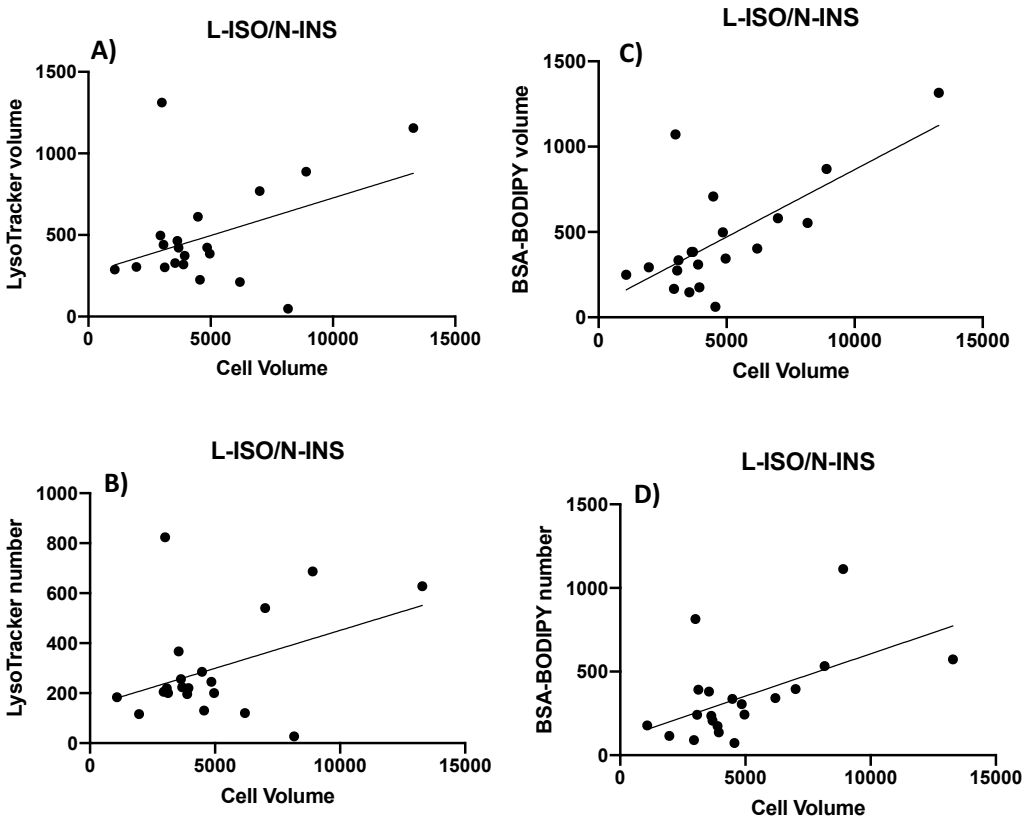

E)

Correlation	Cell Volume vs. BSA-BODIPY Number	Cell Volume vs. BSA-BODIPY volume	Cell Volume vs. LysoTracker number	Cell Volume vs. LysoTracker volume
	Y	Y	Y	Y
Pearson r				
r	0.5494	0.6849	0.4021	0.4037
95% confidence interval	0.1412 to 0.7979	0.3478 to 0.8652	-0.04917 to 0.7170	-0.04731 to 0.7179
R squared	0.3018	0.4691	0.1617	0.1629
P value				
P (two-tailed)	0.0121	0.0009	0.0788	0.0776
P value summary	*	***	ns	ns
Significant? (alpha = 0.05)	Yes	Yes	No	No
Number of XY Pairs	20	20	20	20

Figure 8.23 – Correlation between cell volume and lysoTracker number (A) and volume (B) and BSA-BODIPY number (C) and volume (D) in blastocysts that were cultured from 2-cell stage in NBCAA/N-INS medium. Table E shows the Pearson correlation values (R and R2) as well as P values for each graph.

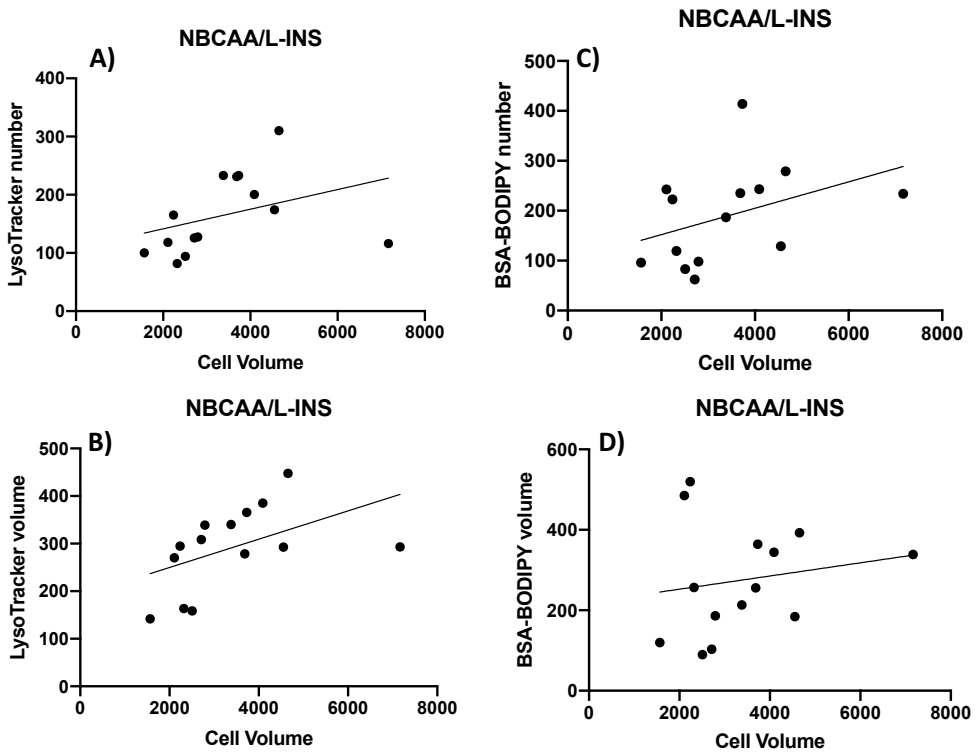

E)

Correlation	Cell Volume vs. BSA-BODIPY Number	Cell Volume vs. BSA-BODIPY volume	Cell Volume vs. LysoTracker number	Cell Volume vs. LysoTracker volume
	Y	Y	Y	Y
Pearson r				
r	0.3921	0.1725	0.3585	0.4862
95% confidence interval	-0.1749 to 0.7638	-0.3942 to 0.6441	-0.2125 to 0.7470	-0.05979 to 0.8083
R squared	0.1537	0.02975	0.1285	0.2364
P value				
P (two-tailed)	0.1656	0.5554	0.2082	0.0779
P value summary	ns	ns	ns	ns
Significant? (alpha = 0.05)	No	No	No	No
Number of XY Pairs	14	14	14	14

Figure 8.24 – Correlation between cell volume and lysoTracker number (A) and volume (B) and BSA-BODIPY number (C) and volume (D) in blastocysts that were cultured from 2-cell stage in NBCAA/L-INS medium. Table E shows the Pearson correlation values (R and R2) as well as P values for each graph.

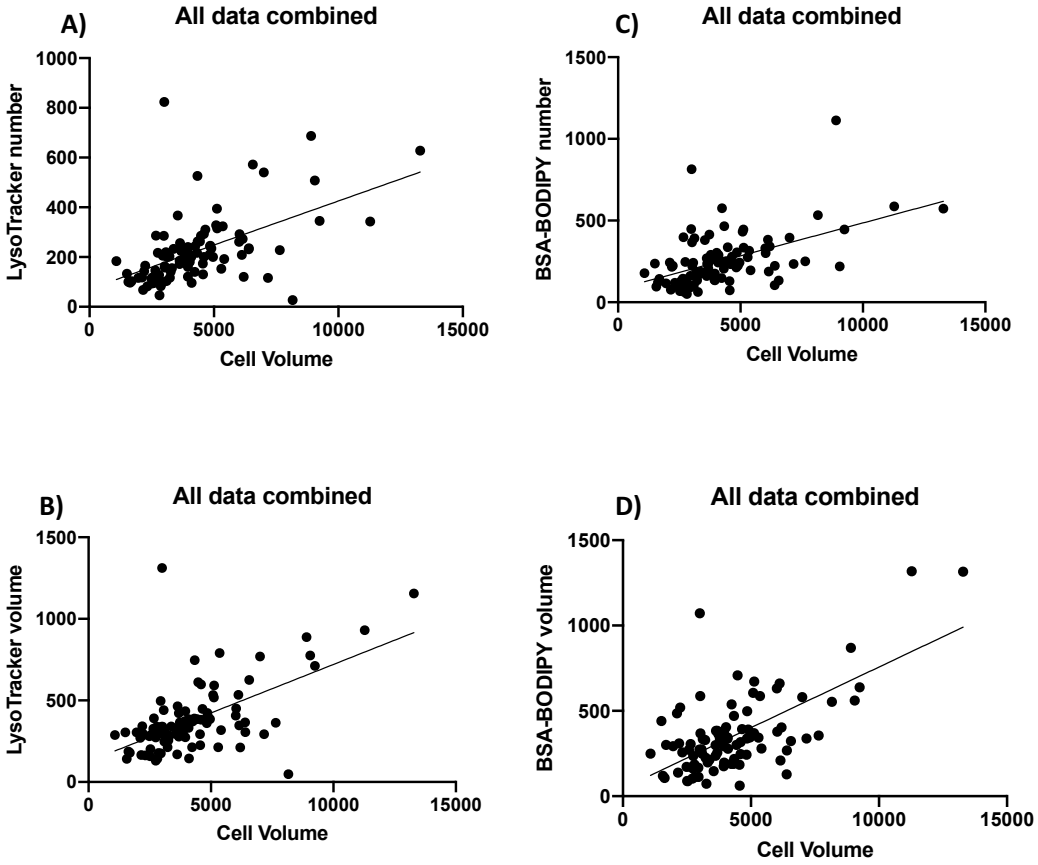

E)

Correlation	Cell Volume vs. BSA-BODIPY Number	Cell Volume vs. BSA-BODIPY volume	Cell Volume vs. LysoTracker number	Cell Volume vs. LysoTracker volume
	Y	Y	Y	Y
Pearson r				
r	0.5122	0.6430	0.5357	0.5840
95% confidence interval	0.3454 to 0.6476	0.5063 to 0.7481	0.3737 to 0.6661	0.4326 to 0.7034
R squared	0.2623	0.4134	0.2870	0.3411
P value				
P (two-tailed)	<0.0001	<0.0001	<0.0001	<0.0001
P value summary	****	****	****	****
Significant? (alpha = 0.05)	Yes	Yes	Yes	Yes
Number of XY Pairs	94	94	94	94

Figure 8.25 – Combination of all correlation data between cell volume and LysoTracker number (A) and volume (B) and BSA-BODIPY number (C) and volume (D) in blastocysts that were cultured from 2-cell stage in medium with different BCAA and insulin compositions (NBCAA/N-INS, L-VAL/N-INS; L-LEU/N-INS, L-ISO/N-INS and NBCAA/L-INS). Table E shows the Pearson correlation values (R and R2) as well as P values for each graph. All graphs show low significant p value <0.05) and relatively high R value (>0.5).

8.11 TFEB – VOLOCITY protocol

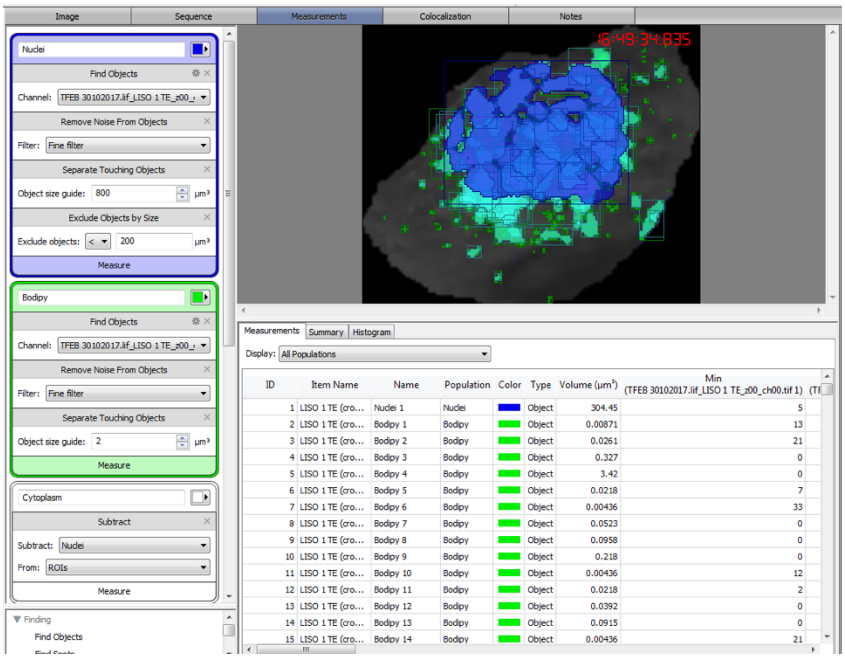

Figure 8.26 - After being cropped, one cell is displayed and the VOLOCITY protocol designed for TFEB was applied. On the left side of the figure there is a part of the set protocol with the definitions used to analyse the nucleus and TFEB. TFEB was measured in the in green channel (with remove noise and separate touching objects settings added) and cytoplasm by subtracting the nucleus from the ROIs (cell).

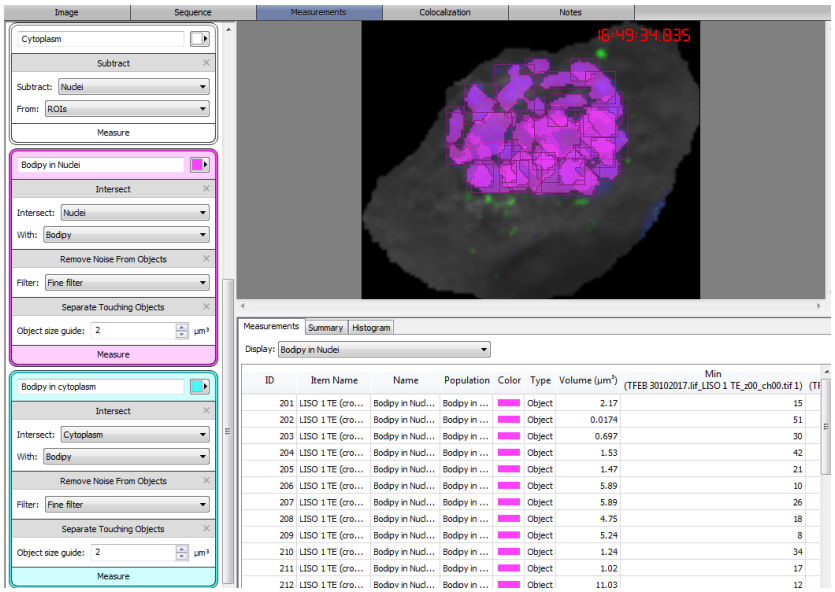

Figure 8.27 – TFEB in nucleus (pink) was designed by intersecting nucleus with TFEB and TFEB in cytoplasm (blue) by intersecting cytoplasm with TFEB.

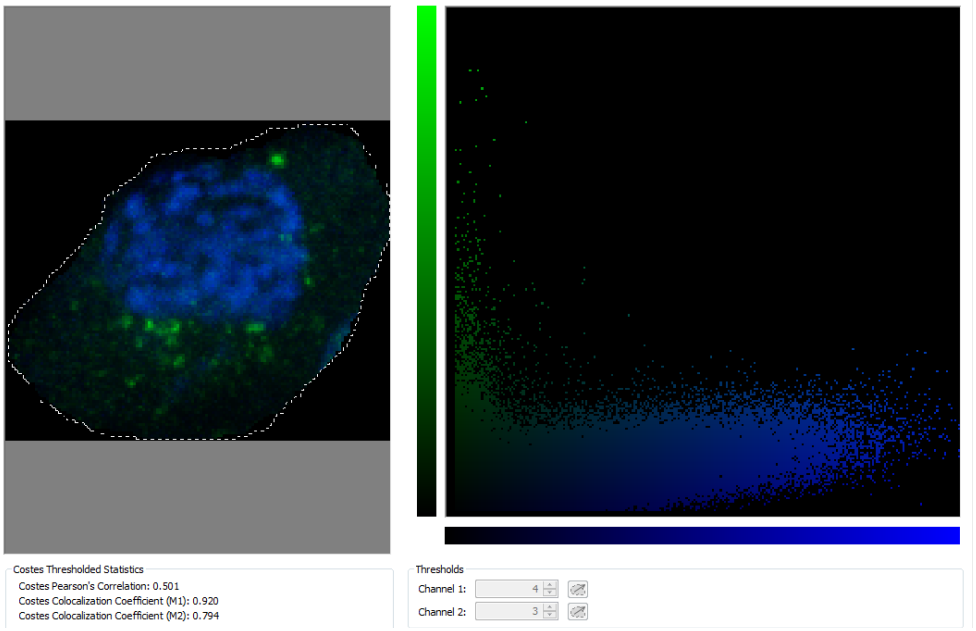

Figure 8.28 – TFEB (green channel) and nucleus (blue channel) colocalisation in one TE cell using VOLOCITY. Automatic Costes threshold was applied.

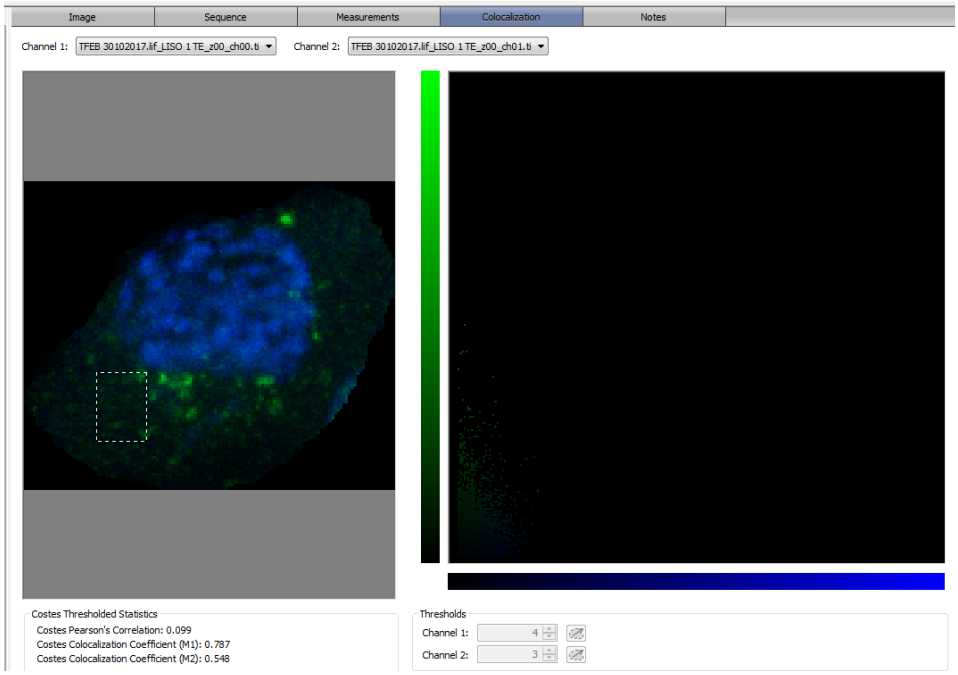

Figure 8.29 – Test for VOLOCITY colocalisation analysis specificity. TFEB (green channel) and nucleus (blue channel - DAPI) colocalisation in one area (square) of one TE cell in the cytoplasm using VOLOCITY. Automatic Costes threshold was applied. Low correlation (0.099) in the cytoplasm (no DAPI in cytoplasm).

8.12 Human embryos – Statistical analysis (SPSS syntax results)

A) **Type III Tests of Fixed Effects[a]**

Source	Numerator df	Denominator df	F	Sig.
Intercept	1	15.396	3.218	.093
HighBMI	1	6.779	10.595	.015
cellvolume	1	15.867	6.582	.021
CellNr	1	20.372	3.974	.060
Born	1	9.930	2.767	.127

B) **Type III Tests of Fixed Effects[a]**

Source	Numerator df	Denominator df	F	Sig.
Intercept	1	9.490	.085	.776
HighBMI	1	8.175	2.645	.142
cellvolume	1	8.174	.130	.727
CellNr	1	8.768	2.960	.120
Born	1	8.507	.066	.804

C) **Type III Tests of Fixed Effects[a]**

Source	Numerator df	Denominator df	F	Sig.
Intercept	1	7.430	5.196	.055
NoICSI	1	6.973	.152	.708
Treatment	1	6.990	5.397	.053
cellvolume	1	13.059	6.245	.027
CellNr	1	18.591	3.639	.072
Born	1	7.995	1.897	.206

D) **Type III Tests of Fixed Effects[a]**

Source	Numerator df	Denominator df	F	Sig.
Intercept	1	7.104	2.517	.156
NoICSI	1	7.041	.592	.467
Treatment	1	7.193	3.933	.087
cellvolume	1	8.161	.109	.749
CellNr	1	8.747	3.112	.113
Born	1	7.386	.337	.579

Figure 8.30 – SPSS syntax results: LysoTracker volume in High Vs normal BMI (A), TFEB and DAPI colocatisation in High Vs normal BMI (B), LysoTracker volume in ICSI vs conventional IVF (non-ICSI) (C) and TFEB and DAPI colocatisation in ICSI vs conventional IVF (non-ICSI) (D). Cofactors used in the High Vs. normal BMI analysis (A,B) were: cell volume, cell number (CellNr), resulted pregnancy from same cycle ("Born"). Cofactors used in the ICSI Vs conventional IVF analysis (C,D) were: treatment (BMI values); cell volume, cell number, resulted pregnancy from same cycle ("Born"). LysoTracker volume was significantly increased in the High BMI group (P value = 0.015) with cell volume surging as a significantly influencing cofactor contributing to the result (P value = 0.021) and cell number as an influencing cofactor contributing to the result at a trend level (P value = 0.060) (A). TFEB and DAPI colocalisation was not altered between High and normal BMI groups (B). LysoTracker volume was not changed between ICSI and conventional IVF groups with BMI, cell volume surging as a significantly influencing cofactor contributing to the result (P value = 0.027) and treatment (BMI) and cell number as influencing cofactors contributing to the result at a trend level (P values = 0.053 and 0.072respectively) (C). TFEB and DAPI colocalisation was not altered between ICSI and conventional IVF groups (D) but with treatment (BMI) surging as influencing cofactor influencing the result at a trend level (P values = 0.087).

8.13 Human embryos – ICSI vs conventional Non-ICSI

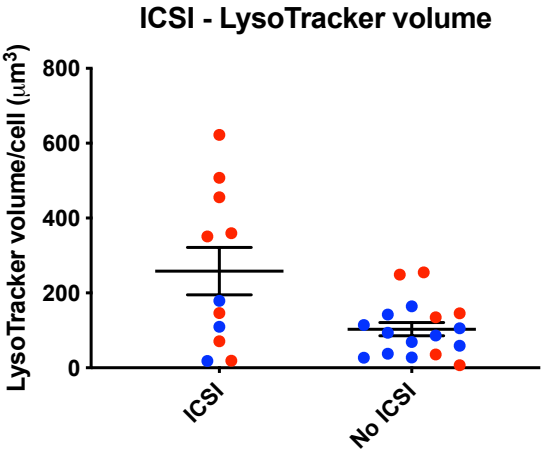

Figure 8.31 - Lysosomes collective volume per cell in blastocyst TE from ICSI and non-ICSI embryos. Red – High BMI embryos; Blue – Normal BMI embryos. Values are presented as mean±SEM. *P value <0.05 (statistical analysis using a multilevel linear regression model); 11-17 embryos per group from 7 mothers per group.

List of References

Adastra, K. L., Chi, M., Riley, J. K., and Moley, K. H. (2011). A differential autophagic response to hyperglycemia in the developing murine embryo. *Reproduction*, *141*(5), 1–16.

Aghayan, M., Rao, L. V, Smith, R. M., Jarett, L., Maureen, J., Thorens, B., and Heyner, S. (1992). Developmental expression and cellular localization of glucose transporter molecules during mouse preimplantation development. *Development*, 312, 305–312.

Aitken, R. J. (1977a). Changes in the protein content of mouse uterine flushings during normal pregnancy and delayed implantation, and after ovariectomy and oestradiol administration. J*ournal of Reproduction and Fertility*, 50(1), 29–36.

Aitken, R. J. (1977b). The protein content of mouse uterine flushings during pseudopregnancy. *J. Reprod. Fert*., 50, 9–11.

Aktories, K., Wilde, C., and Vogelsgesang, M. (2005). Rho-modifying C3-like ADP-ribosyltransferases. *In Reviews of Physiology, Biochemistry and Pharmacology* (pp. 1–22). Berlin, Heidelberg: Springer Berlin Heidelberg.

Alukal, J., and Lamb, D. (2008). Intracytoplasmic Sperm Injection (ICSI) – What are the risks? *Urol. Clin. North Am.*, 35(2), 277–288.

Ameri, K., and Harris, A. L. (2008). Activating transcription factor 4. *The International Journal of Biochemistry and Cell Biology*, 40(1), 14–21.

Appuhamy, J. A. D. R. N., Knoebel, N. A., Nayananjalie, W. A. D., Escobar, J., and Hanigan, M. D. (2012). Isoleucine and Leucine Independently Regulate mTOR Signaling and Protein Synthesis in MAC-T Cells and Bovine Mammary Tissue Slices 1 , 2. *The Journal of Nutrition*, 142(9), 484–491.

Arceci, R. J., King, a a, Simon, M. C., Orkin, S. H., and Wilson, D. B. (1993). Mouse GATA-4: a retinoic acid-inducible GATA-binding transcription factor expressed in endodermally derived tissues and heart. *Molecular and Cellular Biology*, 13(4), 2235–2246.

Arriola Apelo, S. I., Singer, L. M., Lin, X. Y., McGilliard, M. L., St-Pierre, N. R., and Hanigan, M. D. (2014). Isoleucine, leucine, methionine, and threonine effects on mammalian

target of rapamycin signaling in mammary tissue. *Journal of Dairy Science*, 97(2), 1047–1056.

Artus, J., Piliszek, A., and Hadjantonakis, A. K. (2011). The primitive endoderm lineage of the mouse blastocyst: Sequential transcription factor activation and regulation of differentiation by Sox17. *Developmental Biology*, 350(2), 393–404.

Assemat, E. (2005). Expression and Role of Cubilin in the Internalization of Nutrients During the Peri-Implantation Development of the Rodent Embryo. *Biology of Reproduction*, 72(5), 1079–1086.

Assémat, E., Vinot, S., Gofflot, F., Linsel-Nitschke, P., Illien, F., Châtelet, F., Verroust, P., Louvet-Vallée, S., Rinninger, F. and Kozyraki, R. (2005). Expression and Role of Cubilin in the Internalization of Nutrients During the Peri-Implantation Development of the Rodent Embryo. *Biology of Reproduction*, 72, 1079–1086.

Avilion, A. A., Nicolis, S. K., Pevny, L. H., Perez, L., Vivian, N., and Lovell-Badge, R. (2003). Multipotent cell lineages in early mouse development depend on SOX2 function. *Genes and Development*, 17(1), 126–140.

Baird, J., Fisher, D., Lucas, P., Kleijnen, J., Roberts, H., and Law, C. (2005). Being big or growing fast: systematic review of size and growth in infancy and later obesity. *British Medical Journal* 4–9.

Baltz, J. M., and Tartia, A. P. (2010). Cell volume regulation in oocytes and early embryos: connecting physiology to successful culture media. *Human Reproduction Update*, 16(2), 166–176.

Bansal, N., Ayoola, O. O., Gemmell, I., Vyas, A., Koudsi, A., Oldroyd, J., Clayton, P. E., Cruickshank, J. K. (1990). Effects of early growth on blood pressure of infants of British European and South Asian origin at one year of age : the Manchester children's growth and vascular health study. *Journal of Hypertension*, 26, 412-418

Barbacci, E., Reber, M., Ott, M. O., Breillat, C., Huetz, F., and Cereghini, S. (1999). Variant hepatocyte nuclear factor 1 is required for visceral endoderm specification. *Development*, 126(21), 4795–4805.

Barker, D., Eriksson, J., Forsen, T., and Osmond, C. (2002). Fetal origins of adult disease:

strength of effects and biological basis. *Int J Epidemiol*, 31, 1235–1239.

Barker, D. J. P. (2004). The developmental origins of well-being. Philosophical Transactions of the Royal Society of London. *Series B, Biological Sciences,* 359(1449), 1359–1366.

Barker, D. J. P., and Thornburg, K. L. (2013). The obstetric origins of health for a lifetime. *Clinical Obstetrics and Gynecology*, 56(3), 511–9.

Barker M., Dombrowski S. U., Colbourn T., Fall C. H. D., Kriznik N. M., Lawrence W. T., Norris S. A., Ngaiza G., Patel D., Skordis-Worrall J., Sniehotta, F. F., Steegers-Theunissen, R., Vogel, C., Wood-Townsend, K. and Stephenson, J. (2018) Intervention strategies to improve nutrition and health behaviours before conception. *Lancet,* 391, 1853–1864.

Barlev, N. A., Liu, L., Chehab, N. H., Mansfield, K., Harris, K. G., Halazonetis, T. D., and Berger, S. L. (2001). Acetylation of p53 activates transcription through recruitment of coactivators/histone acetyltransferases. *Molecular Cell*, 8(6), 1243–1254.

Basatemur, E., Gardiner, J., Williams, C., Melhuish, E., Barnes, J., and Sutcliffe, A. (2013). Maternal Prepregnancy BMI and Child Cognition: A Longitudinal Cohort Study. *Pediatrics*, 131(1), 56–63.

Bay, B., Lyngsø, J., Hohwu, L., and Kesmodel, U. S. (2019). Childhood growth of singletons conceived following IVF or ICSI: a systematic review and meta-analysis. *British Journal of Obstetrics and Gynaecology*, 126, 158–166.

Beddington, R. S. P., and Robertson, E. J. (1999). Axis development and early asymmetry in mammals. *Cell*, 96(2), 195–209.

Bedzhov, I., and Zernicka-Goetz, M. (2014). Self-organizing properties of mouse pluripotent cells initiate morphogenesis upon implantation. *Cell*, 156(5), 1032–1044.

Belva, F., Bonduelle, M., Roelants, M., Michielsen, D., Steirteghem, A. Van, Verheyen, G., and Tournaye, H. (2016). Semen quality of young adult ICSI offspring : the fi rst results. *Human Reproduction*, 31(12), 2811–2820.

Bergeland, T., Widerberg, J., Bakke, O., and Nordeng, T. W. (2001). Mitotic partitioning of endosomes and lysosomes. *Current Biology*, 11, 644–651.

Bertran, J., Testar, X., Zorzano, A., and Palacin, M. (1994). A new age for mammalian plasma membrane amino acid trasporters. *Cell Physiol Biochem*, 4, 217–241.

Bertrand, E., Van Den Bergh, M., and Englert, Y. (1995). Fertilization and early embryology: Does zona pellucida thickness influence the fertilization rate? *Human Reproduction*, 10(5), 1189–1193.

Besterman, J. M., and Low, R. B. (1983). Endocytosis: a review of mechanisms and plasma membrane dynamics. *The Biochemical Journal*, 210, 1–13.

Bielinska, M., Narita, N., and Wilson, D. B. (1999). Distinct roles for visceral endoderm during embryonic mouse development. *International Journal of Developmental Biology*, 43(3), 183–205.

Biggers, J. D., McGinnis, L. K., and Raffin, M. (2000). Amino acids and preimplantation development of the mouse in protein-free potassium simplex optimized medium. *Biology of Reproduction*, 63(1), 281–293.

Biggers, J. D., Summers, M. C., and McGinnis, L. K. (1997). Polyvinyl alcohol and amino acids as substitutes for bovine serum albumin in culture media for mouse preimplantation embryos. *Human Reproduction Update*, 3(2), 125–35.

Biggers, J. D., Whittingham, D. G., and Donahue, R. P. (1967). The Pattern of Energy Metabolism in the Oocyte and Zygote. *Proceedings of the National Academy of Sciences*, 58(2), 560–567.

Bischoff, M., Parfitt, D.-E., and Zernicka-Goetz, M. (2008). Formation of the embryonic-abembryonic axis of the mouse blastocyst: relationships between orientation of early cleavage divisions and pattern of symmetric/asymmetric divisions. *Development*, 135(5), 953–62.

Bloise, E., Feuer, S. K., and Rinaudo, P. F. (2014). Comparative intrauterine development and placental function of ART concepti: Implications for human reproductive medicine and animal breeding. *Human Reproduction Update*, 20(6), 822–839.

Borgel, J., Guibert, S., Li, Y., Chiba, H., Schübeler, D., Sasaki, H., Forné, T. and Weber, M. (2010). Targets and dynamics of promoter DNA methylation during early mouse development. *Nature Genetics*, 42(12), 1093–100.

Boucher, D. M., and Pedersen, R. a. (1996). Induction and differentiation of extra-embryonic mesoderm in the mouse. *Reproduction, Fertility, and Development*, 8(4), 765–77.

Braude, P., Bolton, V., and Moore, S. (1988). Human gene expression first occurs between the four- and eight-cell stages of preimplantation development. *Nature*, 332(31), 459-461.

Brenseke, B., Prater, M. R., Bahamonde, J., and Gutierrez, J. C. (2013). Current thoughts on maternal nutrition and fetal programming of the metabolic syndrome. *Journal of Pregnancy*, 2013, 1-13.

Brent, R. L., Beckman, D. A., Jensen, M., and Koszalka, T. R. (1990). Experimental yolk sac dysfunction as a model for studying nutritional disturbances in the embryo during early organogenesis. *Teratology*, 41(4), 405–13.

Brinster, R. L. (1965). Studies on the Development of Mouse Embyros i n Vitro. *Journal of Experimental Zoology*, 158, 59–68.

Brinster, R. L., and Thomson, J. L. (1966). Development of eight-cell mouse embryos in vitro. *Experimental Cell Research*, 42(2), 308–315.

Brison, D. R., Roberts, S. A., and Kimber, S. J. (2013). How should we assess the safety of IVF technologies? *Reproductive BioMedicine Online*.

Brown, J. J., and Whittingham, D. G. (1991). The roles of pyruvate, lactate and glucose during preimplantation development of embryos from F1 hybrid mice in vitro. *Development*, 112(1), 99–105.

Brown, K., Legros, S., Artus, J., Doss, M. X., Khanin, R., Hadjantonakis, A. K., and Foley, A. (2010). A comparative analysis of extra-embryonic endoderm cell lines. *PLoS ONE*, 5(8).

Burns, W. N., Gaudet, T. W., Martin, M. B., Leal, Y. R., Schoen, H., Eddy, C. A., and Schenken, R. S. (1999). Survival of cryopreservation and thawing with all blastomeres intact identifies multicell embryos with superior frozen embryo transfer outcome. *Fertility and Sterility*, 72(3), 527–532.

Burruel, V., Klooster, K., Barker, C. M., Pera, R. R., and Meyers, S. (2014). Abnormal early

cleavage events predict early embryo demise: sperm oxidative stress and early abnormal cleavage. *Scientific Reports*, 4, 6598.

Calarco, P. G., and Brown, E. H. (1969). An ultrastructural and cytological study of preimplantation development of the mouse. *The Journal of Experimental Zoology*, 171(3), 253–283.

Calarco, P. G., and Epstein, C. J. (1973). Cell surface changes during preimplantation development in the mouse. *Developmenta Biology*, 32(1), 208–213.

Cantone, I., and Fisher, A. G. (2013). Epigenetic programming and reprogramming during development. N*ature Sructural and Molecular Biology*, 20(3), 282–9.

Carrell, D. (2001). Articles Body mass index is inversely related to intra- follicular HCG concentrations , embryo quality and IVF outcome. *Reproductive BioMedicine Online*, 3(2), 109–111.

Castillo, C. M., Horne, G., Fitzgerald, C. T., Johnstone, E. D., Brison, D. R. and Roberts, S. A. (2019). The impact of IVF on birthweight from 1991 to 2015: a cross-sectional study. *Human Reproduction*, 34(5), 920-931.

Ceelen, M., Van Weissenbruch, M. M., Prein, J., Smit, J. J., Vermeiden, J. P. W., Spreeuwenberg, M., Van Leeuwen, F. E. and Delemarre-Van De Waal, H. A. (2009). Growth during infancy and early childhood in relation to blood pressure and body fat measures at age 8-18 years of IVF children and spontaneously conceived controls born to subfertile parents. *Human Reproduction*, 24(11), 2788–2795.

Chambers, I., Colby, D., Robertson, M., Nichols, J., Lee, S., Tweedie, S., and Smith, A. (2003). Functional expression cloning of Nanog, a pluripotency sustaining factor in embryonic stem cells. *Cell,* 113(5), 643–655.

Chatot, C. L., Lewis-Williams, J., Torres, I., and Ziomek, C. a. (1994). One-minute exposure of 4-cell mouse embryos to glucose overcomes morula block in CZB medium. *Molecular Reproduction and Development*, 37(4), 407–12.

Chatot, C. L., Ziomek, C. a, Bavister, B. D., Lewis, J. L., and Torres, I. (1989). An improved culture medium supports development of random-bred 1-cell mouse embryos in vitro. *Journal of Reproduction and Fertility*, 86(2), 679–688.

Chazaud, C., Yamanaka, Y., Pawson, T., and Rossant, J. (2006). Early Lineage Segregation between Epiblast and Primitive Endoderm in Mouse Blastocysts through the Grb2-MAPK Pathway. *Developmental Cell*, 10(5), 615–624.

Chen, W. S., Manova, K., Weinstein, D. C., Duncan, S. A., Plump, A. S., Prezioso, V. R., Bachvarova, R. F., and Darnell, J. E. (1994). Disruption of the HNF-4 gene, expressed in visceral endoderm, leads to cell death in embryonic ectoderm and impaired gastrulation of mouse embryos. *Genes and Development*, 8(20), 2466–2477.

Christensen, E. I., and Birn, H. (2002). Megalin and cubilin: multifunctional endocytic receptors. *Nature Reviews. Molecular Cell Biology*, 3(4), 256–66.

Collinet, C., Stöter, M., Bradshaw, C. R., Samusik, N., Rink, J. C., Kenski, D., Habermann, B., Buchholz, F., Henschel, R., Mueller, M., Nagel, W., Fava, E., Yannis, K., Zerial, M. (2010). Systems survey of endocytosis by multiparametric image analysis. *Nature*, 464(7286), 243–9.

Cooney, C. A., Dave, A. A., and Wolff, G. L. (2002). Maternal methyl supplements in mice affect epigenetic variation and DNA methylation of offspring. *Journal of Nutrition*, 132, 2393S–2400S.

Daniel, J. C., and Krishnan, R. S. (1969). Studies on the relationship between uterine fluid components and the diapausing state of blastocysts from mammals having delayed implantation. *Journal of Experimental Zoology*, 172(3), 267–281.

Dawson, K. M., and Baltz, J. M. (1997). Organic osmolytes and embryos: substrates of the Gly and beta transport systems protect mouse zygotes against the effects of raised osmolarity. *Biol. Reprod.*, 56(6), 1550–1558.

De Geyter, D. (2018) More than 8 million babies born from IVF since the world's first in 1978. Grimbergen, Belgium: *European Society of Human Reproduction and Embryology* (ESHRE).

Denisenko, O., Lucas, E. S., Sun, C., Watkins, A. J., Mar, D., Bomsztyk, K., and Fleming, T. P. (2016). Regulation of ribosomal RNA expression across the lifespan is fine-tuned by maternal diet before implantation. *Biochimica et Biophysica Acta*, 1–8.

Di Malta, C., Siciliano, D., Calcagni, A., Monfregola, J., Punzi, S., Pastore, N., Eastes, A.,

Davis, O., Cegli, R., Zampelli, A., Giovannantonio, L., Nusco, E., Platt, N., Ogmundsdottir, H., Lanfrancome,L., Perera, R. M., Zoncu, R., Pelicci, P. G., Settembre, C., Ballabio, A. (2017). Transcriptional activation of RAGD GTPase controls mTORC1 and promotes cancer growth. *Science*, 356(6343), 1188–1192.

DiZio, S. M., and Tasca, R. J. (1977). Sodium-Dependent Amino Acid Transport Embryos in Preimplantation Mouse. *Developmental Biology*, 205, 198–205.

Ducibella, T., and Anderson, E. (1975). Cell shape and membrane changes in the eight-cell mouse embryo: Prerequisites for morphogenesis of the blastocyst. *Developmental Biology*, 47(1), 45–58.

Duncan, S. A., Manova, K., Chen, W. S., Hoodless, P., Weinstein, D. C., Bachvarova, R. F., and Darnell Jr., J. E. (1994). Expression of transcription factor HNF-4 in the extraembryonic endoderm, gut, and nephrogenic tissue of the developing mouse embryo: HNF-4 is a marker for primary endoderm in the implanting blastocyst. *Proceedings of the National Academy of Sciences*, 91(16), 7598–7602.

Dunger, D. B., Salgin, B., and Ong, K. K. (2019). Symposium on " Nutrition in early life : new horizons in a new century " Session 7 : Early nutrition and later health Early developmental pathways of obesity and diabetes risk, (2007), 451–457.

Dunglison, G. F., Jane, S. D., Mccaul, T. F., Chad, J. E., Fleming, T. P., Kaye, P. L. (1995). Stimulation of endocytosis in mouse blastocysts by insulin: a quantitative morphological analysis. *Journal of Reproduction and Fertility*, 105(1), 115–23.

Dunglison, G. F., and Kaye, P. L. (1995). Endocytosis in mouse blastocysts: Characterization and quantification of the fluid phase component. *Molecular Reproduction and Development*, 41(2), 225–231.

Dunn, K. W., Kamocka, M. M., and McDonald, J. H. (2011). A practical guide to evaluating colocalization in biological microscopy. *American Journal of Physiology - Cell Physiology*, 300(4), C723–C742.

Ecker, D. J., Stein, P., Xu, Z., Williams, C. J., Kopf, G. S., Bilker, W. B., Schultz, R. M. (2004). Long-term effects of culture of preimplantation mouse embryos on behavior. *Proc Natl Acad Sci U S A,* 101(6), 1595–1600.

Eckert, J. J., and Fleming, T. P. (2008). Tight junction biogenesis during early development. *Biochimica et Biophysica Acta - Biomembranes,* 1778(3), 717–728.

Eckert, J. J., Porter, R., Watkins, A. J., Burt, E., Brooks, S., Leese, H. J., Humpherson, P. G., Cameron, I. T., Fleming, T. P. (2012). Metabolic Induction and Early Responses of Mouse Blastocyst Developmental Programming following Maternal Low Protein Diet Affecting Life-Long Health. *PLoS ONE*, 7 (12), 1-14.

Eckert, J. J., Velazquez, M. A., and Fleming, T. P. (2016). Maternal obesity and programming of the early embryo. In: Green L., Hester R. (eds) Parental Obesity: Intergenerational Programming and Consequences. *Physiology in Health and Disease*. Springer, New York, NY

Enders, A. C., and Schlafke, S. (1967). A morphological analysis of the early implantation stages in the rat. *American Journal of Anatomy*, 125, 1–29.

Epstein, C. J., and Smith, S. A. (1973). Amino acid uptake and protein synthesis in preimplanatation mouse embryos. *Developmental Biology*, 33(1), 171–84.

Epstein, J., and Edwards, F. (1975). Gene Expression and Macromolecular Synthesis During Preimplantation Embryonic Development. *Biology of Reproduction*, 105, 82–105.

Esposito, G. (1984). Intestinal Permeability of Water-Soluble Nonelectrolytes: Sugars, Amino Acids, Peptides. In T. Z. Csáky (Ed.), *Pharmacology of Intestinal Permeation* I (pp. 567–611). Berlin, Heidelberg: Springer Berlin Heidelberg.

Familari, M. (2006). Characteristics of the endoderm: embryonic and extraembryonic in mouse. *TheScientificWorldJournal*, 6, 1815–27.

Feigelson, M., and Kay, E. (1972). Protein Patterns of Rabbit Oviducal Fluid. *Biology of Reproduction*, 252, 244–252.

Feng, Z., and Levine, A. J. (2010). The Regulation of Energy Metabolism and the IGF-1/mTOR Pathways by the p53 Protein. *Trends in Cell Biology*, 20(7), 427–434.

Fernandez-Gonzalez, R., Moreira, P., Bilbao, A., Jime, A., Pe, M., Ramírez, M. A., De Fonseca, F. R., Pintado, B., and Gutie, A. (2004). Long-term effect of in vitro culture of mouse embryos with serum on mRNA expression of imprinting genes , development ,

and behavior. *Proceedings of the National Academy of Sciences*, 101(16), 5880-5885

Fissore, R. A., Jackson, K. V, and Kiessling, A. A. (1989). Mouse zygote development in culture medium without protein in the presence of ethylenediaminetetraacetic acid. *Biol Reprod*, 41(5), 835–841.

Flach, G., Johnson, M. H., Braude, P. R., Taylor, R. a, and Bolton, V. N. (1982). The transition from maternal to embryonic control in the 2-cell mouse embryo. *The EMBO Journal*, 1(6), 681–686.

Fleming, T. P. (1987). A quantitative analysis of cell allocation to trophectoderm and inner cell mass in the mouse blastocyst. *Developmental Biology*, 119(2), 520–531.

Fleming, T. P., Butler, L., Lei, X., and Collins, J. (1994). Molecular maturation of cell adhesion systems during mouse early development. *Histochemistry*, 101, 1–7.

Fleming, T. P., Garrod, D. R., and Elsmore, A. J. (1991). Desmosome biogenesis in the mouse preimplantation embryo. *Development*, 112(2), 527–539. Retrieved from

Fleming, T. P., and Goodall, H. (1986). Endocytic traffic in trophectoderm and polarised blastomeres of the mouse preimplantation embryo. *The Anatomical Record*, 216(4), 490–503.

Fleming, T. P., Lucas, E. S., Watkins, A. J., and Eckert, J. J. (2012). Adaptive responses of the embryo to maternal diet and consequences for post-implantation development. *Reproduction, Fertility and Development*, 24(1), 35–44.

Fleming, T. P., McConnel, J., Johnson, M. H., and Stevenson, B. R. (1989). Development of tight junctions de novo in the mouse early embryo: Control of assembly of the tight junction-specific protein, ZO-1. *Journal of Cell Biology*, 108(4), 1407–1418.

Fleming, T. P., and Pickering, S. J. (1985). Maturation and polarization of the endocytotic system in outside blastomeres during mouse preimplantation development. *Journal of Embryology and Experimental Morphology*, 89, 175–208.

Fleming, T. P., Velazquez, M. a., and Eckert, J. J. (2015). Embryos, DOHaD and David Barker. Journal of Developmental Origins of Health and Disease, 6(5), 377–383.

Fleming, T. P., Velazquez, M. A., Eckert, J. J., Lucas, E. S., and Watkins, A. J. (2012).

Nutrition of females during the peri-conceptional period and effects on foetal programming and health of offspring. *Animal Reproduction Science*, 130(3–4), 193–197.

Fleming, T. P., Watkins, A. J., Sun, C., Velazquez, M. A., Smyth, N. R., and Eckert, J. J. (2015). Do little embryos make big decisions? How maternal dietary protein restriction can permanently change an embryo's potential, affecting adult health. *Reproduction, Fertility and Development*, 27(4), 684–692.

Fleming, T. P., Watkins, A. J., Velazquez, M. A., Mathers, J. C., Prentice, A. M., Stephenson, J., Barker, M. E., Saffery, R., Yajnik, C. S., Eckert, J. J., Hanson, M. A., Forrester, T., Gluckman, P. D. and Godfrey, K. M. (2018). Origins of lifetime health around the time of conception: causes and consequences. *The Lancet*, 391(10132), 1842–1852.

Franke, K., Gaser, C., Rooij, S. R. De, Schwab, M., and Tessa, J. (2017). Premature brain aging in humans exposed to maternal nutrient restriction during early gestation. *NeuroImage,* 173, 460–471.

Friedrich, B., Matskevich, I., and Lang, F. (2006). Cell volume regulatory mechanisms. Contributions to Nephrology, 152, 1–8.

Fujikura, J., and Yamato, E. (2002). Differentiation of embryonic stem cells is induced by GATA factors. *Genes and Development*, 784–789.

Fujimori, T., Kurotaki, Y., Miyazaki, J.-I., and Nabeshima, Y.-I. (2003). Analysis of cell lineage in two- and four-cell mouse embryos. *Development*, 130(21), 5113–22.

Galvez, T., Teruel, M. N., Heo, W. Do, Jones, J. T., Kim, M. L., Liou, J., Myers, J. W. and Meyer, T. (2007). siRNA screen of the human signaling proteome identifies the PtdIns(3,4,5)P3-mTOR signaling pathway as a primary regulator of transferrin uptake. *Genome Biology*, 8(7), R142.

Ganguly, A., McKnight, R. a, Raychaudhuri, S., Shin, B.-C., Ma, Z., Moley, K., and Devaskar, S. U. (2007). Glucose transporter isoform-3 mutations cause early pregnancy loss and fetal growth restriction. American Journal of Physiology. *Endocrinology and Metabolism*, 292(5), E1241-55.

Gardner, D. K., and Balaban, B. (2016). Assessment of human embryo development

using morphological criteria in an era of time-lapse , algorithms and " OMICS " : is looking good still important ? *Molecular and Human Reproduction*, 22(10), 704–718.

Gardner, D. K., and Lane, M. (1993). Amino acids and ammonium regulate mouse embryo development in culture. *Biology of Reproduction*, 48(2), 377–385.

Gardner, D. K., Phil, D., Lane, M., Ph, D., Stevens, J., and Schoolcraft, W. B. (2001). Noninvasive assessment of human embryo nutrient consumption as a measure of developmental potential. *Fertility and Sterility*, 76(6), 1175–1180.

Gardner, H. G., and Kaye, P. L. (1991). Insulin increases cell numbers and morphological development in mouse pre-implantation embryos in vitro. *Reproduction, Fertility, and Development*, 3(1), 79–91.

Gardner, R. L. (1982). Investigation of cell lineage and differentiation in the extraembryonic endoderm of the mouse embryo. *Journal of Embryology and Experimental Morphology*, 68, 175–198.

Gardner, R. L. (2001). Specification of embryonic axes begins before cleavage in normal mouse development. *Development,* 128(6), 839–47.

Gardner, R. L., and Rossant, J. (1979). Investigation of the fate of 4-5 day post-coitum mouse inner cell mass cells by blastocyst injection. *Journal of Embryology and Experimental Morphology*, 52, 141–152.

Garner, W., and McLaren, A. (1974). Cell distribution in chimaeric mouse embryos before implantation. *Journal of Embryology and Experimental Morphology*, 32(2), 495–503.

Garred, Ø., Rodal, S. K., van Deurs, B., and Sandvig, K. (2001). Reconstitution of clathrin-independent endocytosis at the apical domain of permeabilized MDCK II cells: requirement for a Rho-family GTPase. *Traffic,* 2(1), 26–36.

Gonzalez, I. M., Martin, P. M., Burdsal, C., Sloan, J. L., Mager, S., Harris, T., and Sutherland, A. E. (2012). Leucine and arginine regulate trophoblast motility through mTOR-dependent and independent pathways in the preimplantation mouse embryo. *Developmental Biology*, 361(2), 286–300.

Gonzalez, M. B., Lane, M., Knight, E. J. and Robker, R. L. (2018) Inflammatory markers in human follicular fluid correlate with lipid levels and body mass index. *Journal of Reproductive Immunology*, 130, 25–29.

Gould, J. M., Smith, P. J., Airey, C. J., Mort, E. J., Airey, L. E., Warricker, F. D. M., Pearson-farr, J. E., Weston, E. C., Gould, P. J. W., Semmence, O. G., Restall, K. L., Watts, J. A., Mchugh, P. C., Smith, S. J., Dewing, J. M., and Fleming, T. P. (2018). Mouse maternal protein restriction during preimplantation alone permanently alters brain neuron proportion and adult short-term memory. *PNAS,* 115(31).

Grabarek, J. B., Zyzyńska, K., Saiz, N., Piliszek, A., Frankenberg, S., Nichols, J., Hadjantonakis, A. K. and Plusa, B. (2012). Differential plasticity of epiblast and primitive endoderm precursors within the ICM of the early mouse embryo. *Development,* 139(1), 129–39.

Grindler, N. M., and Moley, K. H. (2013). Maternal obesity, infertility and mitochondrial dysfunction: Potential mechanisms emerging from mouse model systems. Molecular *Human Reproduction*, 19(8), 487–494.

Gueth-Hallonet, C., Santa-Maria, A., Verroust, P., and Maro, B. (1994). Gp330 is specifically expressed in outer cells during epithelial differentiation in the preimplantation mouse embryo. *Development*, 120(11), 3289–3299.

Guo, G., Huss, M., Tong, G. Q., Wang, C., Li Sun, L., Clarke, N. D., and Robson, P. (2010). Resolution of Cell Fate Decisions Revealed by Single-Cell Gene Expression Analysis from Zygote to Blastocyst. *Developmental Cell,* 18(4), 675–685.

Guo, X.Y., Liu, X.M., Jin, L., Wang, T.T., Ullah, K., Sheng, J.Z., Huang, H.F. Cardiovascular and metabolic profiles of offspring conceived by assisted re- productive technologies: a systematic review and meta-analysis, *Fertil. Steril*. 107 (2017) 622–631.

Gwinn, D. M., Shackelford, D. B., Egan, D. F., Mihaylova, M. M., Mery, A., Vasquez, D. S., Turk, B. E. and Shaw, R. J. (2008). AMPK Phosphorylation of Raptor Mediates a Metabolic Checkpoint. *Molecular Cell*, 30(2), 214–226.

Handyside, a H. (1978). Time of commitment of inside cells isolated from preimplantation mouse embryos. *Journal of Embryology and Experimental Morphology*,

45, 37–53.

Hanley, B., Dijane, J., Fewtrell, M., Grynberg, A., Hummel, S., Junien, C., Koletzko, B., Lewis, S., Renz, H., Symonds, M., Gros, M., Harthoorn, L., Mace, L., Samuels, F. and van Der Beek, E. (2010). A review of metabolic programming, imprinting and epigenetics. *British Journal of Nutrition*, 104(Suppl 1), S1-25.

Hansen, K. R., Knowlton, N. S., Thyer, A. C., Charleston, J. S., Soules, M. R., and Klein, N. a. (2008). A new model of reproductive aging: The decline in ovarian non-growing follicle number from birth to menopause. *Human Reproduction*, 23(3), 699–708.

Hanson, M. a, and Gluckman, P. D. (2008). Developmental origins of health and disease: new insights. *Basic and Clinical Pharmacology and Toxicology*, 102(2), 90–93.

Hara, K., Maruki, Y., Long, X., Yoshino, K. ichi, Oshiro, N., Hidayat, S., Tokunaga, C., Avruch, J. and Yonezawa, K. (2002). Raptor, a binding partner of target of rapamycin (TOR), mediates TOR action. *Cell*, 110(2), 177–189.

Hardy, K., Hooper, M. A. K., Handyside, A. H., Rutherford, A. J., Winston, R. M. L., and Leese, H. J. (1989). Non-invasive measurement of glucose and pyruvate uptake by individual human oocytes and preimplantation embryos. *Human Reproduction* , 4(2), 188–191.

Harris, S. E., Gopichandran, N., Picton, H. M., Leese, H. J., and Orsi, N. M. (2005). Nutrient concentrations in murine follicular fluid and the female reproductive tract. *Theriogenology*, 64(4), 992–1006.

Hart, R., and Norman, R. J. (2013a). The longer-term health outcomes for children born as a result of ivf treatment: Part I - general health outcomes. *Human Reproduction Update,* 19(3), 232–243.

Hart, R., and Norman, R. J. (2013b). The longer-term health outcomes for children born as a result of ivf treatment. Part II - mental health and development outcomes. *Human Reproduction Update,* 19(3), 244–250.

Hartshorne, G. M., Wick, K., Elder, K., and Dyson, H. (1990). Effect of cell number at freezing upon survival and viability of cleaving embryos generated from stimulated IVF cycles. *Human Reproduction* (Oxford, England), 5(7), 857–61.

Hastings, R. A. 2nd, Enders, A. C., and Schlafke, S. (1972). Permeability of the zona pellucida to protein tracers. *Biology of Reproduction*, 7(2), 288–296.

Hastings 2nd, R. A., and Enders, A. C. (1974). Uptake of exogenous protein by the preimplantation rabbit. *The Anatomical Record*, 179, 311–330.

He, C., and Klionsky, D. J. (2009). Regulation Mechanisms and Signalling Pathways of Autophagy. *Annual Review of Genetics*, 43(68), 67.

Heuser, J. (1989). Changes in lysosome shape and distribution correlated with changes in cytoplasmic pH. *Journal of Cell Biology*, 108(3), 855–864.

Hillman, N., Sherman, M. I., and Graham, C. (1972). The effect of spatial arrangement on cell determination during mouse development. *Journal of Embryology and Experimental Morphology*, 28(2), 263–78.

Hogan, A., Heyner, S., Charron, M. J., Copeland, N. G., Gilbert, D. J., Jenkins, N. A., Thorens, B. and Schultz, G. A. (1991). Glucose transporter gene expression in early mouse embryos. *Development*, 113(1), 363–372.

Hogan, B., and Tilly, R. (1978). In vitro development of inner cell masses isolated immunosurgically from mouse blastocysts. II. Inner cell masses from 3.5- to 4.0-day p.c. blastocysts. *Journal of Embryology and Experimental Morphology*, 45, 107–121.

Holland, M. L., Lowe, R., Caton, P. W., Carbajosa, G., Danson, A. F., Carpenter, A. A., Loche, E., Ozanne, S. E. and Rakyan, V. K. (2016). Early-life nutrition modulates the epigenetic state of specific rDNA genetic variants in mice. *Science.* 353, 495–98.

Hou, Y. J., Zhu, C. C., Duan, X., Liu, H. L., Wang, Q. and Sun, S. C. (2016) Both diet and gene mutation induced obesity affect oocyte quality in mice. *Scientific Reports,* 6(18858)

Hundal, H. S., and Taylor, P. M. (2009). Amino acid transceptors: gate keepers of nutrient exchange and regulators of nutrient signaling. *American Journal of Physiology. Endocrinology and Metabolism*, 296(4), E603-613.

Hyafil, F., Morello, D., Babinet, C., and Jacob, F. (1980). A cell surface glycoprotein involved in the compaction of embryonal carcinoma cells and cleavage stage embryos. *Cell*, 21(3), 927–934.

Hyrapetian, M., Loucaides, E. M., and Sutcliffe, A. G. (2014). Health and disease in children born after assistive reproductive therapies (ART). *Journal of Reproductive Immunology*, 106, 21–26.

Igosheva, N., Abramov, A. Y., Poston, L., Eckert, J. J., Fleming, T. P., Duchen, M. R., McConnell, J. (2010) Maternal diet- induced obesity alters mitochondrial activity and redox status in mouse oocytes and zygotes. *PLoS One*, 5(4):e10074.

Ivanov, A. I. (2008). Pharmacological Inhibition of Endocytic Pathways: Is It Specific Enough to Be Useful? In A. I. Ivanov (Ed.), *Exocytosis and Endocytosis* (pp. 15–33). Totowa, NJ: Humana Press.

Jacinto, E., Loewith, R., Schmidt, A., Lin, S., Rüegg, M. A., Hall, A., and Hall, M. N. (2004). Mammalian TOR complex 2 controls the actin cytoskeleton and is rapamycin insensitive. Nature Cell Biology, 6(11), 1122–1128.

Jahreiss, L., Menzies, F. M., and Rubinsztein, D. C. (2008). The itinerary of autophagosomes: From peripheral formation to kiss-and-run fusion with lysosomes. *Traffic*, 9(4), 574–587.

Jauniaux, E., Gulbis, B., and Burton, G. J. (2003). The human first trimester gestational sac limits rather than facilitates oxygen transfer to the foetus - A review. *Placenta,* 24(SUPPL. A), 86–93.

Johnson, M. H., and Ziomek, C. A. (1981). The foundation of two distinct cell lineages within the mouse morula. *Cell*, 24(1), 71–80.

Jollie, W. P. (1990). Development, morphology, and function of the yolk-sac placenta of laboratory rodents. *Teratology*, 41(4), 361–381.

Jones, C., Ott, E., Keener, J., Curtiss, M., Sandrin, V., and Babst, M. (2012). Regulation of membrane protein degradation by starvation- response pathways. *Traffic*, 13(3), 468–482.

Jones, H. N., Woollett, L. A., Barbour, N., Prasad, P. D., Powell, T. L., and Jansson, T. (2009). High-fat diet before and during pregnancy causes marked up-regulation of placental nutrient transport and fetal overgrowth in C57 / BL6 mice. *FASEB Journal*, 23, 271–278.

Juetten, J., and Bavister, B. D. (1983). The effects of amino acids, cumulus cells, and bovine serum albumin on in vitro fertilization and first cleavage of hamster eggs. *J Exp Zoo.l*, 227(3), 487–490.

Jungheim, E. S., Schoeller, E. L., Marquard, K. L., Louden, E. D., Schaffer, J. E., Moley, K. H. (2010) Diet-induced obesity model: abnormal oocytes and persistent growth abnormalities in the offspring. *Endocrinology*, 151(8):4039–46.

Karnowski, K., Ajduk, A., Wieloch, B., Tamborski, S., Krawiec, K., Wojtkowski, M. and Szkulmowski, M. (2017). Optical coherence microscopy as a novel, non-invasive method for the 4D live imaging of early mammalian embryos. *Scientific Reports*, 7, 4165.

Katz-jaffe, M. G., Ph, D., Gardner, D. K., Ph, D., and Schoolcraft, W. B. (2006). Proteomic analysis of individual human embryos to identify novel biomarkers of development and viability. *Fertility and Sterility*, 85(1), 101–107.

Kaur, J. (2014). A comprehensive review on metabolic syndrome. *Cardiology Research and Practice*, 2014.

Kaye, P. L., and Gardner, H. G. (1999). Preimplantation access to maternal insulin and albumin increases fetal growth rate in mice. *Human Reproduction*, 14(12), 3052–9.

Kaye, P. L., Schultz, G. A., Johnson, M. H., Pratt, H. P. M., and Church, R. B. (1982). Amino acid transport and exchange in preimplantation mouse embyros. *J. Reprod. Fert.*, 65, 367–380.

Kelly, S. J. (1977). Studies of the developmental potential of 4- and 8-cell stage mouse blastomeres. *Journal of Experimental Zoology*, 200(3), 365–376.

Kermack, A. J., Finn-Sell, S., Cheong, Y. C., Brook, N., Eckert, J. J., Macklon, N. S., and Houghton, F. D. (2015). Amino acid composition of human uterine fluid: Association with age, lifestyle and gynaecological pathology. *Human Reproduction*, 30(4), 917–924.

Khosla, S., Dean, W., Brown, D., Reik, W., and Feil, R. (2001). Culture of preimplantation mouse embryos affects fetal development and the expression of imprinted genes. *Biology of Reproduction,* 64(3), 918–926.

Khosla, S., Dean, W., Reik, W., and Feil, R. (2001). Culture of preimplantation embryos

and its long-term effects on gene expression and phenotype. *Human Reproduction* Update, 7(4), 419–427.

Kim, D. H., Sarbassov, D. D., Ali, S. M., King, J. E., Latek, R. R., Erdjument-Bromage, H., Tempst, P. and Sabatini, D. M. (2002). mTOR interacts with raptor to form a nutrient-sensitive complex that signals to the cell growth machinery. *Cell*, 110(2), 163–175.

Kim, E. (2009). Mechanisms of amino acid sensing in mTOR signaling pathway. *Nutrition Research and Practice*, 3(1), 64–71.

Kim, E., Goraksha-Hicks, P., Li, L., Neufeld, T. P., and Guan, K.-L. (2008). Regulation of TORC1 by Rag GTPases in nutrient response. *Nature Cell Biology*, 10(8), 935–945.

Kleijkers, S. H. M., Mantikou, E., Slappendel, E., Consten, D., Echten-arends, J. Van, Wetzels, A. M., Wely, M. V., Smits, L. J. M., Montfoort, A. P. A., Repping, S., Dumoulin, J. C. M. and Mastenbroek, S. (2016). Influence of embryo culture medium (G5 and HTF) on pregnancy and perinatal outcome after IVF : a multicenter RCT. *Human Reproduction,* 31(10), 2219–2230.

Klonoff-Cohen, H. (2005). Female and male lifestyle habits and IVF: What is known and unknown. *Human Reproduction Update*, 11(2), 179–203.

Kolajova, M., and Baltz, J. M. (1999). Volume-regulated anion and organic osmolyte channels in mouse zygotes. *Biology of Reproduction*, 60, 964–972.

Korolchuk, V. I., Saiki, S., Lichtenberg, M., Siddiqi, F. H., Roberts, E. A., Imarisio, S., Jahreiss, L., Sarkar, S., Futter, M., Menzies, F. M., O'Kane, C. J., Deretic, V. and Rubinsztein, D. C. (2011). Lysosomal positioning coordinates cellular nutrient responses. *Nature Cell Biology*, 13(4), 453–60.

Koutsourakis, M., Langeveld, A., Patient, R., Beddington, R., and Grosveld, F. (1999). The transcription factor GATA6 is essential for early extraembryonic development. *Development*, 126(9), 723–32.

Kouzarides, T. (2007). Chromatin Modifications and Their Function. *Cell*, 128(4), 693–705.

Kozyraki, R., and Gofflot, F. (2007). Multiligand endocytosis and congenital defects: roles

of cubilin, megalin and amnionless. *Current Pharmaceutical Design*, 13(29), 3038–3046.

Kuehnel, W. (2003). Color Atlas of Cytology, Histology, and Microscopic Anatomy. Microscopy.

Kulie, T., Slattengren, A., and Redmer, J. (2011). Obesity and Women ' s Health : An Evidence-Based Review. *J Am Board Fam Med*, 24: 75-85.

Kurotaki, Y., Hatta, K., Nabeshima, Y., and Fujimori, T. (2007). Blastocyst Axis Is Specified Independently of Early Cell Lineage But Aligns with the ZP Shape. *Science*, 316, 719–723.

Kwong, W. Y., Miller, D. J., Ursell, E., Wild, A. E., Wilkins, A. P., Osmond, C., Anthony, F. W. and Fleming, T. P. (2006). Imprinted gene expression in the rat embryo-fetal axis is altered in response to periconceptional maternal low protein diet. *Reproduction*, 132(2), 265–277.

Kwong, W. Y., Osmond, C., and Fleming, T. P. (2004). Article Support for Barker hypothesis upheld in rat model of maternal undernutrition during the preimplantation period : application of integrated " random effects " statistical model. *Reproductive BioMedicine Online*, 8(5), 574–576.

Kwong, W. Y., Wild, A. E., Roberts, P., Willis, A. C., and Fleming, T. P. (2000). Maternal undernutrition during the preimplantation period of rat development causes blastocyst abnormalities and programming of postnatal hypertension. *Development,* 127, 4195–4202.

Lane, M., and Gardner, D. K. (1997). Differential regulation of mouse embryo development and viability by amino acids. *Journal of Reproduction and Fertility*, 109(1), 153–164.

Langley-Evans, S. C. (1997). Hypertension induced by foetal exposure to a maternal low-protein diet, in the rat, is prevented by pharmacological blockade of maternal glucocorticoid synthesis. *Journal of Hypertension*, 15(5), 537–544.

Langley-Evans, S. C. (2000). Critical differences between two low protein diet protocols in the programming of hypertension in the rat. *International Journal of Food Sciences and Nutrition*, 51(1), 11–7.

Langley, S. C., and Jackson, a a. (1994). Increased systolic blood pressure in adult rats induced by fetal exposure to maternal low protein diets. *Clinical Science* (London, England : 1979), 86(2), 217–222; discussion 121.

Larue, L., Ohsugi, M., Hirchenhain, J., and Kemler, R. (1994). E-cadherin null mutant embryos fail to form a trophectoderm epithelium. *Proceedings of the National Academy of Sciences of the United States of America*, 91(17), 8263–8267.

Latham, K. E. (1999). Mechanisms and Control of Embryonic Genome Activation in Mammalian Embryos. *International Review of Cytology*, Volume 193, 71–124.

Lazaraviciute, G., Kauser, M., Bhattacharya, S., Haggarty, P., and Bhattacharya, S. (2014). A systematic review and meta-analysis of DNA methylation levels and imprinting disorders in children conceived by IVF / ICSI compared with children conceived spontaneously. *Human Reproduction Update*, 20(6), 840–852.

Leary, C., Leese, H. J., Sturmey, R. G. (2015) Human embryos from overweight and obese women display phenotypic and metabolic abnormalities. *Humam Reproduction*; 30(1):122–32.

Le Panse, S., Ayani, E., Mulliez, N., Chatelet, F., Cywiner-Golenzer, C., Galceran, M., Citadelle, D., Roux, C., Ronco, P. and Verroust, P. (1994). Antibodies to the 280-kd coated pit protein, target of teratogenic antibodies, produce alterations in the traffic of internalized proteins. *American Journal of Pathology*, 145(6), 1526–1536.

Leese, H. J., and Barton, A. M. (1984). Pyruvate and glucose uptake by mouse ova and preimplantation embryos. J*ournal of Reproduction and Fertility*, 72(1), 9–13.

Lei, X., Chen, Y., Ye, J., Ouyang, F., Jiang, F., and Zhang, J. (2015). The Optimal Postnatal Growth Trajectory for Term Small for Gestational Age Babies: A Prospective Cohort Study. *The Journal of Pediatrics*, 166(1), 54–58.

Lewis, W. H., and Wright, E. S. (1935). On the early development of the mouse eg. Washington.

Li, Y., Xu, M., Ding, X., Yan, C., Song, Z., Chen, L., Huang, X., Wang, X., Jian, Y., Tang, G., Tang, C., Di, Y., Mu, S., Liu, X., Liu, X., Li, T., Wang, Y., Miao, L., Guo, W., Hao, X. and Yang, C. (2016). Protein kinase C controls lysosome biogenesis independently of mTORC1.

Nature Cell Biology, 18, 1065.

Lillycrop, K. A., Phillips, E. S., Jackson, A. A., Hanson, M. A., and Burdge, G. C. (2005). Dietary protein restriction of pregnant rats induces and folic acid supplementation prevents epigenetic modification of hepatic gene expression in the offspring. *The Journal of Nutrition*, 135(6), 1382–1386.

Lillycrop, K. a, Slater-Jefferies, J. L., Hanson, M. a, Godfrey, K. M., Jackson, A. a, and Burdge, G. C. (2007). Induction of altered epigenetic regulation of the hepatic glucocorticoid receptor in the offspring of rats fed a protein-restricted diet during pregnancy suggests that reduced DNA methyltransferase-1 expression is involved in impaired DNA methylation and. *The British Journal of Nutrition*, 97(6), 1064–1073.

Ling, R., Bridges, C. C., Sugawara, M., Fujita, T., Leibach, F. H., Prasad, P. D., and Ganapathy, V. (2001). Involvement of transporter recruitment as well as gene expression in the substrate-induced adaptive regulation of amino acid transport system A. *Biochimica et Biophysica Acta - Biomembranes*, 1512(1), 15–21.

Lintsen, A. M. E., Pasker-de Jong, P. C. M., de Boer, E. J., Burger, C. W., Jansen, C. A. M., Braat, D. D. M. and van Leeuwen, F. E. (2005). Effects of subfertility cause, smoking and body weight on the success rate of IVF. *Human Reproduction*, 20(7), 1867–1875.

Lloyd, J. B., Beckman, D. A., and Brent, R. L. (1998). Nutritional role of the visceral yolk sac in organogenesis-stage rat embryos. *Reproductive Toxicology*, 12(2), 193–195.

Lowther, K. M., Nikolaev, V. O., and Mehlmann, L. M. (2011). Endocytosis in the mouse oocyte and its contribution to cAMP signaling during meiotic arrest. *Reproduction*, 141(6), 737–747.

Luzzo, K. M., Wang, Q., Purcell, S. H., Chi, M., Jimenez, P. T., Grindler, N., Schedl, T. and Moley, K.H. (2012) High fat diet induced developmental defects in the mouse: oocyte meiotic aneuploidy and fetal growth retardation/brain defects. *PLoS One*, 7(11):e49217.

Manning, B. D. (2004). Balancing Akt with S6K: Implications for both metabolic diseases and tumorigenesis. *Journal of Cell Biology,* 167(3), 399–403.

Mantikou, E., Youssef, M. A. F. M., van wely, M., van der veen, F., Al-inany, H. G., Repping, S., and Mastenbroek, S. (2013). Embryo culture media and IVF/ICSI success

rates: A systematic review. *Human Reproduction Update*, 19(3), 210–220.

Marikawa, Y., and Alarcon, V. B. (2009). Establishment of trophectoderm and inner cell mass lineages in the mouse embryo. *Molecular Reproduction and Development*, 76(11), 1019–1032.

Martin, K. L., and Leese, H. J. (1995). Role of glucose in mouse preimplantation embryo development. *Molecular Reproduction and Development*, 40(4), 436–443.

Martin, P. M., and Sutherland, a E. (2001). Exogenous amino acids regulate trophectoderm differentiation in the mouse blastocyst through an mTOR-dependent pathway. *Developmental Biology*, 240(1), 182–193.

Martina, J. A., Chen, Y., Gucek, M., and Puertollano, R. (2012). MTORC1 functions as a transcriptional regulator of autophagy by preventing nuclear transport of TFEB. *Autophagy*, 8(6), 903–914.

Martina, J. A., Diab, H. I., Brady, O. A., and Puertollano, R. (2016). TFEB and TFE3 are novel components of the integrated stress response. *The EMBO Journal,* 35(5), 479–495.

Martina, J. A., Diab, H. I., Lishu, L., Jeong-A, L., Patange, S., Raben, N., and Puertollano, R. (2015). The Nutrient-Responsive Transcription Factor TFE3, Promotes Autophagy, Lysosomal Biogenesis, and Clearance of Cellular Debris. *Sci Signal*, 7(309), 1–31.

Martina, J. A., and Puertollano, R. (2013). Rag GTPases mediate amino acid–dependent recruitment of TFEB and MITF to lysosomes. *The Journal of Cell Biology,* 200(4), 475–491.

McKiernan, S., and Bavister, B. (1992). Different lots of bovine serum albumin inhibit or stimulate in vitro development of hamster embryos. *In Vitro Cell Dev. Biol.*, 30(4), 277–280.

Medina, D. L., Fraldi, A., Bouche, V., Annunziata, F., Mansueto, G., Spampanato, C., Puri, C., Pignata, A., Martina, J.m A., Sardiello, M., Palmieri, M., Polishchuk, R., Puertollano,R., Ballabio, A. (2011). Transcriptional activation of lysosomal exocytosis promotes cellular clearance. *Developmental Cell*, 21(3), 421–430.

Mellman, I., Fuchs, R., and Helenius, A. (1986). Acidification of the endocytic and

exocytic pathways. *Annual Review of Biochemistry*, 55, 663–700.

Mieulet, V., and Lamb, R. F. (2010). Tuberous sclerosis complex: Linking cancer to metabolism. T*rends in Molecular Medicine*, 16(7), 329–335.

Miller, J. G. O., and Schultz, G. A. (1985). Amino acid transport in mouse blastocyst compartments. *Journal of Embryology and Experimental Morphology*, 89, 149–158.

Mitsui, K., Tokuzawa, Y., Itoh, H., Segawa, K., Murakami, M., Takahashi, K., Maruyama, M., Maeda, M. and Yamanaka, S. (2003). The Homeoprotein Nanog Is Required for Maintenance of Pluripotency in Mouse Epiblast and ES Cells Kaoru. *Cell*, 113, 631–642.

Moestrup, S. K., Birn, H., Fischer, P. B., Petersen, C. M., Verroust, P. J., Sim, R. B., Christensen, E. I. and Nexo, E. (1996). Megalin-mediated endocytosis of transcobalamin-vitamin-B12 complexes suggests a role of the receptor in vitamin-B12 homeostasis. *Proceedings of the National Academy of Sciences of the United States of America*, 93(16), 8612–8617.

Moestrup, S. K. and Verroust, P. J. (2001). Megalin- and cubilin-mediated endocytosis of protein-bound vitamins, lipids, and hormones in polarized epithelia. *Annu. Rev. Nutr.* 21:407-28.

Monteiro, P. O. A., and Victora, C. G. (2005). Rapid growth in infancy and childhood and obesity in later life – a systematic review. *Obesity reviews*. 6: 143–154.

Morita, Y., Tsutsumi, O., Hosoya, I., Taketani, Y., Oka, Y., and Tako, T. (1992). Expression and possible function of glucose transporter protei GLUT1 during preimplantation development from oocytes to blastocysts. *Biochemical and Biophysical Research Communications*, 188(1), 8–15.

Morris, S. a, Teo, R. T. Y., Li, H., Robson, P., Glover, D. M., and Zernicka-Goetz, M. (2010). Origin and formation of the first two distinct cell types of the inner cell mass in the mouse embryo. *Proceedings of the National Academy of Sciences of the United States of America*, 107(14), 6364–9.

Muhlhausler, B. S., Duffield, J. A., Ozanne, S. E., Pilgrim, C., Turner, N., Morrison, J. L., and McMillen, I. C. (2009). The transition from fetal growth restriction to accelerated postnatal growth: a potential role for insulin signalling in skeletal muscle. *The Journal of*

Physiology, 587(Pt 17), 4199–211.

Murakami, M., and Ichisaka, T. (2004). mTOR is essential for growth and proliferation in early mouse embryos and embryonic stem cells. *Molecular and Cellular Biology*, 24(15), 6710–6718.

Nezich, C. L., Wang, C., Fogel, A. I., and Youle, R. J. (2015). MiT / TFE transcription factors are activated during mitophagy downstream of Parkin and Atg5. *The Journal of Cell Biology*, 210(3), 435–450.

Niakan, K. K., and Eggan, K. (2013). Analysis of human embryos from zygote to blastocyst reveals distinct gene expression patterns relative to the mouse. *Developmental Biology*, 375(1), 54–64.

Niakan, K. K., Ji, H., Maehr, R., Vokes, S. A., Rodolfa, K. T., Sherwood, R. I., Yamaki, M., Dimos, J. T., Chen, A. E., Melton, D. A., McMahon, A. P. and Eggan, K. (2010). Sox17 promotes differentiation in mouse embryonic stem cells by directly regulating extraembryonic gene expression and indirectly antagonizing self-renewal. *Genes and Development*, 24(3), 312–326.

Nicholas, L. M., Rattanatray, L., MacLaughlin, S. M., Ozanne, S. E., Kleemann, D. O., Walker, S. K., Morrison, J. L., Zhang, S., Muhlhausler, B. S., Martin-Gronert, M. S. and McMillen, I. C. (2013) Differential effects of maternal obesity and weight loss in the periconceptional period on the epigenetic regulation of hepatic insulin-signaling pathways in the offspring. *FASEB J.*, 27(9): 3786–96.

Nichols, J., Zevnik, B., Anastassiadis, K., Niwa, H., Klewe-Nebenius, D., Chambers, I., Scholer, H. and Smith, A. (1998). Formation of pluripotent stem cells in the mammalian embryo dependes on the POU transcription factor Oct4. *Cell*, 95, 379–391.

Niwa, H., Miyazaki, J., and Smith, A. G. (2000). Quantitative expression of Oct-3/4 defines differentiation, dedifferentiation or self-renewal of ES cells. *Nature Genetics*, 24(4), 372–376.

Niwa, H., Toyooka, Y., Shimosato, D., Strumpf, D., Takahashi, K., Yagi, R., and Rossant, J. (2005). Interaction between Oct3/4 and Cdx2 determines trophectoderm differentiation. *Cell*, 123(5), 917–929.

Norwitz, E., Schust, D., and Fisher, S. (2001). Implantation and the survival of early pregnancy. *The New England Journal of Medicine Review,* 345(19), 1400–1408.

Palis, J. (2006). Yolk Sac Development in Mice. *In Hematopoietic Stem Cell Development* (pp. 62–71). Boston, MA: Springer US.

Palmieri, M., Impey, S., Kang, H., di Ronza, A., Pelz, C., Sardiello, M., and Ballabio, A. (2011). Characterization of the CLEAR network reveals an integrated control of cellular clearance pathways. *Human Molecular Genetics*, 20(19), 3852–3866.

Palmieri, M., Pal, R., Nelvagal, H. R., Lotfi, P., Stinnett, G. R., Seymour, M. L., Chaudhury, A., Bajaj, L., Bondar, V. V., Bremner, L., Saleem, U., Tse, D. Y., Sanagasetti, D., Wu, S. M., Neilson, J. R., Pereira, F. A., Pautler, R. G., Rodney, G. G., Cooper, J. D. and Sardiello, M. (2017). mTORC1-independent TFEB activation via Akt inhibition promotes cellular clearance in neurodegenerative storage diseases. *Nature Communications*, 8, 1–16.

Pantaleon, M., Harvey, M. B., Pascoe, W. S., James, D. E., and Kaye, P. L. (1997). Glucose transporter GLUT3: ontogeny, targeting, and role in the mouse blastocyst. *Proceedings of the National Academy of Sciences*, 94(8), 3795–3800.

Pantaleon, M., and Kaye, P. L. (1998). Glucose transporters in preimplantation development. *Reviews of Reproduction*, 3, 77–81.

Pantaleon, M., Ryan, J. P., Gil, M., and Kaye, P. L. (2001). An unusual subcellular localization of GLUT1 and link with metabolism in oocytes and preimplantation mouse embryos. *Biology of Reproduction*, 64, 1247–1254.

Pantaleon, M., Scott, J., and Kaye, P. L. (2008). Nutrient sensing by the early mouse embryo: hexosamine biosynthesis and glucose signaling during preimplantation development. *Biology of Reproduction*, 78(4), 595–600.

Parlee, S. D., and MacDougald, O. A. (2015). Maternal Nutrition and Risk of Obesity in Offspring: The Trojan Horse of Developmental Plasticity. *Biochimic and Biophysis Acta*, 1842(3), 495–506.

Pemble, L. B., and Kaye, P. L. (1976). Whole protein uptake and metabolism by mouse blastocysts. *Journal of Reproduction and Fertility*, 78, 146–157.

Pena-Llopis, S., Vega-Rubin-de-Celis, S., Schwartz, J. C., Wolff, N. C., Tran, T. A. T., Zou, L., Xie, X., Corey, D. R. and Brugarolas, J. (2011). Regulation of TFEB and V-ATPases by mTORC1. *The EMBO Journal*, 30(16), 3242–3258.

Piotrowska, K., Wianny, F., Pedersen, R. a, and Zernicka-Goetz, M. (2001). Blastomeres arising from the first cleavage division have distinguishable fates in normal mouse development. *Development*, 128(19), 3739–48.

Plachta, N., Bollenbach, T., Pease, S., Fraser, S. E., and Pantazis, P. (2011). Oct4 kinetics predict cell lineage patterning in the early mammalian embryo. *Nature Cell Biology,* 13(2), 117–123.

Plusa, B., Piliszek, A., Frankenberg, S., Artus, J., and Hadjantonakis, A. (2008). Distinct sequential cell behaviours direct primitive endoderm formation in the mouse blastocyst Berenika. *Development*, 135(18), 3081–3091.

Populo, H., Lopes, J. M., and Soares, P. (2012). The mTOR signalling pathway in human cancer. *International Journal of Molecular Sciences*, 13(2), 1886–1918.

Puertollano, R., Ferguson, S. M., and Brugarolas, J. (2018). The complex relationship between TFEB transcription factor phosphorylation and subcellular localization. *The EMBO Journal*, 37, 1–12.

Pullar, D., Kronnie, G. T. E., Peiris, I. D., Taverne, N., Jeacock, M. K., Stroband, H. W. J., and Shepherd, D. A. L. (1990). Morphological and radiochemical evidence for the metabolism of exogenous proteins by the preimplantation sheep blastocyst. *Development*, 110, 539–546.

Puy, L., Chuva de Sousa Lopes, S., Haagsman, H. P., and Roelen, B. A. J. (2011). Analysis of co-expression of OCT4, NANOG and SOX2 in pluripotent cells of the porcine embryo, in vivo and in vitro. *Theriogenology*, 75(3), 513–526.

Quinn, P. (2014). Culture media and solutions. Culture Media, Solutions, and Systems in Human ART, ed. Patrick Quinn. Published by Cambridge University Press. © Cambridge University Press 2014.

Ralston, A., and Rossant, J. (2005). Genetic regulation of stem cell origins in the mouse embryo. *Clinical Genetics*, 68(2), 106–112.

Rassoulzadegan, M., Rosen, B. S., Gillot, I., and Cuzin, F. (2000). Phagocytosis reveals a reversible differentiated state early in the development of the mouse embryo. The EMBO Journal, 19(13), 3295–3303.

Reiser, J., Adair, B., and Reinheckel, T. (2010). Specialized roles for cysteine cathepsins in health and disease. *Journal of Clinical Investigation*, 120(10), 3421–3431.

Richert, B. T., Goodband, R. D., Tokach, M. D., and Nelssen, J. L. (1997). Increasing Valine, Isoleucine, and Total Branched-Chain Amino Acids for Lactating Sows. *J. Anim. Sci*., 75, 2117–2128.

Riley, J. K., Carayannopoulos, M. O., H. Wyman, A., Chi, M., Ratajczak, C. K., and Moley, K. H. (2005). The PI3K/Akt pathway is present and functional in the preimplantation mouse embryo. *Developmental Biology*, 284(2), 377–386.

Riley, J. K., and Moley, K. H. (2006). Glucose utilization and the PI3-K pathway: mechanisms for cell survival in preimplantation embryos. *Reproduction*, 131(5), 823–35.

Robker, R. L. (2008). Evidence that obesity alters the quality of oocytes and embryos. *Pathophysiology : The Official Journal of the International Society for Pathophysiology*, 15(2), 115–121.

Roseboom, T., de Rooij, S., and Painter, R. (2015). The Dutch famine and its long-term consequences for adult health. *Early Human Development*, 82(8), 485–491.

Roseboom, T. J., Meulen, M. H. Van Der, and Ravelli, a. C. (2001). Effects of prenatal expossure to the Ductch famine on adult disease in later life: an overview. *Mol Cell Endocrinol,* 185, 93–98.

Roseboom, T. J., Painter, R. C., Van Abeelen, A. F. M., Veenendaal, M. V. E., and De Rooij, S. R. (2011). Hungry in the womb: What are the consequences? Lessons from the Dutch famine. *Maturitas,* 70(2), 141–145.

Rossant, J., Chazaud, C., and Yamanaka, Y. (2003). Lineage allocation and asymmetries in the early mouse embryo. *Philosophical Transactions of the Royal Society of London*, 358, 1341–13498.

Rossant, J., and Lis, W. T. (1979). Potential of isolated mouse inner cell masses to form

trophectoderm derivatives in vivo. *Developmental Biology*, 70(1), 255–261.

Rossant, J., and Tam, P. P. L. (2009). Blastocyst lineage formation, early embryonic asymmetries and axis patterning in the mouse. *Development*, 136(5), 701–713.

Roupa, Z., Polikandrioti, M., Sotiropoulou, P., Faros, E., Koulouri, A., Wozniak, G., and Gourni, M. (2009). Causes of infertility in women at reproductive age. *Health Science Journal*, 3(2), 80–87.

Royle, S. J. (2006). The cellular functions of clathrin. *Cell Mol Life Sci*, 63(16), 1823–1832.

Ruane, P. T., Koeck, R., Berneau, S. C., Kimber, S. J., Westwood, M., Brison, D. R. and Aplin, J. D. (2018). Osmotic stress induces JNK-dependent embryo invasion in a model of implantation. *Reproduction*, 156(5), 421-428.

Russ, A. P., Wattler, S., Colledge, W. H., Aparicio, S. A. J. R., Carlton, M. B. L., Pearce, J. J., Barton, S. C., Surani, M. A., Ryan, K., Nehls, M. C., Wilson, V. and Evans, M. J. (2000). Eomesodermin is required for mouse trophoblast development and mesoderm formation. *Nature*, 404(6773), 95–99.

Sahali, D., Mulliez, N., Verroust, P., and Chemicals, F. (1988). Teratogenic Effect of the Specific Monoclonal Antibodies. *The Journal of Experimental Medicine*, 167, 213–218.

Saiz, N., and Plusa, B. (2013). Early cell fate decisions in the mouse embryo. *Reproduction*, 145, R65-80.

Sancak, Y., Peterson, T. R., Shaul, Y. D., Lindquist, R. a, Thoreen, C. C., Bar-peled, L., and Sabatini, D. M. (2008). The Rag GTPases bind raptor and mediate amino acid signaling to mTORC1. *Science*, 320(5882), 1496–1501.

Sarbassov, D. D., Ali, S. M., Kim, D. H., Guertin, D. A., Latek, R. R., Erdjument-Bromage, H., Tempst, P. and Sabatini, D. M. (2004). Rictor, a Novel Binding Partner of mTOR, Defines a Rapamycin-Insensitive and Raptor-Independent Pathway that Regulates the Cytoskeleton. *Current Biology*, 14, 1296–1302.

Sardiello, M., Palmieri, M., Ronza, A., Medina, D., Valnza, M., Gennarino, V., Di Malta, C., Donaudy, F., Embrione, V., Polishchuck, R., Banfi, S., Parenti, G., Cattaneo, E., Ballabio, A. (2009). A Gene Network Regulating Lysosomal Biogenesis and Function

Marco. *Science*, 325, 473–477.

Sato, T., Umetsu, A., and Tamanoi, F. (2008). Characterization of the Rheb-mTOR Signaling Pathway in Mammalian Cells: Constitutive Active Mutants of Rheb and mTOR. *Methods in Enzymology*, 438(7), 307–320.

Schlafke, S., and Enders, A. C. (1972). Protein Uptake by Rat Preimplantation Stages. *The Anatomical Record,* 175, 539–560.

Schmelzle, T., and Hall, M. N. (2000). TOR, a central controller of cell growth. *Cell*, 103(2), 253–262.

Sellens, M. H., and Sherman, M. I. (1981). Protein and free amino acid content in preimplantation embryos and in blastocysts under various culture conditions. *Journal of Reproduction and Fertility*, 61, 307–315.

Sellens, M., and Jenkinson, E. (1975). Permeability of the mouse zona pellucida to immunoglobulin. *Journal of Reproduction and Fertility*, 153–157.

Settembre, C., Fraldi, A., Medina, D. L., Ballabio, A., and Children, T. (2013). Signals for the lysosome: a control center for cellular clearance and energy metabolism Carmine. *Nature Reviews Molecular Cell Biology*, 14(5).

Settembre, C., Polito, V. A., Garcia, M., Vetrini, F., Erdin, S., Erdin, S. U., Huynh, T., Medina, D., Colella, P., Sardiello, M., Rubinsztein, D. C.Rubinsztein, D. C. (2011). TFEB Links Autophagy to Lysosomal Biogenesis Carmine. *Science*, 332(6036), 1429–1433.

Settembre, C., Zoncu, R., Medina, D. L., Vetrini, F., Erdin, S., Erdin, S., Erdin, S. U., Huynh, T., Ferron, M., Karsenty, G., Vellard, M. C., Facchinetti, V., Sabatini, D. M. and Ballabio, A. (2012). A lysosome-to-nucleus signalling mechanism senses and regulates the lysosome via mTOR and TFEB. *The European Molecular Biology Organization Journal*, 31(5), 1095–108.

Shin, B. C., Fujikura, K., Suzuki, T., Tanaka, S., and Takata, K. (1997). Glucose transporter GLUT3 in the rat placental barrier: A possible machinery for the transplacental transfer of glucose. *Endocrinology*, 138(9), 3997–4004.

Simmons, R. (2011). Epigenetics and maternal nutrition: nature v. nurture. *The*

Proceedings of the Nutrition Society, 70(1), 73–81.

Sinclair, K. D., and Watkins, A. J. (2014). Parental diet, pregnancy outcomes and offspring health: Metabolic determinants in developing oocytes and embryos. *Reproduction, Fertility and Development*, 26(1), 99–114.

Singh, A. M., Hamazaki, T., Hankowski, K. E., and Terada, N. (2007). A Heterogeneous Expression Pattern for Nanog in Embryonic Stem Cells. *Stem Cells*, 25(10), 2534–2542.

Smeenk, J. M., Verhaak, C. M., Eugster, a, van Minnen, a, Zielhuis, G. a, and Braat, D. D. (2001). The effect of anxiety and depression on the outcome of in-vitro fertilization. *Human Reproduction* (Oxford, England), 16(7), 1420–1423.

Smith, K. K., and Strickland, S. (1981). Structural components and characteristics of Reichert's membrane, an extra-embryonic basement membrane. *Journal of Biological Chemistry*, 256(9), 4654–4661.

Smith, R., and McLaren, A. (1977). Factors affecting the time of formation of the mouse blastocoele. *Journal of Embryology and Experimental Morphology*, 41(1), 79–92.

Spindle, A. (1978). Trophoblast Regeneration By Inner Cell Masses Isolated From Cultured Mouse Embryos. *Rapid Communication* 483-.489

Steeves, T. E., and Gardner, D. K. (1999). Temporal and Differential Effects of Amino Acids on Bovine Embryo Development. *Biology of Reproduction*, 61, 731–740.

Stephenson J., Heslehurst N., Hall J., Schoenaker D. A. J. M., Hutchinson J., Cade J. E., Poston L., Barrett G., Crozier S. R. and Barker, M., et al. (2018) Before the beginning: nutrition and lifestyle in the preconception period and its importance for future health. *Lancet*, 391, 1830–1841.

Strange, K., Emma, F., and Jackson, P. S. (1996). Cellular and molecular physiology of volume-sensitive anion channels. A*merican Physiological Society*.

Strumpf, D., Mao, C.-A., Yamanaka, Y., Ralston, A., Chawengsaksophak, K., Beck, F., and Rossant, J. (2005). Cdx2 is required for correct cell fate specification and differentiation of trophectoderm in the mouse blastocyst. *Development*, 132(9), 2093–2102.

Summers, M. C., and Biggers, J. D. (2003). Chemically defined media and the culture of

mammalian preimplantation embryos: Historical perspective and current issues. *Human Reproduction Update*, 9(6), 557–582.

Sun, C., Denisenko, O., Sheth, B., Cox, A., Lucas, E. S., Smyth, N. R., and Fleming, T. P. (2015). Epigenetic regulation of histone modifications and Gata6 gene expression induced by maternal diet in mouse embryoid bodies in a model of developmental programming. *BMC Developmental Biology*, 15(1), 3.

Sun, C., Velazquez, M. a, Marfy-Smith, S., Sheth, B., Cox, A., Johnston, D. a, Smyth, N. and Fleming, T. P. (2014). Mouse early extra-embryonic lineages activate compensatory endocytosis in response to poor maternal nutrition. *Development*, 141, 1140–1150.

Sunde, A., Brison, D., Dumoulin, J., Harper, J., Lundin, K., Magli, M. C., Van Den Abbeel, E. and Veiga, A. (2016). Time to take human embryo culture seriously. *Human Reproduction*, 31(10), 2174–2182.

Suwiska, A., Czolowska, R., Ozdzenski, W., and Tarkowski, A. K. (2008). Blastomeres of the mouse embryo lose totipotency after the fifth cleavage division: Expression of Cdx2 and Oct4 and developmental potential of inner and outer blastomeres of 16- and 32-cell embryos. *Developm*ental Biology, 322(1), 133–144.

Takahashi, Y., and First, N. L. (1992). In vitro development of bovine ane-cell embryos: Influence of glucose, lactate, pyruvate, amino acids and vitamins. *Theriogelology*, 37, 963–978.

Tan, B. S. N., Rathjen, P. D., Harvey, A. J., Gardner, D. K., and Rathjen, J. (2016). Regulation of amino acid transporters in pluripotent cell populations in the embryo and in culture; novel roles for sodium-coupled neutral amino acid transporters. *Mechanisms of Development*, 141, 32–39.

Tang, W. W. C., Kobayashi, T., Irie, N., Dietmann, S., and Surani, M. A. (2016). Specification and epigenetic programming of the human germ line. *Nature Reviews Genetics*, 17(10), 585–600.

Tarkowski, A. K., Suwi??ska, A., Czolowska, R., and Ozdzezski, W. (2010). Individual blastomeres of 16- and 32-cell mouse embryos are able to develop into foetuses and mice. *Developmental Biology*, 348(2), 190–198.

Tarkowski, A. K., and Wróblewska, J. (1967). Development of blastomeres of mouse eggs isolated at the 4- and 8-cell stage. *Journal of Embryology and Experimental Morphology*, 18(1), 155–180.

Tenay, B., Kimberlin, E., Williams, M., Denise, J., Fakilahyel, J., and Kim, K. (2013). Inactivation of Tor proteins affects the dynamics of endocytic proteins in early stage of endocytosis. *Journal of Biosciences,* 38(2), 351–361.

Tesařék, J., Kopečný, V., Plachot, M., and Mandelbaum, J. (1988). Early morphological signs of embryonic genome expression in human preimplantation development as revealed by quantitative electron microscopy. *Developmental Biology*, 128(1), 15–20.

Thomas, F. C., Sheth, B., Eckert, J. J., Bazzoni, G., Dejana, E., and Fleming, T. P. (2004). Contribution of JAM-1 to epithelial differentiation and tight-junction biogenesis in the mouse preimplantation embryo. *Journal of Cell Science*, 117, 5599–608.

Thomas, P. Q., Brown, a, and Beddington, R. S. (1998). Hex: a homeobox gene revealing peri-implantation asymmetry in the mouse embryo and an early transient marker of endothelial cell precursors. *Development* (Cambridge, England), 125, 85–94.

Thoreen, C. C., Kang, S. A., Chang, J. W., Liu, Q., Zhang, J., Gao, Y., Reichling, L. J., Sim, T., Sabatini, D. M. and Gray, N. S. (2009). An ATP-competitive Mammalian Target of Rapamycin Inhibitor Reveals Rapamycin-resistant Functions of mTORC1. *The Journal of Biological Chemistry*, 284(12), 8023–8032.

Tonack, S., Fischer, B., and Navarrete Santos, A. (2004). Expression of the insulin-responsive glucose transporter isoform 4 in blastocysts of C57/BL6 mice. *Anat Embryol* (Berl), 208(3), 225–230.

Torres-Padilla, M.-E., Parfitt, D.-E., Kouzarides, T., and Zernicka-Goetz, M. (2007). Histone arginine methylation regulates pluripotency in the early mouse embryo. *Nature*, 445(7124), 214–8.

Trounson, A., and Mohr, L. (1983). Human pregnancy following cryopreservation, thawing and transfer of an eight-Cell embryo. *Nature*, 305(5936), 707–709.

Tsichlaki, E., and Fitzharris, G. (2016). Nucleus downscaling in mouse embryos is regulated by cooperative developmental and geometric programs. *Nature*, (May), 1–7.

Tsukamoto, S., Hara, T., Yamamoto, A., Ohta, Y., Wada, A., Ishida, Y., Kito, S., Nishikawa, T., Minami, N., Sato, K. and Kokubo, T. (2013). Functional analysis of lysosomes during mouse preimplantation embryo development. *The Journal of Reproduction and Development*, 59(1), 33–9.

Tronick, E. and Hunter, R. G. (2016) Waddington, Dynamic Systems, and Epigenetics. *Frontiers in Behaviour Neurosciences*. 10, 107.

Van der Auwera, I. and D'Hooghe, T. (2001). Superovulation of female mice delays embryonic and fetal development. *Human Reproduction* (Oxford, England), 16(6), 1237–1243.

Van Der Steeg, J. W., Steures, P., Eijkemans, M. J. C., Habbema, J. D. F., Hompes, P. G. A., Burggraaff, J. M., Oosterhuis, G. J. E., Bossuyt, P. M. M., Van Der Veen, F. and Mol, B. W. J. (2008). Obesity affects spontaneous pregnancy chances in subfertile, ovulatory women. *Human Reproduction*, 23(2), 324–328.

Van Winkle, L. J. (1981). Activation of Amino Acid Accumulation in Delayed Implantation Mouse B I astocysts. *The Journal of Experimental Zoology*, 218, 239–246.

Van Winkle, L. J. (2001). Amino acid transport regulation and early embryo development. *Biol Reprod,* 64(1), 1–12.

Van Winkle, L. J., Campione, A. L., and Farrington, B. H. (1990). Development of system B0,+ and a broad-scope Na+-dependent transporter of zwitterionic amino acids in preimplantation mouse conceptuses. *BBA - Biomembranes*, 1025(2), 225–233.

Van Winkle, L. J., and Dickinson, H. R. (1995). Differences in amino acid content of preimplantation mouse embryos that develop in vitro versus in vivo: in vitro effects of five amino acids that are abundant in oviductal secretions. *Biol Reprod*, 52(1), 96–104.

Van Winkle, L. J., Mann, D. F., Wasserlauf, H. G., and Patel, M. (1992). Mediated Na+-independent transport of l-glutamate and l-cysine in 1- and 2-cell mouse conceptuses. *BBA - Biomembranes*, 1107(2), 299–304.

Van Winkle, L. J., Patel, M., Wasserlauf, H. G., Dickinson, H. R., and Campione, A. L. (1994). Osmotic regulation of taurine transport via system β and novel processes in mouse preimplantation conceptuses. *BBA - Biomembranes*, 1191(2), 244–255.

Van Winkle, L. J., Tesch, J. K., Shah, A., and Campione, A. L. (2006). System B0,+ amino acid transport regulates the penetration stage of blastocyst implantation with possible long-term developmental consequences through adulthood. *Human Reproduction Update,* 12(2), 145–157.

Van Winkle, L. J. Van, and Campione, A. L. (1996). Amino acid transport regulation in preimplantation mouse embryos: effects on amino acid content and pre- and peri-implantation development. *Theriogelology*, (45), 69–80.

Vandesompele, J., De Preter, K., Pattyn, F., Poppe, B., Van Roy, N., De Paepe, A., Speleman, F. (2002). Accurate normalization of real-time quantitative RT-PCR data by geometric averaging of multiple internal control genes. *Genome Biology*, 3(7), 1-12.

Vega-Rubin-de-Celisa, S., Pena-Llopisa, S., Kondaa, M., and Brugarolas, J. (2017). Multistep regulation of TFEB by MTORC1. *Autophagy*, 13(3), 464–472.

Velazquez, M. A. (2015). Impact of maternal malnutrition during the periconceptional period on mammalian preimplantation embryo development. *Domestic Animal Endocrinology*, 51, 27–45.

Velazquez, M. A., Fleming, T. P., and Watkins, A. J. (2019). Periconceptional environment and the developmental origins of disease. *Journal of Endocrinology*, 242(1), 33–49.

Velazquez, M. A., Sheth, B., Smith, S. J., Eckert, J. J., Osmond, C., and Fleming, T. P. (2018). Insulin and branched-chain amino acid depletion during mouse preimplantation embryo culture programmes body weight gain and raised blood pressure during early postnatal life. *Biochimica et Biophysica Acta*, 1864(2), 590–600.

Valenzuela-Alcaraz,B., Crispi, F., Bijnens, B., Cruz-Lemini, M., Creus, M., Sitges, M., Bartrons, J., Civico, S., Balasch, J., Gratacos, E. Assisted reproductive technologies are associated with cardiovascular remodeling in utero that persists postnatally, *Circulation* 128 (2013) 1442–1450.

Verroust, P. J., and Christensen, E. I. (2002). Megalin and cubilin — the story of two multipurpose receptors unfolds. *Nephrol Dial Transplant*, 17: 1867–1871.

Vestweber, D., and Kemler, R. (1984). Rabbit antiserum against a purified surface glycoprotein decompacts mouse preimplantation embryos and reacts with specific adult

tissues. Experimental Cell Research, 152(1), 169–178.

Wale, P. L., and Gardner, D. K. (2012). Oxygen Regulates Amino Acid Turnover and Carbohydrate Uptake During the Preimplantation Period of Mouse Embryo Development. *Biology of Reproduction,* 87(1), 1–8.

Wallace, M., Cottell, E., Gibney, M. J., McAuliffe, F. M., Wingfield, M., and Brennan, L. (2012). An investigation into the relationship between the metabolic profile of follicular fluid, oocyte developmental potential, and implantation outcome. *Fertility and Sterility*, 97(5).

Wang, C., and Torbett, B. (2015). Role of the mammalian target of rapamycin pathway and rapamycin in lentiviral vector gene transduction of hematopoietic stem cells. C*urr Opin Hematol,* 22(4), 302–308.

Wang, J., and Sauer, M. V. (2006). In vitro fertilization (IVF): A review of 3 decades of clinical innovation and technological advancement. *Therapeutics and Clinical Risk Management*, 2(4), 355–364.

Wang, Q. T., Piotrowska, K., Ciemerych, M. A., Milenkovic, L., Scott, M. P., Davis, R. W., and Zernicka-Goetz, M. (2004). A genome-wide study of gene activity reveals developmental signaling pathways in the preimplantation mouse embryo. *Developmental Cell*, 6(1), 133–144.

Wang, X., and Proud, C. G. (2009). Nutrient control of TORC1, a cell-cycle regulator. *Trends in Cell Biology*, 19(6), 260–267.

Warren, G. (1993). Membrane partitioning during cell division. *Annual Review of Biochemistry*, 323–348.

Watanabe, D., Suetake, I., Tada, T., and Tajima, S. (2002). Stage- and cell-specific expression of Dnmt3a and Dnmt3b during embryogenesis. *Mechanisms of Development*, 118(1–2), 187–190.

Watkins, A. J., Lucas, E. S., Marfy-Smith, S., Bates, N., Kimber, S. J., and Fleming, T. P. (2015). Maternal nutrition modifies trophoblast giant cell phenotype and fetal growth in mice. *Reproduction*, 149(6), 563–75.

Watkins, A. J., Lucas, E. S., Torrens, C., Cleal, J. K., Green, L., Osmond, C., Eckert, J. J., Gray, W. P., Hanson, M. A. and Fleming, T. P. (2010). Maternal low-protein diet during mouse pre-implantation development induces vascular dysfunction and altered renin-angiotensin-system homeostasis in the offspring. *The British Journal of Nutrition*, 103, 1762–1770.

Watkins, A. J., Platt, D., Papenbrock, T., Wilkins, A., Eckert, J. J., Kwong, W. Y., Osmond, C., Hanson, M. and Fleming, T. P. (2007). Mouse embryo culture induces changes in postnatal phenotype including raised systolic blood pressure. *Proceedings of the National Academy of Sciences*, 104(13), 5449–5454.

Watkins, A. J., and Sinclair, K. D. (2014). Paternal low protein diet affects adult offspring cardiovascular and metabolic function in mice. American Journal of Physiology. *Heart and Circulatory Physiology*, 306(10), H1444-52.

Watkins, A. J., Ursell, E., Panton, R., Papenbrock, T., Hollis, L., Cunningham, C., Wilkins, A., Perry, V. H., Kwong, W. Y., Eckert, J. J., Wild, A. E., Hanson, M. A., Osmond, C., Fleming, T. P. (2008a). Adaptive Responses by Mouse Early Embryos to Maternal Diet Protect Fetal Growth but Predispose to Adult Onset Disease. *Biology of Reproduction*, 78(2), 299–306.

Watkins, A., Papenbrock, T., and Fleming, T. P. (2008b). The preimplantation embryo: Handle with care. *Seminars in Reproductive Medicine*, 26(2), 175–185.

Watson AJ, B. L. (2001). Regulation of blastocyst formation. *Front Biosci*., 6, 708–30.

Weitlauf, H. M. (1973). In vitro uptake and incorporation of amino acids by blastocysts from intact and ovariectomized mice. J*ournal of Experimental Zoology*, 183, 303–308.

Welsh, G. I., Hers, I., Berwick, D. C., Dell, G., Wherlock, M., Birkin, R., Leney, S and Tavare, J. M. (2005). Role of protein kinase B in insulin-regulated glucose uptake. *Biochem Soc Trans*, 33(Pt 2), 346–349.

Wheeler, M. B., and Rubessa, M. (2017). Integration of microfluidics in animal in vitro embryo production. *MHR: Basic Science of Reproductive Medicine*, 23(4), 248–256.

Wheeler, T. J., and Hinkle, P. C. (1985). The glucose transporter of mammalian cells. *Annual Review of Physiology*, 47(see 42), 503–517.

Williams, C. L., Teeling, J. L., Perry, V. H., and Fleming, T. P. (2011). Mouse maternal systemic inflammation at the zygote stage causes blunted cytokine responsiveness in lipopolysaccharide-challenged adult offspring. *Journal of Biology*, 9(1), 49.

Wolffe, A. P., and Matzke, M. A. (1999). Epigenetics: Regulation Through Repression. *Science*, 286, 481–486.

Xie, Y., Zhong, W., Wang, Y., Trostinskaia, A., Wang, F., Puscheck, E. E. and Rappolee, D. A. (2007). Using hyperosmolar stress to measure biologic and stress-activated protein kinase responses in preimplantation embryos. *Mol Hum Reprod,* 13, 473-481.

Yang, X., Wu, L. L., Chura, L. R., Liang, X., Lane, M., Norman, R. J. and Robker, R. L. (2012) Exposure to lipid-rich follicular fluid is associated with endoplasmic reticulum stress and impaired oocyte maturation in cumulus- oocyte complexes. *Fertil Steril*., 97(6):1438–43.

Yu, L., McPhee, C. K., Zheng, L., Mardones, G. A., Rong, Y., Peng, J., Mi, N., Zhao, Y., Liu, Z., Wan, F., Hailey, D. W., Oorschot, V., Klumperman, J., Baehrecke, E. H., Lenardo, M. J. (2010). Termination of autophagy and reformation of lysosomes regulated by mTOR. *Nature*, 465(7300), 942–6.

Zaitoun, I., Downs, K. M., Rosa, G. J. M., and Khatib, H. (2010). Upregulation of imprinted genes in mice: An insight into the intensity of gene expression and the evolution of genomic imprinting. *Epigenetics*, 5(2), 149–158.

Zandstra, H., Van Montfoort, A. P. A., and Dumoulin, J. C. M. (2015). Does the type of culture medium used influence birthweight of children born after IVF? *Human Reproduction*, 30(3), 530–542.

Zarogoulidis, P., Lampaki, S., Francis Turner, J., Huang, H., Kakolyris, S., Syrigos, K., and Zarogoulidis, K. (2014). mTOR pathway: A current, up-to-date mini-review. *Oncology Letters*, 8(6), 2367–2370.

Zernicka-Goetz, M. (2006). The first cell-fate decisions in the mouse embryo: destiny is a matter of both chance and choice. *Current Opinion in Genetics and Development*, 16(4), 406–412.

Zhao, J., Yan, Y., Huang, X., and Li, Y. (2018). Do the children born after assisted reproductive technology have an increased risk of birth defects? A systematic review

and meta-analysis. *The Journal of Maternal-Fetal and Neonatal Medicine*, 0(0), 1–12.

Zheng, X., Liu, P., Chen, G., Qiao, J., Wu, Y., and Fan, M. (2008). Viability of frozen-thawed human embryos with one-two blastomeres lysis. *Journal of Assisted Reproduction and Genetics*, 25(7), 281–285.

Zhou, J. Liu, H., Gu, H.T., Cui, Y.G., Zhao, N.N., Chen, J., Gao, L., Zhang, Y., Liu, J.Y. Association of cardiac development with assisted reproductive technology in childhood: a prospective single-blind pilot study, *Cell. Physiol. Biochem*. 34 (2014) 988–1000.

Zollner, K.-P., Zollner, U., Schneider, M., Dietl, J., and Steck, T. (2004). Comparison of two media for sequential culture after IVF and ICSI shows no differences in pregnancy rates: a randomized trial. *Medical Science Monitor : International Medical Journal of Experimental and Clinical Research*, 10(1), CR1-7.

Zoncu, R. (2012). mTORC1 Senses Lysosomal Amino Acids Through an Inside-Out Mechanism That Requires the Vacuolar H + -ATPase Roberto Zoncu. *Science*, 678(2011).